ITERATIVE FORWARD-ADJOINT MONTE CARLO SOLUTIONS OF THE BOLTZMANN TRANSPORT EQUATION

A THESIS

Presented to

The Faculty of the Graduate Division

by

Noel Ricky Byrn

In Partial Fulfillment

of the Requirements for the Degree

Doctor of Philosophy

in the School of Nuclear Engineering

Georgia Institute of Technology

June, 1976

ITERATIVE FORWARD-ADJOINT MONTE CARLO SOLUTIONS

OF THE BOLTZMANN TRANSPORT EQUATION

Approved:

J. D. Clement, Chairman

[redacted]

J. W. Davidson

J. W. Walker

J. R. Williams

Date approved by Chairman: May 25, 1976

ACKNOWLEDGMENTS

It is a sincere pleasure for me to acknowledge the advice, assistance, and encouragement of some of the many people who have had an interest in the research described in this dissertation. Foremost, the direction, critical review, and encouragement by Dr. J. D. Clement, who served as thesis advisor, are gratefully acknowledged. The members of the Reading Committee, Drs. R. W. Carlson, J. N. Davidson, J. W. Walker, and J. R. Williams, have contributed to this research through technical discussions and review of the manuscript. Dr. L. J. Gallaher, now with the School of Information and Computer Science and a former member of the Reading Committee, also critiqued and corrected many of the mathematical equations. I am also grateful to Dr. C. J. Roberts for allowing this research to be done in absentia. Dr. L. E. Weaver, Director of the School of Nuclear Engineering, was very helpful by allowing me to use the remote job entry and time sharing capabilities at the Office of Computer Services. Messrs. J. W. Segers and J. N. Farmer of the Office of Computing Services and John Rutledge of South Central Bell, Birmingham, Alabama, were very gracious and helpful in resolving a number of data communication problems between Georgia Tech and Huntsville.

Most of this research was performed during the week ends and evenings at the offices of Science Applications, Inc. (SAI) in Huntsville, Alabama. The use of SAI facilities and resources for computer communications, typing of the initial draft, and publication of the final manuscript is gratefully acknowledged. I am also grateful to many of my

colleagues at SAI who patiently listened to my explanations of why this equation or algorithm or technique could not be wrong, and then assisted me in finding the errors that I could not find by myself. In particular, C. W. Hill, R. W. Guy, H. T. Smith, and L. C. Allen helped in the manner described. Dr. T. J. Hoffman, now an Associate Professor of Nuclear Engineering, University of Tennessee, Knoxville, also provided valuable suggestions and directions during the initial stages of this research.

This research effort was partially supported under a National Aeronautics and Space Administration Contract, NAS8-27541. The contract monitor, Mr. Henry E. Stern, provided valuable assistance and encouragement in the research, and I am very grateful to both Mr. Stern and NASA.

Mrs. Ann G. Jaynes and Mrs. W. J. Johnson shared the difficult task of typing the initial draft from my handwritten original. I appreciate very much their patience and hard work.

Mrs. Lydia S. Geeslin typed the final manuscript. Her excellent work, especially in seeing that the manuscript conformed to the Graduate Division requirements, is greatly appreciated.

I could not fail to acknowledge the love, patience, and support of my wife, Abby, and our three children, Judy, Janice, and Andy. The sacrifices which they made so that I could work on my thesis will never be forgotten. My parents, Mr. and Mrs. Grady D. Byrn, have also encouraged and supported this dissertation and all of my education. I am forever grateful to them. Finally, I give thanks to God and pray this dissertation and all of my life will be to His honor and glory.

TABLE OF CONTENTS (Concluded)

LIST OF TABLES

LIST OF ILLUSTRATIONS

SUMMARY

A Monte Carlo importance sampling variance reduction technique has been developed for application to complex radiation transport problems. The technique is based on iterative solutions of the forward and adjoint integral transport equations. Importance functions are generated for altering the natural sampling distributions in the forward Monte Carlo simulation from the adjoint flux estimated during the adjoint case. Likewise, the flux estimated during the forward case is used to generate importance functions for altering the adjoint Monte Carlo sampling distributions. The altered distributions are the source energy and direction, the transport kernel and the collision kernel. By iteratively solving the forward and adjoint transport equations, better importance functions are generated which improve the efficiency of the Monte Carlo simulation at successive steps.

The theoretical basis for this technique is developed, with particular emphasis on the selection of the proper quantities for the importance functions. Detailed descriptions of how the importance functions are applied to the sampling distributions are given.

A computer test bed was written by the author for determining the effectiveness of the iterative forward-adjoint variance reduction techniques. The test bed is based on the MORSE Monte Carlo code, but has additional logic so that a series of forward and adjoint cases can be executed in a given run. Data management techniques for reducing the computer core requirement and special purpose routines for handling the

generation of importance functions are described.

The techniques developed and implemented in the computer test bed were evaluated on well-defined test problems. One of these problems is a simulation of the point source in infinite air with a point detector. The iterative forward-adjoint technique produced an improvement in the efficiency when applied to the source energy distribution, but the effectiveness of altering the other sampling functions was inconclusive. A simplified problem was constructed which consisted of a point monoenergetic source and point detector in vacuum, and separated by a disk shield. The efficiency gain due to source direction biasing was found to be a factor of two to three. However, no significant improvement was found when the transport kernel was altered. Conclusions based on these test problems are that the iterative forward-adjoint Monte Carlo variance reduction technique increases the efficiency of the simulation where applied to the source sampling functions, but its effectiveness with the transport and collision kernels is doubtful.

CHAPTER I

INTRODUCTION

1.1 Background

The Monte Carlo method is a numerical technique for solving both physical and mathematical problems. The method has been applied to a wide variety of problems, but has found its widest acceptance and utilization in the solution of nuclear radiation transport problems. Various definitions of the method have been given {1-8}, each emphasizing different aspects. The most important characteristic of the Monte Carlo method is the use of random sampling techniques which are applied to the probability distribution laws that a physical or mathematical process obeys. Conclusions about the outcoming of the process are obtained by statistical analysis of the samples obtained from the random sampling technique.

An important part of the method is the representation of the physical or mathematical process by the correct probability distribution functions. Some processes, such as the diffusion of nuclear particles, seem to obey probabilistic laws, although they can also be defined by deterministic equations. Such processes lend themselves readily to simulation by the Monte Carlo methods. Other processes are deterministic, that is, their outcome is not directly concerned with random processes. An example of such a process is the adjoint transport equation {9-11}.

Note: Numbers inside braces denote references.

Deterministic processes, whether physical or mathematical, are solved by devising wholly artificial probability distribution laws which, when simulated by Monte Carlo, produce statistical results that approach the analytical results. Often analytical results are unattainable, so that some numerical technique is required. Monte Carlo methods provide one technique to solve these deterministic problems.

Because statistic inference is used to determine the results in a Monte Carlo simulation, statistical variation or fluctuations are inherent in the results. To reduce the error between the Monte Carlo results and the true result, large numbers of samples are usually required. This is the principal reason that the Monte Carlo method did not gain widespread utilization until recently, when the advent of the electronic computer provided a means of generating the large sample populations. However, the method was used to solve select problems before the computer age, usually under the title of "model sampling" {2}. Hammersley and Handscomb provide a brief history of the Monte Carlo method in their excellent monograph {7}, including the pre-computer determination of pi(π) by observing the frequency with which a needle thrown on the floor intersects parallel straight lines. Also mentioned is the use of model sampling by Student (W. S. Gosset) to supplement his hypothesis of the t-distribution and in the discovery of the correlation coefficients. In the early 1900's Lord Kelvin published a paper {12} which contained the essence of modern Monte Carlo techniques as applied to the solution of the Boltzmann equation. Unfortunately, the emphasis was on the solution and not the method.

It is generally accepted {1-4,7} that the method now called Monte

Carlo is an outgrowth of the efforts of Stanley Ulan and John von Neumann during the Manhattan Project (the United States' World War II project to build the atomic bomb). Their principal interest was the simulation of neutron transport in fissile material. They soon recognized the need for techniques to reduce the sample size needed to obtain a given accuracy. These techniques, called variance reduction techniques, soon became the major research issue for the Monte Carlo method. An excellent review of the progress of the Monte Carlo method from post-World War II to 1954 is given by A. W. Marshall in Reference 2. During this time, almost all of mathematical foundation of the method was completed and published, with Kahn's efforts most noteworthy [3]. This foundation includes most of the variance reduction techniques which are discussed later, thus leaving future researchers with the principal task of application of the Monte Carlo method.

Applications were also of concern during the late 1940's and early 1950's, with Enrico Fermi and others using Monte Carlo to estimate the eigenvalues associated with the Schrödinger equation, while others solved matrix inversion and operations research problems [2]. Another concern during this period (and one of continuing discussion) is the proper definition of the Monte Carlo method. In particular, what was model sampling and what was Monte Carlo? Most researchers apply "Monte Carlo" to the more sophisticated sampling techniques (e.g., those using variance reduction) while the straightforward simulation of a probabilistic situation is called model sampling. However, this distinction is immaterial to the present research, and the term Monte Carlo will be used to denote both aspects of this numerical technique. Where appropriate, the adjective,

analog, will precede Monte Carlo to denote that method which is a faithful simulation of the probabilistic laws governing a given situation.

From the mid-1950's until the present, much of the effort in Monte Carlo has been in the application of the method to various problems, especially those of nuclear radiation transport. Indicative of this fact is the large number of Monte Carlo computer codes which were developed during the period, a few of which are contained in References 13-23. The greatest effort has been in the development and application of variance reduction techniques. In the discussion which follows, variance reduction techniques will be described which have demonstrated their efficiency in solving radiation transport equations. The analog Monte Carlo method usually requires extensive amounts of computing time to produce accurate results. Variance reduction techniques attempt to reduce the computing time required to obtain a given accuracy, usually by altering the simulation process, but not the result of interest. The figure of merit for a given variance reduction technique is the efficiency {7}, and this is usually taken as inversely proportional to the product of the sampling variance and the computer time or resources expended in obtaining the estimate. More efficient Monte Carlo calculations can also result by the use of approximate or analytical information instead of random sampling and by studying the process or problem within a different context or abstract representation. Examples of variance reduction techniques in these categories are given below.

Importance sampling is the technique of altering the sampling probability functions so that those events of interest are sampled more often than in the analog process. To compensate for the distortion of

the simulation, the value of a given sample must also be altered in order to remove any bias in the estimate of the result or effect of interest. This variance reduction technique is described in considerable detail in Section 2.3, since the major emphasis of this research effort is on this type of variance reduction. The concept of the perfect game or zero-variance importance sampling probably originated by Goertzel [24], but excellent discussions of this technique and importance sampling in general are given in References 3, 4, 8, and 25. One of the most used importance sampling devices is the exponential transformation [26], which can expand or contract the average path length of a particle, thus promoting the transport of particles in preferred directions while discouraging transport in other directions.

Variance reduction techniques are also employed which can limit or kill samples in uninteresting portions of the transport simulation (e.g., regions of a reactor far away from the region of interest) and increase the number of samples in or near important regions. These techniques are called Russian Roulette and splitting, respectively [3-8,10, 27]. These techniques can be formulated in a manner which makes them only slight variations of the same importance sampling technique [10], but a straightforward formulation exists which justifies their inclusion as separate variance reduction techniques.

Two other techniques which are classed as altering the sampling process are systematic sampling and stratified (or quota) sampling. In systematic sampling, the sample space is divided into subspaces with known probability and random samples are distributed according to those probabilities [3-8, 27]. Stratified or quota sampling is similar, but the

random samples are distributed not by the known probabilities, but by a distribution which emphasizes the more important subspaces. This variance reduction technique has application when a priori knowledge of importance exists {3,7,8,27}.

A second category of variance reduction technique consists of those which use analytical or approximate solutions of the Monte Carlo simulation. Since analytical solutions have no variance, replacing a random sampling step by its analytical or approximate solution reduces the fluctuations in the sample results. The expected value technique is a member of this category. Its greatest application in radiation transport simulation by Monte Carlo is in the scoring function {3,8,19,27}. Suppose the fluence at a point detector is desired. Then at each particle collision, the expected value of the fluence at that detector due to a given collision is just the product of the probability that the particle will be scattering toward the detector and the probability that the particle will reach the detector, divided by the collision to detector distance squared. This special analytical scoring technique is also known as statistical estimation. Similar analytical techniques are available for calculating the boundary crossing and volume fluences. Another application of expected value variance reduction techniques in radiation transport is the use of a weight system so that when a particle undergoes a collision, a scattering event always occurs. To compensate for the fact that absorptions are not allowed, the particle's weight is multiplied by the nonabsorption probability.

Hammersley and Handscomb {7} introduced another analytical or approximate technique which usually requires little additional computa-

tion but can often give great improvement in the variance. This technique, called antithetic variates, associates with the outcome of a random event one or more additional events whose contribution to the result or effect of interest is negatively correlated to the original event. For example, during a fission event, the direction of the first neutron is randomly chosen. Then a second neutron in the opposite direction is simulated. Other analytical or approximate variance reduction techniques include correlated sampling, control variates, and history reanalysis {27}.

The final category of variance reduction techniques has found applications in very specialized problems, since they usually required more effort to implement than the above mentioned techniques. Usually they require that the problem be analyzed in a different context or that an abstract representation of the problem be devised. The most straightforward of these techniques is sequential sampling, which consists of performing an initial Monte Carlo simulation with little or no variance reduction techniques, then analyzing the result to develop other variance reduction techniques for the next simulation. Obviously, this technique can be continued for as many iterations as desired, but the efficiency may be low.

Conditional Monte Carlo is another of the specialized techniques. Introduced by Trotter and Tukey {2}, it was applied to radiation transport problems by Drawbaugh {28}. It uses importance sampling to facilitate the sampling of conditional probability distributions in which the transport problem is imbedded. This allows all transport problems to end at the same desired point. Unfortunately, this technique is very difficult to implement and has been used only sparsely.

Other specialized techniques include transformations of the problem [27] and the adjoint formulation [3,4,27]. Only the adjoint technique has enjoyed wide acceptance. It is described in detail in the next chapter.

1.2 Purpose

For a large class of radiation transport problems, only the Monte Carlo method has proven to be a useful tool for effecting solutions. This is due primarily to the fact that three-dimensional, time dependent problems can be solved by the Monte Carlo method, while other methods are usually restricted to only two dimensions. Monte Carlo suffers from the disadvantage that as a probabilistic method, considerable computer time is required for statistically meaningful results. This limitation can be alleviated by the use of variance reduction techniques. The research that has been performed in this study has identified variance reduction techniques based on both the forward or normal Monte Carlo solution and the adjoint Monte Carlo solution which can be used to reduce the variance for a given amount of computation time.

In particular, the techniques utilize the fact that the adjoint fluence determined in an adjoint Monte Carlo calculation can be used to calculate altered sampling distributions (for the source parameters, path length, and post-collision parameters) to be used in the forward calculation. The source term used in the adjoint calculation must be the detector response function in the forward case. Random sampling from these altered distributions, instead of the natural distribution, results in a reduced variance of the effects of interest because the most

"important" part of the distribution is sampled most often. The forward fluence determined in a forward calculation can likewise be used to alter the distribution function for the adjoint calculation. The validity of this technique has been discussed by many researchers [3,4,24,25,29-33]. The earliest reference is contained in Herman Kahn's Application of Monte Carlo (1), first published in 1954. He also suggested the use of the iterative forward-adjoint Monte Carlo (called Method IV), stating "As far as the author knows, Method IV has never been used in a systematic fashion." By iteratively performing the forward and adjoint calculations, updating the altered sampling distributions between each calculation, the variance should be reduced more rapidly with each iteration, since better values of the fluence (forward and adjoint) are being determined.

The principal efforts of this study have been to develop iterative forward-adjoint techniques which can be applied to Monte Carlo computation methods, to write a computer test bed which will perform the appropriate calculations for testing these different techniques of using the forward or adjoint fluence to calculate the altered sampling distributions, and to evaluate the value of the iterative forward-adjoint Monte Carlo techniques which are developed.

The general outline of an iterative forward-adjoint Monte Carlo calculation is given below and diagrammed in Figure 1. It is assumed that the particular problem of interest has been identified and the necessary data obtained and prepared in a form acceptable to the computer program which employs the iterative forward-adjoint variance reduction techniques. A discussion of such a program, called IFAM for Iterative Forward-Adjoint MORSE, is given in Chapter III. The initial step in the

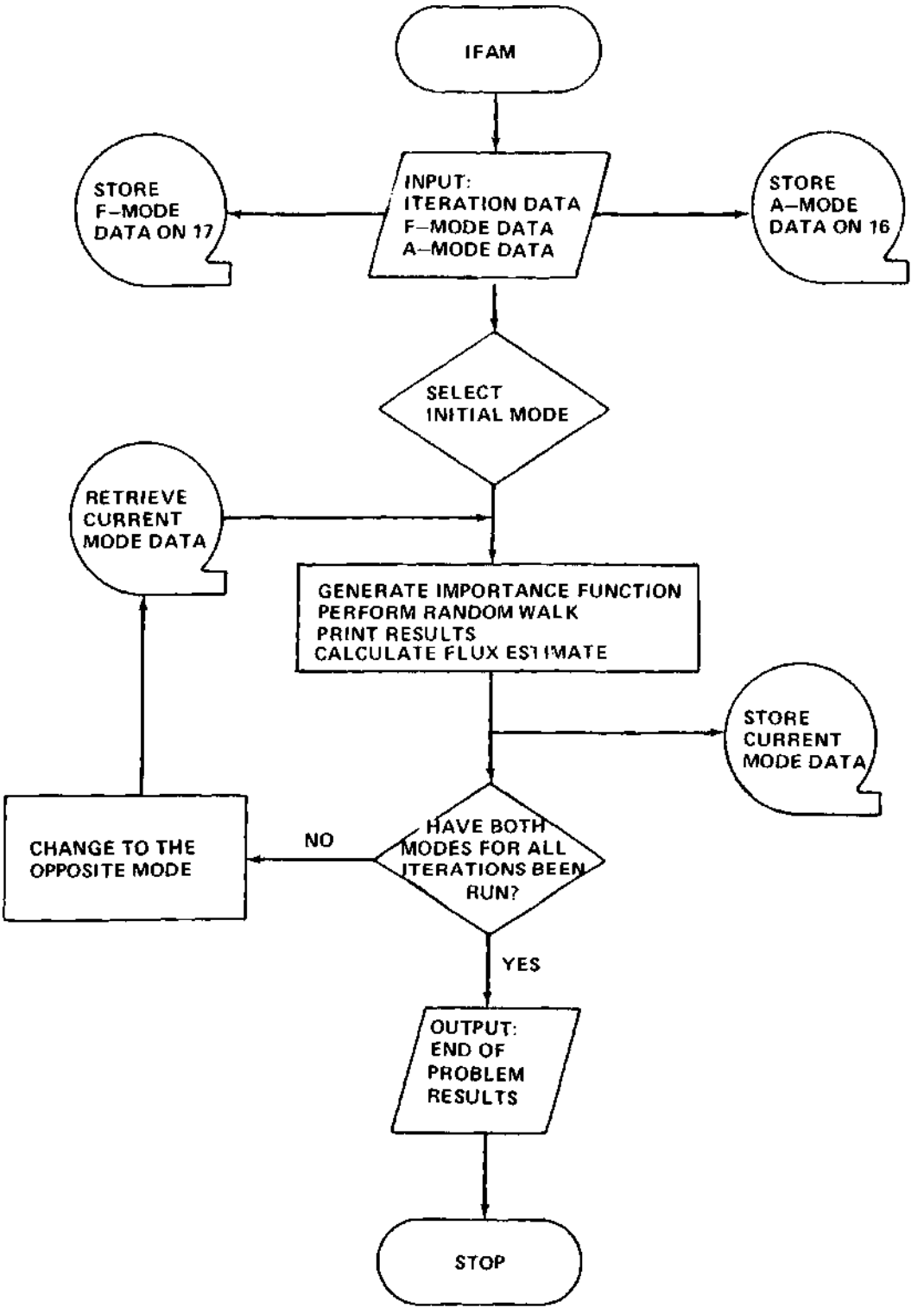

Figure 1. Iterative Forward-Adjoint Monte Carlo Flow Diagram

calculation is the processing of input data. This step is performed for both forward and adjoint data before any of the random walk calculations begin. Data which are not in use (e.g., adjoint data during the forward mode random walk) are stored on bulk storage or data file units such as disk files. The input data must also specify the initial mode - forward or adjoint - to be executed, since this is left to the judgment of the user.

After the processing of the input data, the data for the initial mode are retrieved from the proper data file, data initialization performed, and the data put into core. The initial mode, either forward or adjoint, random walk is begun for the specified number of batches and histories per batch. During this calculation, the program executes only the initial mode type of random walks, but it employs input biasing parameters, if desired, to alter the source particle energy and direction, the path length, and the energy downscattering distribution functions. At the same time, data are stored for estimating the energy and angular dependent fluence in each importance region. Estimates are also made of some effect of interest, such as the dose at the detector. This process is continued until all histories have been completed for the initial mode, at which time the output data are written, including the estimate of the effect of interest and the energy and region dependent fluence estimate. The data used or generated during this calculation are stored back on the data file units for processing and use in the next iteration.

The calculations performed in the second half of this first iteration are very similar to those performed for the initial mode except that

the other mode type random walk will be executed. The distribution functions will be altered by an importance function which is based on both the input biasing functions and the energy, angular, and region dependent fluence from the initial mode. The validity of using the initial mode fluence for altering the distribution functions is discussed in detail in Chapter II, and the form employed in this study is explained in Chapter IV. Retrieval of the opposite mode data from the data file, initialization and generation of the importance function are required before the random walk calculations can occur. At the completion of these calculations, the same results as in the initial mode are output both to the printer and to the data file for this mode. This completes the first iteration which consists of random walk calculations in both the forward and adjoint modes. Note that, at the end of each mode, an estimate of the effect of interest was obtained.

The second and succeeding iterations are identical in format to the first iteration: data are retrieved for the initial mode data file, initialization and importance function calculations are performed, then the effect of interest and the fluence are estimated during the random walk calculations followed by output and data storage for the initial mode. The same steps are then performed for the opposite mode. However, with each iteration, the fluence estimates approach the actual value, thus improving the altered distribution functions and hence reducing the variance of the effect of interest estimator with each iteration.

1.3 Applications

Research on the iterative forward-adjoint Monte Carlo method was motivated primarily by the desire to develop a variance reduction technique that could solve very complex radiation transport problems more efficiently than those techniques discussed above. The discussion below gives both a justification for this research and provides examples of problems for which the technique can be used.

The discovery of the harmful effects of penetrating radiation, such as neutron and gamma-rays, prompted considerable concern and effort about protective shielding. Initially, much of this effort was experimental but with the advent of the atomic bomb and the nuclear reactor during World War II, it was realized that experimental methods were not suitable for determining the radiation environments from these massive sources. Numerical techniques were needed which could accurately predict the radiation transport processes. Since that time, considerable effort and money have been spent in developing methods for solving the transport equation. Although these methods represent a tremendous capability to perform radiation transport calculations, many improvements are still needed, especially in the area of very complex problems requiring three-dimensional geometries, time dependence, and deep penetration.

Deep penetration problems are those in which the flux changes by several orders of magnitude from source to detector. It is not unusual for a reactor shield to be required to reduce the radiation environment by eight orders of magnitude. For land base reactors, where the shield is usually designed within a factor of 10, sophisticated calculational methods are not needed. This is not the case for mobile reactors, such

as in submarines and reactors used for nuclear propulsion or space nuclear power.

In these reactors, where weight is such an important factor, addition of a few inches of shielding to account for calculational uncertainties can be disastrous. A good example of this is a nuclear aircraft. One of the primary reasons that this multi-million dollar program was unable to produce an operational aircraft was because of the excessive shield weight. This is not to imply that the availability of an improved method for solving this radiation transport problem would have changed the outcome of a nuclear aircraft program, but rather that the practicability of the nuclear aircraft would have been known sooner had such a technique been available.

There exist many applications for which the iterative forward-adjoint Monte Carlo calculational technique can be used. For example, the former chairman of the U. S. Atomic Energy Commission, Dr. Glenn Seaborg, has said that the use of nuclear propulsion to reach outer planets such as Jupiter will surely be examined instrumentally in this century and that man is likely to visit Mars by the same means [34]. He has also predicted that large earth stationary satellites bearing compact nuclear reactors will broadcast television programs and other messages directly to home receivers. Clement and Williams have described how gas-core nuclear reactors could be put into space and used to heat the working fluid for magnetohydrodynamic generators [35]. The energy produced could then be beamed to earth by microwaves.

Considerable effort has already been spent in calculating the radiation environment around both nuclear propulsion and space power

systems. It has been found that, without an excessive amount of computational effort, accurate radiation environment calculations cannot be made with present radiation transport methods. Both personnel and equipment on these systems are subject to radiation damage. Personnel can be incapacitated and equipment performance degraded even to the point of malfunction or failure under radiation environment conditions. It is essential that the radiation environment be accurately known before these systems can become operational.

Radiation transport methods are also required for a nuclear weapons program. Because of the atmospheric nuclear test ban, the capabilities of the new nuclear weapons must be determined by sophisticated radiation transport calculations. Another application of the iterative forward-adjoint Monte Carlo methods would be in the design of medical facilities for the bombardment of cancerous cells in the human body by 14 MeV neutrons. An efficient radiation transport calculational scheme capable of handling three-dimensional geometries would be able to reduce the cost of designing and building a collimator for the neutrons. This method can also be used for design of shields for advanced reactor concepts such as the fast breeder and fusion reactors. The above applications provide a few examples of how radiation transport problems can be solved by the iterative forward-adjoint Monte Carlo method.

CHAPTER II

THEORETICAL ASPECTS

The fundamental equation describing the transport of radiation through matter is the Boltzmann transport equation. This linear integro-differential equation is essentially a particle balance equation in phase space. In Section 2.1, each term of this equation is defined by discussing both the physical significance and the mathematical form of each term. The physical assumptions upon which the transport equation is based and which restrict its application are also presented. Whereas the Boltzmann transport equation provides the basis for numerical solution methods such as discrete ordinates and the moments method, an integral transport equation (i.e., Fredholm equation of the second kind) is a better form for stochastic or Monte Carlo method solutions. However, the integro-differential form seems to give a better physical insight into the radiation transport problem, and for that reason the Boltzmann equation was chosen for the introductory discussion of the iterative forward-adjoint Monte Carlo method.

Section 2.2 presents a derivation of the integral transport equation from basic definitions. The concept of the emergent particle density (or the density of particles leaving sources and collisions) is also introduced. This concept is important to the Monte Carlo method because the emergent particle density equation is the one simulated in most Monte Carlo computer programs. The format of the presentation in Section 2.2

and Section 2.3 follows that of the report by Goertzel and Kalos [4], which is an amplification of the fundamental work done by Kahn [3]. Section 2.3 illustrates the Monte Carlo method by an example transport game, and then uses this game to produce the "perfect game" by the introduction of the adjoint or importance function. The implications of these results are then discussed relative to the iterative forward-adjoint Monte Carlo method.

Since the computer test bed used to validate the iterative forward-adjoint variance reduction techniques is a multigroup Monte Carlo code, Section 2.4 contains a discussion of the multigroup integral transport equations in both the forward and adjoint forms. These equations are used to define the proper relationships between the forward and adjoint forms.

2.1 Boltzmann Transport Equation

The Boltzmann transport equation (sometimes called the linear transport equation, Boltzmann equation, or transport equation) describes the distribution of particles such as neutrons or gamma-rays in phase space, P. Phase space will be represented by:

$$P = (\bar{x},\bar{E},t) = (\bar{x},E,\bar{\omega},t) \tag{2-1}$$

where $\bar{x}$ = spatial variable (e.g., $\bar{x} = (x,y,z)$) (vector)

$\bar{E}$ = directed energy variable ($\bar{E} = (E,\bar{\omega})$) (vector)

E = energy variable (scalar)

$\bar{\omega}$ = direction or angular variable ($\bar{\omega} = (\theta,\phi)$) (vector)

t = time variable (scalar)

The Boltzmann equation is usually written in the following form:

$$\left[\frac{1}{v}\frac{\partial}{\partial t}\Phi(\bar{x},\bar{E},t) + \bar{\omega}\cdot\nabla\Phi(\bar{x},\bar{E},t) + \Sigma_t(\bar{x},E)\Phi(\bar{x},\bar{E},t)\right. \tag{2-2}$$

$$\left. = \int\int \Sigma_s(\bar{x},E')\ \Phi(\bar{x},\bar{E}',t)\ f(E,\bar{\omega}|E',\bar{\omega}')dE'd\bar{\omega}' + S(\bar{x},\bar{E},t)\right]d\bar{x}d\bar{E}$$

where

$d\bar{x}$ = differential volume element (e.g., dxdydz) (scalar)

dE = differential energy variable (scalar)

$d\bar{\omega}$ = differential angular variable (e.g., $\sin\theta d\theta d\Phi$) (scalar)

$d\bar{E} = dEd\bar{\omega}$ (scalar)

$\Phi(\bar{x},\bar{E},t)d\bar{x}dEd\bar{\omega}$ = particle flux at time t in the differential volume $d\bar{x}$ about $\bar{x}$ with energies in dE about E and with directions in $d\bar{\omega}$ about $\bar{\omega}$. The units of Φ are particles (or photons)/cm^2/sec/steradians/eV, and the energy E corresponds to the speed v. (scalar)

$\Sigma_t(\bar{x},E)$ = macroscopic total cross section in cm^{-1} at position $\bar{x}$ and energy E (scalar)

$\Sigma_s(\bar{x},E)$ = macroscopic scattering cross section in cm^{-1} at position $\bar{x}$ and energy E (scalar)

$f(E,\bar{\omega}|E',\bar{\omega}')dEd\bar{\omega}$ = the conditional probability of a particle scattering from an initial energy E' and direction $\bar{\omega}'$ into the energy interval dE about E and into the solid angle $d\bar{\omega}$ about the direction $\bar{\omega}$ (scalar)

$S(\bar{x},\bar{E},t)d\bar{x}d\bar{E}$ = the radiation at time t in the differential volume $d\bar{x}$ about $\bar{x}$ with energies in dE about E and with

directions in $d\bar{\omega}$ and $\bar{\omega}$ appearing from sources other than scattering events (e.g., fission neutrons, radioactive decay gamma-rays) (scalar).

The first term on the left side of the Boltzmann equation represents the time rate of change of the radiation in the differential phase cell, $d\bar{x}d\bar{E}$, at time t. This time rate of change can be caused by the following four occurrences:

1) Leakage $[\bar{\omega}\cdot\nabla\Phi(\bar{x},\bar{E},t)d\bar{x}d\bar{E}]$: Net leakage of particles with directions in $d\bar{\omega}$ about $\bar{\omega}$ and with energies in dE about E from the differential volume, $d\bar{x}$ about $\bar{x}$, at time t;

2) Interactions $[\Sigma_t(\bar{x},E)\Phi(\bar{x},\bar{E},t)d\bar{x}d\bar{E}]$: Any interaction of the particles with the medium at time t in $d\bar{x}$ about $\bar{x}$ which removes the particle from either dE about E, or $d\bar{\omega}$ about $\bar{\omega}$;

3) Inscattering $\left[\left(\int\int \Sigma_s(\bar{x},E)\Phi(\bar{x},\bar{E},t)f(E,\bar{\omega}|E',\bar{\omega}')dE'd\bar{\omega}'\right)dEd\bar{\omega}\right]$

A gain in radiation in $d\bar{x}$ about $\bar{x}$ at time t due to any scattering events which redirect the particles into $d\bar{\omega}$ about $\bar{\omega}$ and the energy into dE about E;

4) Sources $[S(\bar{x},\bar{E},t)d\bar{x}d\bar{E}]$: Particles born in $d\bar{x}$ about $\bar{x}$ with the proper energies and directions as defined above.

These four terms constitute the losses (leakage and interactions) and gains (inscattering and sources) which determine the time rate of change. Thus, the Boltzmann equation is essentially a particle balance equation, that is:

Change = Gains - Losses.

It should be noted that Equation 2-2 is not the only form of the Boltzmann

equation. Often the balance is performed on the phase space particle density instead of the particle flux. The independent energy variable E can be replaced by the speed, v. Also, the inscattering term, which includes any scattering event in which the number of particles is not changed, can be replaced by a more general term. This term can include production events such as fission in neutron transport and pair production in gamma-ray transport. When the inscattering term is thus modified, the source term must be modified correspondingly.

The justification of the linear Boltzmann transport equation as given in Equation 2-2 requires that the following assumptions be made (also see Reference 36):

1) Statistical fluctuations are neglected

2) Collision times are negligible

3) Particle correlations are neglected

4) The wave nature and spin of the particle are neglected (except in the computation of the cross sections and scattering kernel, $f(E,\bar{\omega}|E',\bar{\omega}')$)

5) Interactions between particles are negligible

6) The medium in which the particles are being transported is not affected by the presence of the particles (i.e., the cross sections and scattering kernel are assumed not to depend functionally on $\Phi(\bar{x},\bar{E},t)$)

7) Cross sections are assumed independent of $\bar{\omega}$

8) The scattering kernel, $f(E,\bar{\omega}|E',\bar{\omega}')$ depends only on the angle between $\bar{\omega}$ and $\bar{\omega}'$ (or on $\bar{\omega}\cdot\bar{\omega}'$) and on E'.

Assumptions 1) through 4) are required since the Boltzmann equation is derived in the continuous phase space P based on classical physics. This

means that the independent variables, $\bar{x}$, E, $\bar{\omega}$, and t, are assumed to be continuous, not discrete (however, most transport methods use discrete approximations for some or all of these variables). Assumptions 5) and 6) were necessary to keep the Boltzmann equation linear. Thus Equation 2-2 can be used for neutron, gamma-ray, and charged particle transport, but would fail to adequately describe low energy x-ray transport because of stimulated emission and the extreme temperature sensitivity of cross sections. Finally, assumptions 7) and 8) avoid the necessity of having a preferred coordinate system. These assumptions would not be valid for the Bragg (coherent) scattering of low energy neutrons by crystals.

The integral form of the transport equation can be derived from the Boltzmann equation by defining a new quantity of interest, the emergent particle density {37}. A derivation of the integral transport equation in multigroup form has also been derived for the MORSE code {13} from the Boltzmann transport equation (Eq. 2-2). These derivations will be discussed in Section 2.4. However, a derivation of the integral transport equation from more fundamental considerations is given below.

2.2 Integral Transport Equation

The following discussion of the integral transport equation is valid for both neutrons or gamma-rays, provided that the assumptions imposed on the linear Boltzmann equation are valid. Each particle will be described by its position in phase space (P), consisting of the spatial coordinates, $\bar{x}$, energy, E, and direction of motion, $\bar{\omega}$. Only time independent cases will be considered, but addition of time dependence is straightforward. Hence, P can be represented as shown below:

$$P = (\bar{x},\bar{E}) = (\bar{x},E,\bar{\omega}) \ . \qquad (2\text{-}3)$$

The motions of the particles will be described by three terms:

Flux -- $\Phi(P)$

Collision density -- $\psi(P)$

Density of particles leaving collisions (emergent particle density) -- $\chi(P)$.

Note that all three of these terms are functions of phase space, P, and not not just $\bar{x}$ or $(\bar{x},\bar{E})$. As usual, the flux and collision density are related by the total cross section, $\Sigma_t(\bar{x},E)$, which is assumed to be independent of $\bar{\omega}$, so that

$$\psi(\bar{x},E,\omega) = \Sigma_t(\bar{x},E)\ \Phi(\bar{x},E,\bar{\omega}) \ . \qquad (2\text{-}4)$$

In order to derive the transport equation, it is convenient to consider the number of collisions that a given particle has undergone. Therefore, the following definitions are in order:

$\Phi_n(P)$ - flux at P of particles that have undergone n-1 collisions (hence are entering their n^{th} collision)

$\psi_n(P)$ - collision density at P of particles that have undergone n-1 collisions [as for $\Phi_n(P)$]

$\chi_n(P)$ - density of particles at P which have just had their n^{th} collision

$\chi_o(P)$ - density of particles at P which are emitted from the source (consider the source as the zeroth collision)

$C(\bar{E}|\bar{E}';\bar{x})d\bar{E}$ - probability that a particle having a collision at the spatial point $\bar{x}$ and directed energy $\bar{E}'$ will emerge in dE about E [$C(\bar{E}|\bar{E}';\bar{x})$ is called the collision kernel]

$T(\bar{x}|\bar{x}';\bar{E})d\bar{x}$ - probability that a particle leaving a collision at $\bar{x}'$ with directed energy $\bar{E}$ will have its next collision in $d\bar{x}$ about $\bar{x}$ [$T(\bar{x}|\bar{x}';\bar{E})$ is called the transport kernel].

From the above definition, the following relationship can be deduced:

$$\Phi(P) = \sum_{n=1}^{\infty} \Phi_n(P) \tag{2-5}$$

$$\psi(P) = \sum_{n=1}^{\infty} \psi_n(P) \tag{2-6}$$

$$\chi(P) = \sum_{n=0}^{\infty} \chi_n(P) = \chi_0(P) + \sum_{n=1}^{\infty} \chi_n(P) \tag{2-7}$$

$$\chi_0(P) = S(P) \text{ (the source at P)} \tag{2-8}$$

$$\chi_n(\bar{x},\bar{E}) = \int C(\bar{E}|\bar{E}';\bar{x})\ \psi_n(\bar{x},\bar{E}')d\bar{E}' \qquad n = 1,2, \ldots \tag{2-9}$$

$$\psi_{n+1}(\bar{x},\bar{E}) = \int T(\bar{x}|\bar{x}';\bar{E})\ \chi_n(\bar{x}',\bar{E})d\bar{x}' \qquad n = 0,1,2, \ldots \tag{2-10}$$

Note that, in Equations 2-5 and 2-6, the summation begins at n = 1, but in Equation 2-7, it begins at n = 0. The reason for this is that $\Phi_n(P)$ and $\psi_n(P)$ represent the particle immediately before entering a collision,

and since n = 0 denotes the source, $\Phi_0(P)$ or $\psi_0(P)$ are physically meaningless.

The physical significance of the transport kernel can be seen from the fact that $T(\bar{x}|\bar{x}';\bar{E})$ is just $\Sigma_t(\bar{x},E)\exp[\Sigma_t(\bar{x},E)\cdot|\bar{x}-\bar{x}'|]$ if the material property from $\bar{x}'$ to $\bar{x}$ does not change and if the vector from $\bar{x}'$ to $\bar{x}$ is parallel to $\bar{\omega}$, where $\bar{E} = (E,\bar{\omega})$. If the vectors are not parallel, then $T(\bar{x}|\bar{x}';\bar{E})$ is identically zero. Thus the significance of Equation 2-10 is that the collision density at $P = (\bar{x},\bar{E})$ for particles entering their $(n+1)^{th}$ collision is just the integral over all spatial points of the density of particles leaving $\bar{x}'$ with directed energy $\bar{E}$ times the probability that the particle will reach $\bar{x}$ without having a collision. The physical significance of Equation 2-9 is very similar except that the particle entering into the n^{th} collision does not change spatial coordinates, but changes its direction from $\bar{\omega}'$ to $\bar{\omega}$ and its energy from E' to E. Thus $\chi_n(\bar{x},\bar{E})$ is just the integral of the collision density times the collision kernel over all directions and all energies. The exact form of the collision kernel is much more difficult to describe than the transport kernel since it must include all possible types of collision events, such as elastic and inelastic scattering, absorptions, and fissions, whenever applicable.

By substituting Equation 2-9 into Equation 2-10, where $\bar{x}$ is replaced by $\bar{x}'$, then $\chi_n(\bar{x}',\bar{E})$ can be eliminated:

$$\psi_{n+1}(\bar{x},\bar{E}) = \iint T(\bar{x}|\bar{x}';\bar{E})\ C(\bar{E}|\bar{E}';\bar{x}')\ \psi_n(\bar{x}',\bar{E}')d\bar{E}'d\bar{x}' \qquad (2\text{-}11)$$

$$n = 1,2, \ldots$$

For $n = 0$, we use the fact that $\chi_0(P) = S(P)$, so that

$$\psi_1(\bar{x},\bar{E}) = \int T(\bar{x}|\bar{x}';\bar{E})\ S(x,E)d\bar{x}' \ . \tag{2-12}$$

Note that the order in which the collision and transport kernels appear is very important, since the collision density must first be transformed by the collision kernel before the transport kernel can operate on it. Substituting Equation 2-10 into Equation 2-9 for the $(n+1)^{th}$ collision yields:

$$\chi_{n+1}(\bar{x},\bar{E}) = \iint C(\bar{E}|\bar{E}';\bar{x})\ T(\bar{x}|\bar{x}';\bar{E}')\ \chi_n(\bar{x}',\bar{E}')d\bar{x}'d\bar{E}' \tag{2-13}$$

$$n = 0,1,2, \ . \ . \ .$$

In Equation 2-13, the order of the collision and transport kernels is reversed to that of Equation 2-11, as one would expect from physical considerations.

The relationships between $\psi(P)$ and $\chi(P)$ can be derived by summing Equation 2-9 over $n = 1,2, \ . \ . \ .$.

$$\sum_{n=1}^{\infty} \chi_n(\bar{x},\bar{E}) = \sum_{n=1}^{\infty} \int C(\bar{E}|\bar{E}';\bar{x})\ \psi_n(\bar{x},\bar{E}')d\bar{E}' \tag{2-14}$$

or

$$\sum_{n=0}^{\infty} \chi_n(\bar{x},\bar{E}) - \chi_0(\bar{x},\bar{E}) = \int \sum_{n=1}^{\infty} C(\bar{E}|\bar{E}';\bar{x})\ \psi_n(\bar{x},\bar{E})d\bar{E}' \ . \tag{2-15}$$

By Equations 2-6, 2-7, and 2-8, Equation 2-15 can be written

$$\chi(P) = \int C(\bar{E}|\bar{E}';\bar{x})\ \psi(\bar{x},\bar{E})d\bar{E}' + S(P) \tag{2-16}$$

Likewise, by summing Equation 2-10 over n = 0,1,2, . . . :

$$\sum_{n=0}^{\infty} \psi_{n+1}(x,\bar{E}) = \int \sum_{n=0}^{\infty} T(\bar{x}|\bar{x}';\bar{E})\ \chi_n(\bar{x}',\bar{E})d\bar{x}' \tag{2-17}$$

or

$$\psi(\bar{x},\bar{E}) = \int T(\bar{x}|\bar{x}'\bar{E})\ \chi(\bar{x}',\bar{E})d\bar{x}'. \tag{2-18}$$

Substituting Equation 2-18 into Equation 2-16 will clear Equation 2-16 of $\psi(\bar{x},\bar{E}')$ as follows:

$$\chi(\bar{x},\bar{E}) = \iint C(\bar{E}|\bar{E}';\bar{x})\ T(\bar{x}|\bar{x}';\bar{E}')\ \chi(\bar{x}',\bar{E}')d\bar{x}'d\bar{E}' + S(\bar{x},\bar{E}). \tag{2-19}$$

Likewise, $\chi(\bar{x}',\bar{E})$ can be cleared from Equation 2-18 by substituting Equation 2-16:

$$\psi(\bar{x},\bar{E}) = \iint T(\bar{x}|\bar{x}';\bar{E})\ C(\bar{E}|\bar{E}';\bar{x}')\ \psi(\bar{x}',\bar{E}')\ d\bar{E}'d\bar{x}' \tag{2-20}$$

$$+ \int T(\bar{x}|\bar{x}';\bar{E})\ S(\bar{x}',\bar{E})d\bar{x}'.$$

Equation 2-20 can be written in the form:

$$\psi(P) = \int K(P|P')\ \psi(P')dP' + Q(P) \tag{2-21}$$

where

$$K(P|P') = T(\bar{x}|\bar{x}';\bar{E})\ C(\bar{E}|\bar{E}';\bar{x}') \tag{2-22}$$

$$Q(P) = \int T(\bar{x}|\bar{x}';\bar{E})\ S(\bar{x}',\bar{E})d\bar{x}' \tag{2-23}$$

$$dP' = d\bar{E}'d\bar{x}'. \tag{2-24}$$

Equations 2-19 and 2-21 are two forms of the integral transport equation. The equation most often simulated in forward Monte Carlo calculations is Equation 2-19. However, due to the fact that most people have a better understanding of the collision density equation (2-21), this equation will be used in the next section to introduce the concept of the adjoint to an integral equation, to define the term, adjoint, both mathematically and in a physical sense, and to illustrate how the adjoint equation solution can be used to improve the forward Monte Carlo estimate of an effect of interest.

2.3 Monte Carlo Transport Games

Suppose one wants to evaluate an effect of interest defined by:

$$\langle F \rangle = \int \psi(P)\ f(P)dP, \tag{2-25}$$

where $\psi(P)$ is the collision density defined in Equation 2-21 and $f(P)$ is a collision density response or payoff function (see Section 2.4.2 for a discussion of the form of the response functions). Since the calculation of the collision density by analytical techniques is impossible except for very simple problems, one must employ a numerical technique to evalu-

ate or estimate the effect of interest. The Monte Carlo solution of Equation 2-25, which consists of estimating the expected value of Equation 2-25 by a series of random walks based on Equation 2-21 is one possible technique. This procedure, described in detail in Section 3.2, consists of picking "particles" from the first collision source term, Q(P), (i.e., selecting the spatial, energy, and directional parameters of the particle) and then determining the subsequent history of the particle from the kernel, $K(P|P')$. Certain restrictions are imposed due to the statistical nature of this procedure, for example, the first collision source must be a properly normalized probability function, either discrete or continuous. Also, Q(P) and $K(P|P')$ must be nonnegative. Thus, a source normalization factor is required for Q(P). Equation 2-23 indicates that the normalization factor is not the magnitude of the natural source, S(P), for a finite system. The distribution of the particle collisions (and any daughter particles) so transported is proportional to the magnitude of the collision density. Thus, the values of the response function, f(P), at each collision are unbiased estimators of Equation 2-25. An estimate, $\bar{F}$, of $\langle F \rangle$ can be calculated for a finite number of particle histories, as shown below:

$$\bar{F} = \frac{1}{N} \sum_{j=1}^{N} \sum_{n=1}^{C_j} f(P_n^j) \quad , \tag{2-26}$$

where N is the number of histories generated and C_j is the number of collisions which the j^{th} particle and its daughters experience. It has been assumed that each history terminates in a finite number of collisions

(i.e., the process is subcritical and C_j is finite).

It is also possible to generate an unbiased estimator of <F> by choosing from a different or altered source and kernel (say $\tilde{Q}$ and $\tilde{K}$), if the contribution from the response function at each collision is weighted by the product of the ratios of the true to altered source and kernel distribution. This weighting factor after m collision, w_m, which multiplies the response value, can be written as:

$$w_m = \frac{Q(P_1)}{\tilde{Q}(P_1)} \prod_{n=2}^{m} \frac{K(P_n|P_{n-1})}{\tilde{K}(P_n|P_{n-1})} \tag{2-27}$$

$$= W_0(P_1) \prod_{n=2}^{m} W_1(P_n|P_{n-1})$$

Equation 2-27 defines the weighting functions which are used in Figure 2 to illustrate an altered transport game. In order to define the game properly the following requirements on our altered source distribution and kernel are imposed:

$$\left.\begin{aligned} &\tilde{Q}(P) \geq 0 \\ &\int \tilde{Q}(P)\,dP = 1 \end{aligned}\right\} \tag{2-28}$$

and

$$\left.\begin{aligned} &\tilde{K}(P|P') > 0 \\ &\int \tilde{K}(P|P')\,dP \equiv p_1(P') \leq 1 \end{aligned}\right\} \tag{2-29}$$

Equations 2-28 assure that the source term is a properly normalized probability function. Equations 2-29 restrict the transport problem to

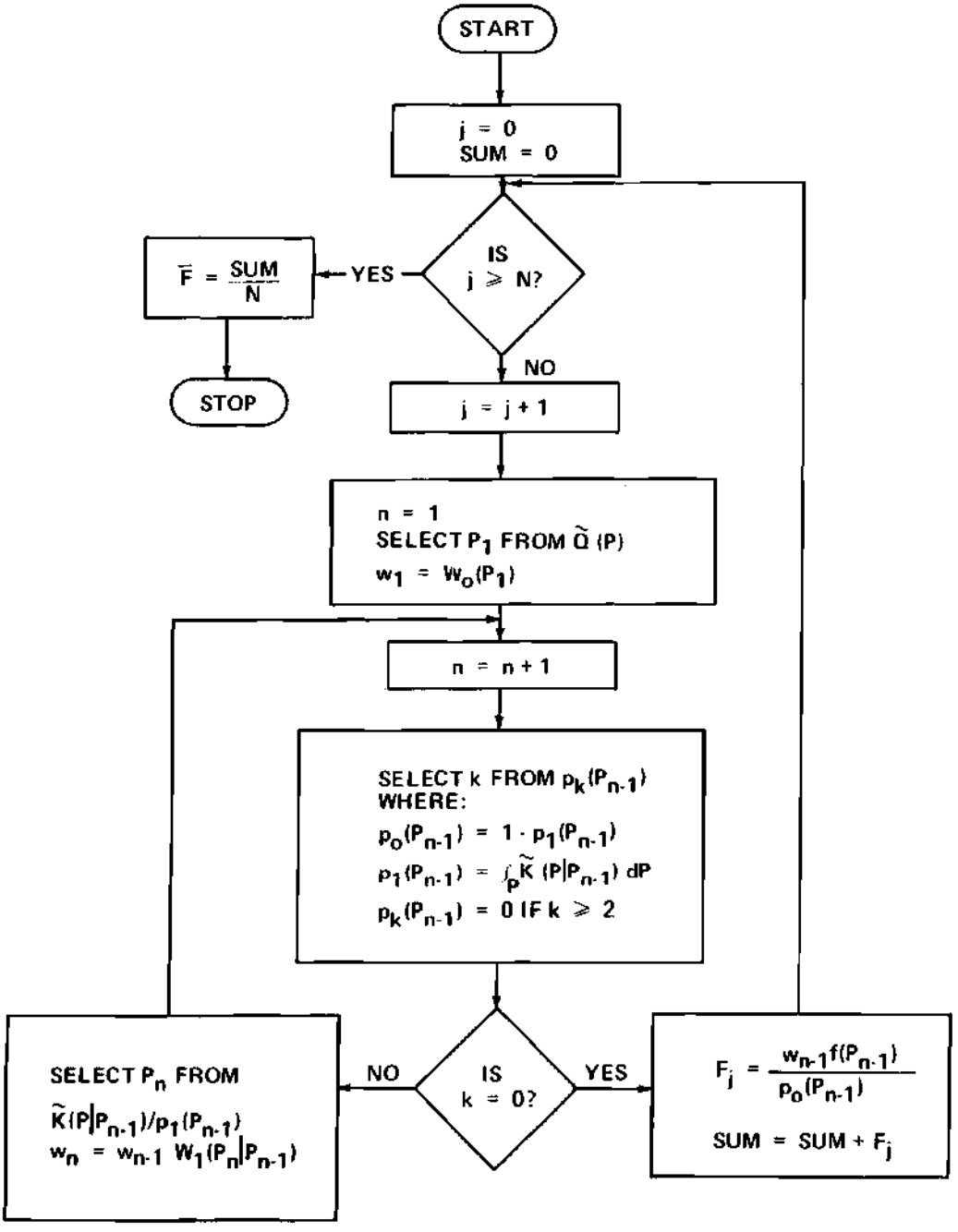

Figure 2. An Altered Transport Game

one in non-multiplying media, thus assuring the convergence of the transport in a finite number of steps if there exists any medium which has a positive absorption probability. This probability, $p_0(P')$, of entering a trapped state at P' is just:

$$p_0(P') = 1 - p_1(P'), \tag{2-30}$$

which is the absorption probability, and it is assumed that each random walk enters a trapped state.

As a further modification to the transport game, instead of evaluating the response function, $f(P')$, at each collision event, score only when P' is a trapped state for the particle. Such a change in the scoring technique requires a change in the response function without changing the expected value. This can be done easily by considering the density of trapped states or absorption event density, which will be denoted by ψ_a. The absorption event density is related to the collision density by:

$$\psi_a(P) = p_0(P)\ \psi(P)\ , \tag{2-31}$$

where $p_0(P)$ is the absorption probability. Thus, the effect of interest in Equation 2-25 could also have been calculated with the integrand, $\psi_a(P)\ f(P)/p_0(P)$, and so the response function defined by $f(P)/p_0(P)$ is also an unbiased estimator of $\langle F \rangle$ when only those collisions resulting in an absorption contribute to the estimate of $\bar{F}$. Combining this new response function with our altered source and kernel produces:

$$\bar{F} = \frac{1}{N} \sum_{j=1}^{N} w_a \, f(P_a^j)/p_0(P_a^j), \tag{2-32}$$

where w_a is the weighting function value calculated at the absorption event, which occurred at P_a^j for the j^{th} particle. The flow diagram of this altered game is depicted in Figure 2. All terms are defined in the convention used above, except the particle superscript, j, has been dropped for clarity purposes. Now consider methods of reducing the variance of the estimate of <F> by utilizing the adjoint equation.

2.3.1 The Adjoint Equation

Although the transport game discussed above was based on altered probability distribution functions, no mention was made of the way in which these distribution functions are chosen (note that $\tilde{K}(P|P')/p_1(P')$ is the distribution function, not $\tilde{K}(P/P')$). Obviously, one wants to alter the distribution functions in such a manner that scores (F) yield a better value of $\bar{F}$ and to do this with smaller sample size (i.e., smaller N). Therefore, one seeks to choose "particles" from Q and points in phase space that lead to higher expected contributions to F. This means that one needs to have some sort of importance function, say I(P), which is at least approximately proportional to the expected value of F from a particle at P. Then with I(P) we can define appropriate values of $\tilde{Q}(P)$, $p_0(P)$, and $\tilde{K}(P|P')$, so that the variance of our calculation is minimized, where the variance is defined as

$$V = \frac{1}{N-1} (\overline{F^2} - \bar{F}^2). \tag{2-33}$$

To motivate our selection of the above values, consider the following discussion of the equation which is adjoint to Equation 2-21. Since $K(P|P')$ is the product of two real kernels, $T(\bar{x}|\bar{x}';\bar{E})$ and $C(\bar{E}|\bar{E}';\bar{x}')$, then $K(P|P')$ is also a real kernel and its adjoint is just $K^*(P|P') = K(P'|P)$.

Therefore, any equation of the form

$$J(P) = \int K(P'|P)\ J(P')dP' + f(P), \tag{2-34}$$

assuming that $J(P)$ and $f(P)$ are quadratically integrable, is an adjoint of Equation 2-21. Defining the operators:

$$K\psi(P) = \int K(P|P')\ \psi(P')dP' \tag{2-35}$$

and

$$K^*J(P) = \int K(P'|P)\ J(P)dP' \tag{2-36}$$

the following relationship is known to be true {38}:

$$\int J(P)\ K\psi(P)dP = \int \psi(P)\ K^*J(P)dP\ . \tag{2-37}$$

The proof is straightforward, requiring only a reversal of the variable of integration and rearranging of terms inside the integrals. Multiplying Equation 2-21 by $J(P)$ and integrating over P and then multiplying Equation 2-34 by $\psi(P)$ and integrating over P, produces another identity:

$$\int \psi(P)\ f(P)dP = \int J(P)\ Q(P)dP\ . \tag{2-38}$$

But from Equation 2-25 it is obvious that:

$$\langle F \rangle = \int J(P)\, Q(P) dP. \tag{2-39}$$

Thus, another method for determining <F> is to perform a transport game by Monte Carlo methods on the adjoint integral Equation (2-34) and estimate the average value of <F> by:

$$\langle F \rangle \approx \frac{1}{N} \sum_{j=1}^{N} \sum_{n=1}^{C_j} Q(P_n^j). \tag{2-40}$$

This method is analogous to the one described earlier in which Equations 2-21 and 2-26 were used.

One other mathematical characteristic of the operator, K, and its adjoint, K^*, is that since:

$$K\psi(P) = \int T(\bar{x}|\bar{x}';\bar{E}) \int C(\bar{E}|\bar{E}';\bar{x}')\, \psi(\bar{x}',\bar{E}') d\bar{E}' d\bar{x}', \tag{2-41}$$

then

$$K^* J(P) = \int C(\bar{E}'|\bar{E};\bar{x}) \int T(\bar{x}'|\bar{x};\bar{E}')\, J(\bar{x}',\bar{E}') d\bar{x}' d\bar{E}'. \tag{2-42}$$

This is due to the fact that the adjoint of the product of two operators is just the project of the adjoint to the operators taken in reverse order. This relationship will be used in Section 2.4.

Now consider the following physical identifications to those terms which are in Equations 2-25 through 2-39 and were not previously identified. In Equation 2-25, the function f(P) shall be a response or detector function which produces some contribution to the effect of interest

due to a particle that has a collision at P in phase space. The effect of interest, <F>, is a physical quantity such as dose, heating rate, or fission per kilogram in uranium-235. The distribution, Q(P), is just the so-called "first collision source," or the distribution point at which particles leaving the real sources, defined by $S(\bar{x},\bar{E})$, experience their initial collision (see Equation 2-23). By choosing to use the response function, f(P), in the adjoint equation (2-34), it was possible to construct a new method of solving for the effect of interest. Mathematically, any suitable (i.e., quadratically integrable) function could have been used instead of f(P) in Equation 2-34, but f(P) was chosen because any other choice would not produce a second method of estimating <F>.

The physical interpretation of our adjoint equation, as given by Goertzel and Kalos {4}, is that J(P) is precisely the expected score of a particle at P. Thus the right hand side of Equation 2-34 consists of:

$f(P) \equiv$ the direct score at P of J(P),

$\int K(P'|P)\, J(P')\, dP' \equiv$ the score after one or more collisions.

Thus, the function, J(P), represents the importance of particles at P in determining <F>. J(P) is commonly called the adjoint function, and this term will be used in this paper. The terminology is somewhat ambiguous due to the fact that choosing another suitable function other than f(P) for Equation 2-34 would have produced a different J(P), and certain authors have objected to this terminology {3}. However, knowledgeable workers in the area of radiation transport understand the context where

the term adjoint is used in conjunction with J(P) and in reference to Equation 2-34.

2.3.2 The Perfect Game

Since the adjoint function represents the importance of a particle, and since a Monte Carlo calculation can be improved by sampling from the important parts of the distribution function (i.e., relative to some effect of interest), the question of how the adjoint function can be used to enhance our Monte Carlo transport game naturally occurs. To elucidate that question, consider the following choices for the parameters in our altered transport game:

$$p_0(P) \equiv \frac{f(P)}{\int K(P'|P)\, J(P')dP' + f(P)} = \frac{f(P)}{J(P)} \tag{2-43}$$

$$p_1(P) = \frac{\int K(P'|P)\, J(P')dP'}{\int K(P'|P)\, J(P')dP + f(P)} \tag{2-44}$$

$$= \frac{\int K(P'|P)\, J(P')dP'}{J(P)}$$

$$\tilde{Q}(P) \equiv \frac{Q(P)\, J(P)}{\int Q(P')\, J(P')dP'} = \frac{Q(P)\, J(P)}{\langle F \rangle} \tag{2-45}$$

$$\tilde{K}(P|P') = \frac{K(P|P')\, J(P)}{\int K(P''|P')\, J(P'')dP'' + f(P')} \tag{2-46}$$

$$= \frac{K(P|P')\, J(P)}{J(P')}$$

Applying these terms to the transport game illustrated in Figure 2, the following parameters can be calculated from the equation whose number is given on the left hand side:

(2-45) $$W_0(P) = \frac{Q(P)}{Q(P')} = \frac{\langle F \rangle}{J(P)} \,, \qquad (2\text{-}47)$$

(2-46) $$W_1(P|P') = \frac{K(P|P')}{\tilde{K}(P|P')} = \frac{J(P')}{J(P)} \,. \qquad (2\text{-}48)$$

As shown in Figure 2, the weight of the transported particle is given by

$$w_n = w_{n-1}\, W_1(P_n|P_{n-1}) \,. \qquad (2\text{-}49)$$

Substituting Equation 2-48 into Equation 2-49 yields

$$w_n = w_{n-1}\, \frac{J(P_{n-1})}{J(P_n)} \,, \qquad (2\text{-}50)$$

or

$$w_n J(P_n) = w_{n-1} J(P_{n-1}) \,.$$

Then it follows that

$$w_n J(P_n) = w_1 J(P_1) \,. \qquad (2\text{-}51)$$

From Figure 2, w_1 is given by

$$w_1 = W_0(P_1) \qquad (2\text{-}52)$$

Substituting Equations 2-47 and 2-52 into Equation 2-51 yields

$$w_n J(P_n) = W_0(P_1)\ J(P_1) = \langle F \rangle \ . \tag{2-53}$$

Now returning to the transport game, if the particle entered a trapped state of the $(n+1)^{th}$ collision, then the score, F, would be

$$F = w_n f(P_n)/p_0(P_n) \ . \tag{2-54}$$

But from Equation 2-43, J(P) can be represented by

$$J(P) = \frac{f(P)}{p_0(P)} \ . \tag{2-55}$$

Hence, substituting Equation 2-55 into Equation 2-54 yields

$$F = w_n J(P_n) \ . \tag{2-56}$$

But from Equation 2-53, $w_n J(P_n) = \langle F \rangle$, hence

$$F = \langle F \rangle \ . \tag{2-57}$$

In other words, the exact answer can be obtained from the result of the transport game with only one particle. All that is required is that the particle be transported until it reaches a trapped state. The variance then is obviously zero, and thus, the game played was a perfect game.

However, consider the assumption made to get the values of $p_0(P)$, p, (P), Q(P), and $\tilde{K}(P|P')$, that is, that J(P) is known. Then it is obvious that <F> can be found by integrating Equation 2-25 by either analytical or numerical technique (i.e., Monte Carlo is no longer needed). Obviously, if one desires to solve for <F> by forward Monte Carlo, then J(P) will probably not be known. One possibility is to replace J(P) by some approximate importance function, I(P). Then the altered probability distribution functions can be found by

$$p_0(P) = \frac{f(P)}{\int K(P'|P)\, I(P')dP' + f(P)} \tag{2-58}$$

$$p_1(P) = 1 - p_0(P) \tag{2-59}$$

$$\tilde{Q}(P) = \frac{I(P)\, Q(P)}{\int I(P')\, Q(P')dP'} \tag{2-60}$$

$$\tilde{K}(P|P') = \frac{K(P|P')\, I(P)}{I(P')} \,. \tag{2-61}$$

Another possibility to compute the altered probability distribution functions is to solve for J(P) and $\psi(P)$ iteratively, using the values of one to define better distribution functions for the other, since if $\psi(P)$ were known exactly, a perfect game could also be constructed for the adjoint Monte Carlo solution. This procedure is called the iterative forward-adjoint Monte Carlo method, and the theoretical validity of this method has been demonstrated above.

2.3.3 Importance and Bias Sampling

In the previous subsection, the concept of an importance function was introduced, including the use of that importance function to alter a physically derived distribution function with the new distribution being sampled to construct the history of our particles. Altering the distribution functions, that is, the kernel, $K(P|P')$, and the first collided source, $Q(P)$, lead to much greater efficiency of our calculation for the given transport game. This process, known as importance sampling, was discussed using the familiar quantity, $\psi(P)$, the collision density. For the remainder of this discussion of importance sampling, the emergent particle density, $\chi(P)$, will be the quantity of interest. Although this quantity is used less frequently in nuclear engineering, it is much easier to work with in Monte Carlo. Thus, the integral emergent particle density equation, as given by Equation 2-19, can be written:

$$\chi(P) = S(P) + \int CT(P|P')\ \chi(P')dP' \ , \tag{2-62}$$

where

$$CT(P|P') = C(\bar{E}|\bar{E}';\bar{x})\ T(\bar{x}|\bar{x}';\bar{E}') \ . \tag{2-63}$$

Note that the new kernel, $CT(P|P')$ is not the same as the kernel, $K(P|P')$, defined by Equation 2-22. $CT(P|P')$ requires that the transport kernel be applied before the collision kernel, a process which is reversed in $K(P|P')$. A given effect of interest (λ), such as energy deposition, biological dose, or particle flux, can be calculated by:

$$\lambda = \int g(P)\ \chi(P)dP, \tag{2-64}$$

where g(P) is the response or payoff function for particles emerging from a collision at P in phase space.

Now consider an arbitrary, but positive, function, I(P), which shall be called an importance function. Multiplying Equation 2-62 by I(P)/N, where N is the normalization factor of the altered source, given by $\int I(P)\, S(P)\, d(P)$, yields:

$$\tilde{\chi}(P) = \tilde{S}(P) + \int \tilde{\tilde{CT}}(P|P')\, \tilde{\chi}(P')dP' \ , \tag{2-65}$$

where:

$$\tilde{\chi}(P) = \chi(P)\, I(P)/N \ , \tag{2-66}$$

$$\tilde{S}(P) = S(P)\, I(P)/N \ , \tag{2-67}$$

$$\tilde{\tilde{CT}}(P|P') = CT(P|P')\, I(P)/I(P') \ . \tag{2-68}$$

Hence, λ can be evaluated by:

$$\lambda = \int \tilde{g}(P)\, \tilde{\chi}(P)dP \ , \tag{2-69}$$

with

$$\tilde{g}(P) = N \cdot g(P)/I(P) \ . \tag{2-70}$$

It does not appear that any more improvement has been made by calculating λ by Equation 2-69 than by Equation 2-64, since only a change in notation has occurred. But in the previous section, the use of the adjoint as the importance function resulted in a game with zero variance for one history. Therefore, it seems reasonable that a choice of I(P)

that approximates J(P) should lead to reduced variance. Many studies support this conclusion {3,4,25,29,30,31,33}.

An alternate technique which is similar but is based more on physical intuition is that of bias sampling. In bias sampling, an altered distribution, such as the source distribution, S'(P), or the kernel CT'(P|P') is used on the basis of an understanding of the physics of the problem and how it relates to the mathematical procedure. In the Monte Carlo game, a source particle is selected from S'(P) and then weighted by the ratio of S(P) to S'(P). Transport and collision parameters are based on the altered kernel CT'(P|P'). Letting $\chi'(P)$ be the weight density of particles emerging from collisions and sources at P, then,

$$\chi'(P) = S'(P)\, W_0(P) + \int CT'(P|P')\, W(P|P')\, \chi'(P')dP' \qquad (2\text{-}71)$$

where

$$W_0(P) = S(P)/S'(P) \ , \qquad (2\text{-}72)$$

and

$$W(P|P') = CT(P|P')/CT'(P|P') \ . \qquad (2\text{-}73)$$

Substitution of Equations 2-72 and 2-73 into 2-71 yields:

$$\chi'(P) = S(P) + \int CT(P|P')\, \chi'(P')dP' \ , \qquad (2\text{-}74)$$

which proves that $\chi(P)$ and $\chi'(P)$ are identical, hence a solution of Equation 2-71 is also a solution of 2-62. The only restrictions on our altered distributions are that all mathematical expressions must be defined over the entire phase space, with the indeterminate, 0/0, defined as 0.

The techniques which have been developed in this research employ aspects of both importance and bias sampling. This is done by using the importance function to alter the source energy and angular distribution functions, the transport kernel, and the collision kernel, then correcting the weight of the particles at each step as in bias sampling. For the forward Monte Carlo calculation, this importance function is based on both the adjoint function and input biasing parameters which allows the use of the researcher's physical intuition to enhance the variance reduction schemes. The equivalent technique is available for the adjoint mode calculation. Thus, the advantages of both importance and biasing are included in the techniques developed. These techniques are discussed in detail in Chapters III through V.

2.4 Multigroup Integral Transport Equations

The computer code from which the test bed for determining the validity of the iterative forward-adjoints variance reduction techniques was derived is MORSE [13-15]. MORSE is a multigroup Monte Carlo transport code, which means that multigroup cross sections are used. Because of the strong interaction which occurs between the forward and adjoint calculations in the variance reduction techniques, an understanding of the multigroup integral equations which are being solved by Monte Carlo is essential. In this section, these equations are discussed in considerable detail. The beginning point for this discussion will be Equation 2-2, the Boltzmann transport equation. The primary emphasis will be placed on those areas where this research has deviated from the efforts of other researchers such as Irving[37], Straker, et al. [13], and Solomito [39],

and how the quantities used in the importance function are derived. For a complete derivation of these equations, Appendix A of Reference 13 should be consulted, although certain exceptions will be noted in this section and Appendix D to that work.

The time dependence of radiation transport is handled in a very straightforward way in Monte Carlo calculations. Each particle is given an initial age at the source and the age at some subsequent time is calculated by a knowledge of the particle's speed and distance traveled. Therefore, consider the time-independent integro-differential form of the Boltzmann transport equation:

$$\bar{\omega}\cdot\nabla\Phi(\bar{x},E,\bar{\omega}) + \Sigma_t(\bar{x},E)\ \Phi(\bar{x},E,\bar{\omega}) = S(\bar{x},E,\bar{\omega}) \qquad (2\text{-}75)$$

$$+ \int\int \Sigma_s(\bar{x},E')\ \Phi(\bar{x},E',\bar{\omega}')\ f(E,\bar{\omega}|E',\bar{\omega}')dE'd\bar{\omega}'$$

where all terms are the same as defined in Section 2.1, except for the assumption of steady state conditions. The multigroup form of Equation 2-75 is obtained by integrating over pre-selected energy intervals, ΔE_g, where:

$$\Delta E_g = E_g - E_{g+1},$$

the energy width of the g^{th} group with the highest energy group being defined as group 1. Obviously, the sum over all groups, say from 1 to N, must be identical to the energy from 0 to E_1. The resulting equation is:

$$\bar{\omega}\cdot\nabla\Phi_g(\bar{x},\bar{\omega}) + \Sigma_t^g(\bar{x})\ \Phi_g(\bar{x},\bar{\omega}) = S_g(\bar{x},\bar{\omega}) \tag{2-76}$$

$$+\sum_{g'}\ \int \Sigma_s^{g'}(\bar{x})\ \Phi_{g'}(\bar{x},\bar{\omega}')\ f^{g\leftarrow g'}(\bar{\omega}|\bar{\omega}')d\bar{\omega}'\ ,$$

where

$$\Phi_g(\bar{x},\bar{\omega}) \equiv \int_{E_{g+1}}^{E_g} \Phi(\bar{x},E,\bar{\omega})dE, \tag{2-77}$$

≡ the multigroup (or group) angular flux for group g;

$$S_g(\bar{x},\bar{\omega}) \equiv \int_{E_{g+1}}^{E_g} S(\bar{x},E,\bar{\omega})dE\ , \tag{2-78}$$

≡ the group source for group g;

$$\Sigma_t^g(x) \equiv \frac{\int_{E_{g+1}}^{E_g} \Sigma_t(\bar{x},E,\bar{\omega})\ \Phi(\bar{x},E,\bar{\omega})dE}{\Phi_g(\bar{x},\bar{\omega})}\ , \tag{2-79}$$

≡ energy-averaged total cross section for group g;

($\Sigma_s^g(\bar{x})$ is defined similarly),

and

$$f^{g\leftarrow g'}(\bar{\omega}|\bar{\omega}') \equiv \frac{\int_{E_{g'+1}}^{E_{g'}} \int_{E_{g+1}}^{E_g} f(E,\bar{\omega}|E',\bar{\omega}')\ \Phi(\bar{x},E,\bar{\omega})dEdE'}{\int_{E_{g'+1}}^{E_{g'}} \Phi(\bar{x},E,\bar{\omega})dE'}\ , \tag{2-80}$$

≡ group g' to group g transfer probability.

In Equation 2-76, the summation over g' allows both upscattering into higher energy groups and downscattering in lower energy groups, although only downscattering is important for the problems being considered.

The right hand side of Equation 2-76 is just the expected number of particles leaving source or collision events (per unit volume solid angle and time) about $\bar{x}$ and $\bar{\omega}$ whose energies lie in energy group g. This is the definition of the group emergent particle density, $\chi_g(\bar{x},\bar{\omega})$, which yields the following identity:

$$\chi_g(\bar{x},\bar{\omega}) = S_g(\bar{x},\bar{\omega}) + \sum_{g'} \int \Sigma_s^{g'}(\bar{x})\ \Phi_{g'}(\bar{x},\bar{\omega}')\ f^{g\leftarrow g'}(\bar{\omega}|\bar{\omega}')d\bar{\omega}' \ . \qquad (2\text{-}81)$$

2.4.1 Forward Multigroup Integral Equations

Transformation of Equation 2-76 into integral form is accomplished by expressing the leakage term in terms of a spatial variable, R (as illustrated in Figure 3):

$$\bar{x}' = \bar{x} - R\bar{\omega} \qquad (2\text{-}82)$$

where $\bar{x}$ is a fixed point in space and $\bar{x}'$ is arbitrary. Taking the total derivative of $\Phi_g(\bar{x},\bar{\omega})$ with respect to R yields:

$$\frac{d}{dR}\Phi_g(x,\omega) = \frac{d\Phi_g}{dx}\frac{dx}{dR} + \frac{d\Phi_g}{dy}\frac{dy}{dR} + \frac{d\Phi_g}{dz}\frac{dz}{dR}$$

$$= -\cos\alpha\ \frac{d\Phi_g}{dx} - \cos\beta\ \frac{d\Phi_g}{dy} - \cos\gamma\ \frac{d\Phi_g}{dz} \ ,$$

where α, β, amd γ are the angles between dR (which is along $\bar{\omega}$) and the x, y, and z axes, respectively. Thus:

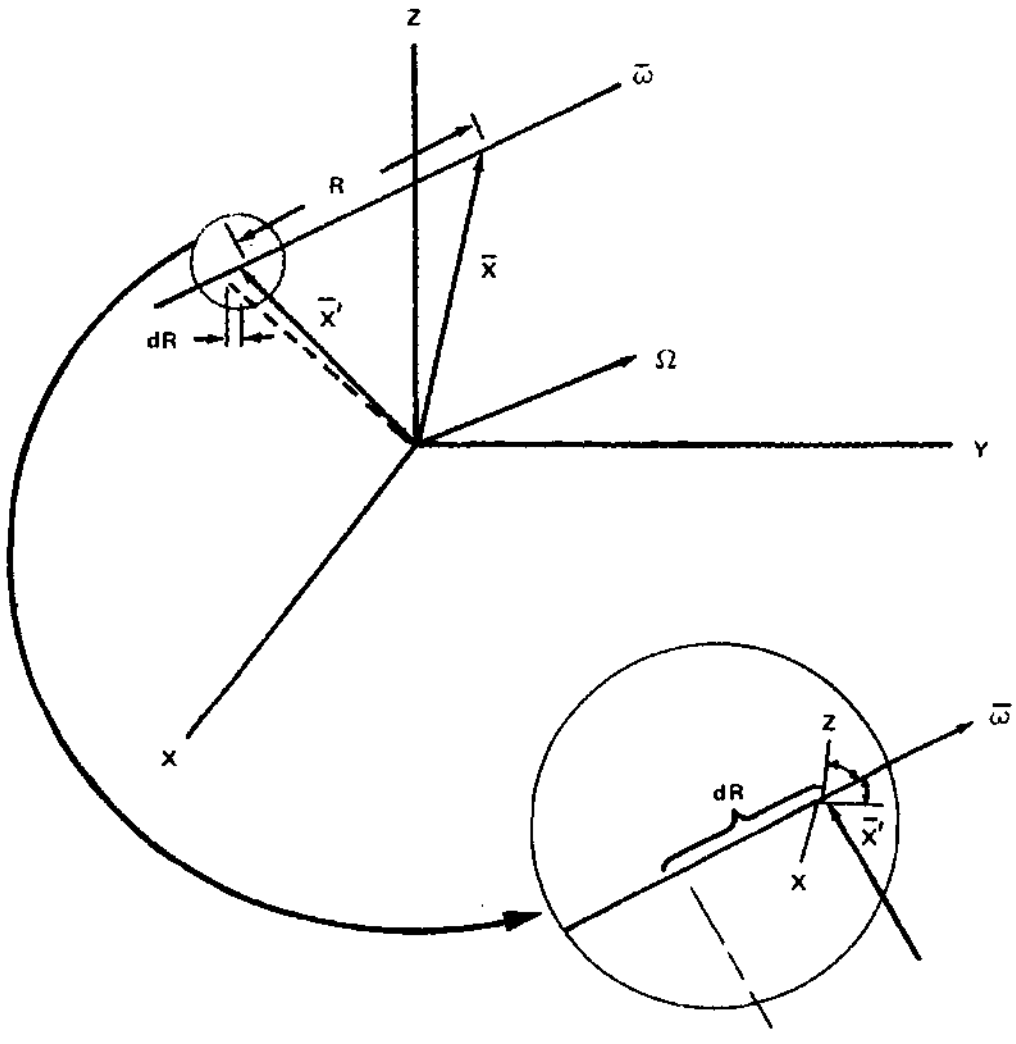

Figure 3. Geometry for Leakage Term

$$\frac{d}{dR}\,\Phi_g(\bar{x},\bar{\omega}) = -\,\bar{\omega}\cdot\nabla\Phi_g(\bar{x},\bar{\omega})\ . \tag{2-83}$$

Substituting the above equation and (2-81) into Equation 2-76 for the point, $\bar{x}'$, yields:

$$-\frac{d}{dR}\,\Phi_g(\bar{x}',\bar{\omega}) + \Sigma_t^g(\bar{x}')\ \Phi_g(\bar{x}',\bar{\omega}) = \chi_g(\bar{x}',\bar{\omega})\ . \tag{2-84}$$

Introducing the integrating factor, $\exp\left[-\int_0^R \Sigma_t^g(\bar{x}-R'\bar{\omega})dR'\right]$, into (2-84), then multiplying by dR and integrating from R=0 to R=∞ results in:

$$\Phi_g(\bar{x},\bar{\omega}) = \int_0^\infty \exp\left[-\int_0^R \Sigma_t^g(\bar{x}-R'\bar{\omega})dR'\right]\chi_g(\bar{x}-R\bar{\omega},\bar{\omega})dR\ , \tag{2-85}$$

or

$$\Phi_g(\bar{x},\bar{\omega}) = \int_0^\infty \exp\left[-\int_0^R \Sigma_t^g(\bar{x}-R'\bar{\omega})dR'\right]\Big\{S_g(\bar{x}-R\bar{\omega},\bar{\omega}) \tag{2-86}$$

$$+\sum_{g'}\int \Sigma_s^{g'}(\bar{x}-R\bar{\omega})\ \Phi_{g'}(\bar{x}-R\bar{\omega},\bar{\omega}')\ f^{g\leftarrow g'}(\bar{\omega}|\bar{\omega}')d\bar{\omega}'\Big\}\,dR.$$

Equation 2-86 is called the multigroup integral flux equation or the integral flux density equation. Equation 2-85, and hence 2-86, can be generalized by performing our integration over all spatial points, $\bar{x}'$, by using the properties of the Dirac delta function {40} and the differential volume element $d\bar{x}'$ about the point $\bar{x}'$:

$$d\bar{x}' \equiv R^2\sin\theta' d\theta'\,d\phi'\,dR = R^2\,d\bar{\omega}'dR\ , \tag{2-87}$$

where $R = |\bar{x} - \bar{x}'|$,

thus:

$$\Phi_g(\bar{x},\bar{\omega}) = \int \exp\left[- \int_{\bar{x}'}^{\bar{x}} \Sigma_t^g(\bar{x}'')ds \right] \chi_g(\bar{x}',\bar{\omega}') \frac{\delta(\bar{\omega}\cdot\bar{\omega}'-1)}{R^2} d\bar{x}' , \qquad (2\text{-}88)$$

where the angular direction vector from any arbitrary $\bar{x}'$ to the fixed point $\bar{x}$ is defined as $\bar{\omega}'$ (note the change in definition) and the integral from $\bar{x}'$ to $\bar{x}'$ is along the straight line path, s, which contains the spatial points, $\bar{x}''$. This integral will also be represented by $\int_0^R \Sigma_t^g(\bar{x}-R'\bar{\omega}')dR'$.

From Equations 2-88 and 2-81, a multigroup integral emergent particle density equation can be constructed in a form analogous to Equation 2-19:

$$\chi_g(\bar{x},\bar{\omega}) = S_g(\bar{x},\bar{\omega}) + \sum_{g'} \iint \frac{\Sigma_s^{g'}(\bar{x})}{\Sigma_t^{g'}(\bar{x})} f^{g\leftarrow g'}(\bar{\omega}|\bar{\omega}') \frac{\delta(\bar{\omega}'\cdot\bar{\omega}''-1)}{R^2} \qquad (2\text{-}89)$$

$$\times \Sigma_t^{g'}(\bar{x}) \exp\left[- \int_0^R \Sigma_t^{g'}(\bar{x}-R'\bar{\omega}')dR' \right] \chi_{g'}(\bar{x}',\bar{\omega}')d\bar{x}'d\bar{\omega}'$$

where $d\bar{x}'$ is defined as $R^2 d\bar{\omega}''dR$ (see Figure 4). The group dependent kernels are just:

$$C^{g\leftarrow g'}(\bar{\omega}|\bar{\omega}';\bar{x}) = \frac{\Sigma_s^g(\bar{x})}{\Sigma_t^g(\bar{x})} f^{g\leftarrow g'}(\bar{\omega}|\bar{\omega}') , \qquad (2\text{-}90)$$

and

$$T^g(\bar{x}|\bar{x}';\bar{\omega}') = \frac{\delta(\bar{\omega}'\cdot\bar{\omega}''-1)}{R^2} \Sigma_t^g(\bar{x}) \exp\left[- \int_0^R \Sigma_t^g(\bar{x}-R'\bar{\omega}')dR' \right] \qquad (2\text{-}91)$$

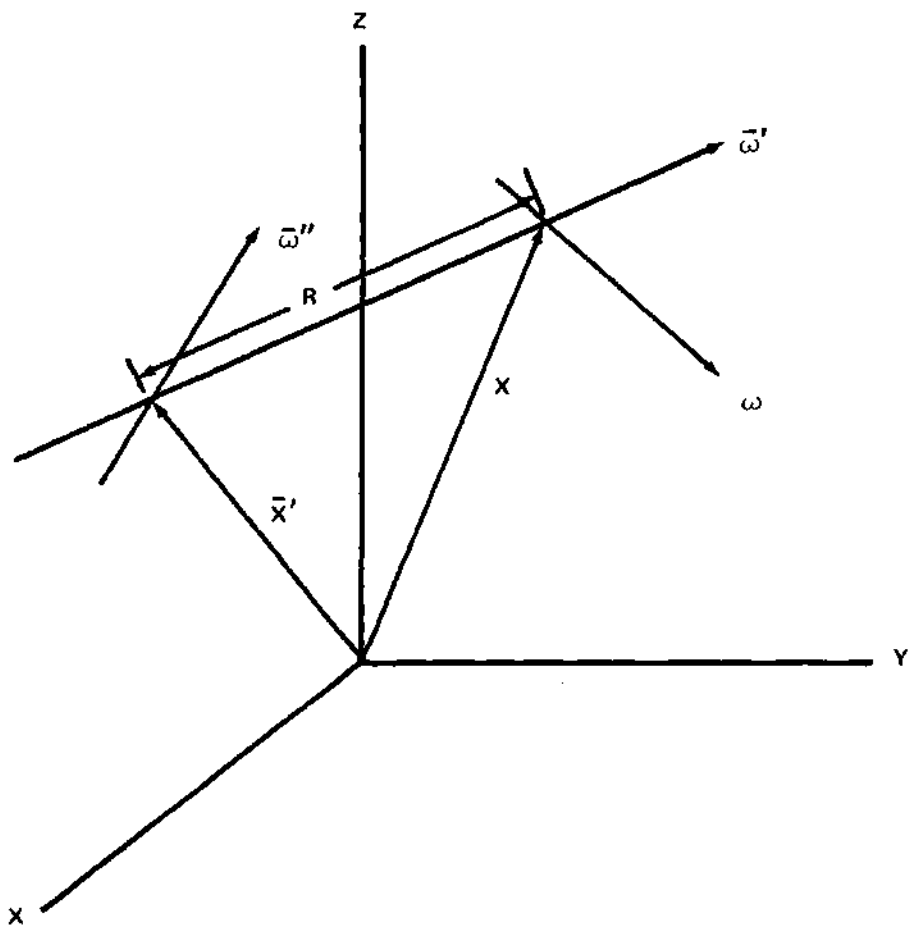

Figure 4. Integral Transport Equation Geometry

However, because of the difficulty in maintaining a consistent notation set due to the change of variables of integration for different integral equations (such as the flux density and the emergent particle density equation) subsequent equations will not use the kernel notation unless that meaning is completely unambiguous. Thus, Equation 2-89 will be written:

$$\chi_g(\bar{x},\bar{\omega}) = S_g(\bar{x},\bar{\omega}) + \sum_{g'} \int \frac{\Sigma_s^{g\leftarrow g'}(\bar{x};\bar{\omega}|\bar{\omega}')}{\Sigma_t^{g'}(\bar{x})} \tag{2-92}$$

$$\times \int_0^\infty \Sigma_t^{g'}(\bar{x}) \exp\left[-\int_0^R \Sigma_t^{g'}(\bar{x}-R'\bar{\omega}')dR'\right] \chi_{g'}(\bar{x}-R\bar{\omega}',\bar{\omega}')d\bar{\omega}'dR \ ,$$

with the scattering cross section denoted by the term, $\Sigma_s^{g\leftarrow g'}(\bar{x};\bar{\omega}|\bar{\omega}')$.

It is also possible to write the multigroup collision density equation, as shown below. Defining the multigroup collision density by:

$$\psi_g(\bar{x},\bar{\omega}') = \Sigma_t^g(\bar{x})\ \Phi_g(\bar{x},\bar{\omega}') \ , \tag{2-93}$$

then from Equation 2-85, and using Figure 4,

$$\psi_g(\bar{x},\bar{\omega}') = \int_0^\infty \Sigma_t^g(\bar{x}) \exp\left[-\int_0^R \Sigma_t^g(\bar{x}-R'\bar{\omega}')dR'\right] S_g(\bar{x}-R\bar{\omega}')dR \tag{2-94}$$

$$+ \int_0^\infty \Sigma_t^g(\bar{x}) \exp\left[-\int_0^R \Sigma_t^g(\bar{x}-R'\bar{\omega}')dR'\right]$$

(continued)

$$\times \sum_{g'} \int \frac{\Sigma_s^{g\leftarrow g'}(\bar{x};\bar{\omega}'|\bar{\omega}'')}{\Sigma_t^{g'}(\bar{x}')} \psi_{g'}(\bar{x}',\bar{\omega}'')d\bar{\omega}''dR \ .$$

The first term on the right hand side is the first collision source in the g^{th} energy group and the second term is the group form of the $K(P|P')$ kernel, where P is defined as $(\bar{x},\bar{E}')$ and P' is $(\bar{x}',\bar{E}'')$. The similarity to Equation 2-20 is obvious. The use of the double prime on the angular variable is necessary to maintain the geometry notation shown in Figure 4. However, should the vector entering a collision at $\bar{x}$ from $\bar{x}'$ be redefined as $\bar{\omega}$, then $\bar{\omega}''$ can be redefined as $\bar{\omega}'$, and the resulting equation is then in a more standard form.

2.4.2 The Effect of Interest

In Section 2.3, the solution of Equation 2-25, <F>, could be estimated by performing a Monte Carlo transport game based on the collision density, $\psi(P)$. <F> was identified as the effect of interest. The effects of interest are some quantities such as the Henderson tissue dose at a detector, the total energy deposited in a given volume, or the energy flux through a bounded surface. Equation 2-25 shows one way in which the effect of interest can be calculated. The response function, $f(P)$, is the payoff per unit collision density at P. In multigroup notation, the response function shall be denoted by $R_g^{\psi}(\bar{x},\bar{\omega})$, which is defined as the response function of the effect of interest due to the particle collision density at $\bar{x}$ and in $\bar{\omega}$ for group g.

Due to the simple relationship between the flux and the collision density (Eq. 2-4), the payoff function for a unit angular flux at $\bar{x}$ in $\bar{\omega}$ for group g, $\Phi_g(\bar{x},\bar{\omega})$, is just:

$$R_g^{\Phi}(\bar{x},\bar{\omega}) = \Sigma_t^g(\bar{x})\ R_g^{\Psi}(\bar{x},\bar{\omega}) \ . \tag{2-95}$$

The response function is most often given for the unit angular flux, since it is usually normalized to the number of particles per centimeter squared (e.g. rad/(neutron cm^2). For general use, the response function can be a function of position, energy, angular direction, and time. However, the response function is usually independent of the particle direction and age, with the response being defined as zero everywhere except at the detector, which could be a point, surface, or volume. The effect of interest for group g can be expressed as:

$$\lambda_g = \iint R_g^{\Phi}(\bar{x},\bar{\omega})\ \Phi_g(\bar{x},\bar{\omega})d\bar{\omega}d\bar{x} \ , \tag{2-96}$$

with the condition placed on λ_g that the total effect of interest, λ, is the sum of the group effects of interest.

Group response functions have been defined which produce the group effect of interest when integrated over the spatial and angular (and time, if desired) variables for both the collision density and flux. A group response function, $R_g^{\chi}(\bar{x},\bar{\omega})$, can also be defined so that:

$$\lambda_g = \iint R_g^{\chi}(\bar{x},\bar{\omega})\ \chi_g(\bar{x},\bar{\omega})d\bar{\omega}d\bar{x} \ . \tag{2-97}$$

This is accomplished by requiring that the group effect of interest due to the emergent particle density be the same as the effect of interest which results from the flux caused by $\chi_g(\bar{x},\bar{\omega})$. Since the group flux caused by $\chi_g(\bar{x},\bar{\omega})$ at some point a distance of R from $\bar{x}$ along $\bar{\omega}$ is

given by:

$$\phi_g(\bar{x}+R\bar{\omega},\bar{\omega}) = \exp\left[\int_0^R \Sigma_t^g(\bar{x}+R'\bar{\omega})dR'\right] \chi_g(\bar{x},\bar{\omega}) \quad , \tag{2-98}$$

$$R_g^{\chi}(\bar{x},\bar{\omega})\ \chi_g(\bar{x},\bar{\omega}) \equiv \int_0^{\infty} R_g^{\phi}(\bar{x}+R\bar{\omega},\bar{\omega})\ \phi(\bar{x}+R\bar{\omega},\bar{\omega})dR \tag{2-99}$$

$$= \int_0^{\infty} \exp\left[-\int_0^R \Sigma_t^g(\bar{x}+R'\bar{\omega})dR'\right] R_g^{\phi}(\bar{x}+R\bar{\omega},\bar{\omega})\ \chi_g(\bar{x},\bar{\omega})dR \quad ,$$

from which the definition of $R_g^{\chi}(\bar{x},\bar{\omega})$ is shown to be:

$$R_g^{\chi}(\bar{x},\bar{\omega}) = \int_0^{\infty} \exp\left[-\int_0^R \Sigma_t^g(\bar{x}+R'\bar{\omega})dR'\right] R_g^{\phi}(\bar{x}+R\bar{\omega},\bar{\omega})dR \quad . \tag{2-100}$$

It is not likely that $R_g^{\chi}(\bar{x},\bar{\omega})$ will be used directly to calculate λ_g, but it will be required in the next section for defining the multigroup integral transport equation which is adjoint to Equation 2-92. Alternate methods of calculating the total effect of interest (λ or $\langle F \rangle$) will also be discussed.

2.4.3 Adjoint Multigroup Integral Equations

In this section, several forms of the multigroup transport equation have been introduced, including the integro-differential Boltzmann equation and the integral collision density, emergent particle density, and flux equations. Likewise, several forms of the adjoint multigroup equation exist, each determining a different adjoint function even when the relationship between the forward and adjoint "source" term is based on the effect of interest calculation (i.e. $\lambda = \int \psi(P)\ f(P)dP =$

$\int S(P)\ J(P)dP)$. Any of these forms can be used to calculate the required importance function, but the forms that should be used are the adjoint integral equations which are simulated in the Monte Carlo random walk procedure in our test bed in the same manner as the emergent particle density equation. It is somewhat surprising that the desired adjoint equation is not the adjoint to the emergent particle density equation. For that reason, this subsection contains a discussion of different adjoint equations and the relationship between these equations which determine the importance function. Due to the adequate descriptions of the derivation of most of these adjoint equations in References 13 and 37, a full derivation of all equations will be omitted. However, errors, other than typographical, in Reference 13 will be discussed and corrected in the following development or in Appendix D.

One method of defining an adjoint equation is to derive the adjoint to the integro-differential Boltzmann equation (2-75) by the requirement that:

$$\int \Phi^*(P)\ L\Phi(P)dP = \int \Phi(P)\ L^*\Phi^*(P)dP\ , \qquad (2\text{-}101)$$

where Φ^* is usually called the adjoint flux and L is the Boltzmann transport operator, defined by:

$$L\Phi(P) = -\bar{\omega}\cdot\nabla\Phi(\bar{x},\bar{E}) - \Sigma_t(\bar{x},E)\ \Phi(\bar{x},E) \qquad (2\text{-}102)$$

$$+ \iint \Sigma_s(\bar{x},E)\ f(E,\bar{\omega}|E',\bar{\omega}')\ \Phi(\bar{x}',\bar{E}')dE'd\bar{\omega}'\ .$$

The resulting adjoint operator, L^*, differs from the forward operator in two ways:

1) The leakage terms have opposite signs,

2) The transfer probability in the inscattering terms has reversed the initial and final direction ($\bar{\omega}$) and energy (E) variables.

$$L^*\Phi^*(P) = \bar{\omega}\cdot\nabla\Phi^*(\bar{x},\bar{E}) - \Sigma_t(\bar{x},E)\ \Phi^*(\bar{x},\bar{E}) \qquad (2\text{-}103)$$

$$+ \iint \Sigma_s(\bar{x},E')\ f(E',\bar{\omega}'|E,\bar{\omega})\ \Phi(\bar{x},\bar{E}')dE'd\bar{\omega}' \ .$$

Defining $S^*(P)$ as the adjoint source term, the multigroup form of the adjoint equation,

$$L^*\Phi^*(P) - S^*(P) = 0 \ , \qquad (2\text{-}104)$$

can be determined as was done for Equation 2-75. If the adjoint flux, $\Phi^*(P)$, is used to define the multigroup cross sections and transfer probability, then the cross sections for the adjoint Monte Carlo calculations will probably differ from these for the forward calculation. However, if the same multigroup cross sections are used and only the transfer probability matrix is transposed, then the multigroup form of Equation 2-104 is identical to the adjoint form of Equation 2-76:

$$-\bar{\omega}\cdot\nabla\Phi_g^*(\bar{x},\bar{\omega}) + \Sigma_t^g(\bar{x})\ \Phi_g^*(\bar{x},\bar{\omega}) = S_g^*,(\bar{x},\bar{\omega}) \qquad (2\text{-}105)$$

$$+ \sum_{g'} \int \Sigma_s^{g'\leftarrow g}(\bar{x};\bar{\omega}'|\bar{\omega})\ \Phi_g^*(\bar{x},\bar{\omega}')d\bar{\omega}' \ .$$

Remember that the choice of $S_g^*(\bar{x},\bar{\omega})$ will determine the solution of $\Phi_g^*(\bar{x},\bar{\omega})$.

Using the same procedure as applied to Equation 2-76, but with $\bar{x}' = \bar{x}+R\bar{\omega}$ and an integrating factor of:

$$\exp\left[-\int_0^R \Sigma_t^g(\bar{x}+R'\bar{\omega})dR'\right],$$

the following integral equation is derived:

$$\Phi_g^*(\bar{x},\bar{\omega}) = \int_0^\infty \exp\left[-\int_0^R \Sigma_t^g(\bar{x}+R'\bar{\omega})dR'\right] S_g^*(\bar{x}+R\bar{\omega},\bar{\omega})\,dR \qquad (2\text{-}106)$$

$$+ \int_0^\infty \Sigma_t^g(\bar{x}+R\bar{\omega})\,\exp\left[-\int_0^R \Sigma_t^g(\bar{x}+R'\bar{\omega})dR'\right]$$

$$\times \sum_{g'} \int \frac{\Sigma_s^{g'\leftarrow g}(\bar{x}+R\bar{\omega};\bar{\omega}'\,|\,\bar{\omega})}{\Sigma_t^g(\bar{x}+R\bar{\omega})}\,\Phi_{g'}^*(\bar{x}+R\bar{\omega},\bar{\omega}')d\bar{\omega}'dR\ .$$

The above equation is adjoint to Equation 2-92, the emergent particle density equation, since the second term on the right hand side is just the adjoint (or transpose in this case) of the corresponding term above. The above equation was derived from the integro-differential equation and is not the adjoint of the integral flux equation (2-86). Because of the ambiguity of terminology introduced by $\Phi_g^*(\bar{x},\bar{\omega})$, Equation 2-106 will be denoted by $\chi_g^*(\bar{x},\bar{\omega})$. That is:

$$\chi_g^*(\bar{x},\bar{\omega}) \equiv \Phi_g^*(\bar{x},\bar{\omega})\ . \qquad (2\text{-}107)$$

At this time, the source or first term of Equation 2-106 is unspecified (which means that $\chi_g^*(\bar{x},\bar{\omega})$ is unspecified). As discussed in Section 2.3.1, the choice of the source term should be the one which allows the effect of interest to be calculated by either the forward or adjoint function. This means that since:

$$\lambda = \sum_g \iint \chi_g(\bar{x},\bar{\omega})\ R_g^{\chi}(\bar{x},\bar{\omega})d\bar{\omega}d\bar{x} \tag{2-108}$$

then the adjoint source term is:

$$R_g^{\chi}(\bar{x},\bar{\omega}) = \int_0^{\infty} \exp\left[-\int_0^R \Sigma_t^g(\bar{x}+R'\bar{\omega})dR'\right] S_g^*(\bar{x}+R\bar{\omega},\bar{\omega})dR\ . \tag{2-109}$$

Equation 2-106, which is called the integral point value equation, can be written:

$$\chi_g^*(\bar{x},\bar{\omega}) = R_g^{\chi}(\bar{x},\bar{\omega}) + \int_0^{\infty} \Sigma_t^g(\bar{x}+R\bar{\omega})\ \exp\left[-\int_0^R \Sigma_t^g(\bar{x}+R'\bar{\omega})dR'\right] \tag{2-110}$$

$$\times \sum_{g'} \int \frac{\Sigma_s^{g'\leftarrow g}(\bar{x}+R\bar{\omega};\bar{\omega}'|\bar{\omega})}{\Sigma_t^g(\bar{x}+R\bar{\omega})}\ \chi_{g'}^*(\bar{x}+R\bar{\omega},\bar{\omega}')d\bar{\omega}'dR\ .$$

Comparison of Equation 2-109 with Equation 2-100 provides the identification of the adjoint source term, $S_g^*(\bar{x},\bar{\omega})$, which was first used in multigroup integro-differential adjoint equation (2-105):

$$S_g^*(\bar{x},\bar{\omega}) = R_g^{\Phi}(\bar{x},\bar{\omega})\ , \tag{2-111}$$

the angular flux response function. It is this function that should be input as the adjoint source into computer programs such as ANISN {41} and DOT {42} which solve the multigroup adjoint integro-differential equations using finite difference techniques.

Equation 2-110 represents one form of the multigroup adjoint integral transport equation. While this form is solvable by Monte Carlo methods, it is not solvable by the same techniques used in the test bed to solve the forward emergent particle density equation (2-92). This is obvious because the first step after the source particle selection is the collision kernel step, whereas that step in simulation of $\chi_g(\bar{x},\bar{\omega})$ is the transport step. Therefore, consider the adjoint form of the collision density equation (2-94):

$$\psi_g^*(\bar{x},\bar{\omega}) = R_g^{\psi}(\bar{x},\bar{\omega}) + \sum_{g'} \int \frac{\Sigma_s^{g',g}(\bar{x};\bar{\omega}'|\bar{\omega})}{\Sigma_t^g(\bar{x})} \int_0^{\infty} \Sigma_t^{g'}(\bar{x}+R\bar{\omega}') \qquad (2\text{-}112)$$

$$\times \exp\left[-\int_0^R \Sigma_t^{g'}(\bar{x}+R'\bar{\omega}')dR'\right] \psi_g^*(\bar{x}+R\bar{\omega}',\bar{\omega}')dRd\bar{\omega}' .$$

This equation is the multigroup form of the adjoint equation for J(P) derived in Section 2.3.1. It is also called the value, importance, and integral event-value equation. The designation in this paper will be the value equation, because the equation can be derived by defining $\psi_g^*(\bar{x},\bar{\omega})$ to be the value of an event or collision at $\bar{x}$ to the effect of interest for a particle in group g entering a collision with direction $\bar{\omega}$. R_g^{ψ} is the immediate payoff and the second term represents all subsequent contributions. It can also be shown that χ_g^* and ψ_g^* are related by:

At this time, the source or first term of Equation 2-106 is unspecified (which means that $\chi_g^*(\bar{x},\bar{\omega})$ is unspecified). As discussed in Section 2.3.1, the choice of the source term should be the one which allows the effect of interest to be calculated by either the forward or adjoint function. This means that since:

$$\lambda = \sum_g \iint \chi_g(\bar{x},\bar{\omega})\ R_g^{\chi}(\bar{x},\bar{\omega})d\bar{\omega}d\bar{x} \tag{2-108}$$

then the adjoint source term is:

$$R_g^{\chi}(\bar{x},\bar{\omega}) = \int_0^{\infty} \exp\left[-\int_0^R \Sigma_t^g(\bar{x}+R'\bar{\omega})dR'\right] S_g^*(\bar{x}+R\bar{\omega},\bar{\omega})dR\ . \tag{2-109}$$

Equation 2-106, which is called the integral point value equation, can be written:

$$\chi_g^*(\bar{x},\bar{\omega}) = R_g^{\chi}(\bar{x},\bar{\omega}) + \int_0^{\infty} \Sigma_t^g(\bar{x}+R\bar{\omega})\ \exp\left[-\int_0^R \Sigma_t^g(\bar{x}+R'\bar{\omega})dR'\right] \tag{2-110}$$

$$\times \sum_{g'} \int \frac{\Sigma_s^{g'\leftarrow g}(\bar{x}+R\bar{\omega};\bar{\omega}'|\bar{\omega})}{\Sigma_t^g(\bar{x}+R\bar{\omega})} \chi_{g'}^*(\bar{x}+R\bar{\omega},\bar{\omega}')d\bar{\omega}'dR\ .$$

Comparison of Equation 2-109 with Equation 2-100 provides the identification of the adjoint source term, $S_g^*(\bar{x},\bar{\omega})$, which was first used in multigroup integro-differential adjoint equation (2-105):

$$S_g^*(\bar{x},\bar{\omega}) = R_g^{\Phi}(\bar{x},\bar{\omega})\ , \tag{2-111}$$

$$\chi_g^*(\bar{x},\bar{\omega}) = \int_0^\infty \Sigma_t^g(\bar{x}+R\bar{\omega}) \exp\left[-\int_0^R \Sigma_t^g(\bar{x}+R'\bar{\omega})dR'\right] \psi_g^*(\bar{x}+R\bar{\omega},\bar{\omega})dR. \quad (2\text{-}113)$$

Thus, if ψ_g^* is the value for a particle upon entering a collision, then the above equation indicates that χ_g^* is the value for a particle leaving a collision. That this is the case is also indicated by the fact that the source term in Equation 2-110 is R_g^χ, the response function due to the emergent particle density.

Inspection of value equation indicates that it is in the same form as the emergent particle density equation ($\chi_g(\bar{x},\bar{\omega})$), which means that it may be simulated by the same Monte Carlo methods. However, implementation of the simulation for the value equation soon experiences difficulties. After selection of an "adjoint particle" for $\bar{x}',\bar{\omega}'$, and g' from $R_g^\psi(\bar{x}',\bar{\omega}')$, the adjoint particle is not only traveling in a direction opposite to the direction $\bar{\omega}$ (i.e., from $\bar{x}+R\bar{\omega}$ to $\bar{x}$), but the transport kernel is not normalized, since (with $\bar{x}+R\bar{\omega}'=\bar{x}'$):

$$\Sigma_t^{g'}(\bar{x}+R\bar{\omega}') \exp\left[-\int_0^R \Sigma_t^{g'}(\bar{x}+R'\bar{\omega}')dR'\right] = \Sigma_t^{g'}(\bar{x}') \exp\left[-\int_0^R \Sigma_t^{g'}(\bar{x}'-R''\bar{\omega}')dR''\right],$$

and our object is to pick a point $\bar{x} = \bar{x}' - R\bar{\omega}'$. This obstacle can be overcome by choosing from a properly normalized kernel and correcting the weight of the adjoint particle by $\Sigma_t^{g'}(\bar{x}',\bar{\omega})/\Sigma_t^{g'}(\bar{x},\bar{\omega})$. However, this calculation is not required in the simulation of $\chi_g(\bar{x},\bar{\omega})$, so it would be better to avoid the correction in the adjoint equation simulation. In addition, implementation of the collision kernel reveals that is is also unnormalized, and that the corrections required are even more extensive and

time consuming. Our problem with the transport kernel can be circumvented by defining a new function which is the product of ψ_g^* and Σ_t^g, since the introduction of $\Sigma_t^g(\bar{x})$ produces a properly normalized transport kernel.

The new function will be denoted by $G_g(\bar{x},\bar{\omega})$ and will be defined by:

$$G_g(\bar{x},\bar{\omega}) = \Sigma_t^g(\bar{x})\ \psi_g^*(\bar{x},\bar{\omega}) \ . \tag{2-114}$$

Substituting the equation for $\psi_g^*(\bar{x},\bar{\omega})$ into the above equation yields:

$$G_g(\bar{x},\bar{\omega}) = \Sigma_t^g(\bar{x})\ R_g^{\psi}(\bar{x},\bar{\omega}) + \sum_{g'} \int \Sigma_t^g(\bar{x})\ \frac{\Sigma_s^{g'\leftarrow g}(\bar{x}',\bar{\omega}'|\bar{\omega})}{\Sigma_t^g(\bar{x})} \tag{2-115}$$

$$\times \int_0^{\infty} \exp\left[-\int_0^R \Sigma_t^{g'}(\bar{x}+R'\omega')dR'\right] \Sigma_t^{g'}(\bar{x}+R\bar{\omega}')\ \psi_{g'}^*(\bar{x}+R\bar{\omega}',\bar{\omega})dRd\bar{\omega}' \ ,$$

which can be written as:

$$G_g(x,\omega) = R_g^{\Phi}(x,\omega) + \sum_{g'} \int \frac{\Sigma_s^{g'\leftarrow g}(\bar{x};\bar{\omega}'|\bar{\omega})}{\Sigma_t^{g'}(\bar{x})} \tag{2-116}$$

$$\times \int_0^{\infty} \Sigma_t^{g'}(\bar{x})\ \exp\left[-\int_0^R \Sigma_t^{g'}(\bar{x}+R'\bar{\omega}')dR'\right] G_{g'}(\bar{x}+R\bar{\omega}',\bar{\omega}')dRd\bar{\omega}'$$

Equation 2-95 was used to define $R_g^{\Phi}(\bar{x},\bar{\omega})$ and the unity ratio, $\Sigma_t^{g'}(\bar{x})/\Sigma_t^{g'}(\bar{x})$, was distributed in the second term to normalize the transport kernel. The above equation also allows the adjoint particles to travel in a direction opposite to their velocity vector. To overcome this somewhat confusing convention, define the adjuncton, an "adjoint particle" that obeys Equation 2-116, except that the directions have all been

reversed. This allows the adjuncton to travel in the same sense as the velocity vectors, but also requires special attention in the interpretation of the results of this adjoint calculation, since all results will be in the opposite sense to the value calculated by Equation 2-112. The new equation defined is:

$$\bar{G}_g(\bar{x},\bar{\omega}) = \bar{R}_g^{\phi}(\bar{x},\bar{\omega}) + \sum_{g'} \int \frac{\Sigma_s^{g'\leftarrow g}(\bar{x};\bar{\omega}'|\bar{\omega})}{\Sigma_t^g(\bar{x})} \tag{2-117}$$

$$\times \int_0^{\infty} \Sigma_t^{g'}(\bar{x}) \exp\left[-\int_0^R \Sigma_t^{g'}(\bar{x}-R'\bar{\omega}')dR'\right] \bar{G}_{g'}(\bar{x}-R\bar{\omega}',\bar{\omega}')d\bar{\omega}'\,dR \ .$$

Equation 2-117 will be called the integral emergent adjuncton density equation, which is in agreement with Appendix A of Reference 13. However, the approach taken here is different from that taken in Reference 13, an approach which is patterned after Irving {37}. The derivation of the emergent adjuncton density equation contained in Reference 13 has several errors, mostly in terminology (e.g., no distinction is made between G_g and $\bar{G}_g$). Appendix D contains a corrected derivation of the multigroup emergent adjuncton density equation which is consistent with the definition of $G_g(\bar{x},\bar{\omega})$ in Reference 13. The result in Reference 13 is similar to Equation 2-117, but it requires considerably more effort than is required by the derivation of $G_g(\bar{x},\bar{\omega})$ based on its relationship to the value equation. Comparison of the emergent adjuncton density equation (2-117) and the emergent particle density equation (2-92) shows that the Monte Carlo method used to simulate the emergent particle density equation can be used to simulate the emergent adjuncton density

equation. Only the source functions, $S_g(\bar{x},\bar{\omega})$ and $\bar{R}_g^{\Phi}(\bar{x},\bar{\omega})$ and the scattering kernels are different. A description of this simulation will be given in the next chapter.

2.4.4 Effect of Interest and Importance Function Estimation

Now that the integral transport equation, both forward and adjoint, which will be simulated has been chosen, two other questions must be considered:

1) How will the effect of interest be calculated?

2) What functions will be used in determining the importance function?

Most of the necessary information for considering these two questions has already been developed in this section and only needs to be summarized at this time.

Consider first the relationship which was required between the forward integral equation and its adjoint; that is, the adjoint function must not only meet the mathematical requirements but also the adjoint source term must be the response function used to generate the effect of interest in the forward mode. This uniquely related the following sets of equations:

(a) collision density (ψ_g) -- value (ψ_g^*)

(b) emergent particle density (χ_g) -- point value (χ_g^*) or adjoint flux (Φ_g^*)

(c) flux density (Φ_g) -- emergent adjuncton density (G_g or $\bar{G}_g$)

Since the most natural method of calculating the effect of interest, λ, is:

$$\lambda = \sum \iint R_g^{\Phi}(\bar{x},\bar{\omega})\ \Phi_g(\bar{x},\bar{\omega})d\bar{\omega}d\bar{x}\ , \tag{2-118}$$

and the source term for $\Phi_g(\bar{x},\bar{\omega})$ from Equation 2-86 is:

$$\int_0^{\infty} \exp\left[-\int_0^R \Sigma_t^g(\bar{x}-R'\bar{\omega}')dR'\right] S_g(\bar{x}-R\bar{\omega},\bar{\omega})dR\ ,$$

then the effect of interest can also be expressed as:

$$\lambda = \sum_g \iint \left\{\int_o^{\infty} \exp\left[-\int_0^R \Sigma_t^g(\bar{x}-R'\bar{\omega})dR'\right] S_g(\bar{x}-R\bar{\omega},\bar{\omega})dR\right\} \tag{2-119}$$

$$\times\ \bar{G}_g(\bar{x},\bar{\omega})d\bar{\omega}d\bar{x}\ .$$

Obviously, the above expression is not a very desirable method to calculate λ. But since the emergent adjuncton density equation is being simulated, and the flux density is not, won't it be necessary to use Equation 2-119, instead of 2-118? The answer is, fortunately, no, since in the forward Monte Carlo random walk, each of the quantities, ψ_g, χ_g, and Φ_g, can be estimated if desired. Likewise, although the emergent adjuncton density, $\bar{G}_g$, is being simulated, it is also possible to estimate χ_g^* and ψ_g^*. While this procedure will be discussed in the next section, equations such as 2-85, which relates Φ_g to χ_g, and 2-114, relating G_g and ψ_g^*, provide an insight into how this is accomplished. Therefore, there is no restriction as to what quantities, either forward or adjoint, can be used in the effect of interest estimation.

The forward estimation of λ will probably be with the angular flux,

$\Phi_g(\bar{x},\bar{\omega})$, in the Monte Carlo approximation of Equation 2-118, because the response function R_g^{Φ} is the one most often used in radiation transport calculations. For the adjoint estimation of λ, the adjoint response function most likely to be available is the source function, $S_g(\bar{x},\bar{\omega})$. This means that the adjoint flux, $\Phi_g^*(\bar{x},\bar{\omega})$ or $\chi_g^*(\bar{x},\bar{\omega})$, will be determined in the $\bar{G}_g(\bar{x},\bar{\omega})$ simulation and the contribution to effect of interest calculated. This estimation is based on the fact that:

$$\lambda = \sum_g \iint S_g(\bar{x},\bar{\omega})\ \chi_g^*(\bar{x},\bar{\omega})d\bar{x}d\bar{\omega}\ . \qquad (2\text{-}120)$$

It should be recognized that while the group effect of interest, λ_g or λ_g^*, can be defined for each group in both the forward and adjoint calculations, these values are not necessarily equivalent, contrary to the many equations in Reference 13 which state that they are. This fact can be demonstrated by considering a two group problem, where all neutrons are emitted in the first or fast group and where the detector has a non-zero response only for neutrons in the second or thermal group. Assuming an infinite, non-absorbing system, then the forward and adjoint fluxes will be non-zero for both groups, but the adjoint source (or forward response) is zero of the fast group. If the thermal group effect of interest is evaluated by the forward flux, then:

$$\lambda_T = \iint R_T^{\Phi}(\bar{x},\bar{\omega})\ \Phi_T(\bar{x},\bar{\omega})d\bar{\omega}d\bar{x} > 0\ , \qquad (2\text{-}121)$$

since both R_T^{Φ} and Φ_T are positive definite values. However, if the thermal group effect of interest is evaluated by the adjoint flux, then

$$\lambda_T^* = \iint S_T(\bar{x},\bar{\omega})\ \Phi_T^*(\bar{x},\bar{\omega})d\bar{\omega}d\bar{x} = 0\ , \qquad (2\text{-}122)$$

since the thermal source, S_T, is identically zero. Therefore, λ_T is not equal to λ_T^*, and the forward and adjoint group effects of interest cannot be compared directly.

Selection of the functions to be used for determining the importance is a much more difficult problem than that of the effect of interest calculation. However, it was shown in Section 2.3.2 that the adjoint or value function, J(P), could produce a perfect game for the specified transport game which simulated the collision density equation. This result was investigated even more thoroughly and extended to other transport game and biasing schemes in Reference 3. The authors concluded that the value function is always a good choice for importance function biasing of the collision density equation. Therefore, it was decided on the basis of the conclusions above and because the effect of interest estimation required the same functions that the following functions would be used in the importance function:

Forward: The adjoint flux, $\chi_g^*(\bar{x},\bar{\omega})$, for biasing the emergent particle density equation simulation.

Adjoint: The angular flux, $\Phi_g(\bar{x},\bar{\omega})$, for biasing the emergent adjuncton density equation simulation.

This procedure is illustrated by the diagram below. The arrow from the "Importance Function Estimated" column to the "Equation Simulated" column indicates the equation in which the importance function is used. The exact form of the importance functions will be discussed in Chapter IV.

Mode:

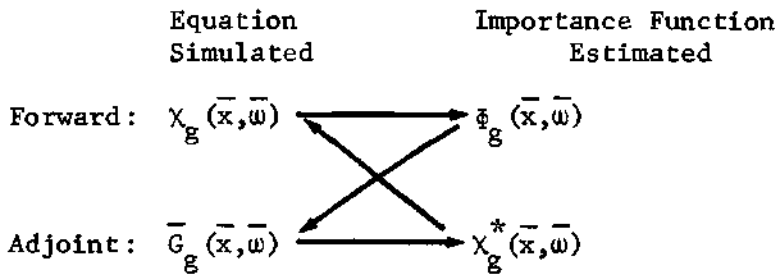
Equation Simulated
Importance Function Estimated
Forward: $\chi_g(\bar{x},\bar{\omega})$
$\Phi_g(\bar{x},\bar{\omega})$
Adjoint: $\bar{G}_g(\bar{x},\bar{\omega})$
$\chi_g^*(\bar{x},\bar{\omega})$

CHAPTER III

THE IFAM TEST BED

The principal objective of this research is to develop and evaluate variance reduction techniques which utilize the iterative forward-adjoint Monte Carlo method. A necessary tool for accomplishing this objective is a computer program which utilizes these techniques while performing the Monte Carlo simulation of the integral transport equations. No such computer program existed, so one had to be developed, coded, and validated as part of this research effort. Because this program must be capable of accepting several different importance and biasing functions, it was decided that the proper approach would be to develop a computer software test bed. The test bed must handle, for both forward and adjoint modes, all input and output of data, cross section manipulations, tracking of particles in complex geometries, and provide the framework for the Monte Carlo random walk, importance function estimation, and effect of interest calculations. A test bed is distinguished from a computer program or code by the fact that the test bed requires the addition of subprograms or portions of a subprogram which perform specific functions (in this case, the particular variance reduction schemes) before it is a complete and executable program.

A test bed is written in such a manner as to minimize the impact of adding the coding required to perform these functions. This is necessary since a major consideration in the evaluation of the different

algorithms is computation time, and the time required for computing activities independent of the algorithms should be constant. Also, the testing of a particular algorithm should require only the validation of the coding for that algorithm, and not the validation of the entire software package. These requirements were implemented in the development of IFAM (Iterative Forward-Adjoint MORSE), the name of the test bed utilized in the evaluation of the variance reduction technique.

This chapter contains a description of the IFAM test bed. This description is necessary for an understanding of the evaluation of the different techniques which will be discussed in Chapter IV. In many ways, the test bed represents to the analyst what equipment and instrumentation represent to the experimenter. Therefore, the IFAM description has been placed in the main body of this paper, beginning with a brief description of the computer code MORSE [14], which forms the basis of IFAM. The rationale for selecting MORSE instead of other codes as the IFAM basis is also discussed. The simulation of the integral forward ($\chi_g(\bar{x},\bar{\omega})$) and adjoint ($\bar{G}_g(\bar{x},\bar{\omega})$) transport equations is also described, followed by a discussion of the test bed logic or flow and a short description of IFAM-peculiar subroutines (e.g., FAIF, which is used to calculate the importance and biasing functions).

3.1 The MORSE Code

Since there was no computer program which performed the iterative forward-adjoint Monte Carlo radiation transport calculation, development of the test bed was essential. One approach was to develop and code the test bed from "scratch," except for the cannibalization of certain parts

of other transport codes. However, in order to include the capability to solve a wide range of transport problems in complex geometries, this approach would require many man-years of effort. A much faster approach is to utilize one of the already developed Monte Carlo transport codes and make appropriate changes so that the iterative forward-adjoint calculations can be performed. Those codes which were considered as the basis for the forward and/or adjoint Monte Carlo calculations include MORSE [14], CAVEAT [19], 06R [17], 06R-D [42], SAM-CE [22], ANTE-II [23], and GADJET [21]. The criteria on which the code selections were based included speed, accuracy, representation of the physical phenomenology, geometry handling schemes, input and output compatability between the forward and adjoint modes, ability to perform both forward and adjoint calculation, and applicability to the iterative forward-adjoint method. Also, the author's familiarity with the code and the effort required to modify into the test bed were considered. Comparison of the above codes soon revealed that MORSE was far superior as the basis for the test bed.

MORSE is a multigroup code which handles neutron, gamma ray, and coupled neutron-gamma ray problems for both the forward and adjoint modes. The SAM-CE code system can perform forward neutron and both forward and adjoint gamma ray problems. However, SAM-CE requires three separate programs to accomplish these calculations and it does not have a provision for neutron adjoint calculations. CAVEAT is also a code system which handles the forward calculation of neutron, gamma ray, and coupled problems, but performs no adjoint calculation. Thus both CAVEAT and SAM-CE would require additional code development to completely handle the adjoint calculation. The other code candidates are restricted to either neutron

(O6R, O6R-D, ANTE-II) or gamma ray (GADJET) problems and only in one mode (forward or adjoint).

Therefore, the MORSE code definitely is better in respect to the ability to perform both forward and adjoint calculation and applicability to the iterative method. The criteria of speed and accuracy are very difficult to evaluate, but it is generally accepted that MORSE is faster than the other candidate because of its use of multigroup cross section, although comparisons of accuracy {44} have been inconclusive. Only MORSE is a multigroup code, the other candidates use point cross sections. This means that the physics of the collision process is contained in the multigroup cross sections in MORSE, but is handled explicitly in the other codes. However, any disadvantage which MORSE may acquire in the representation of the physical phenomenology is balanced by the advantage of the multigroup code in the ease of generating the adjoint cross sections.

Of all the geometry schemes studies, the combinatorial geometry package, developed for the SAM-CE codes, is best. Since there exists a version of MORSE which contains this geometry scheme {14}, then only O6R, O6R-D, and CAVEAT are at a disadvantage to the other code candidates. MORSE also shows a very definite advantage over the other candidates in input and output compatability, since only a few input quantities need to be changed to go from a forward to an adjoint calculation. Only for one criterion does MORSE take a definite second place, and that is in the author's familiarity with the code. At the time the selection was performed, the author had a detailed understanding of all aspects of CAVEAT, but only the combinatorial geometry package in MORSE.

MORSE was also considered to require less effort to modify into the test bed. The obvious choice for the test bed basis was MORSE, and the test bed name, IFAM or Iterative Forward-Adjoint MORSE, reflects that choice. The major modifications required to execute this transformation were:

1) New logic so that both forward and adjoint calculation can be performed in the same run;

2) New logic for inputting both forward and adjoint data and the temporary storage of the data for the mode not being calculated;

3) Estimation and storage of the quantity to be used in the opposite mode importance function;

4) Storage and application of the importance function for biasing the distribution functions;

5) Calculation of the new importance and biasing functions between the mode calculations;

6) Setting up an overlay (or segmentation) map to increase the amount of core storage available for the importance function.

Other modifications for convenience (e.g. storing the cross section input for the forward mode so they can be read from a data file instead of the input unit during the adjoint input operations) were also implemented.

In order to understand IFAM, a familiarity with the MORSE code is required. Many of the features and attributes of MORSE have been discussed above. Other characteristics that are needed to understand IFAM are given below. Complete details on MORSE and its analysis package, SAMBO, are contained in References 13-15. In this summation, the term MORSE will include the basic code package [13], revisions to MORSE such

as those to the geometry routines [14], and the analysis package [15].

As discussed above, MORSE is a multipurpose Monte Carlo transport code for both neutrons and gamma rays. Both forward and adjoint problems can be solved with little change in input data since multigroup cross sections are used. All large data arrays have been included in the variable dimensioning feature to optimize the use of core storage. Complex three-dimensional, time dependence problems can be solved. In addition, several types of importance sampling options are available, including:

Source energy biasing,

Path length stretching,

Downscatter energy biasing,

Russian roulette and splitting.

(These options have been maintained or upgraded with data from the importance function in IFAM.)

By employing multigroup cross sections for each different material in the problem geometry, the physics of the interaction or collision process is contained implicitly in the cross sections. The type of particle, neutron or gamma ray, transported affects only the cross sections, so that the logic is the same for both, except for certain "editorial" exceptions. The multigroup cross sections account for anisotropic scattering by requiring that each group-to-group transfer has an associated angular distribution which is calculated from the input Legendre coefficients using a generalized Gaussian quadrature. Isotropic scattering is handled by randomly selecting the outgoing angles or direction cosines. The cross section module processes the input data so as to produce a normalized collision kernel which is multiplied by the nonabsorption probability for

the forward mode and by the analogous but non-physical weight factor for the adjoint mode. (This weight factor will be defined later.)

The geometry module in the MORSE version used as the IFAM basis is the Combinatorial Geometry package [14]. This package describes general three-dimensional material configurations or regions by performing the union, differences, and intersections of simple bodies such as spheres, boxes, cylinders, wedges, cones, and ellipsoids, and a more complex arbitrary convex polyhedron of four, five, or six sides. Experience has shown that almost any configuration can be represented in this manner.

Scoring options include those available in the SAMBO analysis package [15] plus built-in collision density and track length fluence estimators [14]. SAMBO allows an arbitrary number of detectors, energy-dependent response functions, energy bins, angle bins, and time bins. The scoring can be divided into:

Uncollided and total response,

Fluence versus energy and detector,

Time dependent response,

Fluence versus time, energy, and detector,

Fluence versus angle, energy, and detector.

The standard deviation is calculated for each of the above quantities. Estimators for point, surface, and volume detectors are available. The technique of estimating the above quantities by simulating the forward or adjoint integral transport equation is explained in the next section.

3.2 Monte Carlo Simulation of Integral Transport Equations

Both the forward and the adjoint transport equations are simulated in the IFAM test bed. The same coding is used for both of these simulations, with changes only in input data (e.g., the source term and the cross section scattering matrix) and the identification of the quantities calculated. The Monte Carlo simulation of the integral equations is discussed below in a very simplified manner. Details of how the specific phase space components are selected are contained in Chapter IV. This discussion emphasizes the mathematical and physical aspects of the simulation. Also, explanation of the effect of importance sampling on the probability distribution functions will be delayed until Chapter IV.

The simulation of the forward integral transport equation (2-92) and the adjoint equation (2-117) will be considered simultaneously. Thus it is possible to compare both the similarities and differences in each of the three simulation steps. Table 1 shows the major elements of the simulation. For each of the three steps, the table defines integral equation terms which are simulated, radiation quantities which are estimated, and the expression for the value of the estimate. The treatment of both discrete and continuous probability distributions will be considered achievable in the sense of the Lebesque-Stieltjes integral. That is, the probability of the events between x_1 and x_2 is just:

$$\Pr\ [x_1 < X \leq x_2] = \int_{x_1}^{x_2} dF(X) \qquad (3\text{-}1)$$

where X is a random variable with values X, and $F(x) = \Pr\ [X \leq x]$ is the cumulative distribution function. Assuming the existence of a set of

Table 1. Monte Carlo Simulation Outline

Step Mode	Term Simulated	Quantities Estimated	Value of Estimate
Source: $(g', \bar{x}', \bar{\omega}')$			
Forward	$S_{g'}(\bar{x}', \bar{\omega}')$	$\chi_{g'}(\bar{x}', \bar{\omega}')$	$\sum_{g'} \iint S_{g'}(\bar{x}', \bar{\omega}') d\bar{x}' d\bar{\omega}'$
Adjoint	$\bar{R}_{g'}^{\Phi}(\bar{x}', \bar{\omega}')$	$\bar{G}_{g'}(\bar{x}', \bar{\omega}')$	$\sum_{g'} \iint \bar{R}_{g'}^{\Phi}(\bar{x}', \bar{\omega}') d\bar{x}' d\bar{\omega}'$
Transport: $(\bar{x}' \rightarrow \bar{x})$			
Forward	$\Sigma_t^{g'}(\bar{x}) \exp\left[-\int_0^R \Sigma_t^{g'}(\bar{x}-R'\bar{\omega}')dR'\right]$	$\psi_{g'}(\bar{x}, \bar{\omega}')$	W_s (statistical weight)
		$\Phi_{g'}(\bar{x}, \bar{\omega}')$	$W_s/\Sigma_t^{g'}$
		$\Phi_{g'}(\bar{x}'', \bar{\omega}')$	$W_s \cdot S/V$ (track length)
Adjoint	$\Sigma_t^{g'}(\bar{x}) \exp\left[-\int_0^R \Sigma_t^{g'}(\bar{x}-R'\bar{\omega}')dR'\right]$	$\chi_{g'}^{*}(\bar{x}, -\bar{\omega}')$	$W_s/\Sigma_t^{g'}$
		$\chi_{g'}^{*}(\bar{x}'', -\bar{\omega}')$	$W_s \cdot S/V$
Collision: $(g' \rightarrow g; \bar{\omega}' \rightarrow \bar{\omega})$			
Forward	$\Sigma_s^{g \leftarrow g'}(\bar{x}; \bar{\omega} \mid \bar{\omega}')/\Sigma_t^{g'}(\bar{x})$	$\chi_g(\bar{x}, \bar{\omega})$	W_s
Adjoint	$\Sigma_s^{g' \leftarrow g}(\bar{x}; \bar{\omega}' \mid \bar{\omega})/\Sigma_t^{g}(\bar{x})$	$\bar{G}_g(\bar{x}, \bar{\omega})$	W_s

random numbers uniformly distributed on the interval from 0 to 1, then a specific value of x can be selected from F(x) by the following relationship:

$$\rho = \int_{-\infty}^{x} dF(X) \tag{3-2}$$

where ρ has been randomly chosen from the uniform set of random numbers. When the above relationship is solved repeatedly for x with ρ's taken from the uniform random number set, then the x's will be distributed as F(X). This principle is the basis for the Monte Carlo technique, and it is in this sense that the expression "select . . ." is used below.

3.2.1 Source Selection

The source term in Equation 2-92 is expressed as $S_g(\bar{x},\bar{\omega})$. This term is completely general, and its exact form depends on the physical problem being solved. If our source is an isotropic, mono-energetic point source, then the source selection requires that only the energy group and spatial coordinates be specified in the input. The angular coordinate, usually expressed by the direction cosines, can be selected rather simply by assuming a uniform distribution over the unit sphere. Details of this selection will not be necessary for this discussion, since it will be assumed that the selection of the energy group, position, and direction is possible from a properly defined source term. Thus, select the source parameters $(g',\bar{x}',\bar{\omega}')$ from $W_s^{-1}\cdot S_{g'}(\bar{x}',\bar{\omega}')$, where:

$$W_s = \sum_g \iint S_{g'}(\bar{x}',\bar{\omega}')\,d\bar{\omega}'\,d\bar{x}' \ . \tag{3-3}$$

The term, W_s^{-1}, normalizes our source term so that the selection is performed on a properly normalized distribution function. W_s is also the statistical weight assigned to each particle whose parameters are selected from the source distribution function.

Since the particle selected above is emerging from the source, then the weight of the particles, W_s, is an estimate of the emergent particle density, $\chi_{g'}(\bar{x}',\bar{\omega}')$. At this time in the simulation, W_s should be used to "score" the emergent particle density, if desired. This is usually done by keeping a running sum of the statistical weights in finite elements of phase space.

The adjoint source term, given in Equation 2-117, is $\bar{R}_g^{\Phi}(\bar{x},\bar{\omega})$. This function of g, $\bar{x}$, and $\bar{\omega}$ must also be normalized so that these adjoint source or adjuncton parameters can be selected. After the adjuncton parameters $(\bar{g}',\bar{x}',\bar{\omega}')$ have been selected, the adjuncton is assigned a statistical weight of:

$$W_s^* = \sum_{g'} \iint \bar{R}_{g'}^{\Phi}(\bar{x}',\bar{\omega}')\, d\bar{\omega}'\, d\bar{x}' \quad . \tag{3-4}$$

As in the forward source selection, the emergent adjuncton density, $\bar{G}_{g'}(\bar{x},\bar{\omega}')$, can be scored by keeping a running sum of W_s^* and other adjuncton weights as discussed below. However, neither $\bar{G}_g(\bar{x}',\bar{\omega}')$ nor $\chi_{g'}(\bar{x}',\bar{\omega}')$ are usually scored since they do not yield estimates of the effect of interest when multiplied by the normal response functions (e.g., see Equations 2-97 and 2-100 or 2-119).

3.2.2 Transport Step

Inspection of the integral term equations (2-92 and 2-117) shows

that the next step in the simulation of the emergent particle density or emergent adjuncton density is the transport of our "particle" from $\bar{x}'$ to $\bar{x}$ along the $\bar{\omega}'$ direction. The next collision site, $\bar{x}$, is selected from the probability distribution function:

$$\Sigma_t^{g'}(\bar{x}) \exp\left[- \int_0^R \Sigma_t^{g'}(\bar{x}-R'\bar{\omega}')dR' \right] \tag{3-5}$$

It is possible that the new collision site is outside the region of interest or has escaped into a non-reentrant void. In this case the history of this particle (or adjuncton for the adjoint mode) is terminated and a new source particle is selected. If $\bar{x}$ is within the region of interest, then this transport step can be used to estimate the collision density, $\psi_{g'}(\bar{x},\bar{\omega}')$, and hence the flux, $\Phi_{g'}(\bar{x},\bar{\omega})$, in the forward mode. The estimate for the collision density is just the statistical weight, W_s, while the estimate of the flux is $W_s/\Sigma_t^{g'}(\bar{x})$. These estimates are also made for finite elements of phase space, with the spatial bin being that geometric region which contains $\bar{x}$.

It is also possible to get an estimate of the fluence in those geometric regions through which the particle passes in traveling from $\bar{x}'$ to $\bar{x}$. This estimate is based on the fact that the fluence can be defined as the path length per unit volume. Therefore, the contributions to the estimate of the average fluence in a given geometric region when a particle travels a distance S through the region are just the product of the statistical weight times the distance S, and divided by the region volume V (i.e., $S \cdot W_s/V$). A running sum is usually kept of the product of S and W_s for each energy group and region during the random walk calculations.

The sum is normalized by dividing by the region volume and the total number of source particles at the conclusion of the calculation, producing an estimate of the fluence. Flux estimates can also be calculated for time dependent problems by dividing the time range into time bins, recording the running sum estimate for each time bin as well as energy and region, then including the time difference in the normalization term. For time dependent problems, the flux estimate calculation is identical to the fluence calculation, except the source term is in units of per second.

Similarly, the transport step of the adjoint simulation produces estimates of the adjoint flux. The statistical weight at each collision point can be divided by the total cross section to produce an estimate of the adjoint flux, $\chi_g^*(\bar{x},-\bar{\omega})$. Track length estimates of the adjoint flux during the adjoint simulation are calculated in the same manner and use the same computer coding as the forward flux. Running sums of these quantities are calculated by IFAM for each energy group, region, and angular bin.

3.2.3 Collision Step

After the particle or adjuncton has been transported from either a source or a previous collision site to a new collision site (e.g., from $\bar{x}'$ to $\bar{x}$), the physics of interaction as a nucleus must be simulated. This process is usually assumed to occur instantaneously and at the selected collision site. Mathematically, the collision step is a simulation of the scattering or collision kernel, which results in the selection of a new energy or energy group (g' to g) and a new direction ($\bar{\omega}'$ to $\bar{\omega}$). In order to make this selection of a new energy group and direction, the

collision kernel must be properly normalized. This normalization for the forward mode can be performed in two ways:

1) Terminate (or kill) the particle or adjuncton with an expectation proportional to the absorption probability.

2) Adjust the statistical weight W_s by multiplying by the non-absorption probability.

The second method is the one most commonly used, and is the method used in IFAM.

This method has the effect of dividing the collision term into two parts:

$$\frac{\Sigma_s^{g'}(\bar{x})}{\Sigma_t^{g'}(\bar{x})} \cdot \frac{\Sigma_s^{g \leftarrow g'}(\bar{x},\bar{\omega}|\bar{\omega}')}{\Sigma_s^{g'}(\bar{x})} ,$$

which is the same as the term shown in Table 1. However, in this form, the first ratio represents the probability that the collision event will not terminate the particle. Reducing the statistical weight by multiplying by this ratio has the effects of "killing" that fraction of the particle that would "on the average" terminate at the collision site. Of course, a part of a particle cannot be terminated in the physical process, but this mathematical technique is perfectly correct. It then allows the selection of the new energy group and direction from a normalized function, as shown in the second part of the above term.

For the adjoint simulation, an equivalent mathematical procedure is used to simulate the adjoint collision term. However, the adjustment of the statistical weight by

$$\left[\sum_{g''}\int \Sigma_s^{g'\leftarrow g''}(\bar{x};\bar{\omega}'|\bar{\omega}'')\,d\bar{\omega}''\right]/\Sigma_t^{g'}(\bar{x})$$

has no physical analog such as the non-absorption probability. In fact, the above term can have a value greater than one, unlike the non-absorption probability. Use of the above term does allow simulation of the adjoint integral equation for $\bar{G}_g(\bar{x},\bar{\omega})$ in a manner identical to the forward integral equation for $\chi_g(\bar{x},\bar{\omega})$. It also allows the transport step to be performed with a normalized kernel, as discussed in Chapter II. Only the cross sections, which are usually input for each problem, differ in the simulation of the particle (neutron and gamma ray) and adjuncton transport.

After the adjustment of the statistical weight to allow normalization of the collision kernel, selection of the new energy group and direction is performed from the following term:

$$\Sigma_s^{g'\leftarrow g}(\bar{x};\bar{\omega}'|\bar{\omega})\Big/\left[\sum_{g''}\int \Sigma_s^{g'\leftarrow g}(\bar{x};\bar{\omega}'|\bar{\omega}'')\,d\bar{\omega}''\right]$$

The general procedure for this selection is to determine the downscattering probabilities into each group g from the current group g'. These probabilities are precomputed and stored by the IFAM test bed. Then the outgoing angle is selected from the discrete angle probability matrix which corresponds to the selected downscatter energy. If the new energy group is outside the range of interest (e.g., below the energy at which the response function for the effort of interest is zero), then the particle or adjuncton history is terminated and a new source is selected. If the history is not terminated, the transport step is performed with the new parameters $(g,\bar{x},\bar{\omega})$.

The estimation of quantities of interest at the conclusion of the collision step is very similar to that of the source selection step. The outgoing statistical weight is an estimate of the emergent particle density $\chi_g(\bar{x},\bar{\omega})$ for the forward mode and the emergent adjuncton density $\bar{G}_g(\bar{x},\bar{\omega})$ for the adjoint mode. Of course, the statistical weights can change from step to step, especially at the weight adjustment in the collision step. For a problem in which importance sampling techniques are utilized, weight adjustments will occur at other times during the simulation. Chapter IV will contain further discussion of these adjustments for the techniques considered during this research.

3.3 IFAM Logic Design

The efficient implementation of the IFAM test bed on a computer with limited core storage such as the $200K_8$ UNIVAC 1108 was a significant problem. Both forward and adjoint data would be required during a single run. Additional core storage would be required by the importance function for the current mode and the flux estimator to generate the importance function for the next mode. Both of these data arrays are functions of three parameters: position, energy, and direction. Additional storage area is required for manipulation of the raw importance data to prepare it for the next mode calculation. The core storage required for a typical problem with 40 importance regions, 20 energy groups, and 18 angular bins is 14,400 words for the importance function. The same number of words is needed for storage of the data which will be used to generate the opposite mode importance function. Additional storage is required for marginal probability distributions of the importance function. If

scratch areas are set aside for data manipulation, then the core storage requirements for IFAM--peculiar data exceed 44,000 words for either mode. The total for both forward and adjoint modes is greater than the 65,536 ($200K_8$) words of UNIVAC 1108 storage. The 44,000 words does not include storage for the instruction bank and for random walk, geometry, cross section, and analysis data.

Obviously, techniques for reducing core storage requirements are required. Use of readily available techniques such as segmentation of the program provided some reduction, but not enough. Data could be stored on data files, but the increase in run time and input/output operations to retrieve and store data from data files during the random walk computation was intolerable. It was obvious that all data needed for a given mode calculation must be in core. To meet this condition and to allow sufficient core storage for the additional data arrays, the logic flow of IFAM was designed as shown in Figure 5. This design is such that both segmentation and data storage or retrieval on data files can be utilized. In addition, only that portion of the input or generated data that is required during a given mode calculation resides in core. Scratch areas of core have been eliminated by dynamic allocation of data array storage for temporary data arrays. The result of this design is that the amount of core storage available for data is more than 18,000 words greater than that for the MORSE code even though IFAM requires a larger instruction bank. Thus, iterative forward-adjoint Monte Carlo problems can be executed on the UNIVAC 1108 without removal of any of the MORSE code capabilities. Subsequent paragraphs will describe the IFAM logic design in more detail.

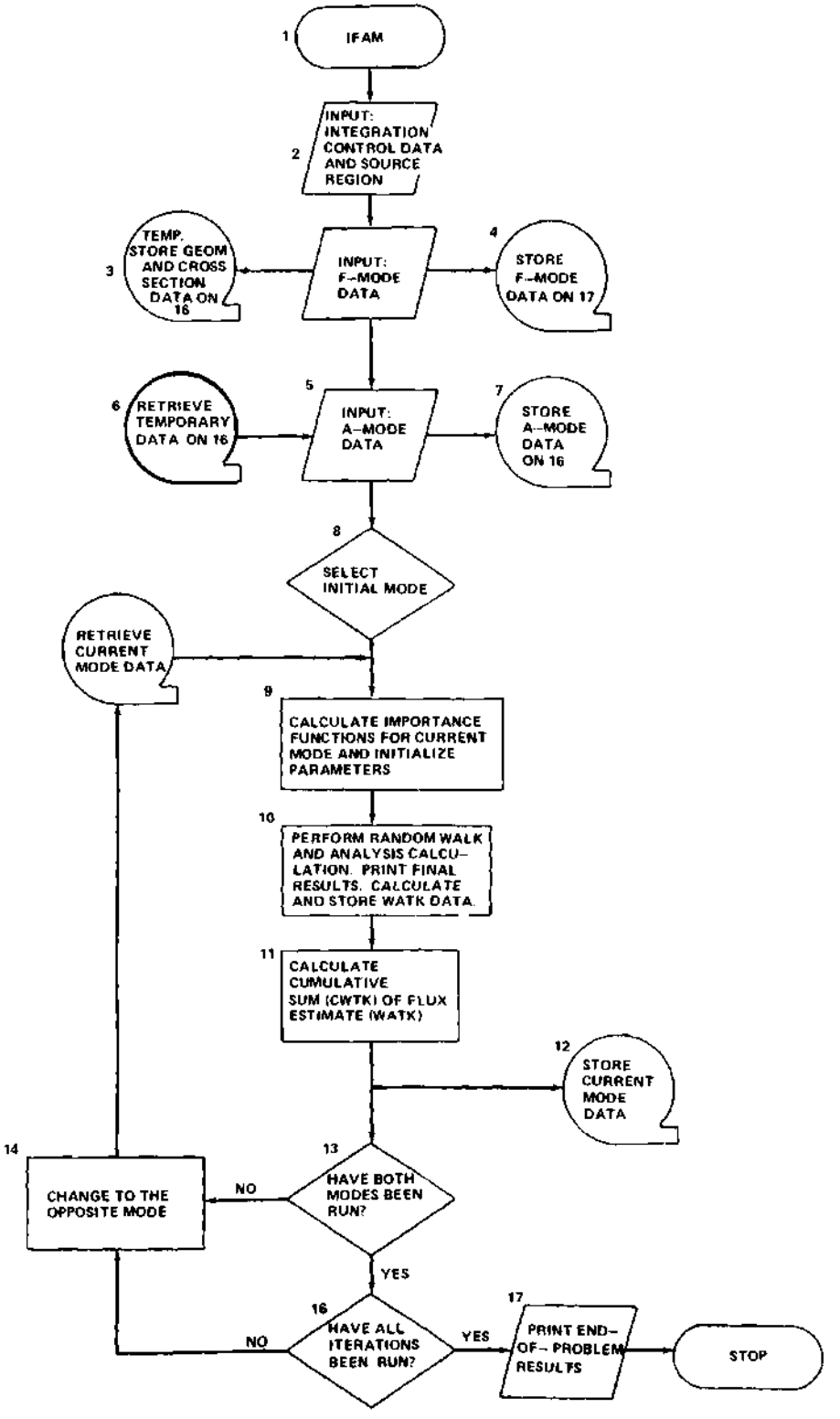

Figure 5. IFAM Logic Design

As explained in Section 3.1, the IFAM test bed is built around the MORSE code. The overall design of IFAM is based on the calculation of both forward and adjoint MORSE solutions alternately for a specified number of iterations. Before each mode calculation, an importance function is computed and used during the mode calculation to alter the sampling distributions. This importance function is derived from the flux estimate stored during the Monte Carlo simulation of the opposite mode problem. Figure 5 is a simplified diagram of the logic flow of this design. Each process, input/output and decision operation has been numbered for ease of reference in the following discussion. Some of these numbered operations are much more complex than others. For example, operation 14 consists of one line of FORTRAN code, while operation 2 and a subset of operation 10 encompass a complete MORSE forward mode calculation. However, these operations do illustrate the major logic design of IFAM.

The initial IFAM-peculiar operation occurs in the executive or controller subroutine for IFAM, MORSE/IFA. Iteration control and source region information are obtained by input operation 1. The iteration control data include the number of iterations, initial mode, the number of batches, and the number of particles or adjunctons per batch for each iteration. Operation 2 is the input of the forward or F-mode data. These data include the random walk, geometry, cross section, and analysis data as described in Appendix B. During the F-mode data input operation, both the combinatorial geometry and the cross section data are temporarily stored on data file 16. These data are read during the A-mode input operations. After all F-mode data have been read into the appropriate common

areas, the FAMS subroutine is called and the data in these common areas are written onto data file 17. This data file always contains the F-mode data which are transmitted back into the appropriate core storage data array at the beginning of an F-mode calculation (represented by operation 14). Following the F-mode data input is the A-mode data input. The A-mode must follow the F-mode data input operation, but the initial random walk calculation is arbitrary. The A-mode data are read from cards (or card images) which are on the input file and data file 17. A-mode data are stored in the same areas of core storage as the F-mode data, and likewise, written onto the A-mode data file (16) by the FAMS subroutine.

After all input data have been read and stored on the appropriate data file, the iterative forward-adjoint calculation begins. The initial mode (forward or adjoint) is determined during operation 8 and the data for that mode are retrieved from their data file. For example, if the initial mode is forward, then data file 17 is read and the F-mode data put into the core storage data arrays. This operation (15) is performed by the FAMS subroutine. FAMS also initiates operation 9, which consists of calling the FAIF subroutine for determining the importance functions and initializing certain variables and parameters. With these operations, IFAM is now ready to begin the random walk and analysis steps that constitute the major part of the computation. The logic flow for this part of IFAM is very similar to the MORSE random walk, except for modifications to accommodate the distribution functions which have been altered by the importance function. In addition the data which will be used to generate the importance function for the opposite mode (i.e., the track length or collision density) are also stored by angular bin. In MORSE, only energy

group and importance region dependent quantities were stored. After each source selection and collision event, flux estimates are made to the point detectors using statistical estimation techniques. These data are cumulated and then output at the completion of operation 10 for the initial mode of the first iteration, the equivalent of one complete (but short) MORSE run is terminated.

Of course, IFAM does not terminate, but performs operation 11 of Figure 5. This operation, executed in the FAMS subroutine, is the first step in generating the importance function for the next mode calculation. It is followed by an output of the initial mode data at the completion of the calculation to the appropriate data file. While many of the data arrays written on the data file are the same as the input data for that mode, some arrays will have been updated. These arrays include the geometry arrays, the scattering and track length counters, and the user (analysis) arrays. The data arrays at the completion of this initial mode are then stored on the initial mode data file, as indicated by operation 12.

Since the above discussion was for the initial mode calculation for the first iteration, then decision operation 13 will be negative, and the mode will be changed to the next or opposite mode from the initial mode at operation 14. The data stored on the data file for this mode will be read and placed in core storage. For example, if the adjoint mode had been specified to be the initial mode, then at operation 15, the F-mode data are stored in core so that a forward Monte Carlo simulation can be performed by operation 10. Assuming that more than one iteration is requested, then the next time that operation 15 is executed, A-mode data will be put into core. In any case, data for the "non-initial" mode

are now in core storage. The importance functions for this mode are calculated in the FAIF subroutine and are passed to the random walk routines by operation 9. At operation 10, another complete Monte Carlo calculation is performed, including the output of the results. This calculation is for the opposite mode from the initial model, but uses data from the initial mode calculation in the importance function to alter the sampling distributions.

After operations 11 and 12, a check is made to determine if all iterations have been completed. If not, then the mode is changed again, this time from the "non-initial" to the initial mode. The initial mode data are stored in core, new importance functions are calculated from the previous run data, and the Monte Carlo simulation routines of operation 10 are executed. After operations 11, 12, and 13 are performed, the "non-initial" mode calculations for the second iteration are executed.

This procedure continues until both mode calculations are performed for all iterations. Then decision operation 13 is affirmative, and the end-of-problem results are printed. Note that the above logic design never requires both forward and adjoint data in core storage at the same time. In fact, the only significant amount of additional data is the array used to store the flux estimator (WATK). Further reduction in core requirements is obtained by segmentation of the program into a main segment and four subsegments, with nearly 19,000 words saved. Appendix A contains a more detailed description of the segmentation of IFAM. Finally, the requirement for scratch area in core was overcome by storing data on the F- and A-mode data files until it could be placed in the blank common area used by the flux estimator without destroying useful data. This

logic design resulted in a factor of three reduction of total core storage requirement, making possible the utilization of the IFAM test bed on the 65K word UNIVAC 1108.

3.4 Special IFAM Subroutines

Twenty two of the subroutines contained in the MORSE code had to be modified in order to be compatible with the IFAM test bed. In some cases, the subroutine had to be completely revised for IFAM (e.g. NXTCOL), while others required only minor changes. In addition to these twenty two subroutines, three new subroutines were required. Two of these subroutines, FAMS and FAIF, are required to manipulate the data between the two mode calculations and to generate the importance functions. The third subroutine, ANGBIN, determines the angular bin for directional dependent storage or selects an outgoing angular direction isotropically over a specified angular bin.

These subroutines have functions that are central to the design of IFAM and are described in the following sections to provide a better understanding of the IFAM test bed.

3.4.1 Subroutine FAMS

Very early in the design of the IFAM test bed, it was recognized that a software routine would be required to handle the exchange of forward and adjoint data between mode calculations and control the calculation of the importance functions. Consideration was also given to using the same routine as the executive controller for IFAM, but further analysis revealed that this function could be handled easier by modifying the MORSE code controller (which is the MORSE subroutine). The modified

MORSE subroutine, MORSE/IFA, is now used as the executive controller for IFAM, but it calls the FAMS subroutine for mode data exchange and importance function control. Almost all of the data used in FAMS are transmitted through the common areas. Only two parameters are passed through the subroutine agreement list, IADJ and MSR. IADJ specifies the current mode under consideration. MSR specifies whether the mode data are to be stored on or retrieved from the data files. The value of MRS also determines what data manipulation will occur, as shown in Figure 6.

During the read operation, the flux estimate from previous mode calculations is read into the FAI data array, which contains the importance function during the random walk. For the first iteration and initial mode, where no estimate exists, the FAI array is initialized to zero. The design of the FAMS subroutine is such that either the cumulative sum of all appropriate mode calculations or just the previous mode results are retrieved. Next, the input data are read from the mode data file and loaded into labeled and blank common areas of core storage. Only those data which are required for this particular mode are put into the core. This read operation performs the same function for IFAM as the input operation does for the MORSE code. It is followed by a call to the FAIF subroutine, where the importance functions are generated for the present mode calculation. The initialization of blank common storage areas and other variables completes the read option tasks of FAMS. The store option (MSR $\leqq$ 0) tasks are performed at the conclusion of operation 10 on Figure 5, which includes the random walk calculations for the current mode. The flux estimate determined during the random walk is either transferred to the FAI data array or it is summed to all previous estimates

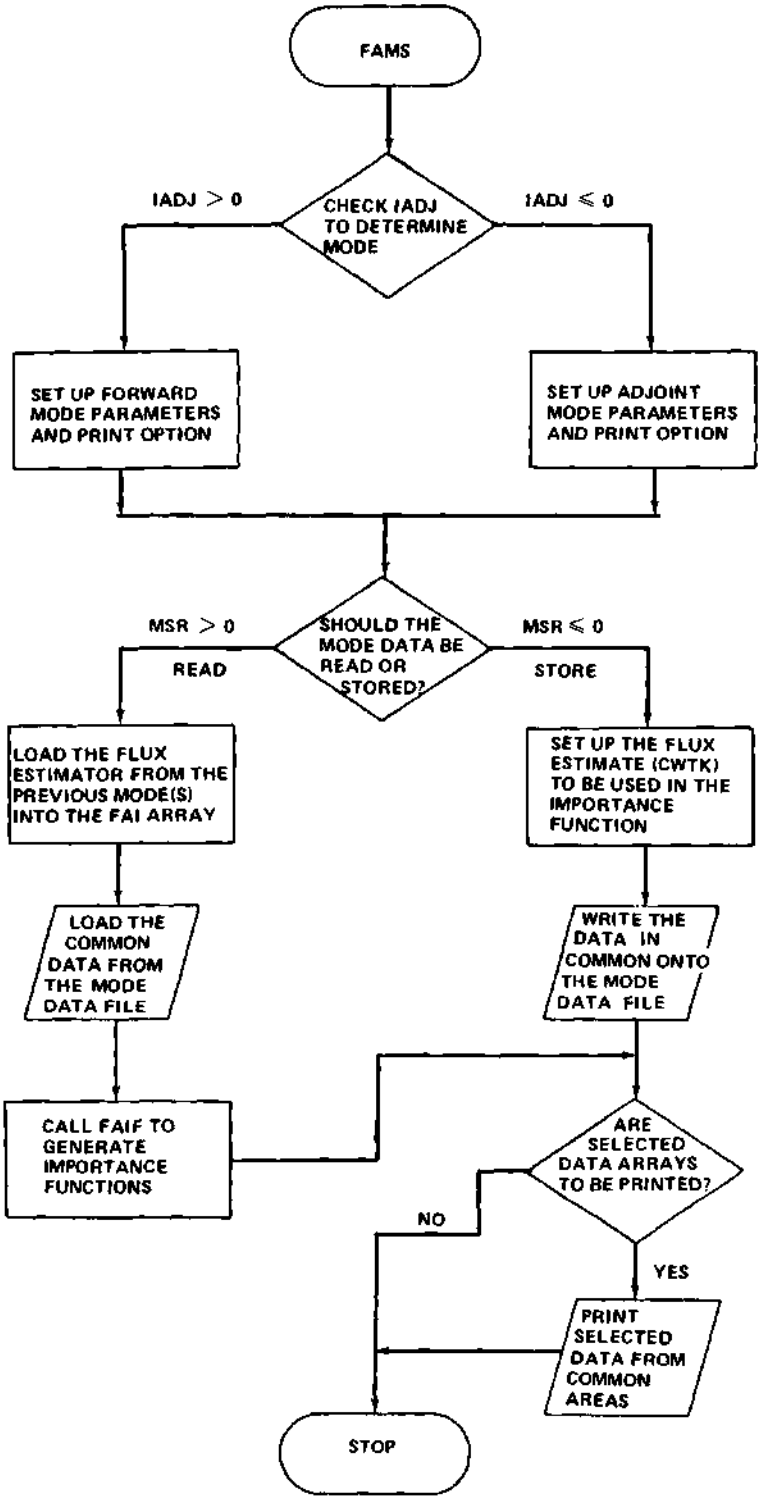

Figure 6. FAMS Subroutine Flow Diagram

of the flux for this mode (for cumulative sum importance functions). In either case, these data are written onto the current mode data file along with the other labeled and blank common data arrays. The final flux estimate is retrieved from this data file during the next mode calculation and used to generate the importance functions.

FAMS will also print the contents of all the labeled common data arrays which it handles and of selected portions of blank common. This print is controlled by input data and provides a valuable aid in debugging operations for both coding and input data checkout.

3.4.2 Subroutine FAIF

The generation of the importance functions which are used to alter the source, transport, and collision distributions functions is performed in the FAIF subroutine. While the exact design of this subroutine is dependent on the particular form of the importance function being tested, several general features of FAIF are common to most cases. These features are described in the context of the version of FAIF that normalizes the importance function array FAI and the input energy importance array EPROB on a region basis. Justification of any particular method of generating the importance functions will not be discussed until Chapter IV.

Figure 7 indicates the major features of the FAIF subroutine logic flow. During the initial mode of the first iteration, no flux estimate exists, so only the input energy importance array EPROB requires normalization. These data are then used to calculate the initial importance functions. The functions calculated are:

1. RI -- the region importance function
2. FAI -- the energy and angular importance function normalized

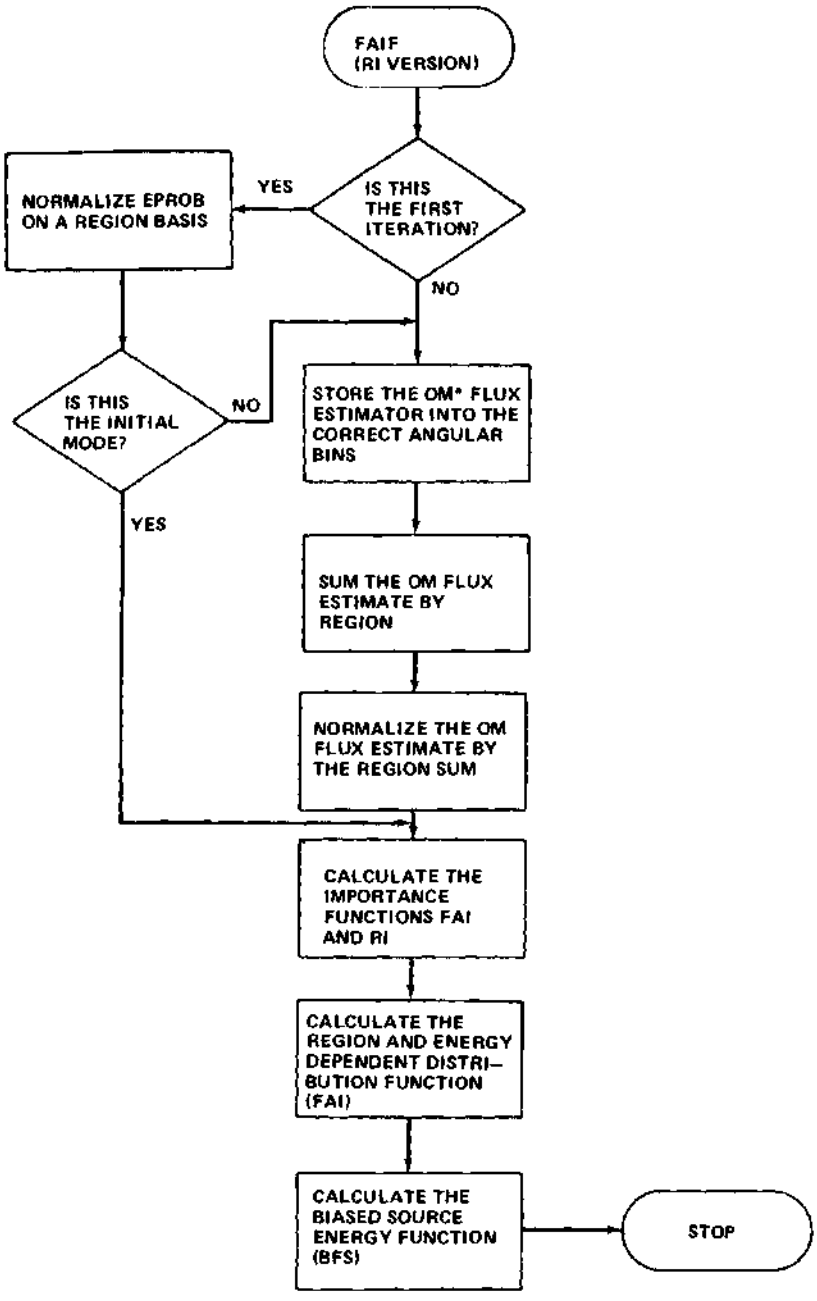

* OM – OPPOSITE MODE. IF THE FORWARD MODE CALCULATION TO BE PERFORMED NEXT, THEN THE OPPOSITE MODE IS THE ADJOINT MODE, AND VICE–VERSA.

Figure 7. FAIF Subroutine Flow Diagram

for each region

3. FAI^+ -- the energy importance function for each region

4. BFS -- the biased source energy function.

Details on how these functions are employed in IFAM are given in Chapter IV. However, it should be noted that FAI^+ is generated by summing the FAI data array over all angular bins. The biased source energy function BFS is calculated by multiplying the input source energy function by FAI^+ for the source region and then normalizing. The above functions are calculated prior to each new mode calculation.

Whenever the FAIF subroutine is called after the initial mode of the first iteration, the flux estimate from the opposite mode random walk must be normalized and stored in the correct angular bin for the current mode importance function. Storage in the correct angular bin is required because the flux estimate was stored in such a way that the particle or adjuncton is traveling along its velocity vector instead of in the opposite direction as required by the importance function (explained in Section 2.4.3 and Appendix D). Correcting the angular direction or bin is handled by a transformation or permutation array defined in FAIF. The flux estimates are also divided by the region volume. It should be noted that the flux estimate has been stored in the FAI array by the FAMS subroutine. Also, all operations on the flux estimate, including the angular bin correction, are performed in a manner that requires no additional storage area.

Once the flux estimate has been properly normalized and transformed, the final form of the importance function is calculated by a linear combination of the input energy importance function EPROB and the flux estimate.

The final form of the region importance function RI is also calculated. RI is stored in the unused fission weight array FWLO of blank common. Next, the FAI^{+} and BFS arrays are calculated from the FAI array. Thus, the importance functions and, in one case, a biased distribution function (BFS), are computed by the FAIF subroutine for the iterative forward-adjoint Monte Carlo random walk.

3.4.3 Subroutine ANGBIN

In order to satisfy the requirement for angular biasing with the importance function, the flux estimate taken during a given mode calculation must be stored as a function of direction. The MORSE code provides for angular data at detector points, but not as part of the region and energy dependent random walk arrays. Therefore, it was necessary to set aside core storage for the region, energy, and angular dependent flux estimate array. To handle the angular dependence, an angular bin structure was designed as shown in Figure 8. Also, the ANGBIN subroutine is written to place each particle or adjuncton in the correct bin. In addition, a software routine is required to select the specific direction of an emerging particle or adjuncton after an outgoing angular bin has been selected. ANGBIN also performs this task. Figure 9 illustrates how these two tasks are accomplished. Discussion of the methodology used by ANGBIN and a description of the ANGBIN operations are given below.

The angular bin structure was defined by defining eighteen equal solid angle bins. These bins can be defined on a sphere (see Figure 8) as follows:

Bin 1 - Polar cap about the +z-axis which is subtended by the cone whose polar angle has a cosine of 8/9.

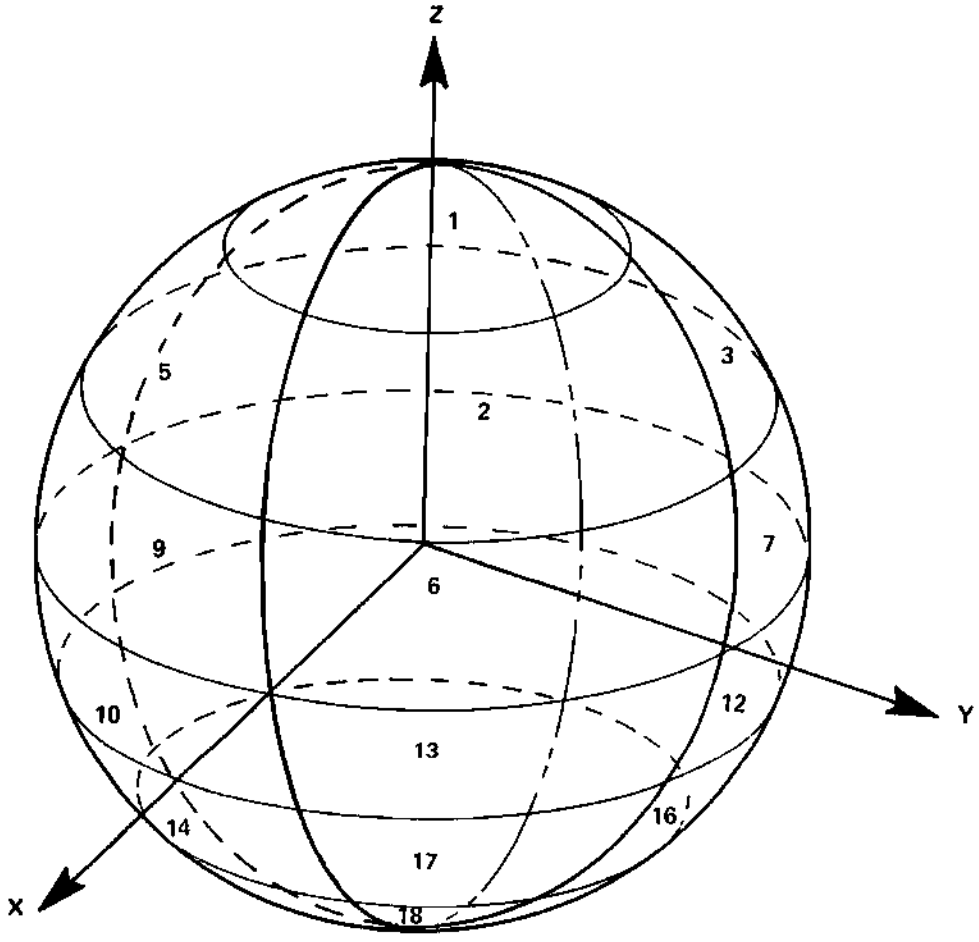

Figure 8. Angular Bin Structure

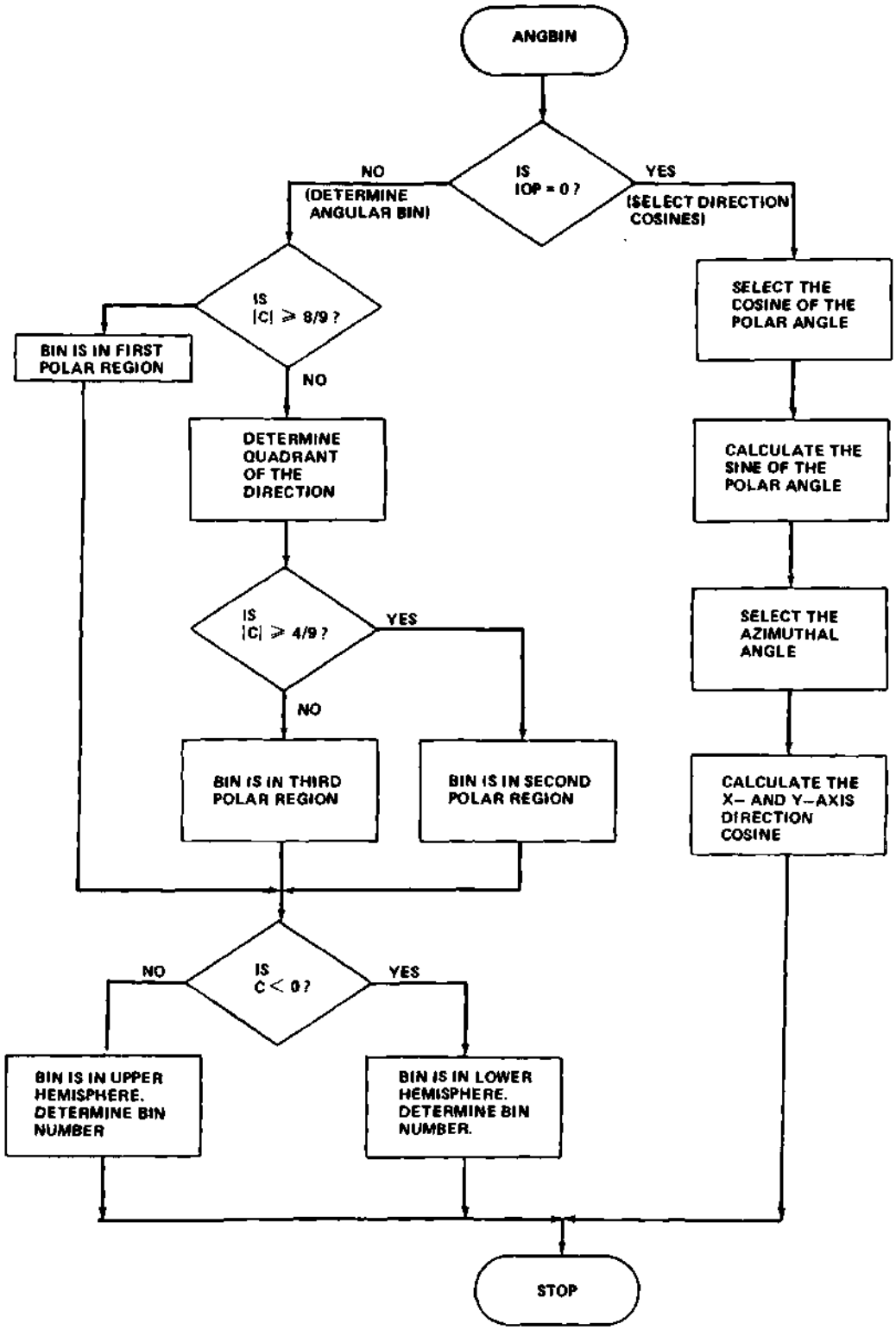

Figure 9. ANGBIN Subroutine Flow Diagram

Bin 2 to 5 - Surface areas lying between the polar angles whose cosines are 8/9 and 4/9, each of which occupies one quadrant, with bin 2 in the first quadrant, bin 3 in the second, bin 4 in the third, and bin 5 in the fourth.

Bin 6 to 9 - Surface areas lying between the polar angles whose cosines are 4/9 and 0 (the equator), each occupying one quadrant in sequential order.

Bin 10 to 18 - These bins lie in the -z hemisphere and were determined by taking absolute value of the z-axis direction cosine, locating the +z bin, then determining the bin number by the formula: bin m = 19-n, where n is the +z bin.

This angular bin structure allows for the rapid determination of the bin from the direction cosines of the particle or adjuncton path. Each angular bin has a solid angle of one-eighteenth of the total solid angle (i.e., $(2\pi)/9$). Once the polar region of the direction has been determined, the quadrant is found by checking the sign of the x- and y-direction cosines. This eliminates the necessity for any complex arithmetic calculations. Figure 9 shows the logic flow for determining the angular bin from the direction cosines.

ANGBIN also selects the direction cosine uniformly over the input angular bin whenever the option variable, IOP, is input as zero. Since each angular bin is limited in its polar and azimuthal angle extent, then the cosine of the polar angle and the azimuthal angle are selected uniformly over the limits of the input bin. This can be done quite simply by adding the product of a uniformly distributed random number times the angular interval to the lower limit. If the lower azimuthal angle of the

input bin is θ_L, and the bin width is $\Delta\theta_L$, then the azimuthal angle θ is calculated by:

$$\theta = \theta_L + R_n \cdot \Delta\theta_L \ , \tag{3-6}$$

where R_n is the random number. Since the polar angle is cosine distributed, then the cosine of the polar angle is uniformly distributed. Thus, the z-axis direction cosine C can be computed from knowing the cosine of the lower limit C_L and the cosine width ΔC_L. Selecting another uniformly distributed random number R_n, C is calculated as shown below:

$$C = C_L + R_n \cdot \Delta C_L \ . \tag{3-7}$$

The direction cosines for the x- and y-axes can now be calculated from the trigometric relations:

$$A = \cos\theta \sqrt{1 - C^2} \ , \tag{3-8}$$

$$B = \sin\theta \sqrt{1 - C^2} \ , \tag{3-9}$$

where $\sqrt{1 - C^2}$ is the sin of the polar angle. In this manner, ANGBIN determines the direction cosine (A, B, C) of a direction uniformly distributed over the input angular bin.

CHAPTER IV

METHODS DEVELOPMENT

The theoretical discussion of the iterative forward-adjoint Monte Carlo method in Chapter II demonstrated the validity of the method for biasing the sampling distributions in continuous phase space. However, the solution of most practical radiation transport problems requires the use of high speed computers and the reduction of continuous phase space to finite phase cells in energy, position, and direction. Chapter III has already introduced the phase cell structure which is employed in IFAM, but it did not answer the important question of the validity of the finite cell's approach. This question can only be answered by the development of methods for applying the information obtained during the opposite mode calculation and then testing these methods on real radiation transport problems. Methods development will be addressed in this chapter, and the results of applying these methods to radiation transport problems are given in Chapter V.

The central problem in the development of methods for biasing of our sampling distributions is to define the importance function. This problem is discussed in Section 4.1, where the form, format, and restrictions which were placed on the importance functions are described in detail. Application of the importance function to the sampling distributions is discussed in the order that IFAM employs them. Section 4.2 describes the biasing on the source distribution in both energy and

direction. The transport of the particle or adjuncton is next in IFAM, so Section 4.3 defines various techniques considered for the biasing of the transport kernel. The mathematical justification of these techniques is given and inherent problems and restrictions are discussed. The major problems encountered during this research were caused by the use of importance sampling techniques on the transport kernel. However, since many important radiation transport problems (e.g., any involving deep penetrations) require altered transport kernels, considerable effort was spent in resolving these difficulties.

Following selection of the collision site with the altered transport kernel, the outgoing energy and direction must be selected from the collision kernel. Methods were also developed for altering the sampling from the collision kernel by using the importance function. These methods are discussed in Section 4.4. The first four sections emphasize the development of importance sampling methods. Section 4.5, which is independent of importance sampling, contains a brief description of a technique for avoiding the infinite variance problem when estimating the response at a point detector with the statistical estimation or expected value method. This technique was required because the detector is contained in a scattering region, thus allowing the possibility of an "infinite" estimate.

4.1 The Importance Function

The theoretical application of an importance function for altering or biasing the sampling distributions in a Monte Carlo radiation transport calculation were discussed in Section 2.3. In Section 3.4, the

computer routines which generate the importance function were described in sufficient detail to explain the logical flow of the IFAM test bed. In this section, the analytical and computational rationale for the specific forms of the importance function will be given. As stated in Section 2.3, the importance function was used to alter the sampling distributions, but the bias introduced was removed by correcting the weight (e.g., the source particle is selected from the altered source distribution S'(P), but the weight assigned to that particle is the ratio of the natural or true distribution, S(P), to S'(P)).

The initial consideration in developing the importance function was what quantity should be stored during a given mode (forward or adjoint) calculation for defining the importance function for the opposite mode. The theoretical considerations of Chapter II indicated that a proper quantity would be the adjoint to the integral equation being simulated by the Monte Carlo procedure. Analysis revealed the fact that the adjoint angular flux, $\chi_g^*(\bar{x},\bar{\omega})$ or $\Phi_g^*(\bar{x},\bar{\omega})$, is adjoint to the emergent particle density (equation 2-92). The forward angular flux, $\Phi_g(\bar{x},\bar{\omega})$, is the quantity "adjoint" to the integral equation (2-117) simulated during the adjoint mode (i.e., the "adjoint" to the adjoint equation is the "forward" angular flux). Table 1, page 76, shows that each of these two quantities can be estimated by two different techniques. The first technique is based on the collision density (i.e., $\psi = \Sigma_t \Phi$). The forward or adjoint flux is estimated by dividing the statistical weight at a collision point by the group cross section. The second technique is based on the track length in a region. Since the average flux in a given region is equal to the total track length of all particles crossing the region divided by the

region volume, then the flux (forward or adjoint) can be estimated during the Monte Carlo simulation by dividing the product of the statistical weight times the path length in a given region by the region volume. Both of these techniques have the attribute of requiring the same code design for both the forward and adjoint mode calculations.

For a given test run, only one of these techniques can be used to estimate the forward or adjoint angular flux. Therefore, it is not necessary to store both the collision density and track length flux estimators, and core storage is set aside for only one of these estimates. The track length estimator has been examined most thoroughly, since it provides an estimate of the flux in a region whenever the particle's path intercepts the region, although no collision occurs there. The track length estimates are stored in the IFA version of the NXTCOL subroutine. The statistical weight used to multiply the track length in each region is computed at the next collision point or at the escape point. Track length data are stored in NXTCOL/IFA until this weight is determined, and then a running sum of the product of the weight and track length is stored as a function of energy, region, and direction. Division by the region volume is performed for the sum of these estimates in the FAIF subroutine.

Storage of the collision density estimator occurs after the transport step (CALL NXTCOL) and before the collision step (CALL COLISN) in the MORSE subroutine. Like the track length estimator, a running sum of the statistical weight is stored for the energy group, region, and angular bin of the particle at the collision point. This sum is divided by the group cross section to produce the proper angular flux estimate. Because of the similarities between these calculations and those for the MORSE

scattering counters, these data have been put in blank common immediately following the energy and region dependent track length array.

At the beginning of the subsequent mode calculation, these data are summed with the track length or collision density estimates from previous IFAM iterations. Provision has been made to use only the previous mode data for the estimates, but the statistics are very poor. This practice was soon discounted as a reasonable method of determining the track length or collision density estimates for the importance function.

Although the theoretical analysis indicated that the adjoint to the integral equation being simulated was a proper choice for the importance function, computational considerations place certain restrictions on this choice. The initial restriction is due to the fact that it is highly unlikely for each finite cell in phase space to have an accurate estimate of the forward or adjoint flux. For example, consider the test problem, which has 15 energy groups, 42 importance regions, and 18 angular bins, or a total of 11,340 phase cells. Even if the histories were uniformly distributed over these cells (of course they are not), ten percent accuracy would require over a million estimates. This is an impractical requirement, so a procedure was developed to use already available importance information in addition to the Monte Carlo "adjoint function" estimate. This procedure can be represented by the following equation:

$$I(i,j,k) = a_n \, J(i,j,k) + (1-a_n) \, C(i,j,k) \ , \qquad (4\text{-}1)$$

where

$(i,j,k) \equiv$ indices of the phase cell for the energy group, region, and angular bin, respectively,

$I(i,j,k) \equiv$ importance function for the (i,j,k) phase cell,

$a_n \equiv$ a parameter which is dependent on the number of iterations or histories that have been executed ($0 < a_n < 1$),

$J(i,j,k) \equiv$ normalized angular flux estimate from the opposite mode calculations for the (i,j,k) phase cell,

$C(i,j,k) \equiv$ normalized input value for the (i,j,k) phase cell.

Equation 4-1 allows the IFAM test bed to increase the reliance on the "adjoint" flux (which is the forward angular flux for altering the distributions for the adjoint integral equation simulation) as the statistical accuracy of that estimate increases. This is done by increasing a_n. One method that has been used is to define a_n by $n/(n+1)$, where n is the number of iterations. Another possibility is to pick some minimum number of histories, say m, then set a_n to $n/(n+m)$, where n is the total number of histories completed for the specified mode. The importance function thus approaches the J(i,j,k) value as the number of histories increases. Also, requiring that C(i,j,k) must be positive (> 0) and that a_n must be less than one assumes that no cell in phase space will have zero importance. This is a potential danger when only J(i,j,k) is used in the importance function. One very good choice of C(i,j,k) is the adjoint flux from discrete ordinates calculation where the finite cells in phase space used in the discrete ordinates and IFAM are matched as closely as possible.

The importance function defined by Equation 4-1 provides the basis for altering the Monte Carlo sampling distributions in IFAM. As discussed above, there exist several options for determining each of the major parameters in the equation (a_n, J(i,j,k), and C(i,j,k)). The result of choosing a representative range is given in the next chapter. In

addition, the most useful form of the importance function depends on the particular sampling distribution being altered. The next three sections discuss the forms in which I(i,j,k) is applied.

4.2 Source Biasing

Selection of a source particle usually requires that an energy group, spatial position, direction, and age be selected from the distribution functions. For the IFAM test bed, the age is assumed to be zero and the spatial position assigned at the input source point. Then an energy group and direction are selected from the altered distribution functions. While selection of an energy group and angular bin is possible from a joint probability distribution function, the method used in IFAM is consistent with the MORSE procedure of selecting the energy group from the marginal distribution function, then selecting the angular bin from the conditional probability function given in the above energy group. The specific direction is defined by selecting the direction cosines so that the direction vector is uniform over the previously chosen angular bin. Details of this methodology are discussed below.

Consider first the selection of an energy group. The natural energy dependent source distribution is one of the default input options for IFAM. To generate the altered energy group distribution function, the energy and region dependent marginal importance function is computed as shown below:

$$I'(i,j,k) = I(i,j,k) \Big/ \sum_i \sum_k I(i,j,k) \,, \qquad (4\text{-}2)$$

where I(j,j,k) is defined by Equation 4-1. This new importance function, I'(i,j,k) is now normalized on a region basis. Next, the marginal distribution for the energy groups and importance regions is computed from I'(i,j,k):

$$I'_k(i,j) = \sum_k I'(i,j,k) \quad . \tag{4-3}$$

The final step in defining the altered energy dependent source distribution, $\tilde{S}(i)$ is:

$$\tilde{S}(i) = S(i)\cdot I'_k(i,j_s) / \sum_i [S(i)\cdot I'_k(i,j_s)] \quad , \tag{4-4}$$

where S(i) is the input natural distribution and j_s is the importance region which contains the source. Note that the distribution has been normalized, so that the initial statistical weight for a source energy group of i_s is given by:

$$W_s^i = S(i_s)/\tilde{S}(i_s) \quad . \tag{4-4}$$

Only the source direction remains to be determined. As in the source energy selection, the importance function for the region containing the source point is used to supply angular biasing information. Since the energy group and region are known, then the proper importance function to be used is $I'(i_s,j_s,k)$. Defining $D(i_s,j_s,k)$ as the angular bin distribution function, then the angular bin is chosen from:

$$\tilde{D}(i_s,j_s,k) = D(i_s,j_s,k)\cdot I'(i_s,j_s,k) \div \sum_k [D(i_s,j_s,k)\ I'(i_s,j_s,k)] \quad . \tag{4-5}$$

After the angular bin, k_s, has been randomly chosen from (4-5), the direction cosines from the direction vector are determined in the ANGBIN subroutine, as discussed in Section 3.4. However, the use of $\tilde{D}(i_s,j_s,k)$ instead of $D(i_s,j_s,k)$ for the selection of the outgoing angular bin means that the statistical weight must be corrected. The final statistical weight for the source is given by:

$$W_s^f = W_s^i \cdot D(i_s,j_s,k_s)/\tilde{D}(i_s,j_s,k_s) \quad . \tag{4-6}$$

For the special case where the source is isotropic, Equations 4-5 and 4-6 can be written in a much simpler form:

$$\tilde{D}(i_s,j_s,k) = I'(i_s,j_s,k)/I'_k(i_s,j_s) \quad , \tag{4-7}$$

$$W_s^f = W_s^i/[k_{max} \cdot I'_k(i_s,j_s)] \quad , \tag{4-8}$$

where $I'_k(i_s,j_s)$ is defined by Equation 4-3 and k_{max} is the total number of angular bins. The two equations above were used for the test problem.

4.3 The Altered Transport Kernel

The most difficult of the regular Monte Carlo sampling distributions to alter with the generated importance function is the transport kernel. The reason is that the transport kernel is a continuous exponential function, whereas the importance function is a set of numerical values, one for each finite cell in phase space. The importance function is easily applied to the discrete sample space of the source and collision

kernel, but this is not the case for the transport kernel. To better understand the mathematical foundation, consider the following form of Equation 2-62:

$$\chi(\bar{x},\bar{E}) = S(\bar{x},\bar{E}) + \int C(\bar{E}|\bar{E}';\bar{x})\ T(\bar{x}|\bar{x}';\bar{E}')\ \chi(\bar{x}',\bar{E}')d\bar{x}'d\bar{E}' \ . \tag{4-9}$$

All quantities are defined the same as in Chapter II.

Now, as in Section 2.3, multiply the equation above by the importance function, represented by $I(\bar{x},\bar{E})$. Letting:

$$\chi(\bar{x},\bar{E})\ I(\bar{x},\bar{E}) \equiv \hat{\chi}(\bar{x},\bar{E}) \ , \tag{4-10}$$

and

$$S(\bar{x},\bar{E})\ I(\bar{x},\bar{E}) \equiv \hat{S}(\bar{x},\bar{E}) \ , \tag{4-11}$$

then

$$\hat{\chi}(\bar{x},\bar{E}) = \hat{S}(\bar{x},\bar{E}) + \int C(\bar{E}|\bar{E}';\bar{x})\ T(\bar{x}|\bar{x}';\bar{E}') \tag{4-12}$$

$$\times\ [I(\bar{x},\bar{E})/I(\bar{x}',\bar{E}')]\ \hat{\chi}(\bar{x}',\bar{E}')d\bar{x}'d\bar{E}' \ .$$

Consider the following part of the integral term of (4-12):

$$C(\bar{E}|\bar{E}';\bar{x})\ T(\bar{x}|\bar{x}';\bar{E}')[I(\bar{x},\bar{E})/I(\bar{x}',\bar{E}')] = [I(\bar{x},\bar{E})/I(\bar{x},\bar{E}')] \tag{4-13}$$

$$\times\ C(\bar{E}|\bar{E}';\bar{x})[I(\bar{x},\bar{E}')/I(\bar{x}',\bar{E}')]\ T(\bar{x}|\bar{x}';\bar{E}') \ .$$

Inspection of the right hand side of the above equation shows that the importance function ratio has been separated into the product of two

ratios, the first of which seems to apply naturally to altering the collision kernel and the second to the transport kernel. For example, the ratio multiplying the transport kernel is just the ratio of the importance functions at the beginning of the transport step ($\bar{x}'$) to that which describes the energy and direction during the transport step, as would be expected from physical considerations.

To use the altered transport kernel, some method for sampling must be devised. This is a non-trivial problem, since the representation of the kernel in the Monte Carlo simulation for the discrete phase is:

$$\bar{T}(0\rightarrow R)dR = (I_n/I_1)\ \mu_n \exp - \left[\sum_{j=1}^{n-1} \mu_j(R_j-R_{j-1}) + \mu_n(R-R_{n-1})\right]dR, \quad (4\text{-}14)$$

where I_i is the importance function value in the i^{th} region which the path of the particle intersects, with the collision assumed to occur in the n^{th} region. The total group cross section for region i is represented by μ_i, and R_i is the distance to the i^{th} region boundary. The distance from the source point to the collision point is R, and R_o is defined as 0. If the collision occurs in the same region as the starting point, then the summation term (from j = 1 to 0) is just 0. Note that, if the importance function ratio in the right hand side of Equation 4-14 is dropped, then the remaining statement is just the natural transport kernel, T(0→R)dR.

The problem with sampling from Equation 4-14 is that the kernel is not in general normalized, that is:

$$\int_0^\infty \bar{T}(0\rightarrow R)dR \neq 1 \quad (4\text{-}15)$$

This can be seen from the following representation:

$$\int_0^\infty \bar{T}(0\to R)\,dR = \sum_{i=1}^{\infty} \int_{R_{i-1}}^{R_i} (I_i/I_1)\,\mu_i \exp - \Big[\sum_{j=1}^{i-1} \mu_j (R_j - R_{j-1}) + \mu_i (R - R_{i-1}) \Big]\, dR \qquad (4\text{-}16)$$

$$\int_0^\infty \bar{T}(0\to R)\,dR = I_1^{-1} \Big[I_1 + (I_2 - I_1) \exp - (\mu_1 R_1) + (I_3 - I_2) \exp - \Big(\sum_{j-1}^{2} \mu_j (R_j - R_{j-1}) \Big) + \ldots \Big] \qquad (4\text{-}17)$$

or

$$\int_0^\infty \bar{T}(0\to R)\,dR = 1 + I_1^{-1} \cdot \sum_{i=1}^{\infty} (I_{i+1} - I_i) \exp - \Big[\sum_{j=1}^{i} \mu_j (R_j - R_{j-1}) \Big] . \qquad (4\text{-}18)$$

Note that, for the special case where all I_i's are equal, then the altered kernel reduces to the natural kernel and is, of course, normalized.

By forcing each path to an escape boundary and determining the value of Equation 4-18, a normalized kernel can be constructed, but the additional computation time will be excessively large for problems with many regions. If this procedure is used, then the new kernel is defined by:

$$\hat{T}(0\to R)\,dR = \bar{T}(0\to R)\,dR \Big/ \int_0^\infty \bar{T}(0\to R)\,dR \ , \qquad (4\text{-}19)$$

where the integral must be evaluated for every transport step.

The usual procedure employed in the alteration or biasing of the transport kernel is to multiply the total group cross section term, μ_i, by a fixed value. This technique can be extended to multiplication by a

variable which depends on the position. For the problems of interest, the assumption of a region dependent parameter is valid, as shown below. Let:

$$\mu_i' = C_i \mu_i \ , \tag{4-20}$$

where C_i is the region dependent parameter for a given path. This means that C_i can be energy, direction, and even initial position dependent. Defining the altered transport kernel by:

$$\bar{T}(0 \to R)dR = \mu_i' \exp - \left[\sum_{j=1}^{i-1} \mu_j'(R_j - R_{j-1}) + \mu_i'(R - R_{i-1}) \right] dR \ , \tag{4-21}$$

produces a normalization factor of:

$$\int_0^\infty \bar{T}(0 \to R)dR = \sum_{i=1}^{\infty} \int_{R_{i-1}}^{R_i} C_i \mu_i \exp - \left[\sum_{j=1}^{i-1} C_j \mu_j (R_j - R_{j-1}) \right. \tag{4-22}$$

$$\left. + C_i \mu_i (R - R_{i-1}) \right] dR \ ,$$

$$= \sum_{i=1}^{\infty} \left\{ \exp - \left[\sum_{j=1}^{i-1} C_j \mu_j (R_j - R_{j-1}) \right] \int_{R_{i-1}}^{R_i} C_i \mu_i \right. \tag{4-23}$$

$$\left. \times \exp - \left[C_i \mu_i (R_i - R_{i-1}) \right] dR \right\} \ ,$$

$$= \sum_{i-1}^{\infty} \exp - \left[\sum_{j=1}^{i-1} C_j \mu_j (R_j - R_{j-1}) \right] \tag{4-24}$$

$$\times \left\{ 1 - \exp - \left[C_i \mu_i (R_i - R_{i-1}) \right] \right\} \ ,$$

$$= \sum_{i=1}^{\infty} \left\{ \exp - \left[\sum_{j=1}^{i-1} C_j \mu_j (R_j - R_{j-1}) \right] \right. \tag{4-25}$$

$$\left. - \exp - \left[\sum_{j=1}^{i} C_j \mu_j (R_j - R_{j-1}) \right] \right\} .$$

Expansion of the above equation reveals that the negative exponential term for i = n is the same as the positive exponential term for i = n+1. Thus, each of these pairs cancels, leaving only the positive term for i = 1. Since the summation from j = 1 to 0 was previously shown to be 0, then the normalization factor is the exponential of 0 or:

$$\int_0^{\infty} \bar{T}(0 \rightarrow R)\, dR = 1 . \tag{4-26}$$

This proves that any altered transport kernel which is based on replacing the total group cross section μ_i with the product of a region-dependent parameter C_i and μ_i is normalized. An example of C_i is the reciprocal of the constant path length stretching parameter BIAS used in MORSE code. (Note that, although BIAS is computed as a region, energy- and direction-dependent parameter, only the one value for the starting point of the path is used to alter the cross section for all subsequent regions intersected by that path.) Another example of C_i is the region importance function I_i for a specified path (and hence energy group and angular bin). Usually I_i is put through some normalization process, such as:

$$C_i = I_i / I_1 , \tag{4-27}$$

or:

$$C_i = I_i \sum_j \lambda_j / \sum_j I_j \lambda_j \quad . \tag{4-28}$$

The summation of j is for the regions along the projected path of the particle or adjuncton, and λ_j could be the mean free path through region j.

Two methods have been examined for the implementation of the importance function in the altered transport kernel. Both methods use the concept of total cross section alteration by C_i, since the normalization factor for the altered kernel is unity. The first method will be described without including the path length stretching capabilities available in the MORSE code. However, these capabilities are included in the methods implemented in IFAM and their addition to the method will be discussed later. The notation will continue to denote region dependence only, since the energy and direction are fixed during the transport step. The major steps of the first method are outlined and described below:

1. Select MFP, the number of mean free paths, from an exponential distribution. Both the natural and altered transport kernels are exponentially distributed, as indicated by Equation 4-21, where C_i is unity in every region for the natural distribution. For this method, our next collision point will occur at MFP mean free paths along the path as determined by the altered cross sections. The collision point will, in general, be different from the point at which MFP mean free path is reached by using the real cross section along the path.

2. Determine the search length, ETA, from a preselected input value. The purpose of ETA is to define the number of mean free paths

along the projected path at which the importance function I_i, cross section μ_i, and path length t_i data will be found. Beyond this search length, the cross sections will not be altered. ETA is arbitrary, but should be sufficiently large to assure that more than one region is intersected before ETA mean free paths are reached. ETA should not be so large that the probability of reaching ETA mean free paths is very small (e.g., 10 mean free paths). IF MFP is greater than ETA, then a normal transport game will be played.

3. Using the combinatorial geometry routines of IFAM, step through the geometry, determining for each region which the path intersects (out to ETA mean free paths):

I_i = importance function value for the i^{th} region intersected by the path (i = 1 is the starting point region)

t_i = track length through the i^{th} region

μ_i = group cross section for the i^{th} region

λ_i = mean free path through the i^{th} region ($\lambda_i = \mu_i t_i$).

The I_i, t_i, and λ_i data are stored for future use. The region cross section is not stored since λ_i and t_i define μ_i, and μ_i is not needed in the computation technique. As a mathematical convenience, the region containing the end of the search length ETA will be assigned two index numbers. That portion of the region beyond ETA will be m+1, and that part of the path will not require an altered cross section.

4. Calculate the altered mean free path through each region based on the constraint that the sum of the altered mean free paths, λ_i', equals the sum of the real mean free paths, λ_i. That is:

$$\sum_{i=1}^{m} \lambda_i = \sum_{i=1}^{m} \lambda_i' \ , \tag{4-29}$$

where λ_i' is defined as:

$$\lambda_i' = C \ I_i \lambda_i \ . \tag{4-30}$$

The constant of proportionality, C, for Equation 4-30, can be calculated from Equation 4-29:

$$C = \sum_{i=1}^{m} \lambda_i / \sum_{i=1}^{m} I_i \lambda_i \ . \tag{4-31}$$

Inspection of the above equations reveals the fact that the altered cross section that corresponds to λ_i' can be written in the form of Equation 4-28, where:

$$C_i = C \ I_i \ . \tag{4-32}$$

Therefore, the altered transport kernel has the same form as Equation 4-21 and hence is properly normalized to unity.

5. Calculate the distance along the path at which MFP mean free paths have been traversed as determined by the altered mean free paths in each region. This step is equivalent to selecting the distance R from the altered transport kernel. The computational procedure is shown below:

a) Define the ℓ^{th} region by:

$$\sum_{i=1}^{\ell-1} \lambda_i' \leq \text{MFP} < \sum_{i=1}^{\ell} \lambda_i' \ . \tag{4-33}$$

b) Determine the distance R from the starting point by:

$$R = \sum_{i=1}^{\ell-1} t_i + t_\ell \cdot \left(MFP - \sum_{i=1}^{\ell-1} \lambda_i'\right)/\lambda_\ell' \quad . \tag{4-34}$$

The calculation of R consists of accumulating the distance up to the ℓ^{th} region and then adding that fraction of the distance that R goes into the ℓ^{th} region. The collision point, $\bar{r}$, in three dimensional space is calculated quite easily since the starting point, $\bar{r}'$, and the direction cosines of the path are known.

6. Since the above procedure produced a collision point different from that which would be obtained in selecting from the natural transport kernel, the statistical weight will be corrected to remove the bias. The weight correction is just the ratio of the natural to the altered transport kernel evaluated at the selected distance (R).

$$W_c = \frac{T(0\rightarrow R)}{\tilde{T}(0\rightarrow R)} = \frac{\mu_\ell \exp - \left[\sum_{i=1}^{\ell-1} \lambda_i + \mu_\ell (R-R_{\ell-1})\right]}{\mu_\ell' \exp - \left[\sum_{j=1}^{\ell-1} \lambda_j' + \mu_\ell' (R-R_{\ell-1})\right]} \quad , \tag{4-35}$$

where

$$R_{\ell-1} = \sum_{i=1}^{\ell-1} t_i \quad .$$

Since the ratio of μ_ℓ to μ_ℓ' is the same as λ_ℓ to λ_ℓ', and the exponential factor in the denominator is MFP, then the weight correction is just:

$$W_c = \frac{\lambda_\ell}{\lambda_\ell'} \exp(MFP - CMFP) \quad . \tag{4-36}$$

The term CMFP is just the true mean free path from the starting point to the collision point. It is computed in the same manner as R in Equation 4-34, with the t_i and t_ℓ replaced by λ_i and λ_ℓ, respectively.

The above procedure should produce an unbiased game, since the bias introduced by altering the transport kernel (Steps 1-4) is compensated by correcting the statistical weight. Additional changes have been made to the procedure to allow for the regular path length stretching. The technique implemented requires only that the search length ETA be multiplied by the bias term (BIAS) in Step 2 and then Equation 4-31, which defines the constant of proportionality, must include a division by BIAS. No other changes are necessary to implement the use of MORSE path length stretching. Some additional logic was added to handle the special cases where the search length is contained in one region and where an escape occurs. The computational requirement for a single region path is much less than for the above procedure. The logic for the escape condition is such that the above procedure is used unless the escape would have occurred in a regular MORSE run.

The second method which was investigated for application of the importance function attempts to determine a pseudo-cross section which produces the same transport kernel as given by Equation 4-14. This method is based on Equations 4-14 to 4-21, and requires a solution of C_i. That is, set:

$$C_i\mu_i \exp - \left[\sum_{j=1}^{i} C_j\mu_j(R_j-R_{j-1})\right] \tag{4-37}$$

$$= (I_i/I_1)\mu_i \exp - \left[\sum_{j=1}^{i} \mu_j(R_j-R_{j-1})\right] .$$

This equation can be written in the following form:

$$C_i = (I_i/I_1) \prod_{j=1}^{i} \exp - \left[(1-C_j)\ \mu_j(R_j-R_{j-1})\right] . \qquad (4\text{-}38)$$

Equation 4-38 is transcendental, but solution by trial and error seemed feasible. It can be shown that:

$$C_i = (I_i/I_{i-1})\ C_{i-1} \exp - \left[(1-C_i)\ \mu_i(R_i-R_{i-1})\right] \qquad (4\text{-}39)$$

and

$$C_1 = 1 . \qquad (4\text{-}40)$$

Thus, it is possible to solve (4-39) recursively. However, not all combinations of $(I_i/I_{i-1})\ C_{i-1}$ and $\mu_i(R_i-R_{i-1})$ allow a real solution, so the use of this procedure is severely restricted.

4.4 The Altered Collision Kernel

The collision step takes the incoming energy and direction parameters at the collision point selected by the transport step and generates the outgoing energy and direction parameters. The major effort in altering the collision kernel with the importance function during this research has been to bias the selection of the energy group toward the more important groups. Equation 4-13 indicates that a proper importance function is just the ratio of the importance, $I(\bar{x},\bar{E})$, for the possible outgoing energies and directions to the incoming importance, $I(\bar{x},\bar{E}')$. Representing the kernel in the finite phase cell indices format yields:

$$[I(i_c,j,k)/I(i_c,j_c,k_c)]\cdot C(i_c;j_e\rightarrow j,k_c\rightarrow k)$$

as the altered kernel, where the subscript c on the indices denotes the incoming collision parameters.

To select from the altered kernel, it must be normalized at each scattering event. This is done by adjusting the statistical weight to account for the absorption probability as discussed in Section 3.2. Normalization to account for the importance function in the altered collision kernel is performed as shown below:

$$\bar{C}_E(i_c,j_c\rightarrow j) = N_E^{-1} \cdot I_k'(i_c,j)\cdot P(i_c,j_c\rightarrow j) \qquad (4\text{-}41)$$

where $I_k'(i_c,j)$ is defined by Equation 4-3. $P(i_c,j_c\rightarrow j)$ is the natural probability of scattering from group j_c into group j. N_E is the normalization factor, given by:

$$N_E = \sum_{j=1}^{NDS} I_k'(i_c,j)\ P(i_c,j_c\rightarrow j)\ , \qquad (4\text{-}42)$$

where NDS is the number of down scattering groups. This method was easily adapted to the available MORSE coding with the energy importance data being replaced by $I_k'(i,j)$.

Methods to alter the selection of the direction have not been implemented for the collision step. Work by other researchers has revealed that the technique of sampling from the importance function suffers from the generation of negative weights [45]. This is due to the fact that the reconstruction of the natural scattering distribution from the

Legendre moments results in negative values. For some problems, as many as 20 percent of the weights may be negative after correcting for sampling from the importance function. These researchers are examining the feasibility of altering just the probability of scattering into the discrete angles used in MORSE. This technique avoids the negative weight problem, and preliminary calculations indicate a variance reduction for a highly directional problem.

4.5 Exclusion Volume Contribution

The methods developed in this research are to be applied to the difficult point source - point detector problem. This class of transport problem usually uses "statistical" or "test flight" estimations to evaluate the detector response. However, these problems suffer from the so-called "infinite variance" problems whenever the detector is located in a scattering region. The infinite variance problem is due to the fact that the response estimator has an R^{-2} term, where R is the collision to detector point separation. For collisions very near the detector point, R^{-2} is very large, and hence the contribution from those collisions dominates the response estimate and produces a much larger response than the actual value. One method of overcoming this problem is to place an exclusion region about the detector point. The response contribution from any collision occurring in the region is neglected. This procedure obviously produces low response estimates.

To prevent the "infinite variance" problem and at the same time include the contributions from collisions near the detector, the following technique was developed. Assume that the collision density within

the exclusion region is uniform, then a collision of point $\bar{r}$ within the region could have occurred with equal probability at any point in the region. Thus, a collision with incoming energy E_i and direction $\bar{\omega}_i$ which has a statistical weight of W_i will have the following flux contribution:

$$<\Phi(E)> = \frac{W_i}{V_{exc}} \iint \mu_s(E_i)/\mu(E_i)\ P(E_i \rightarrow E, \bar{\omega}_i \rightarrow \bar{\omega}) \tag{4-43}$$

$$\times \exp - \left[\int_0^r \mu(r')dr'\right]/r^2\ d\bar{\omega}d\bar{r}\ ,$$

where

V_{exc} = volume of the exclusion region

$\mu_s(E_i)$ = scattering cross section for energy E_i.

If we make the exclusion region a sphere of radius R, then:

$$<\Phi(E)> = \frac{W_i}{V_{exc}} \left[\frac{\mu_s(E_i)}{\mu(E_i)} P(E_i \rightarrow E)\right] \int_0^R r^2 \exp - \left[\int_0^r \mu(R')dR'\right]/r^2 \tag{4-44}$$

$$\times \int P(\bar{\omega}_i \cdot \bar{\omega})d\bar{\omega}dr\ .$$

The term in brackets outside of the integral is just the post collision weight W_s, and the integral over the direction $\bar{\omega}$ is unity. The integral over r can be evaluated if a $\mu(E)$ term is introduced. This yields:

$$<\Phi(E)> = [W_s/(\mu(E) \cdot V_{exc})] \cdot [1 - \exp(\mu(E) \cdot R)]\ . \tag{4-45}$$

This contribution is computed for each collision in the exclusion region and added to the total flux calculation so that the response due to these collisions can be estimated.

CHAPTER V

RESULTS AND CONCLUSIONS

The purpose of this research effort was to develop a computer test bed for examining the iterative forward-adjoint Monte Carlo method and to evaluate that method. Chapters II, III, and IV contain a comprehensive discussion of the theoretical basis for the forward-adjoint Monte Carlo method, the development of the IFAM test bed, and the variance reduction techniques that have been implemented in IFAM. In this chapter, a summary of computation results will be given to support the conclusions which are presented.

The first results discussed here are for IFAM runs of three iterations with various importance biasing methods in effect. These methods include source direction biasing, source energy biasing, and transport kernel biasing. For comparison, a run with no biasing and another run with all of the biasing methods discussed in Chapter IV were made. The problem considered is a cylinder of air with a point fission source and point detector. The detector response function is the Henderson tissue dose. Appendix C contains a detailed description of this problem. However, the example output is for a source-detector separation of 600 meters, whereas the results discussed in this chapter are for a separation of 300 meters. The reason for selecting this particular problem is the existence of extensive analytical and experimental results which can be used to validate the IFAM results [46-48].

Table 2 contains a summary of the IFAM results for the five runs. The uncollided dose is denoted by D_u, D_{exc} is the contribution of collisions in the exclusion volume (see Section 4.5) to the total dose estimate, and the total dose is denoted by D_T. The symbol FSD following each dose value stands for the fractional standard deviation, which is defined as the square root of the sample variance of the mean divided by the mean value of the dose estimate. This quantity is the statistical estimate calculated by the MORSE and IFAM codes. The UNIVAC 1108 run time is also given, as well as the number of scattering events for each mode. Two estimates of the "goodness" of the variance reduction method are also presented. The efficiency is defined as the reciprocals of the square of the fractional standard deviation times the relative run time (which is 0.1 times the run time). The use of the relative run time was for convenience in plotting the results, and since the efficiency is a relative measure of goodness instead of an absolute measure, it has no effect on the conclusions. The second measure is denoted as the "% Error" and is based on the Henderson tissue dose calculated by the two-dimensional DOT-III Discrete Ordinates computer code for the cylinder of air. That is:

$$\% \text{ Error} = 100 \cdot (D_s - D_T)/D_s \ , \qquad (5\text{-}1)$$

where D_s is the DOT-III calculated value of 3.408×10^{-19} rads. Note that this measure does not include any consideration for the computational effort required (such as the run time).

The arrangement of Table 2 is such that both mode calculation results for a given iteration are adjacent and are in the same row as the

Table 2. Air Cylinder Calculations

1st Iteration	No Biasing		Source Direction Biasing		Source Energy Biasing		Transport Kernel Biasing		All Biasing	
	A	F	A	F	A	F	A	F	A	F
D_u	0.211	0.214	0.211	0.214	0.211	0.214	0.210	0.213	0.211	0.205
FSD	.013	.017	.013	.022	.013	.014	.014	.012	.013	.020
D_{exc}	0.953	1.351	0.953	1.986	0.953	1.616	1.238	1.197	0.953	3.139
FSD	.627	.156	.627	.213	.627	.223	.539	.287	.627	.744
D_T-D_{exc}	2.359	2.012	2.359	2.084	2.359	2.042	2.629	2.137	2.359	2.439
D_T	3.312	3.363	3.312	4.070	3.312	3.658	3.867	3.336	3.312	5.578
FSD	.189	.074	.189	.120	.189	.116	.168	.123	.189	.452
Run Time	400	1030	330	970	390	1020	390	1030	390	990
Scattering	21927	77121	21927	84503	21927	77135	21654	79910	21927	74830
Efficiency	0.699	1.772	0.848	0.715	0.717	0.728	0.908	0.642	0.717	0.049
% Error	2.816	1.320	2.816	-19.424	2.816	-7.335	-13.468	2.112	2.816	-63.673

Table 2. Continued

2nd Iteration	No Biasing		Source Direction Biasing		Source Energy Biasing		Transport Kernel Biasing		All Biasing	
	A	F	A	F	A	F	A	F	A	F
D_u	0.208	0.213	0.213	0.214	0.206	0.210	0.207	0.209	0.210	0.219
FSD	.013	.013	.027	.026	.011	.013	.009	.011	.018	.028
D_{exc}	0.999	1.344	0.679	1.007	1.878	1.371	0.034	1.187	0.658	1.114
FSD	.652	.138	.801	.234	.383	.173	.576	.220	.276	.234
D_T-D_{exc}	2.637	2.079	2.722	2.264	2.274	2.106	2.323	1.935	2.141	2.019
D_T	3.636	3.423	3.401	3.271	4.152	3.477	2.357	3.122	2.799	3.133
FSD	.192	.071	.243	.112	.200	.087	.138	.104	.177	.095
Run Time	370	1030	310	920	480	1000	380	970	420	920
Scattering	21467	77504	21775	80086	29133	76311	22310	74532	24966	69531
Efficiency	0.733	1.925	0.546	0.866	0.520	1.321	1.381	0.953	0.759	1.204
% Error	-6.690	-0.44	0.205	4.019	-21.830	-2.024	30.839	8.392	17.869	8.069

Table 2. Concluded

3rd Iteration	No Biasing		Source Direction Biasing		Source Energy Biasing		Transport Kernel Biasing		All Biasing	
	A	F	A	F	A	F	A	F	A	F
D_u	0.211	0.212	0.207	0.208	0.209	0.206	0.205	0.213	0.221	0.212
FSD	.012	.015	.020	.028	.013	.012	.013	.013	.022	.035
D_{exc}	0.769	1.326	1.648	1.079	1.350	1.174	0.908	1.293	0.921	1.195
FSD	.781	.178	.374	.273	.344	.180	.413	.195	.268	.216
D_T-D_{exc}	2.445	2.279	2.077	1.964	2.492	2.125	2.604	2.005	2.478	1.918
D_T	3.214	3.605	3.725	3.043	3.842	3.299	3.512	3.298	3.399	3.113
FSD	.273	.088	.213	.123	.127	.082	.306	.114	.171	.096
Run Time	390	1030	320	920	530	990	370	940	470	870
Scattering	21887	77907	21718	80917	31953	75313	21208	72161	28080	64843
Efficiency	0.344	1.253	0.688	0.718	1.169	1.502	0.288	0.818	0.727	1.247
% Error	5.692	-5.78	-9.30	10.71	-12.734	3.198	-3.051	3.227	0.264	8.656

results for the other cases for that iteration. The headings A and F denote the adjoint and forward modes, respectively. The total dose estimate, D_T, the total dose estimate from collisions outside the exclusion volume, D_T-D_{exc}, and the efficiency have been plotted as a function of the iteration/mode sequence for the five test cases in Figure 10. Figures 11-15 show the total dose for five cases and include error bars representing plus and minus one standard deviation.

Inspection of Table 2 and Figures 10 and 15 indicates that the utility of the "all FAI biasing" technique for the air cylinder problem is questionable. However, it should be noted that the dose calculated for the first mode - first iteration, which is done with no biasing, is a particularly good result. Other calculations, which were identical except for the starting random number, are not as close to the DOT-III value as the one shown. The results of Table 2 are based on 200 neutrons for each of the 20 batches in each mode calculation. In all cases, except the transport kernel biasing case, the initial total dose is 3.312×10^{-19} rads per source neutron. This gives an error of 2.82 percent. The transport kernel biasing case required a different number of random numbers so that the initial total dose had an error of -13.47 percent for the same number of neutrons. An even more erroneous result of 3.976×10^{-19} rads per source neutron was computed for a run in which 60 batches were used. This represents an error of -16.67 percent, even though three times as many neutron histories were executed. Thus, the apparent increase in error from the initial to the final estimate of the total dose is not necessarily real.

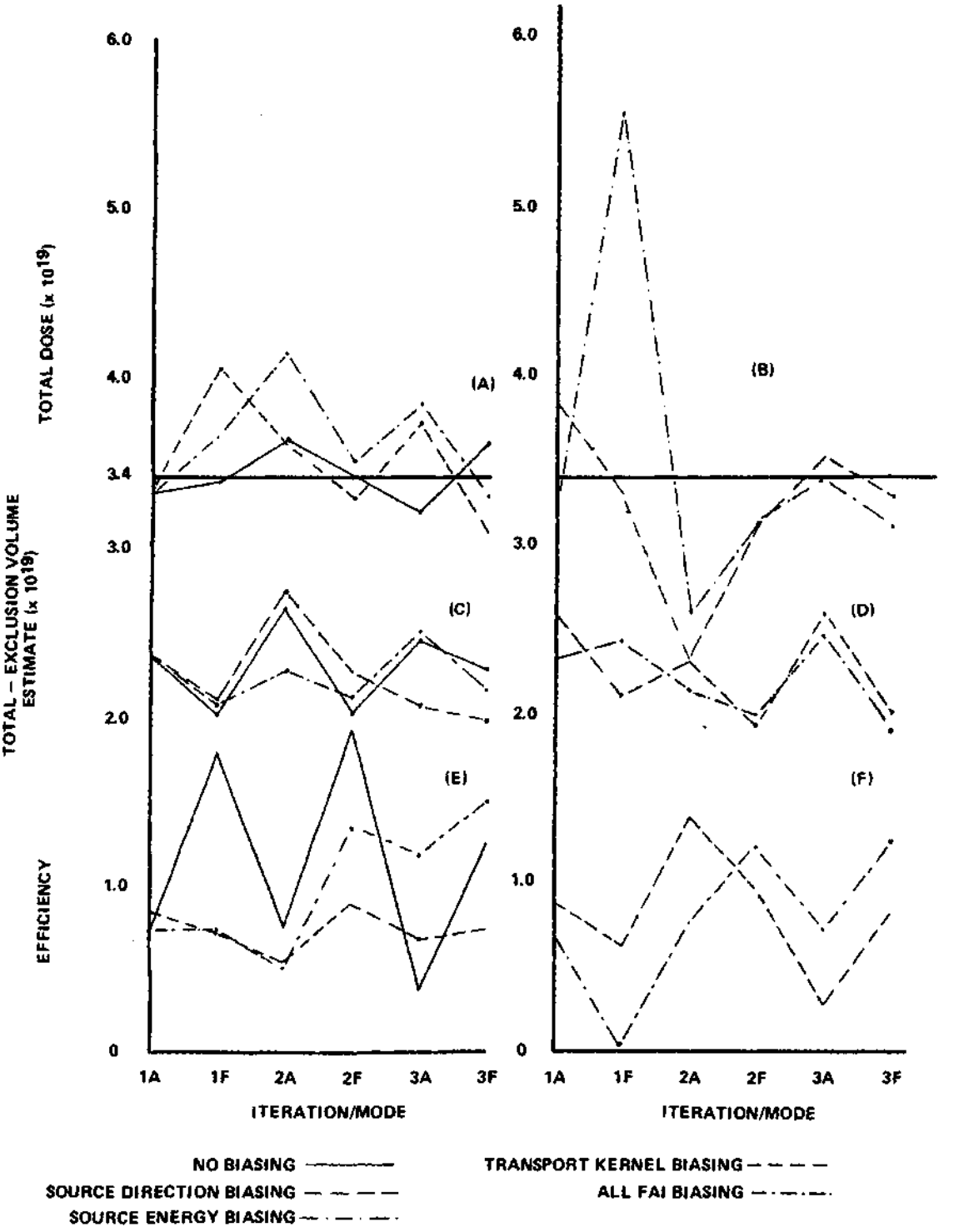

Figure 10. Total Dose, Total Dose Estimate from Outside the Exclusion Volume, and Efficiency Results

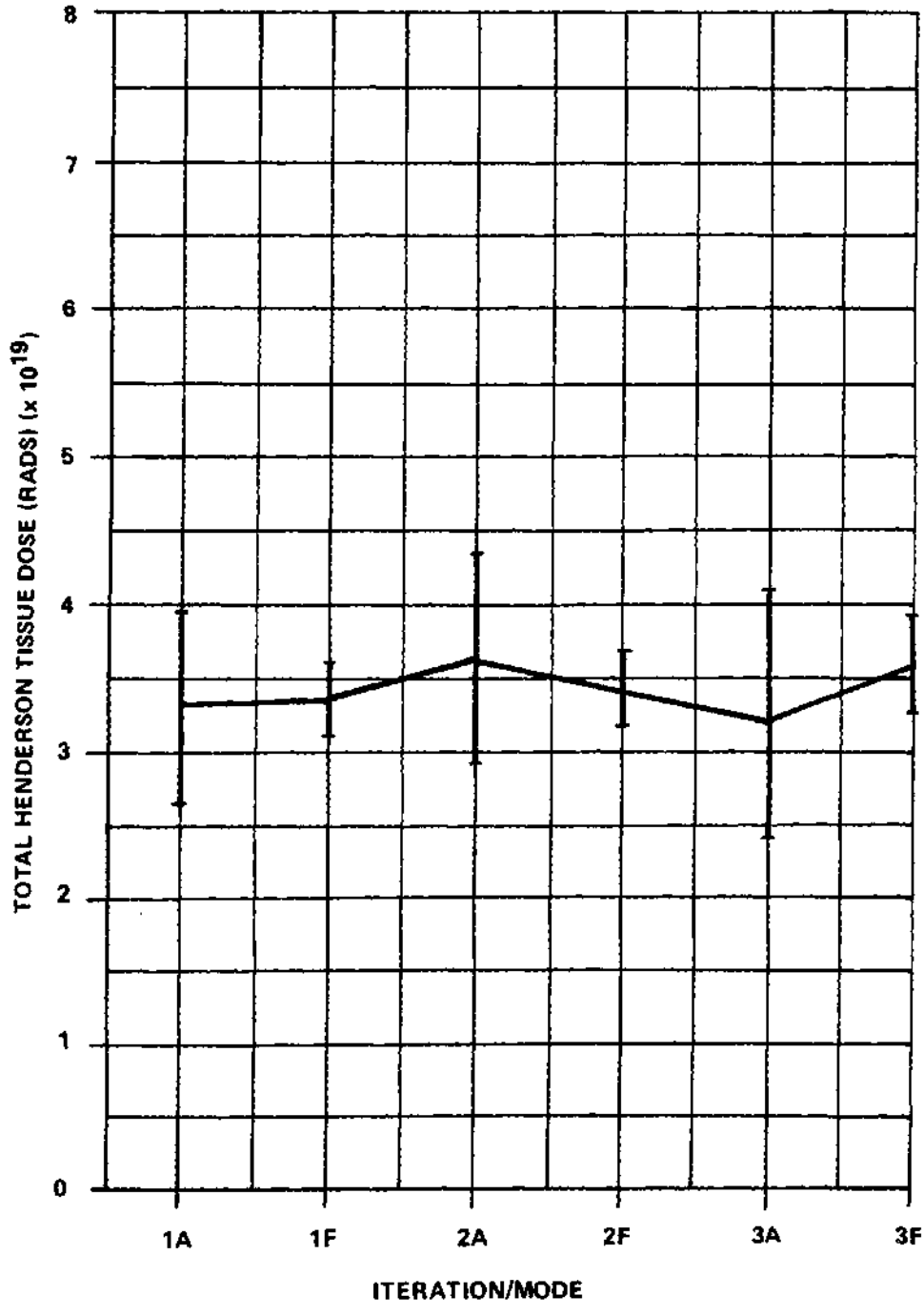

Figure 11. Total Dose and Error Bars for the No Biasing Case

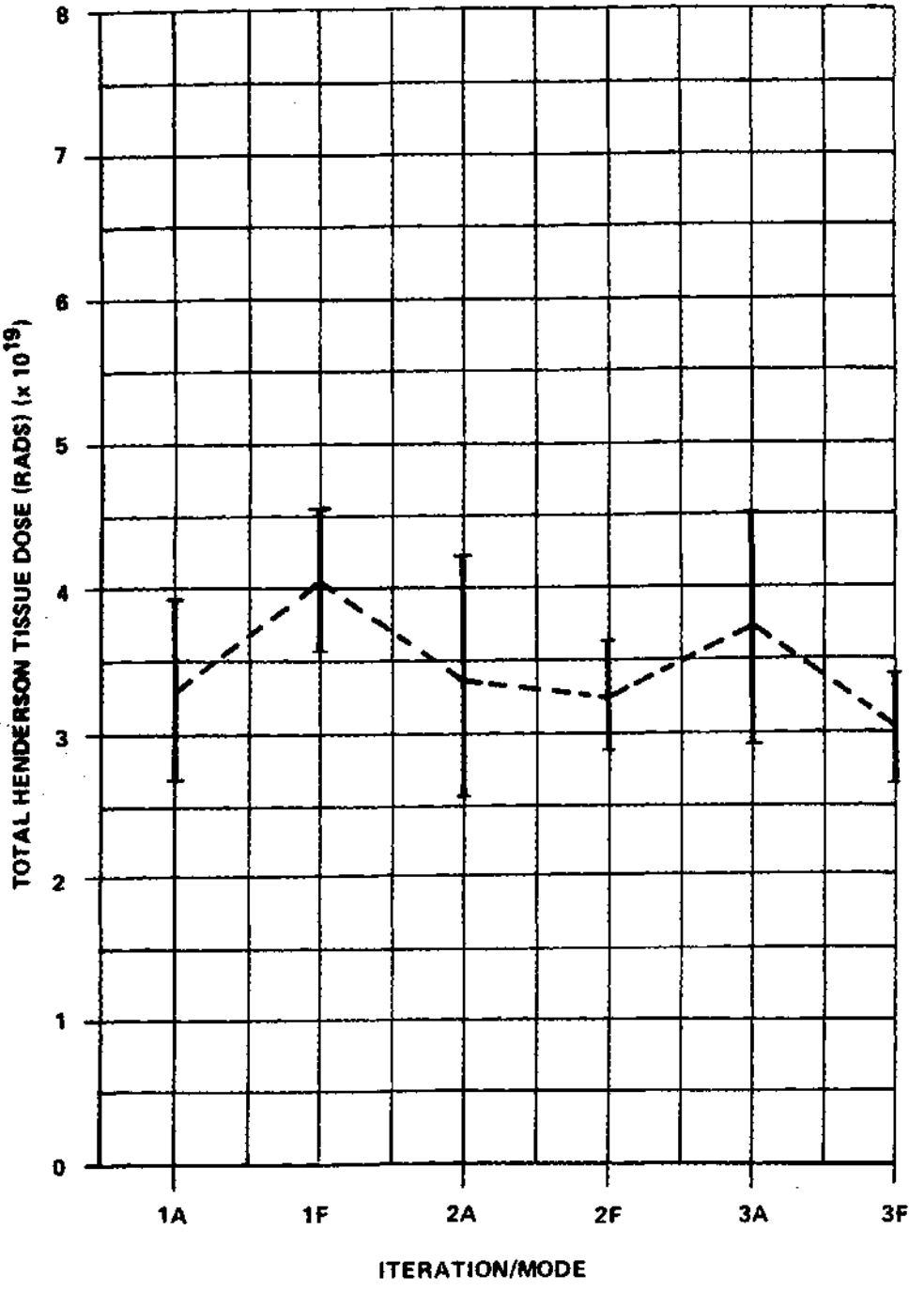

Figure 12. Total Dose and Error Bars for the Source Direction Biasing Case

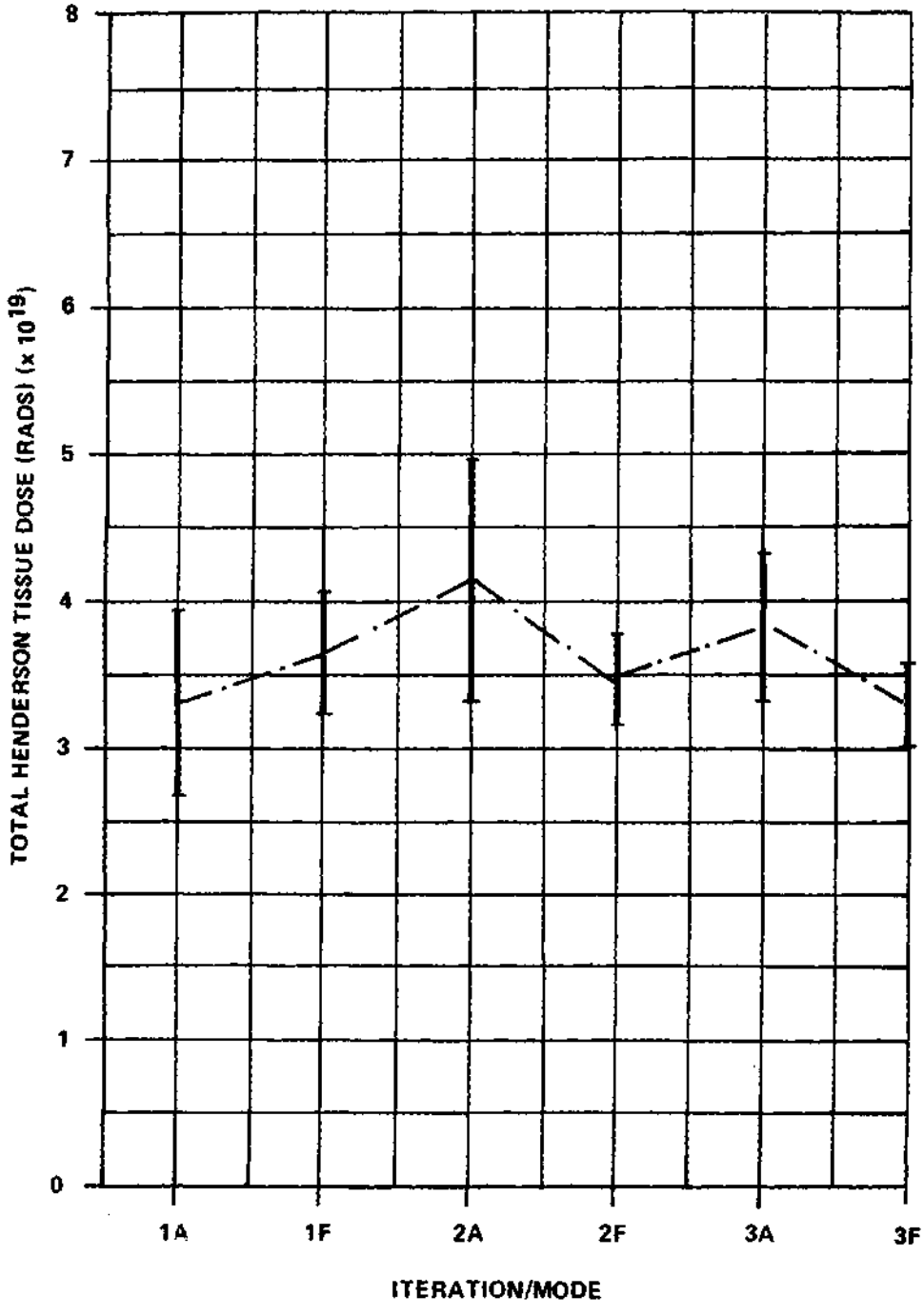

Figure 13. Total Dose and Error Bars for the Source Energy Biasing Case

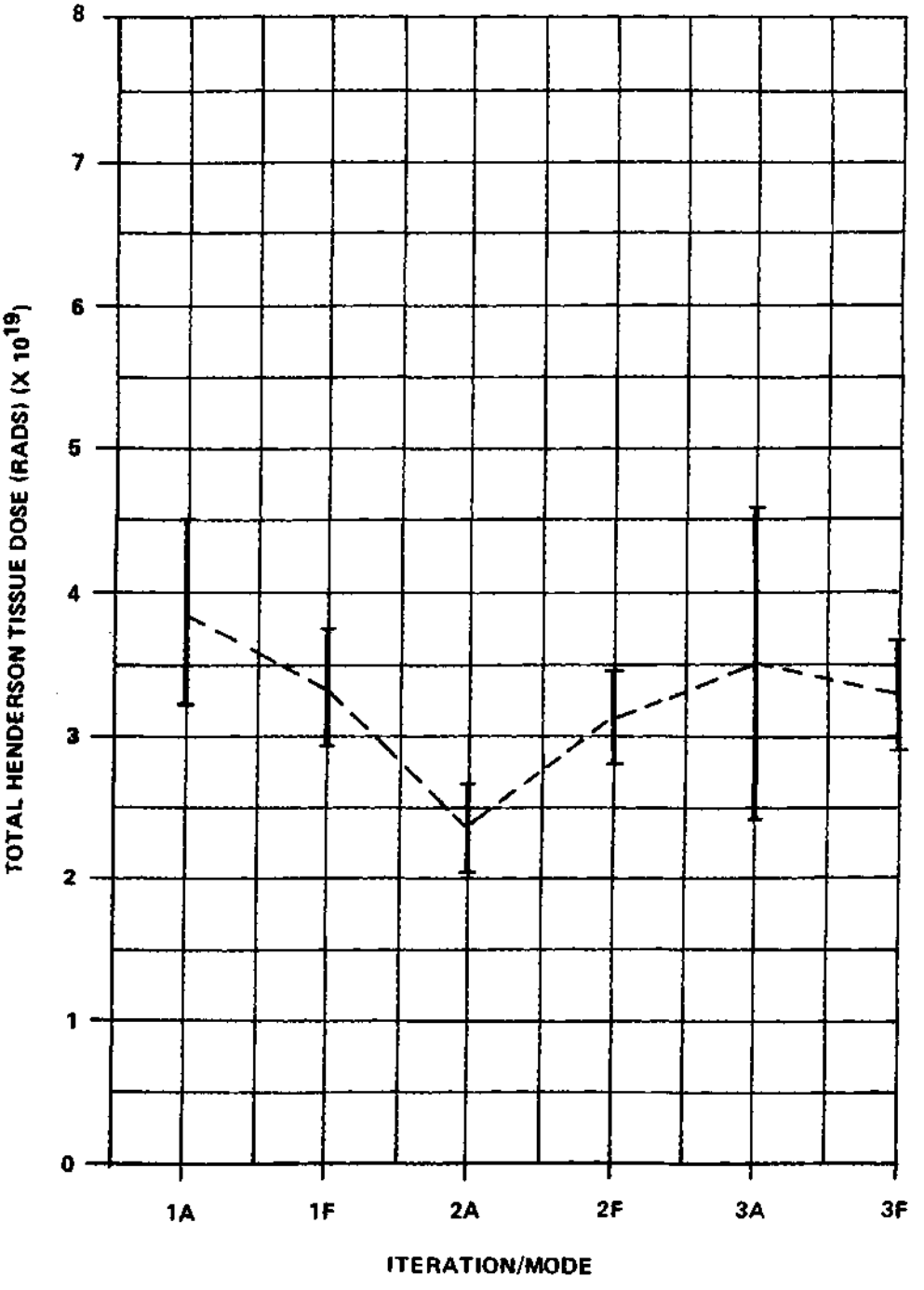

Figure 14. Total Dose and Error Bars for the Transport Kernel Biasing Case

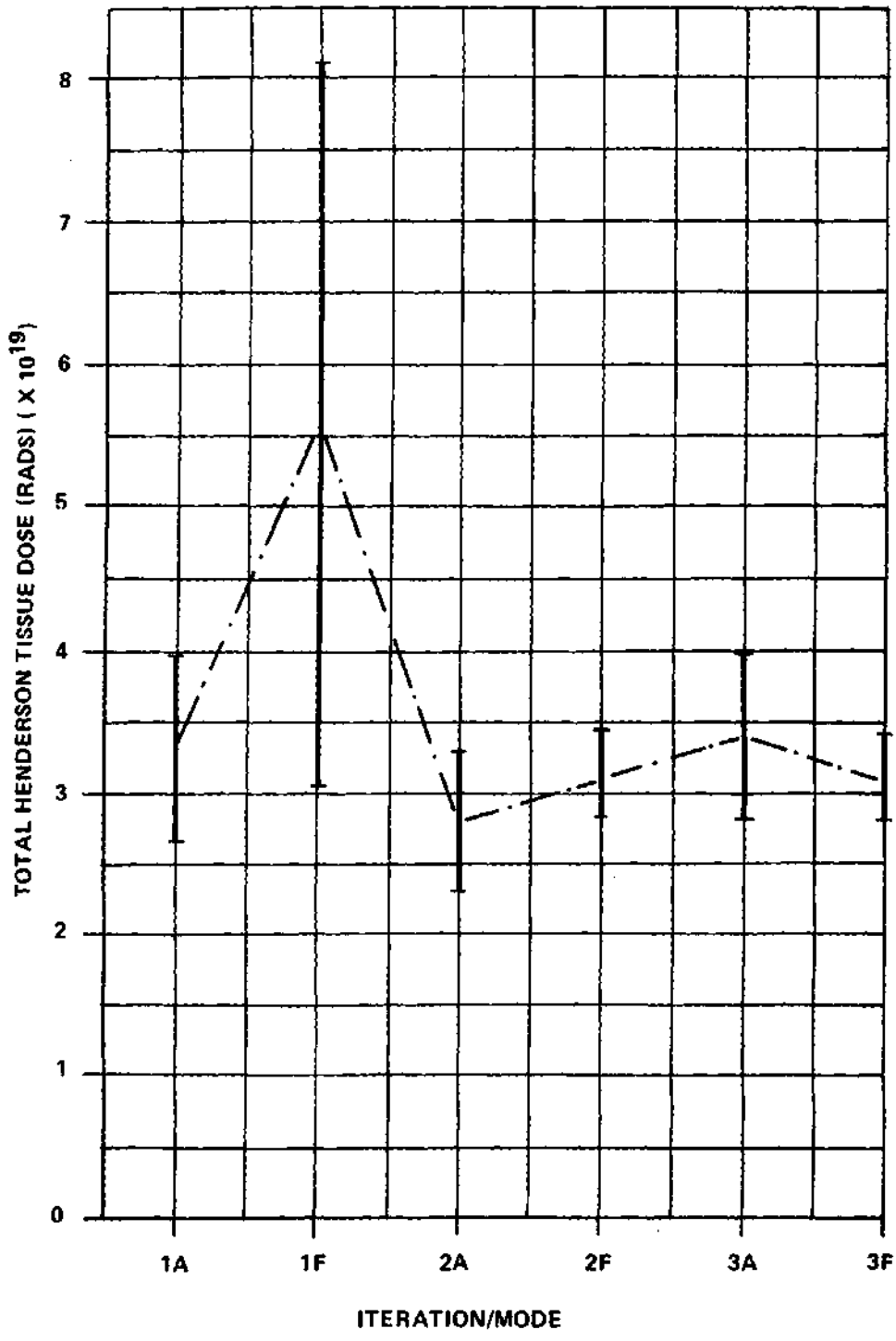

Figure 15. Total Dose and Error Bars for the All Biasing Case

One problem observed in the air cylinder problem with the iterative forward-adjoint method is an increase in the error (and decrease in efficiency) in the second mode of the first iteration and the first mode of the second iteration. The apparent reason for this effect is that the importance function is poorly defined due to the small number of histories contributing to the estimate of the importance function. Analysis of the importance functions generated by IFAM indicates substantial differences in the values of the importance function in phase cells which should have identical estimates (e.g., the source region importance function for a given energy group in symmetrical angular bins such as 2, 3, 4, and 5). Figure 10 (A) and (B) seem to indicate that this problem is less severe in the latter iterations which have data from a large number of histories with which to generate the importance function.

Another interesting feature of the iterative forward-adjoint method is that the dose estimates tend to oscillate about the correct value. This behavior is obvious in Figure 10. Unfortunately, the errors are not consistently smaller, but this behavior can be explained on the basis of the statistical deviations from the correct dose value. It is possible that the importance function may cause fluctuations that hinder the convergence to a very accurate result rather than assist that convergence, as predicted by the "perfect game" in Chapter II. This effect may be caused by "bad actor" histories, which produce a much larger importance in a given phase cell than that particular phase cell actually has. These "bad actors" have been noted in detailed studies of the energy, angle, and region dependent importance functions generated by IFAM. Some of these importance function values can be an order of magnitude above

the expected value.

Figure 10 (C) and (D) are plots of the total dose estimate in which the contribution from collisions in the exclusion volume has been removed. While the resulting dose still oscillates, the amount of oscillation is much less than for the total dose. This is especially true for the case where only the transport kernel biasing was used and where all of the methods described in Chapter IV were in effect. As part (D) of Figure 10 and Table 2 illustrate, the wild fluctuations in total dose were largely due to collisions (or lack of collisions) in the exclusion volume. Analysis of the exclusion volume estimator revealed no apparent deficiencies, and the results given below indicate that problems not needing the exclusion volume are better behaved.

Examination of Figure (E) for the efficiency of the source energy biasing shows that this particular technique is increasing the efficiency of the Monte Carlo calculation. Although the efficiency shows a drop at the initial mode of the second iteration, from that point on it increases in both of the forward and adjoint modes. For the air cylinder problem, only the source energy biasing appears to improve the efficiency of the calculation.

In order to resolve some of the questions raised by the air cylinder problem, simplified problems were constructed and solved by IFAM. The problem geometry is depicted in Figure 16. It consists of an isotropic point source and a detector placed on opposite sides and along the centerline of a cylindrical shield. Both the source and detector are in a vacuum and are five centimeters away from the nearest shield surface. The shield has a radius and thickness of 10 centimeters. Various problems

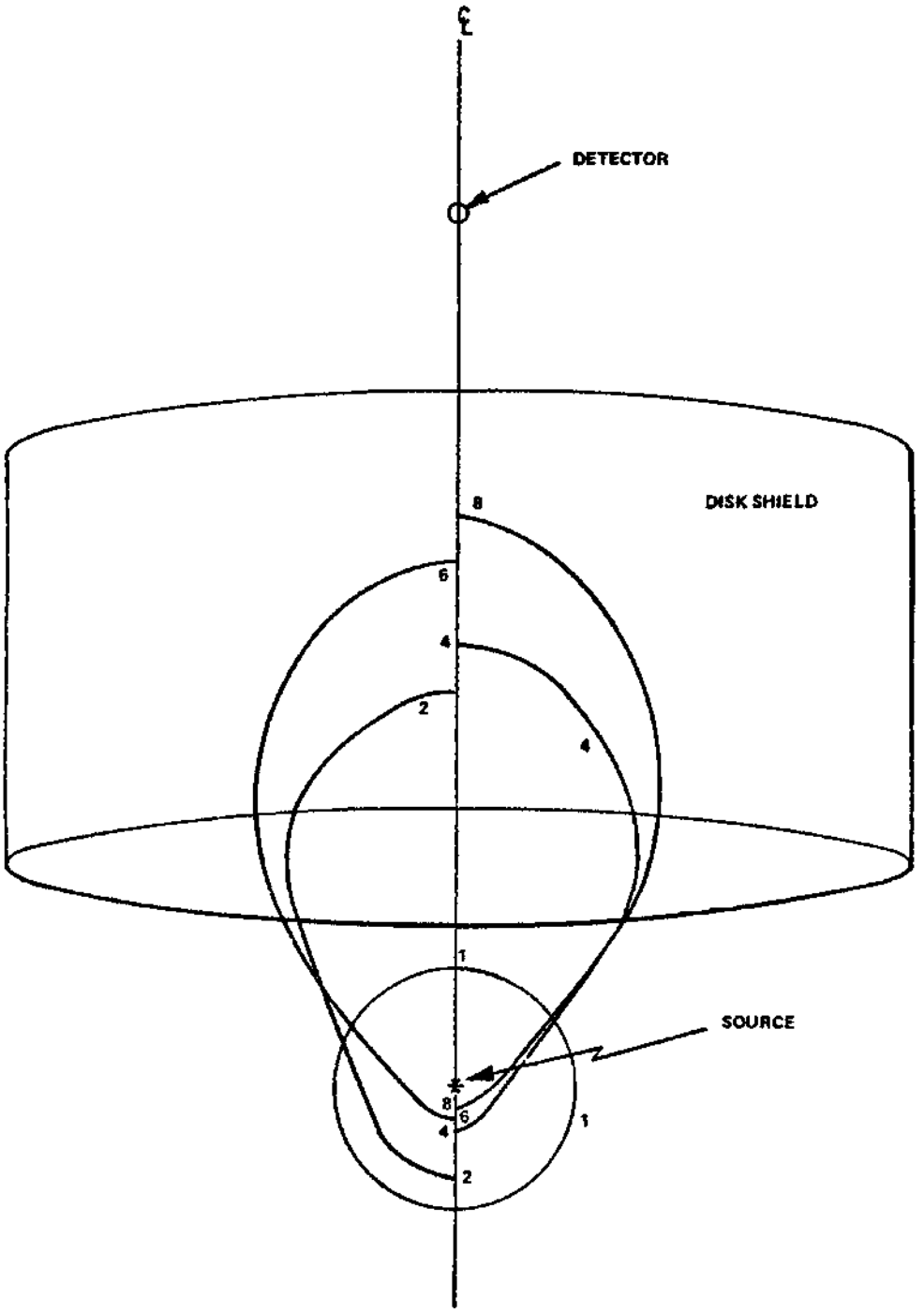

Figure 16. Simplified Problem Geometry and Source Direction Biasing

were obtained by changing the total macroscopic cross section of the shield material to obtain various mean free paths along the centerline (from 2 to 4). Only one energy group was used, so that the in-group scattering cross section is just the non-absorption cross section. By varying the ratio of the in-group to total cross section, the non-absorption probability can be changed.

The result from one simplified problem is illustrated in Figure 16. Drawn about the source is the source angular distribution for the initial mode (adjoint) for iterations 1, 2, 4, 6, and 8. The angular distributions are drawn to scale, with the distribution for iteration 1 representing an isotropic source. The distributions were symmetrical in the azimuthal direction, and the centerline represents the polar axis. The curves for iterations 2 and 6 are plotted on the opposite side of the centerline from iterations 4 and 6 for the sake of clarity. The curves are the results from an IFAM calculation with a non-absorption probability of 0.9 and a shield thickness of two mean free paths. A total of 12 iterations was performed, but the angular distribution change after the eighth iteration was not significant. For this problem, only 50 particles per batch and five batches per iteration were used. The IFAM angular flux at the source was compared with DOT calculations using 96 angles. Good agreement was obtained at polar angles less than 40 degrees and excellent agreement was found after six iterations.

Table 3 shows the scattered fluence from three computer runs on the same simplified problem, but with a different number of source particles for each mode of each iteration. The non-absorption probability was set at 0.25 and the shield thickness was four mean free paths. The

Table 3. Results of Three Source Direction Biasing Problems

Iteration	Mode	Fluence ($\times 10^{-6}$ Part./cm^2)	FSD	Efficiency ($\times 10^{-3}$)
		500 Particles		
1	A	1.741	.173	5.56
1	F	1.333	.120	9.27
2	A	1.662	.148	5.44
2	F	1.721	.107	11.02
3	A	1.510	.116	8.74
3	F	1.756	.099	12.63
4	A	1.966	.094	12.62
4	F	1.603	.097	12.51
Average Fluence		1.661		
		2000 Particles		
1	A	1.437	.096	4.87
1	F	1.815	.056	9.80
2	A	1.744	.058	8.46
2	F	1.646	.054	10.30
3	A	1.781	.064	7.08
3	F	1.606	.055	9.81
4	A	1.735	.060	7.88
4	F	1.675	.051	11.70
Average Fluence		1.680		

Table 3. Concluded

Iteration	Mode	Fluence ($\times 10^{-6}$ Part./cm^2)	FSD	Efficiency ($\times 10^{-3}$)
		16,000 Particles		
1	A	1.653	.045	2.85
1	F	1.696	.015	17.65
2	A	1.731	.020	8.87
2	F	1.722	.019	10.12
3	A	1.819	.019	9.33
3	F	1.802	.018	11.22
4	A	1.730	.023	6.45
4	F	1.708	.021	8.51
Average Fluence		1.733		

scattered fluence was also calculated with the DOT computer code and found to be 1.74×10^{-6} particles/cm^2. Since DOT is a discrete ordinate code, it does not have the statistical variations of a Monte Carlo code like IFAM. However, it is subject to numerical errors and the DOT result is only accurate within a few percent.

It is interesting to note that the closest IFAM fluence to the DOT fluence occurs at the first iteration, initial mode for the smallest number of source particles. The result is coincidental, since this IFAM case also has the largest fractional standard deviation (FSD). Note that, for the 2000 and 16,000 source particle runs, the IFAM result which differs the most from the DOT fluence occurs at the first iteration, initial mode case, as expected.

Examination of each run in Table 3 indicates that the efficiency does increase with the use of source direction biasing after the initial case, but not monotonically with iteration number. The reason for the lack of increase of efficiency with each iteration is due to the fact that statistical variation in the fractional standard deviation offsets the gain in source biasing. However, Table 3 clearly indicates a factor of two to three gain in efficiency. This gain is due only to the use of one of the iterative-forward Monte Carlo biasing techniques discussed in Chapter IV, that of source direction biasing. Thus the utility of this technique for source direction biasing is established.

Table 4 depicts the final results of three transport kernel biasing problems on the simplified geometry of Figure 16. The shield has been divided into 48 regions, consisting of three radial zones, four angular zones, and four axial zones. The results shown are for a shield thickness

Table 4. Results of Three Transport Kernel Biasing Problems

Iteration	Mode	Fluence ($\times 10^{-6}$ Part./cm^2)	FSD	Efficiency ($\times 10^{-3}$)
		1000 Particles		
1	A	2.145	.179	0.88
1	F	1.484	.100	2.88
2	A	1.447	.092	3.48
2	F	1.656	.148	1.37
3	A	1.773	.130	1.80
3	F	2.187	.145	1.39
4	A	1.594	.122	1.87
4	F	1.882	.162	1.10
5	A	1.548	.120	2.01
5	F	1.835	.130	1.77
6	A	1.613	.157	1.19
6	F	1.595	.126	2.00
7	A	1.214	.132	1.68
7	F	1.937	.149	1.30

Table 4. Concluded

Iteration	Mode	Fluence ($\times 10^{-6}$ Part./cm^2)	FSD	Efficiency ($\times 10^{-3}$)
		4000 Particles		
1	A	1.733	.066	1.63
1	F	1.813	.078	1.23
2	A	1.773	.093	0.84
2	F	1.431	.054	2.61
3	A	1.630	.076	1.31
3	F	1.640	.073	1.43
4	A	1.755	.074	1.31
4	F	1.539	.064	1.88
		16,000 Particles		
1	A	1.653	.036	1.36
1	F	1.794	.041	1.14
2	A	1.787	.037	1.32
2	F	1.718	.037	1.37

of four mean free paths and a non-absorption probability of 0.25. As in Table 3, the fluence, fractional standard deviation, and efficiency are given for three different numbers of particles per case. Examination of these results indicates that the technique developed to alter the transport kernel produced little if any improvement in the efficiency of the Monte Carlo calculations. Problems were also run at different shield thicknesses and non-absorption probabilities. In none of these problems was the improvement in efficiency sufficient to warrant the expenditure of computer resources in time and core storage. This conclusion is consistent with the implications of the air cylinder problem discussed earlier.

Therefore, this research indicates that the iterative forward-adjoint Monte Carlo is beneficial for biasing the source energy and direction, but does not improve the efficiency when used in biasing the transport kernel. In addition, this research has resulted in the development of the modular test bed IFAM that can be used for performing a wide variety of radiation transport problems. IFAM has several intrinsic attributes that can be used to good advantage by the analyst.

One major advantage is that IFAM can be used to compare run time, efficiency, or other measures of "goodness" between the forward and adjoint modes of a given problem. Table 2 shows that the adjoint mode requires less run time for a given number of histories than the forward mode for the air problem. The percent error for the no biasing case is also comparable for the forward and adjoint modes. Therefore, the adjoint mode is the better one to use to calculate the air cylinder dose. IFAM can be used to aid the researcher in determining the proper mode for a

given problem. Since very little time is required to set up most problems in the adjoint mode once the forward mode data have been designed, it seems advisable to make a preliminary IFAM calculation with both modes before selecting the single mode which will be used in the final calculation.

Another advantage of IFAM is that the importance function generated usually agrees quite well with calculations made by other methods (e.g., ANISN and DOT) once the statistical fluctuations have been removed. Thus, the forward and adjoint importance functions from an initial one iteration IFAM calculation can be used to suggest subsequent biasing parameters for MORSE or IFAM calculations.

APPENDICES

APPENDIX A

IFAM STRUCTURE AND OPERATING INSTRUCTIONS

IFAM is a very large and complex piece of computer software. Depending on the particular problem, over 100 subprograms may be required for a given run. The complexity of IFAM is illustrated by Figure 17, which depicts the interrelationship of the main routine, called IFAM, and the various subroutines and functions. Only system mathematic library and intrinsic functions have been omitted. Also, the subroutines may have more than one version. All of these subprograms have been included on a FURPUR tape for the IFAM user. If the user wishes to use a specific version, he can easily use the @MAP to input a set of source language control statements to specify the version.

A listing of the control statements used to run an IFAM problem is given in Figure 18. Note that the main segment of our overlay contains both the main routine, called AAFAM, and the MORSE subroutine. There are four first level segments: (1) DATAIN, (2) CRANK, (3) FAMSEG, and (4) NOTUSED. DATAIN is a segment that performs all of the input functions except for those few handled by MORSE. It is further segmented into the specific random walk problem data segment, RWALK, the cross section data segment, XSECIN, and the analysis data segment, ANALYSIS. These three segments are represented in Figure 17 by subroutines INPUT1, INPUT2, and INPUT 3, respectively. This can also be seen in the control statement list by the fact that the IN control statement after each SEG statement

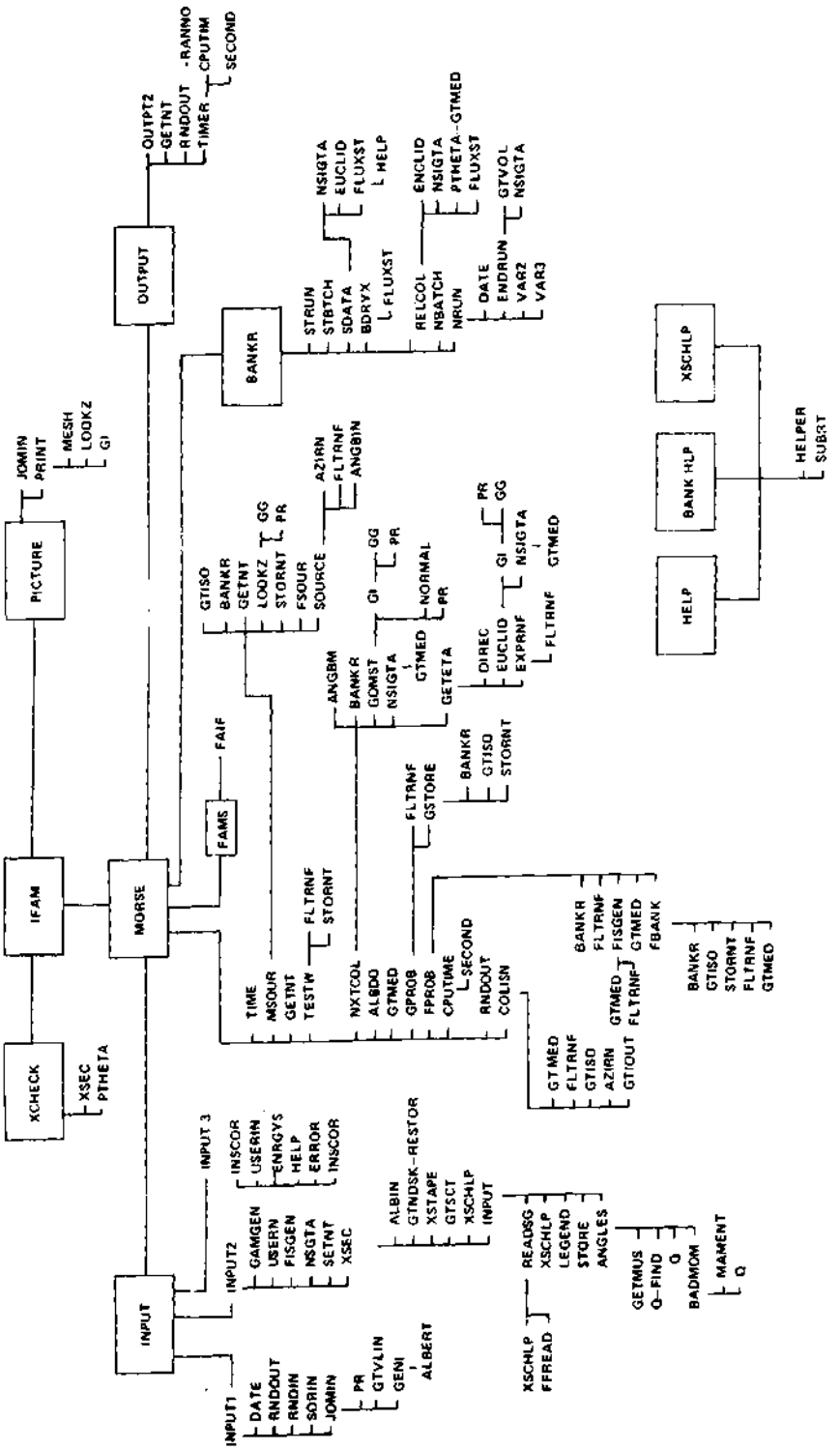

Figure 17. IFAM Subroutine Structure

```
@MAP      FAMSEG,FAMSEG
MAP2BR1 RL71-3 05/03/7o 21:58:16 (0,)
    1.NEW     LIB      SYS$*MSFC$.
    2.        CLASS IFA**********
    3.        SEG      MAIN
    4.         IN        AAFAM,MORSE,BLANK$COMMON
    5.-01     SEG      DATAIN*,(MAIN)
    6.         IN        INPUT
    7.        SEG      RWALK*,(DATAIN)
    8.         IN        INPUT1
    9.        SEG      XSECIN*,(DATAIN)
   10.         IN        INPUT2
   11.        SEG      ANALYSIS*,(DATAIN)
   12.         IN        INPUT3
   13.        SEG      CRANK*,(MAIN)
   14.         IN        MSOUR,NXTCOL,COLISN,BANKR,TESTw
   15.         IN        OUTPT
   16.        SEG      FAMSEG*,(MAIN)
   17.         IN        FAMS
   18.        SEG      NOTUSED*,(MAIN)
   19.         IN        ALBDO,FPROB,GPROB
   20.         IN        FSOUR
   21.       END
```

Figure 18. IFAM Control Statement

has these element names. IFAM was broken into three input segments so that the CRANK segment would dominate the core storage requirements.

The CRANK segment handles the random walk calculations and the output. The output can be handled in a separate segment, but the core storage savings are small. Since the output routines are called at the end of each mode, it was decided that the core storage savings were less important than the extra time for segment interchange. Most of the changes made in the Monte Carlo procedure are in the CRANK segments.

The manipulation of the importance information between mode calculations is handled by the third segment, FAMSEG. The driver subroutine is FAMS, as shown by the element name. (With few exceptions, the element name and a given subroutine name are identical.) The fourth segment is made up of subroutines that are referenced in one of the above subroutines but are never called due to the IFAM problem options. Those subroutines include the albedo, fission, and secondary gamma ray options as indicated by the IN statement in Figure 18. Thus, this segment is called NOTUSED. By placing subroutines that are referenced but never called, core storage is saved with essentially no loss of computer run time.

As mentioned above, IFAM has some subroutines with multiple versions. Most of the original and unchanged subroutines have no version identifier, so they can be considered as having the version name of "blank." Those subroutines modified for the IFAM test bed were given a version name of IFA. New subroutines written for IFAM may have either the "blank" or IFA version name. The CLASS control statement has been used as shown in Figure 18 to tell the collector that the IFA version of subroutines with multiple version names should be included in the collection.

A listing of the subroutines stored on the FURPUR tape will also show that some subroutines are available with DLP version. Subroutines with the DLP version are used in conjunction with the IFA versions to reduce the large amount of output, especially of the input data. The DLP version is especially useful during coding checkout where the same input data are used several times and a full output each time is unnecessary.

The execution of an IFAM job is illustrated by Figure 19. The stream of control and update cards is representative of that required to execute the sample problem (see Appendix C). The tape which is assigned as FAMT contains three files, the first of which is a FURPUR file and then the next two are data files, written with an @DATA statement. However, before the FURPUR file can be copied into the temporary program file, TPF$, more mass storage must be assigned to TPF$. This is accomplished by first releasing it (@FREE TPF$.) and then assigning a new TPF$ of sufficient FASTRAND area.

Next, the source and relocatable elements on the FURPUR file are copies into TPF$. (If only an absolute element is to be read in and executed, the default TPF$ storage is sufficient.) This tape read is followed by the assignment of a data file DTFF for the forward mode input data, which is read from the second file of the FAMT tape. This file was written with an @DATA statement and consists of card images. During the read, columns 52 through 55 in the fourth card are corrected. Next, another data file is assigned and the adjoint mode input data are read from the third file of FAMT and the same correction made to the second card. Since the program and data are now on FASTRAND, the tape (and tape drive) can be released with an @FREE.

```
@RUN SAIFAM,1HNTSV452045,NRBYRNBIN441,2C,400
@ASG,T      FAMT,T,12315
@FREE TPF$.
@ASG,T TPF$,F/2/POS/10
@COPIN,RS  FAMT.,TPF$.
@ASG,T DTFF,F
@DATA,L  FAMT.,DTFF.
-4,4-
52,55$25.0$
@END
@ASG,T DTFA,F
@DATA,L  FAMT.,DTFA.
-2,2-
52,55$25.0$
@END
@FREE       FAMT.
@FOR,US     AAFAM/IFA,AAFAM/IFA          . REDUCE BC TO 40000
-2,2
      COMMON NC(40000)
-25,25
      NLFT = 40000
@DELETE,RS TPF$.CPUTIM/GT
@PREP
@MAP,L   FAMSEG,FAMSEG
 LIB     SYS$*MSFC$.
-4,4
@PRT,T      TPF$.
@ASG,T 16,F/1/POS/4
@ASG,T 17,F/1/POS/4
@XQT        FAMSEG
@ADD,P DTFF.
@ADD,P      DTFA.
@FIN
```

Figure 19. Control Stream for IFAM Job

The next six cards in the control stream are for processing the source programs on TPF$. The main routine is updated to reduce the size of blank common and the source and relocatable subprograms of CPUTIM are deleted. This allows the system routine, CPUTIM/MSFC, to replace the one on the FURPUR tape.

After preparing an entry point table, the @MAP statement is used with its control statements to determine the final executable program. FAMSEG is the name of a source language control element on TPF$ (and hence on the FURPUR file of FAMT). This element is to be updated by the addition of a library (SYS$*MSFC$) and the deletion of control statement four. The result of these corrections to FAMSEG was shown in Figure 18. A table of the elements in TPF$ is listed as a result of the @PRT,T statement.

As explained in Chapter IV, data files 16 and 17 are requires for every IFAM run, and they are assigned to FASTRAND as shown. Now the execution of the absolute element FAMSEG generated by the collector is initiated. The input card images stored on DTFF and DTFA are added to the run stream by the two @ADD statements. The result of this operation will be the IFAM test bed as illustrated in Appendix C.

APPENDIX B

IFAM INPUT INSTRUCTIONS

The input data required by IFAM are essentially the same as those required by the Combinatorial Geometry Version of MORSE (see Reference 14). However, becamse IFAM requires both forward and adjoint mode data for a single run and because some of the MORSE options are not implemented in IFAM (e.g., coupled neutron-gamma ray, fissions and albedo calculations), this appendix contains a complete set of input instructions for IFAM. Input data which may be different in IFAM than in MORSE have been caveated by placing an asterisk before the input symbol in the input data format tables. The change or restriction is given in the description for that input symbol or in supplemental notes. The input data have been divided into four sections:

B.1	Random Walk and Iteration Data	(B.1 of Ref. 14)
B.2	Combinatorial Geometry Data	(B.3 of Ref. 14)
B.3	Cross-Section Data	(B.4 of Ref. 14)
B.4	Analysis Data	(B.5 of Ref. 14)

Each subsection below contains an introduction to the data format tables and defines the subroutines in which the data are read and the differences between the forward mode (or F-mode) and adjoint mode (or A-mode) input.

IFAM is so structured that the F-mode data are required to be read initially. Three new data cards are required before the old B.1 MORSE input data are read. These cards are now included as part of the new B.1

F-mode input data. After reading and performing necessary calculations with these data, IFAM reads the F-mode data defined in B.2, B.3, and B.4 in order. These data are processed and then stored on temporary data file unit 17. Then IFAM reads the A-mode data, beginning with Card Type A of Table 5. To enhance the clarity of the output, all title cards should specify the input data mode (i.e., F or A). In order to reduce the amount of input data required, certain parts of the geometry (B.2) and cross section (B.3) data are stored on temporary data file unit 16 during F-mode input and are retrieved during the A-mode input instead of reading these redundant data from cards. The data handled in this way are explained in Sections B.2 and B.3. The input and output logical unit numbers have been set to 5 and 6, respectively. These units are defined both in MAIN and in G1, and must be changed in both subroutines if other unit numbers are required.

As explained in Appendix A, it is possible to execute the Combinatorial Geometry Version of MORSE by supplying the proper MAP statements to the UNIVAC 1108 Collector under EXEC-VIII. The input data defined in this appendix contain all the necessary information for MORSE data preparation. Cards 1-3 in Section B.1 apply only to IFAM and should not be input for MORSE runs.

B.1 Random Walk and Iteration Data

This section contains all input data for IFAM or MORSE except the geometry, cross-section, and analysis data. The first three input cards (labeled 1, 2, and 3) are peculiar to IFAM and are not required by MORSE. They are read by the MORSE/IFA subroutine for the F-mode input only. MORSE then calls INPUT which calls INPUT1/IFA. INPUT1/IFA handles all

Table 5. Random Walk and Iteration Data

CARD TYPE	FIELD/FORMAT	INPUT SYMBOL	DESCRIPTION
1	1-5/I5	*IMOD	IFAM: Initial mode to be executed. 0: F-Mode 1: A-Mode
	6-10/I5	*NITP	IFAM: Number of iterations for this run ($\leq$15).
	11-80/14I5 1-80/16I5	*NPPB(I) *NBTI(I)	IFAM: NITP order pairs giving the number of particles per batch (NPPB(I) and the number of batches (NBTI) for the I-th iteration.
2	1-5/I5	*NSRF	IFAM: Source region number for the F-Mode.
	6-10/I5	*NSRA	IFAM: Source region number for the A-Mode.
	11-20/E10.4	*PSC	IFAM: Search length constant for the transport kernel routine (NXTCOL) in mean free paths.
3	Intermediate print and mode data write options executed at the end of each mode. INTPR(1) - INTPR(12) are for selected labeled commons and blank common. INTPR(13) and INTPR(14) control mode data writes to data file. Options are:		
	0 - Off	Do not write,	
	1 - On	Write information on appropriate output unit,	
	– 1 - End	Terminate search for any further output determined by INTPR(1) through INTPR(12). Doesn't affect INTPR(13) and INTPR(14).	
	1-5/I5	*INTPR(1)	IFAM: Labeled common APOLLO.
	6-10/I5	*INTPR(2)	IFAM: Labeled common USER.
	11-15/I5	*INTPR(3)	IFAM: Labeled common GOMLOC.
	16-20/I5	*INTPR(4)	IFAM: Labeled common LOCSIG.
	21-25/I5	*INTPR(5)	IFAM: Labeled common PDET.
	26-30/I5	*INTPR(6)	IFAM: Labeled common BNKNMC.
	31-35/I5	*INTPR(7)	IFAM: Labeled common BANK.
	36-40/I5	*INTPR(8)	IFAM: Labeled common RANDOM.
	41-45/I5	*INTPR(9)	IFAM: Blank common from I=1 to 4*NMTG.
	46-50/I5	*INTPR(10)	IFAM: Blank common containing the Region Importance (RI).
	51-55/I5	*INTPR(11)	IFAM: Blank common containing source region FAI values.

Table 5. Continued

CARD TYPE	FIELD/FORMAT	INPUT SYMBOL	DESCRIPTION
3	56-60/I5	*INTPR(12)	IFAM: Labeled common FAM.
	61-65/I5	*INTPR(13)	IFAM: Forward Mode output on data file 20†.
	66-70/I5	*INTPR(14)	IFAM: Adjoint Mode output on data file 20†.
			†Includes all of blank common and the following labeled commons: APOLLO, USER, GOMLOC, LOGSIG, POET, BNKNMC, BANK, RANDOM and FAM.
A	1-80/20A4	TITLE(I)	Title Card. Any character other than a blank or alphanumeric in Column 1 will terminate the job.
B	1-5/I5	*NSTRT	Number of particles per batch. IFAM: INSTRT is overridden by NPPB(I).
	6-10/I5	NMOST	Maximum number of particles allowed for in the bank(s); may equal NSTRT if there are no splitting, fission, and secondary generation during execution. If bank size is exceeded by more than 50 due to fission or secondary gamma ray generation, the job is terminated.
	11-15/I5	*NITS	Number of batches. IFAM: Overridden by NBTI(I).
	16-20/I5	*NQUIT	Number of sets of NITS batches to be run without calling subroutine INPUT. IFAM: Restricted to 1.
	21-25/I5	NGPQTN	Number of neutron groups being analyzed.
	26-30/I5	NGPQTG	Number of gamma-ray groups being analyzed.
	31-35/I5	NMGP	Number of primary particle groups for which cross sections are stored ; should be same as NGP (or the same as NGG when NGP=0) on Card XB read by subroutine XSEC.
	36-40/I5	NMTG	Total number of groups for which cross sections are stored; should be same as NGP + NGG as read on Card AB read by subroutine XSEC.

Table 5. Continued

CARD TYPE	FIELD/FORMAT	INPUT SYMBOL	DESCRIPTION
B	41-45/I5	NCOLTP	Set greater than zero if a collission tape is desired; the collision tape is written by the user routine BANKR.
	46-50/I5	*IADJM	Mode switch, ≤ 0 for F-Mode; >0 for A-Mode IFAM: Overridden by IMOD.
	51-55/F5.0	AXTIM	Maximum clock time in minutes allowed for the problem to be on the computer.
	56-60/I5	MEDIA	Number of cross-section media; should agree with NMED on Card XB read in by subroutine XSEC.
	61-65/I5	*MEDALB	Albedo scattering medium is absolute value of MEDALB: if = 0, no albedo information to be read in, <0, albedo only problem – *no* cross sections are to be read, >0, coupled albedo and transport problem IFAM: Set = 0 only.
C	1-5/I5	ISOUR	Source energy group if >0, if ISOUR ≤ 0, SORIN is called for input of Cards E1 and E2.
	6-10/I5	NGPFS	Number of groups for which the source spectrum is to be defined. If ISOUR ≤ 0, NGPFS ≥ 2.
	11-15/I5	*ISBIAS	No source energy biasing if set less than or equal to zero ; otherwise, the source energy is to be biased, and Cards E2 are required. IFAM: Source biasing is handled by code. Sets ISBIAS >0 at input completion.
	16-20/I5	NOTUSD	An unused variable.
	21-30/E10.5	WTSTRT	Weight assigned to each source particle.
	31-40/E10.5	EBOTN	Lower energy limit of lowest neutron group (eV) (group NMGP).

Table 5. Continued

CARD TYPE	FIELD/FORMAT	INPUT SYMBOL	DESCRIPTION
C	41-50/E10.5	EBOTG	Lower energy limit of lowest gamma-ray group (eV) (group NMTG).
	51-60/E10.5	TCUT	Age in sec at which particles are retired; *if* TCUT = 0, no time kill is performed.
	61-70/E10.5	VELTH	Velocity of group NMGP when NGPOTN >0; i.e., thermal-neutron velocity (cm/sec).
D	1-10/E10.4	XSTRT	Starting coordinates for source particles (may be overridden by changes in subroutine SOURCE).
	11-20/E10.4	YSTRT	
	21-30/E10.4	ZSTART	
	31-40/E10.4	AGSTRT	Starting age for source particles (see above note).
	41-50/E10.4	*UINP	Source particle direction cosines; if all are zero, isotropic direction are chosen. IFAM: Selection based on FAI array.
	51-60/E10.4	*VINP	
	61-70/E10.4	*WINP	
E1	1-70/7E10.4	FS(I)	NGPFS values of FS, where FS equals the unnormalized fraction of source particles in each group. (Omit if ISOUR on Card C is >0.)
E2	1-70/7E10.4	*BFS(I)	NGPFS values of BFS(I), where FBS(I) is the relative importance of a source in group I. Needed only if ISOUR ≤ 0 and ISBIAS >0. IFAM: BFS values are not input.
F	1-70/7E10.4	ENER(I)	NMTG values of the energy (in eV) at the upper edge of the energy group boundaries.
G	(Omit if NCOLTP on Card B ≤0, otherwise see Ref. 13).		
	1-5/I5	*NHISTR	Logical tape number for the first collision tape. IFAM: NHISTR cannot be the same for F- and A-modes.
	6-10/I5	NHISMX	The highest logical number that a collision tape may be assigned.
	11-46/36I1	NBIND(J)	An index to indicate the collision parameters to be written on tape (J=1, 36).
	47-59/13I1	NCOLLS(J)	An index to indicate the types of collisions to be put on tape.

Table 5. Continued

CARD TYPE	FIELD/FORMAT	INPUT SYMBOL	DESCRIPTION
H	1-24/4X,D20	RANDOM	Starting random number.
I	1-5/I5	NSPLT	Index indicating that splitting is allowed if >0.
	6-10/I5	NKILL	Index indicating that Russian roulette is allowed if >0.
	11-15/I5	NPAST	Index indicating that exponential transform is invoked if >0 (subroutine DIREC required).
	16-20/I5	NOLEAK	Index indicating that non-leakage is invoked if >0.
	21-25/I5	IEBIAS	Index indicating that energy biasing is allowed if >0. IFAM: If IEBIAS ≤ 0, EPROB will be set to $(NGPREG)^{-1}$, and IEBIAS to 1 by INPUT1/IFA.
	26-30/I5	MXREG	Number of regions described by geometry input (will be set to one if ≤ 0). If ENDRUN is used, a data array relating media number to region numbers must be given in a data statement in ENDRUN.
	31-35/I5	MAXGP	Group number of last group for which Russian roulette or splitting or exponential transform is to be performed.
J	(Omit if NSPLT + NKILL + NPAST = 0; Repeat the data set given below until all groups and regions input; terminate Card J read with negative value of NGP1.)		
	1-5/I5	NGP1	From energy group NGP1 to energy group NGP2, inclusive, in steps of NDG and from region NRG1 to NRG2, inclusive, in steps to NDRG, the following weight standards and path-stretching parameters are assigned. If NGP1 = 0, groups 1 to MAXGP will be used; if NRG1 = 0, regions 1 to MXREG will be used (both in steps of one). Usually NDG = 1 and NDRG = 1.
	6-10/I5	NDG	
	11-15/I5	NGP2	
	16-20/I5	NRG1	
	21-25/I5	NDRG	
	26-30/I5	NRG2	
	31-40/E10.5	WTHIH1	Weight above which splitting will occur.
	41-50/E10.5	WTLOW1	Weight below which Russian roulette is played.

Table 5. Continued

CARD TYPE	FIELD/FORMAT	INPUT SYMBOL	DESCRIPTION
J	51-60/E10.5	WTAVE1	Weight given those particles surviving Russian roulette.
	61-70/E10.5	PATH	Path-length stretching parameters for use in exponential transform (usually $0 \leq PATH < 1$).
K	(Omit if IEBIAS on Card I ≤ 0)		
	1-70/7E10.4	*EPROB (IG;NREG)	Values of the relative energy importance of particles leave a collision or source in region NREG for IG=1, NMTG. Input for each region (NREG=1, MXREG) must begin on a new card. IFAM: EPROB is assumed uniform if IEBIAS ≤ 0. (IG=1, NMTG:NREG = 1, MXREG).
L	(IFAM: All variables must be ≤ 0)		
	1-5/I5	*NSOUR	Set ≤ 0 for a fixed source problem; otherwise, the source is from fissions generated in a previous batch.
	6-10/I5	*MFISTP	Index for fission problem, if ≤ 0 no fissions are allowed.
	11-15/I5	*NKCALC	The number of the first batch to be included in the estimate of k; if ≤ 0 no estimate of k is made.
	16-20/I5	*NORMF	The weight standards and fission weights are unchanged if ≤ 0; otherwise, fission weights will be multiplied at the end of each batch, by the latest estimate of k and the weight stnadards are multiplied at the end of each batch by the latest estimate of k and the weight standards are systems, NORMF should be > 0.
M	(Omit if MFISTP ≤ 0 on Card L)		
	1-70/7E10.4	*FWLO(I)	Values of the weights to be assigned to fission neutrons (I = 1, MXREG). IFAM: No fission problems allowed.

Table 5. Concluded

CARD TYPE	FIELD/FORMAT	INPUT SYMBOL	DESCRIPTION
N	(Omit if MFISTP ≤ 0 on Card L)		
	1-70/7E10.4	*FSE(IG, IMED)	Fraction of fission-induced source particles in group IG (IG = 1, NMGP) and medium IMED (begin a new card for each medium where IMED = 1, MEDIA). IFAM: No fission problems allowed.
0	(Required input only for coupled neutron-gamma ray problem)		
	1-70/7E10.4	*GWLO(IG,NREG)	Values of the weight to be assigned to the secondary particles being generated. NMGP groups are read for each region in a forward problem and NMTG-NMGP for an adjoint. Input for each region must start on a new card. IFAM: No coupled problems allowed.

of this input for the data defined in this section.

If a description of the input data contains "IFAM:", then any information following this symbol pertains only to IFAM input.

B.2 Combinatorial Geometry Data

The combinatorial geometry data are read by the JOMIN/IFA subroutine, except for the region volumes VNOR(I), which are read by the GTVLIN subroutine. JOMIN/IFA is called from INPUT1/IFA. During the initial (F-mode) input, all specified data must be in the input stream. However, during the next (A-mode) call to JOMIN/IFA, card types CGB (body data) and CGC (input zone data are omitted. Since the data on the CGB and CGC cards must be identical for both the F- and A-modes, these data are temporarily stored on data file unit 16 during the F-mode input. They are later read by the GENI subroutine and processed for both the F- and A-mode calculations.

Details of the combinatorial geometry package and its utilization are given in Reference 14. However, the information given below is sufficiently complete so that anyone familiar with combinatorial geometry can prepare input data for most problems. Because the combinatorial geometry package was originally written for the SAM codes {22} and MORSE originally used the 05R geometry package {17}, confusion in terminology has occurred. The term zone used below is the same as the "region" used in the original combinatorial geometry package, whereas a region as used in this document corresponds to "region" of the 05R geometry package, just as a media corresponds to the 05R "media." However, regions* and

*Note: If ENDRUN is used to obtain collision density and track length per unit volume estimate of fluence, then a data statement in

media are defined by combining zones for IFAM applications, which differs from the construction in the 05R package. The term body has the same meaning as in the original combinatorial geometry package, but it has no counterpart in the 05R package.

The required combinatorial geometry input data are defined in Table 6. A summary of the input data required for each body type is given in Table 7.

B.3 Cross-Section Data

The cross section input data required by IFAM are the same as for the MORSE forward and adjoint modes. In order to reduce the amount of input data cards for IFAM, the multigroup cross section tables (card type XE) are read only during the initial or F-mode input. At that time, these tables are stored on data file unit 16 and are automatically read by READSG from unit 16 during the A-mode input instead of being read from the input data file. In order to implement this labor saving change, the READSG subroutine was revised, producing the READSG/IFA version for IFAM.

To facilitate interpretation of the output cross-section data, the title card (XA) should indicate whether F- or A-mode output is being performed. The data on card XC for the F- and A-mode input need not be identical, except for the IDTF switch, since the A-mode cross-section setup uses the same data as read during the F-mode input and stored on data file unit 16. All other card types (XB, XD, XF, XG) require identical data for F- and A-mode input, as shown in Table 8.

ENDRUN must give a relationship between region and media. In this case only one medium may be in a region.

Table 6. Combinatorial Geometry Data

CARD TYPE	FIELD/FORMAT	INPUT SYMBOL	DESCRIPTION
CGA	1-5/I5	IVOPT	Option which defines the method by which region volumes are determined; if IVOPT = 0, volumes set equal to 1., IVOPT = 1, concentric sphere volumes are calculated, IVOPT = 2, slab volumes (1-dim.) are calculated (not operational), IVOPT = 3, volumes are input by card type CGF
	6-10/I5	IDBG	If IDBG >0, subroutine PR is called to print results of combinatorial geometry calculations during execution. Use only for debugging.
	21-80/10A6	JTY	Alphanumeric title for geometry input (columns 21 - 80).
CGB	(One set of cards is required for each body and for the END card. Leave columns 1 - 10 blank for continuation cards. See Table 7 for more input information. IFAM: Not required for A-mode input.)		
	1-5/2X,A3	*ITYPE	Specifies body type or END to terminate reading of body data (for example BOX, RPP, ARB, etc.). Leave blank for continuation cards.
	6-10/I5	*IALP	Body number assigned by user (all input body numbers must form a sequence set beginning at 1). If left blank, numbers are assigned sequentially. Either assign all or none of the numbers. Leave blank for continuation cards
	11-70/6E10.3	*FPD(I)	Real data required for the given body as shown in Table 7.
CGC	(One set of cards for each input zone. Input zone numbers are assigned sequentially. IFAM: Not required for A-mode input.)		
	1-5/2X, A3	IALP	IALP must be a non-blank for the first card of each set of cards defining an input zone. If IALP is blank, this card is treated as a continuation of the previous zone card. IALP = END denotes the end of zone description.

Table 6. Concluded

CARD TYPE	FIELD/FORMAT	INPUT SYMBOL	DESCRIPTION
CGC	6-10/I5	NAZ	Total number of zones that can be entered upon leaving any of the bodies used in defining this input zones (some zones may be counted more than once). Leave blank for continuation cards for a given zone. (If NAZ $\leq$0 on the first card of the zone card set, then it is set to 5). NAZ is used to allocate blank common.
	(Alternate IIBIAS(I) and JTY(I) for all bodies defining this input zone.)		
	11-73/6(A2,I5)	IIBIAS(I)	Specific the "OR" operator if required for the JTY(I) body
		JTY(I)	Body number with the (+) or (–) sign as required for the zone description.
CGD	1-70/1415	MRIZ(I)	MRIZ(I) is the region number in which the I^{th} input zone is contained (I = 1, to the number of input zones). Region numbers must be sequentially defined from 1.
CGE	1-70/1415	MMIZ(I)	MMIZ(I) is the medium number in which the I^{th} input zone is contained (I = 1, to the number of input zones). Medium numbers must be sequentially defined from 1.
CGF	(Omit if IVOPT $\neq$ 3 in card CGA)		
	1-70/7E10.5	VNOR(I)	Volume of the I^{th} region (I = 1 to MXREG, the number of regions).

Table 7. Input Required on CGB Cards for Each Body Type

CARD COLUMNS BODY TYPE	ITYPE 3 - 5	IALP 7 - 10	REAL DATA DEFINING PARTICULAR BODY						NUMBER OF CARDS NEEDED
			11 - 20	21 - 30	31 - 40	41 - 50	51 - 60	61 - 70	
Box	BOX	IALP is assigned by the user or by the code if left blank.	Vx H2x	Vy H2y	Vz H2z	H1x H3x	H1y H3y	H1z H3z	1 of 2 2 of 2
Right Parallelepiped	RPP		Xmin	Xmax	Ymin	Ymax	Zmin	Zmax	1
Sphere	SPH		Vx	Vy	Vz	R	–	–	1
Right Circular Cylinder	RCC		Vx R	Vy –	Vz –	Hx –	Hy –	Hz –	1 of 2 2 of 2
Right Elliptic Cylinder	REC		Vx R1x	Vy R1y	Vz R1z	Hx R2x	Hy R2y	Hz R2z	1 of 2 2 of 2
Ellipsoid	ELL		V1x L	V1y –	V1z –	V2x –	V2y –	V2z –	1 of 2 2 of 2
Truncated Right Cone	TRC		Vx L1	Vy L2	Vz –	Hx –	Hy –	Hz –	1 of 2 2 of 2
Right Angle Wedge	WED		Vx H2x	Vy H2y	Vz H2z	H1x H3x	H1y H3y	H1z H3z	1 of 2 2 of 2
Arbitrary Polyhedron	ARB		V1x V3x V5x V7x	V1y V3y V5y V7y	V1z V3z V5z V7z	V2x V4x V6x V8x	V2y V4y V6y V8y	V2z V4z V6z V8z	1 of 5 2 of 5 3 of 5 4 of 5 5 of 5
			FACE DESCRIPTIONS (see note below)						
Termination of Body Input Data	END								

NOTE: Card 5 of the arbitrary polyhedron input contains a four-digit integer for each of the six faces of an ARB body. The format is 6(1X, I4), beginning in column 11. See the ARB write-up in Section 2.1 of Reference 14 for an example.

Table 8. Cross Section Input Data

CARD TYPE	FIELD/FORMAT	INPUT SYMBOL	DESCRIPTION
XA	1-80/20AA	TITLE	Title card for cross sections. This title is also written on tape if a processed tape is generated; therefore, it is suggested that the title be definitive.
XB	1-5/I5	NGP	The number of primary groups for which there are cross sections to be stored. Should be same as NMGP input in MORSE.
	6-10/I5	NDS	Number of primary downscatters for NGP (usually NGP).
	11-15/I5	NGG	Number of secondary groups for which there are cross sections to be stored.
	16-20/I5	NDSG	Number of secondary downscatters for NGG (usually NGG).
	21-25/I5	INGP	Total number of groups for which cross sections are to be input.
	26-30/I5	ITBL	Table length, i.e., the number of cross sections for each group (usually equal to number of downscatters + number of upscatters +3).
	31-35/I5	ISGG	Location of within-group scattering cross sections (usually equal to number of upscatters +4).
	36-40/I5	NMED	Number of media for which cross sections are to be stored – should be same as MEDIA input in MORSE.
	41-45/I5	NELEM	Number of elements for which cross sections are to be read.
	46-50/I5	NMIX	Number of mixing operations (elements times density operations) to be performed (must be ≥ 1).
	51-55/I5	NCOEF	Number of coefficients for each element, including P_0.
	56-60/I5	NSCT	Number of discrete angles (usually $NCOEF/2_{Integral}$).

Table 8. Continued

CARD TYPE	FIELD/FORMAT	INPUT SYMBOL	DESCRIPTION
XB	61-65/I5	ISTAT	Flag to store Legendre coeffiicents if greater than zero. Must be >0 if RELCOL is used.
XC	1-5/I5	*IRDSG†	Switch to print the cross sections as they are read if 0, if 0 card sequence is not checked. IFAM: Cross sections are also printed if IRDSG = –99.
	6-10/I5	ISTR†	Switch to print cross sections as they are stored if >0.
	11-15/I5	IFMU†	Switch to print intermediate results of μ's calculation if >0.
	16-20/I5	IMOM†	Switch to print moments of angular distribution if >0.
	21-25/I5	IPRIN†	Switch to print angles and probabilities if >0.
	26-30/I5	IPUN†	Switch to print results of bad Legendre coefficients if >0.
	31-35/I5	*IDTF†	Switch to signal that input format is DTF-IV format if >0; otherwise, ANISN format is assumed. IFAM Must be same for F- and A-modes.
	36-40/I5	IXTAPE	Logical tape unit if binary cross-section tape, set equal to 0 if cross sections are from cards. If negative, then the processed cross sections and other necessary data from a previous run will be read; in this case (IXTAPE <0) no cross sections from cards and no mixing cards may be input. The absolute value of IXTAPE is the logical tape unit.
	41-45/I5	JXTAPE	Logical tape unit of a processed cross-section tape to be written. This processed tape will contain the title card, the variables from common LOCSIG and the pertinent cross sections from blank common.
	46-50/I5	IO6RT	Logical tape unit of a point cross-section tape in O6R format.

Table 8. Concluded

CARD TYPE	FIELD/FORMAT	INPUT SYMBOL	DESCRIPTION
XC	51-55/I5	IGQPT	Last group (MORSE multigroup structure) for which the O6R point cross sections are to be used (NMGP).
	†Switches are ignored if IXTAPE <0.		
XD	(Omit if IXTAPE ≤ 0 on card XC)		
	1-70/14I5	NSIG(I)	Element identifiers for cross-section tape. If element identifiers are in the same order as element on tape, the efficiency of the code is increased due to fewer tape rewinds.
XE	(Omit if IXTAPE ≤ 0 on card XC)		
			Cross sections in ANISN format if IDTF ≤ 0, otherwise, DTF-IV format. Cross sections for INGP groups with a table length of ITBL for NELEM elements each with NCOEFF coefficients. IFAM: Not required for A-mode input.
XF	(NMIX cards are required. Omit if IXTAPE <0 on card XC)		
	1-5/I5	KM	Medium number (media numbers from 1 to MEDIA, see Card B, must appear on some XF card).
	6-10/I5	KE	Element number occurring in medium KM (negative value indicates last mixing operation for that medium and at least one negative value is required for each medium).
	11-20/E10.5	RHO	Density of element KE in medium KM in units of atoms/(barn·cm).
XG	(Omit if IO6RT ≤ 0)		
	1-5/I5	NXPM	Number of point cross-section sets per medium found on an O6R tape, = 1, total cross section only, = 2, total and scattering cross section, = 3, total scattering and ν^* fission cross section.

B.4 Analysis Data

The SAMBO analysis package was written for use with MORSE into the IFAM test bed. The capabilities of this package were sufficient that only minor modifications were required in the analysis subroutines. No changes were required in the input data format or processing by the SAMBO package. The input analysis data, as specified in Table 9, are read by the SCORIN subroutine for both the forward and adjoint modes. A complete set of applicable cards is needed during analysis input for both modes.

Input data for the user written routines, INSCOR, SOURCE, and ENDRUN, will be inserted into the input data deck (or run stream) following the AM cards of the analysis input.

The input cards for user written subroutines are inserted into the input deck after the analysis data. IFAM (and MORSE) calls INSCOR from SCORIN, then returns to INPUT3 (may be INPUT or INPUT2 in some MORSE versions), which calls USERN. USERN can be used for the input of additional data for other user written subroutines.

Table 9. Analysis Input Data

CARD TYPE	FIELD/FORMAT	INPUT SYMBOL	DESCRIPTION
AA	1-80/20A4	IHOL(I)	Title information describing the analysis input data (I=1, 20)
AB	1-5/I5	ND	Number of detectors (set=1 if 0).
	6-10/I5	NNE	Number of primary particle energy bins to be used (must be $\leq$NE)
	11-15/I5	NE	Total number of energy bins (set=0 if 1).
	16-20/I5	NT	Number of time bins for each detector (may be negative, in which case, NT values are to be read used for every detector)(set=0 if NT = ±1).
	21-25/I5	NA	Number of angle bins (set=0 if 1).
	26-30/I5	NRESP	Number of energy-dependent response functions to be used (set=1 if 0).
	31-35/I5	NEX	Number of extra arrays of size NMTG to be set aside (useful, for example, as a place to store an array of group transfer probabilities for estimator routines. If the subroutine ENDRUN which outputs fluence estimates from collision and track lengths is used, then this number must be at least MXREG + 2 (see Card 1 for MXREG).
	36-40/I5	NEXND	Number of extra arrays to size ND to be set aside (useful, for example, as a place to store detector-dependent counters). If RELCOL is used, then NEXND must be at least 1 for an event counter.
AC	(ND cards will be read, i.e., I=1, ND)		
	1-10/E10.4	XD(I)	Point detector position. The distance between this point and XSTRT, YSTRT, ZSTRT of Card D will be used along with the initial age, AGSTRT, to define the lower limit of the first time bin. If other than point detectors are desired, the point positions must still be input and can be combined with additional data built in to user routines to fully define each detector.
	11-20/E10.4	YD(I)	
	21-30/E10.4	ZD(I)	

Table 9. Continued

CARD TYPE	FIELD/FORMAT	INPUT SYMBOL	DESCRIPTION
AD	1-80/20A4	LNK*	Title or units for total response for all detectors. Will be used in columns 54 through 133 of the title for the print of these arrays.
(NRESP sets of AE and AF card types will be input, with each AE card followed by the NMTG response values on AF card types for each response).			
AE	1-80/20A4	LABEL	Title or units for each total response for all detectors.
AF	1-70/7E10.4	RESP(I)	Response function values. NMTG values will be read in for each total response function in order of decreasing energy. Each set of NMTG response function values will be headed by its AE card (I=1, NMTG).
AG	(Omit if NE $\leq$1)		
	1-80/20A4	LNK*	Units for energy-dependent fluence for all detectors.
AH	(Omit if NE $\leq$1)		
	1-70/1415	IB	Energy group numbers defining lower limit of analysis energy bins (in order of increasing group number). The NNE entry must equal NGPQTN and NE must be set to NMTG + NGPQTG for a combined problem, or else to NGPQTG or NGPQTN.
AI	(Omit if |NT| $\leq$1)		
	1-80/20A4	LNK*	Units for time dependent total response for all detectors.
AJ	(Omit if |NT| $\leq$1 or NE $\leq$1)		
	1-80/20A4	LNK*	Units for time and energy dependent fluence for all detectors.
AK	(Omit if |NT| $\leq$1)		
	1-70/7E10.4	T(IT,TD)	NT values of the upper limits of time bins for each detector in order of increasing time and detector number. The values for each detector must start on a new card. If NT on card AB is negative, then only NT values are read and used for every detector.

Table 9. Concluded

CARD TYPE	FIELD/FORMAT	INPUT SYMBOL	DESCRIPTION
AL	(Omit if NA ≤ 1)		
	1-80/20A4	LNK*	Units for angle and energy dependent fluence for all detectors.
AM	(Omit if NA ≤ 1)		
	1-70/7E10.4	COS(I)	Angle bins are defined by the upper limits of the cosine of the angle (i.e., the cosine of the lower angle limit). Thus, the NAth value must equal 1.

*The input symbol LNK is a generic variable name for data which is stored in blank common and addressed by its location instead of the usual mnemonic name.

APPENDIX C

IFAM SAMPLE PROBLEM

The IFAM sample problem was not chosen because it was the best example of the types of problems for which IFAM should be used, but because of the availability of experimental and analytical data with which to compare results. In addition, important features such as a point source and point detector, the need to do biasing to get adequate results in a reasonable time, and simplicity of the geometry were taken into consideration. These features are present in the point source/point detector configuration shown in Figure 20. Another attractive feature that has been used in testing IFAM is that data for many different source/detector separations are available, so the difficulty of the transport problem can be changed readily. At the same time, the amount of effort required to make these changes is minimum.

The source for the sample point is a point isotropic fission source located at (0,0,0). The detector is also isotropic, has a Henderson tissue dose response, and is located at (0,0,Z), where Z is the source/detector separation. Test cases have been run for Z = 150, 300, 600, and 1200 meters. Note that, for the adjoint mode, the source is located at (0,0,Z), and the adjoint detector (or forward source) at (0,0,0). The medium in the volume is uniform air at a density of 1.11 grams per liter. The fission source spectrum, cross sections, and response function used are the same as those used for the benchmark calculations described in refer-

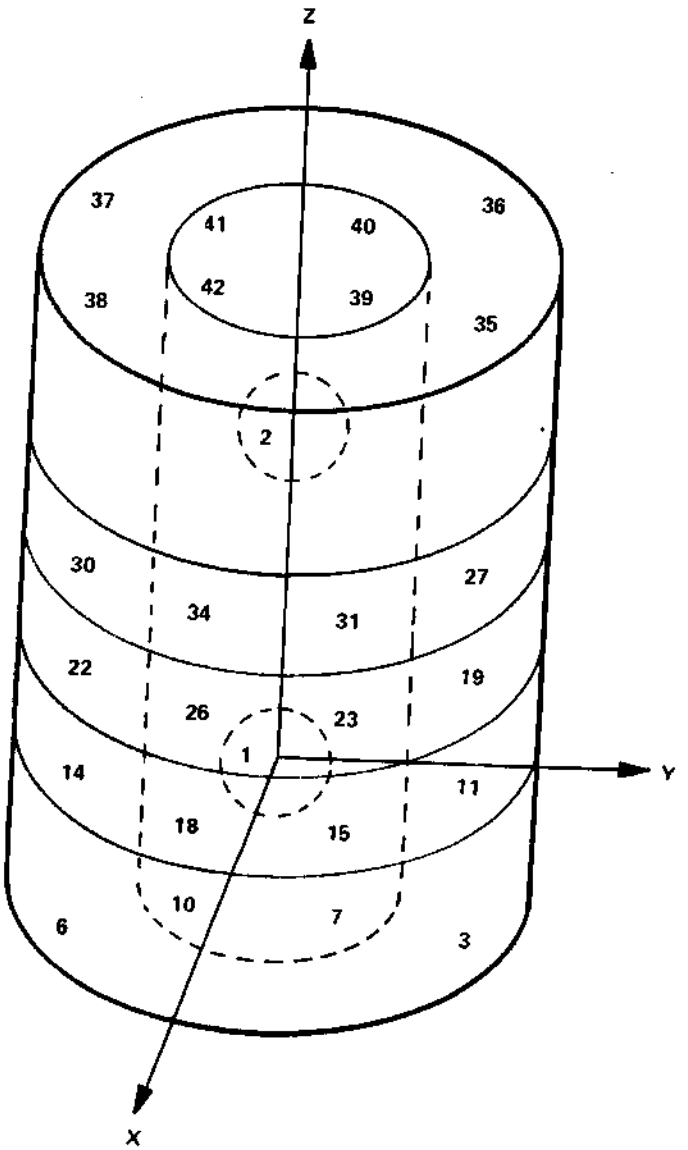

Figure 20. Sample Problem Geometry

ences 46 through 48 which were used to compare results. Of course, allowance must be made for the fact that the geometry used in this sample problem is finite, while the results of the above references are for infinite geometries.

In order to obtain spatial dependent importance data, 42 importance regions were defined as illustrated in Figure 20. Regions 1 and 2 are spheres centered about the source and detector, respectively. In the radial direction, the overall cylindrical geometry was divided into an inside cylinder and an outside annular volume. In the axial direction, five sectors were defined, one below the source, one above the detector, and three equally spaced between the source and detector. To consider the angular dependence, both the inside cylindrical and outside annular regions were divided into quadrants for each axial sector. In this manner, forty-two importance regions were defined. Energy and angular fluxes and importance data were stored for each region, as described in Chapter IV. The input card images, as listed by the control stream of Figure 19, are shown on pages 179 through 183.

Selected pages of the IFAM random walk and analysis output are shown on pages 184 through 233. Output from both the forward and adjoint modes is given.

```
*DATA,L  FAMT.,DTFF.
DATA 7 RL70-5 05/10-23:42:52
    1.  NEW      1     2  100    10  100    10
    2.  NEW      1     2 2.5
    3.  NEW      0     0    0     0    0     0    0    0    0    0    0    0    1    0    0
    4.  -03   1 F A M  REDUCED PT. SOURCE/DETECTOR IN AIR PROBLEM - EXC, VOL. IN
    5.           1   100     1     1   14     0   15   15     0    0 25.0     1    0
    6.           0    14     0       1.0        0.025      0.          0.           2.2E+5
    7.        0.001       0.001      0.001      0.0        0.0         0.0        0.0
    8.         1.568E-4   8.932E-4   3.480E-3   1.392E-2   3.457E-2   3.507E-2   1.072E-1
    9.         8.898E-2   2.323E-2   1.203E-1   2.181E-1   1.983E-1   1.403E-1   1.550E-2
   10.       1.5000E 071.2200E 071.0000E 078.1800E 066.3600E 064.9600E 064.0600E 06
   11.        3.01 E 06 2.46 E 06 2.35 E 06 1.826E 06 1.108E 06 5.502E 05 1.109E 05
   12.        3.3546E+3
   13.                  346122764532
   14.          0    0     0    0    0   42    0
   15.          0    0     0    0    0
   16.          3    0            REDUCED GEOMETRY FOR POINT SOURCE/DETECTOR PROBLEM
   17.         SPH    1 0.0        0.0        0.0         9999.9
   18.         SPH    2 0.0        0.0        60000.0     9999.9
   19.         RCC    3 0.0        0.0       -20000.0     0.0         0.0         20000.1
   20.                  80000.0
   21.         RCC    4 0.0        0.0        0.0         0.0         0.0         20000.1
   22.                  80000.0
   23.         RCC    5 0.0        0.0        20000.0     0.0         0.0         20000.1
   24.                  80000.0
   25.         RCC    6 0.0        0.0        40000.0     0.0         0.0         20000.1
   26.                  80000.0
   27.         RCC    7 0.0        0.0        60000.0     0.0         0.0         20000.0
   28.                  80000.0
   29.         RCC    8 0.0        0.0       -20000.0     0.0         0.0         100000.0
   30.                  40000.0
   31.         RPP     9-0.1       130000.0  -0.1         130000.0  -50000.0     170000.0
   32.         RPP    10-130000.0  0.0        0.0         130000.0  -50000.0     170000.0
   33.         RPP    11-130000.0  0.1       -130000.0    0.1       -50000.0     170000.0
   34.         RPP    12 0.0       130000.0  -130000.0    0.0       -50000.0     170000.0
   35.         RCC    13 0.0       0.0       -19999.9     0.0        0.0         99999.8
   36.                  79999.9
   37.         SPH    14 0.0       0.0        30000.0     200000.0
   38.         END
   39.           1    8    + 1
   40.           2    8    + 2
   41.           3   20    + 3    - 8    + 9
   42.           4   20    + 3    - 8    +10
   43.           5   20    + 3    - 8    +11
   44.           6   20    + 3    - 8    +12
   45.           7   20    + 3    + 8    + 9    - 1
   46.           8   20    + 3    + 8    +10    - 1
   47.           9   20    + 3    + 8    +11    - 1
   48.          10   20    + 3    + 8    +12    - 1
   49.          11   20    + 4    - 8    + 9
   50.          12   20    + 4    - 8    +10
   51.          13   20    + 4    - 8    +11
   52.          14   20    + 4    - 8    +12
   53.          15   20    + 4    + 8    + 9    - 1
   54.          16   20    + 4    + 8    +10    - 1
   55.          17   20    + 4    + 8    +11    - 1
```

```
 56.        18   20    + 4    + 8    +12    - 1
 57.        19   20    + 5    - 8    + 9
 58.        20   20    + 5    - 8    +10
 59.        21   20    + 5    - 8    +11
 60.        22   20    + 5    - 8    +12
 61.        23   20    + 5    + 8    + 9
 62.        24   20    + 5    + 8    +10
 63.        25   20    + 5    + 8    +11
 64.        26   20    + 5    + 8    +12
 65.        27   20    + 6    - 8    + 9
 66.        28   20    + 6    - 8    +10
 67.        29   20    + 6    - 8    +11
 68.        30   20    + 6    - 8    +12
 69.        31   20    + 6    + 8    + 9    - 2
 70.        32   20    + 6    + 8    +10    - 2
 71.        33   20    + 6    + 8    +11    - 2
 72.        34   20    + 6    + 8    +12    - 2
 73.        35   20    + 7    - 8    + 9
 74.        36   20    + 7    - 8    +10
 75.        37   20    + 7    - 8    +11
 76.        38   20    + 7    - 8    +12
 77.        39   20    + 7    + 8    + 9    - 2
 78.        40   20    + 7    + 8    +10    - 2
 79.        41   20    + 7    + 8    +11    - 2
 80.        42   20    + 7    + 8    +12    - 2
 81.        43    0    + 9    -13
 82.        44    0    +10    -13
 83.        45    0    +11    -13
 84.        46    0    +12    -13
 85.       END
 86.         1    2    3    4    5    6    7    8    9   10   11   12   13   14
 87.        15   16   17   18   19   20   21   22   23   24   25   26   27   28
 88.        29   30   31   32   33   34   35   36   37   38   39   40   41   42
 89.        19   20   21   22
 90.         1    1    1    1    1    1    1    1    1    1    1    1    1    1
 91.         1    1    1    1    1    1    1    1    1    1    1    1    1    1
 92.         1    1    1    1    1    1    1    1    1    1    1    1    1    1
 93.         0    0    0    0
 94.       4.189E12  4.189E12  7.540E13  7.540E13  7.540E13  7.540E13  2.461E13
 95.       2.461E13  2.461E13  2.461E13  7.540E13  7.540E13  7.540E13  7.540E13
 96.       2.461E13  2.461E13  2.461E13  2.461E13  7.540E13  7.540E13  7.540E13
 97.       7.540E13  2.513E13  2.513E13  2.513E13  2.513E13  7.540E13  7.540E13
 98.       7.540E13  7.540E13  2.461E13  2.461E13  2.461E13  2.461E13  7.540E13
 99.       7.540E13  7.540E13  7.540E13  2.461E13  2.461E13  2.461E13  2.461E13
100.       14-MEV WT XSECTIONS FOR AIR  -  F-MODE INPUT
101.        15   15    0    0   15   18    4    1    1    1    6    3    1
102.         0    0    0    0    1    0    0    0    0    0    0
103.       0 +12811- 9 0 +    0+ 0 0 +71737- 9 0 +28052- 914R+    0+ 0 0 +11464- 9
104.       0 +    0+ 0 0 +66814- 9 0 +24956- 9 0 +94300-1013R+    0+ 0 0 +10423- 9
105.       0 +    0+ 0 0 +58432- 9 0 +21479- 9 0 +12113- 9 0 +22328-1012R+    0+ 0
106.       0 +95534-10 0 +    0+ 0 0 +58510- 9 0 +26748- 9 0 +14392- 9 0 +28688-10
107.       0 +33637-1011R+    0+ 0 0 +89562-10 0 +    0+ 0 0 +62953- 9 0 +29353- 9
108.       0 +16856- 9 0 +16751-10 0 +25094-10 0 +34893-1010R+    0+ 0 0 +14483- 9
109.       0 +    0+ 0 0 +69968- 9 0 +30362- 9 0 +20862- 9 0 +72731-11 0 +13547-10
110.       0 +23529-10 0 +25826-10 9R+    0+ 0 0 +13445- 9 0 +    0+ 0 0 +87048- 9
111.       0 +44742- 9 0 +24518- 9 0 +24633-10 0 +10373-10 0 +21696-10 0 +33153-10
112.       0 +32199-10 8R+    0+ 0 0 +71867-10 0 +    0+ 0 0 +62301- 9 0 +2396R- 9
```

```
113.      0 +25238- 9 0 +54870-15 0 +24505-11 0 +59374-11 0 +17235-10 0 +17735-10
114.      0 +16667-10 7R+     0+ 0 0 +33771-10 0 +     0+ 0 0 +53538- 9 0 +75580-10
115.      0 +86990-10 0 +26800-10 0 +39854-13 0 +64939-12 0 +12810-11 0 +35461-11
116.      0 +37327-11 0 +34617-11 6R+     0+ 0 0 +37277-10 0 +     0+ 0 0 +74152- 9
117.      0 +36852- 9 0 +41220- 9 0 +22359- 9 0 +68149-11 0 +98214-12 0 +29624-11
118.      0 +57393-11 0 +20241-10 0 +16330-10 0 +14954-10 5R+     0+ 0 0 +27427-10
119.      0 +     0+ 0 0 +10091- 8 0 +73914- 9 0 +33574- 9 0 +13828-10 0 +     0+ 0
120.      0 +34969-12 0 +26103-11 0 +38480-11 0 +11041-10 0 +18843-10 0 +19574-10
121.      0 +17493-10 4R+     0+ 0 0 +13455-10 0 +     0+ 0 0 +10158- 8 0 +82427- 9
122.      0 +24250- 9 3R+     0+ 0 0 +12688-11 0 +16947-11 0 +22987-11 0 +86922-11
123.      0 +69962-11 0 +10765-10 0 +93813-11 3R+     0+ 0 0 +24733-11 0 +     0+ 0
124.      0 +15923- 8 0 +14583- 8 0 +17805- 9 3R+     0+ 0 0 +63358-12 0 +94586-12
125.      0 +69167-12 0 +91322-12 0 +30896-11 0 +23956-11 0 +40186-11 0 +34365-11
126.      2R+     0+ 0 0 +56793-12 0 +     0+ 0 0 +27448- 8 0 +26386- 8 0 +13153- 9
127.      4R+     0+ 0 0 +23709-12 0 +49054-13 0 +34984-13 0 +45466-13 0 +10321-12
128.      0 +11601-12 0 +19316-12 0 +16352-12 0 +     0+ 0 0 +27307-11 0 +     0+ 0
129.      0 +35854- 8 0 +33087- 8 0 +10558- 9 5R+     0+ 0 0 +51624-15 0 +59272-16
130.      0 +44238-16 0 +58578-16 0 +10406-15 0 +15472-15 0 +27307-15 0 +23940-15
131.      2R+     0+ 0 0 +71737- 9 0 +62324- 916R+     0+ 0 0 +66814- 9 0 +57256- 9
132.      0 -69780-1015R+     0+ 0 0 +58432- 9 0 +48822- 9 0 -45010-10 0 -73052-11
133.     14R+     0+ 0 0 +58510- 9 0 +55266- 9 0 -74323-10 0 -19936-1014R+     0+ 0
134.      0 +62953- 9 0 +57183- 9 0 -10865- 9 0 -28880-1114R+     0+ 0 0 +69968- 9
135.      0 +67342- 9 0 -17548- 9 0 -63890-1114R+     0+ 0 0 +87048- 9 0 +76541- 9
136.      0 -18406- 9 0 -57853-1014R+     0+ 0 0 +62301- 9 0 +47045- 9 0 -31315- 9
137.     15R+     0+ 0 0 +53538- 9 0 +20210- 9 0 +60591-10 0 -66006-1014R+     0+ 0
138.      0 +74152- 9 0 +57960- 9 0 +84142-10 0 -29566- 9 0 -18801-1013R+     0+ 0
139.      0 +10091- 8 0 +63141- 9 0 -26123- 9 0 -38164-1014R+     0+ 0 0 +10158- 8
140.      0 +41610- 9 0 -22009- 915R+     0+ 0 0 +15923- 8 0 +37023- 9 0 -12991- 9
141.     15R+     0+ 0 0 +27448- 8 0 +47311- 9 0 -12126- 915R+     0+ 0 0 +35854- 8
142.      0 +76560- 9 0 -95609-1013R+     0+ 0
143.      2R+     0+ 0 0 +71737- 9 0 +66432- 916R+     0+ 0 0 +66814- 9 0 +63555- 9
144.      0 -15801-1015R+     0+ 0 0 +58432- 9 0 +54024- 9 0 -46953-10 0 +86841-11
145.     14R+     0+ 0 0 +58510- 9 0 +57256- 9 0 -55345-10 0 +22853-1014R+     0+ 0
146.      0 +62953- 9 0 +53302- 9 0 -26705-10 0 +41050-1114R+     0+ 0 0 +69968- 9
147.      0 +66706- 9 0 +33950-11 0 +88731-1114R+     0+ 0 0 +87048- 9 0 +75699- 9
148.      0 +12897- 9 0 +64789-1014R+     0+ 0 0 +62301- 9 0 +34405- 9 0 +23756- 9
149.     15R+     0+ 0 0 +53538- 9 0 +26501- 9 0 -46770-10 0 +71874-1014R+     0+ 0
150.      0 +74152- 9 0 +26898- 9 0 -15857- 9 0 +55263-10 0 +26371-1013R+     0+ 0
151.      0 +10091- 8 0 +39879- 9 0 +53853-12 0 +53547-1014R+     0+ 0 0 +10158- 8
152.      0 +23791- 9 0 +94525-1015R+     0+ 0 0 +15923- 8 0 +14323- 9 0 -27310-10
153.     15R+     0+ 0 0 +27448- 8 0 +48387-10 0 -95624-1115R+     0+ 0 0 +35854- 8
154.      0 +75791-10 0 -90535-1113R+     0+ 0
155.      2R+     0+ 0 0 +71737- 9 0 +66798- 916R+     0+ 0 0 +66814- 9 0 +63598- 9
156.      0 +18659-1015R+     0+ 0 0 +58432- 9 0 +54167- 9 0 +28071-10 0 -73195-11
157.     14R+     0+ 0 0 +58510- 9 0 +57006- 9 0 +51355-10 0 -17927-1014R+     0+ 0
158.      0 +62953- 9 0 +48554- 9 0 +66673-10 0 -44739-1114R+     0+ 0 0 +69968- 9
159.      0 +51154- 9 0 +47356-10 0 -93130-1114R+     0+ 0 0 +87048- 9 0 +56220- 9
160.      0 -43396-10 0 -46247-1014R+     0+ 0 0 +62301- 9 0 +17629- 9 0 -11925- 9
161.     15R+     0+ 0 0 +53538- 9 0 +25118- 9 0 -34954-10 0 -47340-1014R+     0+ 0
162.      0 +74152- 9 0 +97542-10 0 -12354- 9 0 -30491-10 0 -28123-1013R+     0+ 0
163.      0 +10091- 8 0 +18685- 9 0 -38599-10 0 -57015-1014R+     0+ 0 0 +10158- 8
164.      0 +10648-10 0 -52105-1015R+     0+ 0 0 +15923- 8 0 +15514-10 0 -15685-10
165.     15R+     0+ 0 0 +27448- 8 0 -29427-10 0 -11076-1115R+     0+ 0 0 +35854- 8
166.      0 -40830-10 0 -22525-1113R+     0+ 0
167.      2R+     0+ 0 0 +71737- 9 0 +65721- 916R+     0+ 0 0 +66814- 9 0 +61170- 9
168.      0 +65066-1015R+     0+ 0 0 +58432- 9 0 +49760- 9 0 +77413-10 0 +49903-11
169.     14R+     0+ 0 0 +58510- 9 0 +44618- 9 0 +82665-10 0 +10878-1014R+     0+ 0
```

```
  170.        0 +62953- 9 0 +32879- 9 0 +39054-10 0 +40112-1114R+     0+ 0 0 +69968- 9
  171.        0 +31802- 9 0 -60433-10 0 +78861-1114R+     0+ 0 0 +87048- 9 0 +21403- 9
  172.        0 -83035-10 0 +18621-1014R+     0+ 0 0 +62301- 9 0 +10070- 9 0 -42677-10
  173.       15R+     0+ 0 0 +53538- 9 0 +17702- 9 0 -56282-10 0 +12804-1014R+     0+ 0
  174.        0 +74152- 9 0 +46310-10 0 -20232- 9 0 +47279-10 0 +24381-1013R+     0+ 0
  175.        0 +10091- 8 0 +69673-10 0 -81954-11 0 +49040-1014R+     0+ 0 0 +10158- 8
  176.        0 +98537-11 0 -40840-1015R+     0+ 0 0 +15923- 8 0 +94455-11 0 -84847-11
  177.       15R+     0+ 0 0 +27448- 8 0 +83147-10 0 +21092-1115R+     0+ 0 0 +35854- 8
  178.        0 +75510-10 0 +52835-1113R+     0+ 0
  179.        2R+     0+ 0 0 +71737- 9 0 +48892- 916R+     0+ 0 0 +66814- 9 0 +46730- 9
  180.        0 -71214-1015R+     0+ 0 0 +58432- 9 0 +33260- 9 0 -69421-10 0 -33858-11
  181.       14R+     0+ 0 0 +58510- 9 0 +19606- 9 0 -83740-10 0 -67045-1114R+     0+ 0
  182.        0 +62953- 9 0 +10468- 9 0 -11460- 9 0 -29492-1114R+     0+ 0 0 +69968- 9
  183.        0 +11358- 9 0 -19435-10 0 -53062-1114R+     0+ 0 0 +87048- 9 0 +64865-10
  184.        0 -61525-10 0 +67070-1214R+     0+ 0 0 +62301- 9 0 +43271-10 0 -16926-10
  185.       15R+     0+ 0 0 +53538- 9 0 +78886-10 0 -38251-10 0 +99866-1114R+     0+ 0
  186.        0 +74152- 9 0 +57932-11 0 -60885-10 0 +22736-10 0 -16971-1013R+     0+ 0
  187.        0 +10091- 8 0 +84702-11 0 -14016-10 0 -33189-1014R+     0+ 0 0 +10158- 8
  188.        0 -31196-11 0 -20379-1015R+     0+ 0 0 +15923- 8 0 -10389-10 0 -18648-11
  189.       15R+     0+ 0 0 +27448- 8 0 -75909-10 0 -19472-1115R+     0+ 0 0 +35854- 8
  190.        0 -97342-10 0 -11546-1013R+     0+ 0
  191.          1    -1   1.0
  192.         F-MODE POINT SOURCE/DETECTOR TEST CASE  -  ANALYSIS INPUT
  193.           2    9    9    0    6    1    2    0
  194.        0.001      0.001      59999.9
  195.        0.001      0.001      59999.9
  196.         TOTAL RESPONSE - NEUTRON RESPONSE FUNCTION FROM ORNL 4464
  197.         HENDERSON TISSUE DOSE - RADS[T]
  198.         5.46E-09  5.13E-09  4.84E-09  4.61E-09  4.44E-09  4.13E-09  4.01E-09
  199.         3.39E-09  3.15E-09  3.09E-09  2.64E-09  1.97E-09  1.12E-09  2.29E-10
  200.         0.0
  201.         ENERGY DEPENDENT FLUENCE - NEUTRONS/CMSQ/EV/SOURCE
  202.           1    2    3    4    6    9   11   13   14
  203.         ENERGY AND ANGULAR DEPENDENT FLUENCE
  204.        -.8888889 -.4444444 0.0       0.4444444 0.8888889 1.0
END DATA.


@ASG,T DTFA,F2
```

```
*DATA,L  FAMT.,DTFA.
DATA 7 RL70-5 05/10-23:42:57
    1.        ADJOINT MODE INPUT - REDUCED PT. SOURCE/DETECTOR PROBLEM
    2.           1  100    1    1   14    0   15   15    0    1 25.0    1    0
    3.           0   14    0       1.0       0.025      0.0       0.0          2.2E+5
    4.       0.001      0.001      59999.9   0.0        0.0       0.0       0.0
    5.        5.46E-09  5.13E-09  4.84E-09  4.61E-09  4.44E-09  4.13E-09  4.01E-09
    6.        3.39E-09  3.15E-09  3.09E-09  2.64E-09  1.97E-09  1.12E-09  2.29E-10
    7.      1.5000E 071.2200E 071.0000E 078.1800E 066.3600E 064.9600E 064.0600E 06
    8.       3.01 E 06 2.46 E 06 2.35 E 06 1.826E 06 1.108E 06 5.502E 05 1.109E 05
    9.       3.3546E+3
   10.                 346122764532
   11.          0    0    0    0    0   42    0
   12.          0    0    0    0    0
   13.          3    0    A-MODE GEOMETRY INPUT - REDUCED PT. S/D PROBLEM
   14.          1    2    3    4    5    6    7    8    9   10   11   12   13   14
   15.         15   16   17   18   19   20   21   22   23   24   25   26   27   28
   16.         29   30   31   32   33   34   35   36   37   38   39   40   41   42
   17.         19   20   21   22
   18.          1    1    1    1    1    1    1    1    1    1    1    1    1    1
   19.          1    1    1    1    1    1    1    1    1    1    1    1    1    1
   20.          1    1    1    1    1    1    1    1    1    1    1    1    1    1
   21.          0    0    0    0
   22.       4.189E12  4.189E12  7.540E13  7.540E13  7.540E13  7.540E13  2.461E13
   23.       2.461E13  2.461E13  2.461E13  7.540E13  7.540E13  7.540E13  7.540E13
   24.       2.461E13  2.461E13  2.461E13  2.461E13  7.540E13  7.540E13  7.540E13
   25.       7.540E13  2.513E13  2.513E13  2.513E13  2.513E13  7.540E13  7.540E13
   26.       7.540E13  7.540E13  2.461E13  2.461E13  2.461E13  2.461E13  7.540E13
   27.       7.540E13  7.540E13  7.540E13  2.461E13  2.461E13  2.461E13  2.461E13
   28.       14-MEV WT XSECTIONS FOR AIR - A-MODE INPUT
   29.        15   15    0    0   15   18    4    1    1    1    6    3    1
   30.         0    0    0    0    0    0    0    0    0    0    0
   31.         1   -1  1.0
   32.       A-MODE POINT SOURCE/DETECTOR TEST CASE  -  ANALYSIS INPUT
   33.         2    9    9    0    6    1    2    0
   34.      1.0       1.0       1.0
   35.      1.0       1.0       1.0
   36.       ADJOINT RESPONSE VALUES BASED ON HENDERSON TISSUE DOSE
   37.       ORNL 4464 FISSION SOURCE
   38.       1.568E-4  8.932E-4  3.480E-3  1.392E-2  3.457E-2  3.507E-2  1.072E-1
   39.       8.898E-2  2.323E-2  1.203E-1  2.181E-1  1.983E-1  1.403E-1  1.550E-2
   40.       0.0
   41.       ENERGY DEPENDENT ADJOINT FLUENCE - IMPORTANCE/CMSQ/EV/SOURCE
   42.         1    2    3    4    6    9   11   13   14
   43.       ENERGY AND ANGULAR DEPENDENT ADJOINT FLUENCE
   44.      -.8888889 -.4444444 0.0       0.4444444 0.8888889 1.0
END DATA.
```

```
          ITERATION DATA FOR IFAM PROBLEM

     INITIAL MODE -- 1     (0-FORWARD / 1-ADJOINT)
     NUMBER OF ITERATIONS =  2

           I   NPPB(I)   NBTI(I)
           1       100        10
           2       100        10


NSRF = 1      NSRA = 2      PATH SEARCH CONSTANT IN MFP (PSC) =      2.500

                          INTERMEDIATE PRINT OPTIONS (0-OFF/1-ON/-1-END)
 0-(1)APOLLO          0-(2)USER          0-(3)GOMLOC        0-(4)LOCSIG        0-(5)PDET          0-(6)BNKNMC
 0-(7)BANK            0-(8)RANDOM        0-(9)/1-4*NMTG/    0-(10)REG. IMP.    0-(11)FAI REG.1-2  1-(12)FAM
 0-(13)F-MODE WRITE   0-(14)A-MODE WRITE
```

```
I F A M  REDUCED PT. SOURCE/DETECTOR IN AIR PROBLEM - EXC. VOL. IN      29MAR75

    THIS PRINT OCCURRED ON THE  3 DAY OF THE  5 MONTH IN THE YEAR 1976
        AT  0 MINUTES PAST THE HOUR OF 10 PM .

  NSTRT   NMOST    NITS   NQUIT  NGPQTN  NGPQTG    NMGP    NMTG  NCOLTP   IADJM  MAXTIM   MEDIA  MEDALB
      1     100       1       1      14       0      15      15       0       0   25.00       1       0

  ISOUR   NGPFS  ISBIAS              WTSTRT      EBOTN      EBOTG       TCUT       VELTH
      0      14       1          1.000+00   2.500-02   0.000      0.000      2.200+05

              XSTRT      YSTRT      ZSTRT      AGSTRT       UINP       VINP       WINP
          1.000-03   1.000-03   1.000-03   0.000        .000000    .000000    .000000

                SOURCE DATA
     FS(31) =   .0001568      FS(32) =   .0008932      FS(33) =   .0034800      FS(34) =   .0139200
     FS(35) =   .0345700      FS(36) =   .0350700      FS(37) =   .1072000      FS(38) =   .0889800
     FS(39) =   .0232300      FS(40) =   .1203000      FS(41) =   .2181000      FS(42) =   .1983000
     FS(43) =   .1403000      FS(44) =   .0155000      FS(45) =   .0000000

GROUP PARAMETERS, GROUP NUMBERS GREATER THAN   15 CORRESPOND TO SECONDARY PARTICLES

   GROUP      UPPER EDGE        VELOCITY
                 (EV)          (CM/SEC)
     1        1.5000+07       5.1003+09
     2        1.2200+07       4.6077+09
     3        1.0000+07       4.1697+09
     4        8.1800+06       3.7290+09
     5        6.3600+06       3.2903+09
     6        4.9600+06       2.9370+09
     7        4.0600+06       2.6003+09
     8        3.0100+06       2.2872+09
     9        2.4600+06       2.1448+09
    10        2.3500+06       1.9984+09
    11        1.8260+06       1.6751+09
    12        1.1080+06       1.2593+09
    13        5.5020+05       7.9513+08
    14        1.1090+05       3.3056+08
    15        3.3546+03       2.2000+05

INITIAL RANDOM NUMBER =          346122764532

NSPLT= 0     NKILL= 0     NPAST= 0     NOLEAK= 0     IEBIAS= 0     MXREG= 42     MAXGP=  0

NSOUR= 0     MFISTP=  0     NKCALC= 0     NORMF= 0
```

REDUCED GEOMETRY FOR POINT SOURCE/DETECTOR PROBLEM 10JAN

IVOPT= 3 IDBG= 0

BODY DATA

SPH	1	.0000000	.0000000	.0000000	.9999900+04	.0000000	.0000000	3
SPH	2	.0000000	.0000000	.6000000+05	.9999900+04	.0000000	.0000000	11
RCC	3	.0000000	.0000000	-.2000000+05	.0000000	.0000000	.2000010+05	19
		.8000000+05						
RCC	4	.0000000	.0000000	.0000000	.0000000	.0000000	.2000010+05	28
		.8000000+05						
RCC	5	.0000000	.0000000	.2000000+05	.0000000	.0000000	.2000010+05	37
		.8000000+05						
RCC	6	.0000000	.0000000	.4000000+05	.0000000	.0000000	.2000010+05	46
		.8000000+05						
RCC	7	.0000000	.0000000	.6000000+05	.0000000	.0000000	.2000000+05	55
		.8000000+05						
RCC	8	.0000000	.0000000	-.2000000+05	.0000000	.0000000	.1000000+06	64
		.4000000+05						
RPP	9	-.1000000+00	.1300000+06	-.1000000+00	.1300000+06	-.5000000+05	.1700000+06	73
RPP	10	-.1300000+06	.0000000	.0000000	.1300000+06	-.5000000+05	.1700000+06	81
RPP	11	-.1300000+06	.1000000+00	-.1300000+06	.1000000+00	-.5000000+05	.1700000+06	89
RPP	12	.0000000	.1300000+06	-.1300000+06	.0000000	-.5000000+05	.1700000+06	97
RCC	13	.0000000	.0000000	-.1999990+05	.0000000	.0000000	.9999980+05	105
		.7999990+05						
SPH	14	.0000000	.0000000	.3000000+05	.2000000+06	.0000000	.0000000	114
END	15	.0000000	.0000000	.0000000	.0000000	.0000000	.0000000	122

NUMBER OF BODIES 14
LENGTH OF FPD-ARRAY 127

INPUT ZONE DATA

1	8	1	0	0	0	0	0	0	0	Z	1
2	8	2	0	0	0	0	0	0	0	Z	2
3	20	3	-8	9	0	0	0	0	0	Z	3
4	20	3	-8	10	0	0	0	0	0	Z	4
5	20	3	-8	11	0	0	0	0	0	Z	5
6	20	3	-8	12	0	0	0	0	0	Z	6
7	20	3	8	9	-1	0	0	0	0	Z	7
8	20	3	8	10	-1	0	0	0	0	Z	8
9	20	3	8	11	-1	0	0	0	0	Z	9
10	20	3	8	12	-1	0	0	0	0	Z	10
11	20	4	-8	9	0	0	0	0	0	Z	11
12	20	4	-8	10	0	0	0	0	0	Z	12
13	20	4	-8	11	0	0	0	0	0	Z	13
14	20	4	-8	12	0	0	0	0	0	Z	14

15	20	4	8	9	-1	0	0	0	0	0	Z 15
16	20	4	8	10	-1	0	0	0	0	0	Z 16
17	20	4	8	11	-1	0	0	0	0	0	Z 17
18	20	4	8	12	-1	0	0	0	0	0	Z 18
19	20	5	-8	9	0	0	0	0	0	0	Z 19
20	20	5	-8	10	0	0	0	0	0	0	Z 20
21	20	5	-8	11	0	0	0	0	0	0	Z 21
22	20	5	-8	12	0	0	0	0	0	0	Z 22
23	20	5	8	9	0	0	0	0	0	0	Z 23
24	20	5	8	10	0	0	0	0	0	0	Z 24
25	20	5	8	11	0	0	0	0	0	0	Z 25
26	20	5	8	12	0	0	0	0	0	0	Z 26
27	20	6	-8	9	0	0	0	0	0	0	Z 27
28	20	6	-8	10	0	0	0	0	0	0	Z 28
29	20	6	-8	11	0	0	0	0	0	0	Z 29
30	20	6	-8	12	0	0	0	0	0	0	Z 30
31	20	6	8	9	-2	0	0	0	0	0	Z 31
32	20	6	8	10	-2	0	0	0	0	0	Z 32
33	20	6	8	11	-2	0	0	0	0	0	Z 33
34	20	6	8	12	-2	0	0	0	0	0	Z 34
35	20	7	-8	9	0	0	0	0	0	0	Z 35
36	20	7	-8	10	0	0	0	0	0	0	Z 36
37	20	7	-8	11	0	0	0	0	0	0	Z 37
38	20	7	-8	12	0	0	0	0	0	0	Z 38
39	20	7	8	9	-2	0	0	0	0	0	Z 39
40	20	7	8	10	-2	0	0	0	0	0	Z 40
41	20	7	8	11	-2	0	0	0	0	0	Z 41
42	20	7	8	12	-2	0	0	0	0	0	Z 42
43	0	9	-13	0	0	0	0	0	0	0	Z 43
44	0	10	-13	0	0	0	0	0	0	0	Z 44
45	0	11	-13	0	0	0	0	0	0	0	Z 45
46	0	12	-13	0	0	0	0	0	0	0	Z 46
END	0	0	0	0	0	0	0	0	0	0	Z 47

NUMBER OF INPUT ZONES 46
NUMBER OF CODE ZONES 46
LENGTH OF INTEGER ARRAY 2401

CODE ZONE	INPUT ZONE	ZONE DATA LOC.	NO. OF BODIES	REGION NO.	MEDIA NO.
1	1	99	1	1	1
2	2	104	1	2	1
3	3	109	3	3	1
4	4	122	3	4	1
5	5	135	3	5	1
6	6	148	3	6	1
7	7	161	4	7	1
8	8	178	4	8	1
9	9	195	4	9	1
10	10	212	4	10	1
11	11	229	3	11	1

12	12	242	3	12	1
13	13	255	3	13	1
14	14	268	3	14	1
15	15	281	4	15	1
16	16	298	4	16	1
17	17	315	4	17	1
18	18	332	4	18	1
19	19	349	3	19	1
20	20	362	3	20	1
21	21	375	3	21	1
22	22	388	3	22	1
23	23	401	3	23	1
24	24	414	3	24	1
25	25	427	3	25	1
26	26	440	3	26	1
27	27	453	3	27	1
28	28	466	3	28	1
29	29	479	3	29	1
30	30	492	3	30	1
31	31	505	4	31	1
32	32	522	4	32	1
33	33	539	4	33	1
34	34	556	4	34	1
35	35	573	3	35	1
36	36	586	3	36	1
37	37	599	3	37	1
38	38	612	3	38	1
39	39	625	4	39	1
40	40	642	4	40	1
41	41	659	4	41	1
42	42	676	4	42	1
43	43	693	2	19	0
44	44	702	2	20	0
45	45	711	2	21	0
46	46	720	2	22	0

I	KR1(I)	KR2(I)
1	1	1
2	2	2
3	3	3
4	4	4
5	5	5
6	6	6
7	7	7
8	8	8
9	9	9
10	10	10
11	11	11
12	12	12

13	13	13
14	14	14
15	15	15
16	16	16
17	17	17
18	18	18
19	19	19
20	20	20
21	21	21
22	22	22
23	23	23
24	24	24
25	25	25
26	26	26
27	27	27
28	28	28
29	29	29
30	30	30
31	31	31
32	32	32
33	33	33
34	34	34
35	35	35
36	36	36
37	37	37
38	38	38
39	39	39
40	40	40
41	41	41
42	42	42
43	43	43
44	44	44
45	45	45
46	46	46

MORSE REGION IN INPUT ZONE(I) ARRAY MRIZ(I),I=1,46)

1	2	3	4	5	6	7	8	9	10	11	12	13	14	15	16	17	18	19	20	21	22	23	24	25
26	27	28	29	30	31	32	33	34	35	36	37	38	39	40	41	42	19	20	21	22				

MORSE MEDIA IN INPUT ZONE(I) ARRAY MMIZ(I),I=1,46)

1	1	1	1	1	1	1	1	1	1	1	1	1	1	1	1	1	1	1	1	1	1	1	1	1
1	1	1	1	1	1	1	1	1	1	1	1	1	1	1	1	1	1	0	0	0	0			

OPTION 3 WAS USED IN CALCULATING VOLUMES. FOR 42 REGIONS
0-SET VOLUMES = 1. 1-CONCENTRIC SPHERES. 2-SLABS. 3-INPUTVOLUMES.

VOLUMES (CM**) USED IN COLLISIONS DENSITY AND TRACK LENGTH ESTIMATORS.

REG	1	2	3	4	5	6	7	8	9	10
VOLUME	4.189+12	4.189+12	7.540+13	7.540+13	7.540+13	7.540+13	2.461+13	2.461+13	2.461+13	2.461+13
REG	11	12	13	14	15	16	17	18	19	20
VOLUME	7.540+13	7.540+13	7.540+13	7.540+13	2.461+13	2.461+13	2.461+13	2.461+13	7.540+13	7.540+13
REG	21	22	23	24	25	26	27	28	29	30
VOLUME	7.540+13	7.540+13	2.513+13	2.513+13	2.513+13	2.513+13	7.540+13	7.540+13	7.540+13	7.540+13
REG	31	32	33	34	35	36	37	38	39	40
VOLUME	2.461+13	2.461+13	2.461+13	2.461+13	7.540+13	7.540+13	7.540+13	7.540+13	2.461+13	2.461+13
REG	41	42								
VOLUME	2.461+13	2.461+13								

NGEOM= 19721. NGLAST= 22751

```
  14-REV WT XSECTIONS FOR AIR  -  F-MODE INPUT

NUMBER OF PRIMARY GROUPS (NGP)              15
NUMBER OF PRIMARY DOWNSCATTERS (NDS)        15
NUMBER OF SECONDARY GROUPS (NGG)             0
NUMBER OF SECONDARY DOWNSCATTERS (NDSG)      0
NUMBER OF PRIM+SEC GROUPS (INGP)            15
TABLE LENGTH (ITBL)                         18
LOC OF WITHIN GROUP (SIG GG) (ISGG)          4
NUMBER OF MEDIA (NMED)                       1
NUMBER OF INPUT ELEMENTS (NELEM)             1
NUMBER OF MIXING ENTRIES (NMIX)              1
NUMBER OF COEFFICIENTS (NCOEF)               6
NUMBER OF ANGLES (NSCT)                      3
RESTORE COEFF (ISTAT)                        1
ADJOINT SWITCH (FROM MORSE)                  0


INPUT/OUTPUT OPTIONS
     IRDSG (AS READ)          0
     ISTR (AS STORE)          0
     IFMU (MUS)               0
     IMOM (MOMENTS)           0
     IPRIN (ANGLES,PROB)      1
     IPUN (IMPOSSIBLE COEF)   0
     CARD FORMAT (IDTF)       0
     INPUT TAPE (IXTAPE)      0
     MORSEC TAPE (JXTAPE)     0
     06R TAPE (I06RT)         0


PACKING VARIABLES
     SCALE FACTOR       1.00+03
     SHIFT FACTOR          2000
     XSECS PER WORD           3

STORAGE ALLOCATIONS
CROSS SECTIONS START AT     22752
LAST LOCATION USED (PERM)   23835
TEMP LOCATIONS USED         37145 TO   38000
EXCESS STORAGE (TEMP)       13310
START OF LEGENDRE COEFF     23235
CARD     0 WAS READ WHEN CARD      1 WAS EXPECTED  CHECK CROSS SECTION CARD SEQUENCE IN  ELEMENT      1 COEFFICIENT      1
CARD  1028 WAS READ WHEN CARD      1 WAS EXPECTED  CHECK CROSS SECTION CARD SEQUENCE IN  ELEMENT      1 COEFFICIENT      2
CARD  2040 WAS READ WHEN CARD      1 WAS EXPECTED  CHECK CROSS SECTION CARD SEQUENCE IN  ELEMENT      1 COEFFICIENT      3
CARD  3052 WAS READ WHEN CARD      1 WAS EXPECTED  CHECK CROSS SECTION CARD SEQUENCE IN  ELEMENT      1 COEFFICIENT      4
CARD  4064 WAS READ WHEN CARD      1 WAS EXPECTED  CHECK CROSS SECTION CARD SEQUENCE IN  ELEMENT      1 COEFFICIENT      5
CARD  5076 WAS READ WHEN CARD      1 WAS EXPECTED  CHECK CROSS SECTION CARD SEQUENCE IN  ELEMENT      1 COEFFICIENT      6
```

MIXING TABLE

MEDIA 1 CONTAINS ELEMENT 1 WITH DENSITY 1.0000+00

CROSS SECTIONS FOR MEDIA 1

GROUP	SIGT	SIGST	PNUP	PNABS	GAMGEN	NU*FIS	DOWNSCATTER PROBABILITY							
1	7.174-05	5.893-05	.0000	.8214	.0000	.0000	.4761	.1600	.0379	.0571	.0592	.0438	.0546	.0283
							.0059	.0254	.0297	.0159	.0058	.0003	.0000	
2	6.681-05	5.535-05	.0000	.8284	.0000	.0000	.4509	.2188	.0518	.0453	.0425	.0599	.0320	.0067
							.0295	.0354	.0194	.0073	.0003	.0000		
3	5.843-05	4.801-05	.0000	.8216	.0000	.0000	.4474	.2998	.0349	.0282	.0452	.0359	.0074	.0422
							.0392	.0146	.0050	.0002	.0000			
4	5.851-05	4.896-05	.0000	.8367	.0000	.0000	.5464	.3443	.0149	.0212	.0121	.0026	.0117	.0226
							.0178	.0063	.0002	.0000				
5	6.295-05	5.400-05	.0000	.8577	.0000	.0000	.5436	.3864	.0456	.0045	.0012	.0055	.0071	.0043
							.0017	.0001	.0000					
6	6.997-05	5.549-05	.0000	.7930	.0000	.0000	.5472	.4419	.0000	.0001	.0018	.0047	.0031	.0012
							.0001	.0000						
7	8.705-05	7.360-05	.0000	.8455	.0000	.0000	.6079	.3429	.0364	.0093	.0005	.0017	.0013	.0001
							.0000							
8	6.230-05	5.511-05	.0000	.8846	.0000	.0000	.4349	.1578	.4057	.0000	.0000	.0011	.0004	.0000
9	5.354-05	5.016-05	.0000	.9369	.0000	.0000	.1507	.8218	.0276	.0000	.0000	.0000	.0000	
10	7.415-05	7.043-05	.0000	.9498	.0000	.0000	.5233	.4767	.0000	.0000	.0000	.0000		
11	1.009-04	9.816-05	.0000	.9728	.0000	.0000	.7530	.2470	.0000	.0000	.0000			
12	1.016-04	1.002-04	.0000	.9867	.0000	.0000	.8224	.1776	.0000	.0000				
13	1.592-04	1.590-04	.0000	.9984	.0000	.0000	.9173	.0827	.0000					
14	2.745-04	2.744-04	.0000	.9998	.0000	.0000	.9615	.0385						
15	3.585-04	3.309-04	.0000	.9228	.0000	.0000	1.0000							

SCATTERING PROBABILITIES AND ANGLES FOR MEDIA NUMBER 1

GP	TO GP	PROB	ANGLE	PROB	ANGLE	PROB	ANGLE
1	1	.6950	.9300	.9250	.4470	1.0000	-.1240
1	2	.5370	-.1350	.8650	-.8330	1.0000	.7390
1	3	.4050	-.0370	.7490	-.8300	1.0000	.7660
1	4	-1.0000	-2.0000	.0000	.0000	.0000	.0000
1	5	-1.0000	-2.0000	.0000	.0000	.0000	.0000
1	6	-1.0000	-2.0000	.0000	.0000	.0000	.0000
1	7	-1.0000	-2.0000	.0000	.0000	.0000	.0000
1	8	-1.0000	-2.0000	.0000	.0000	.0000	.0000
1	9	-1.0000	-2.0000	.0000	.0000	.0000	.0000
1	10	-1.0000	-2.0000	.0000	.0000	.0000	.0000
1	11	-1.0000	-2.0000	.0000	.0000	.0000	.0000
1	12	-1.0000	-2.0000	.0000	.0000	.0000	.0000
1	13	-1.0000	-2.0000	.0000	.0000	.0000	.0000
1	14	-1.0000	-2.0000	.0000	.0000	.0000	.0000
1	15	-1.0000	-2.0000	.0000	.0000	.0000	.0000
2	2	.7130	.9330	.9330	.4790	1.0000	-.1000
2	3	.5490	-.0830	.8180	-.8040	1.0000	.7570
2	4	.4300	-.8550	.7860	-.0740	1.0000	.7600
2	5	-1.0000	-2.0000	.0000	.0000	.0000	.0000
2	6	-1.0000	-2.0000	.0000	.0000	.0000	.0000
2	7	-1.0000	-2.0000	.0000	.0000	.0000	.0000
2	8	-1.0000	-2.0000	.0000	.0000	.0000	.0000
2	9	-1.0000	-2.0000	.0000	.0000	.0000	.0000
2	10	-1.0000	-2.0000	.0000	.0000	.0000	.0000
2	11	-1.0000	-2.0000	.0000	.0000	.0000	.0000
2	12	-1.0000	-2.0000	.0000	.0000	.0000	.0000
2	13	-1.0000	-2.0000	.0000	.0000	.0000	.0000
2	14	-1.0000	-2.0000	.0000	.0000	.0000	.0000
2	15	-1.0000	-2.0000	.0000	.0000	.0000	.0000
3	3	.7190	.9280	.9270	.4730	1.0000	-.1280
3	4	.5510	-.1050	.8420	-.8020	1.0000	.7530
3	5	.4250	-.0210	.7340	-.8220	1.0000	.7690
3	6	-1.0000	-2.0000	.0000	.0000	.0000	.0000
3	7	-1.0000	-2.0000	.0000	.0000	.0000	.0000
3	8	-1.0000	-2.0000	.0000	.0000	.0000	.0000
3	9	-1.0000	-2.0000	.0000	.0000	.0000	.0000
3	10	-1.0000	-2.0000	.0000	.0000	.0000	.0000
3	11	-1.0000	-2.0000	.0000	.0000	.0000	.0000
3	12	-1.0000	-2.0000	.0000	.0000	.0000	.0000
3	13	-1.0000	-2.0000	.0000	.0000	.0000	.0000
3	14	-1.0000	-2.0000	.0000	.0000	.0000	.0000
3	15	-1.0000	-2.0000	.0000	.0000	.0000	.0000
4	4	.7090	.9080	.9300	.3210	1.0000	-.3900
4	5	.5100	-.1410	.8370	-.8070	1.0000	.7420
4	6	.4790	-.8900	.8000	-.0580	1.0000	.7620
4	7	-1.0000	-2.0000	.0000	.0000	.0000	.0000
4	8	-1.0000	-2.0000	.0000	.0000	.0000	.0000
4	9	-1.0000	-2.0000	.0000	.0000	.0000	.0000

4	10	-1.0000	-2.0000	.0000	.0000	.0000	.0000
4	11	-1.0000	-2.0000	.0000	.0000	.0000	.0000
4	12	-1.0000	-2.0000	.0000	.0000	.0000	.0000
4	13	-1.0000	-2.0000	.0000	.0000	.0000	.0000
4	14	-1.0000	-2.0000	.0000	.0000	.0000	.0000
4	15	-1.0000	-2.0000	.0000	.0000	.0000	.0000
5	5	.6580	.8990	.9190	.3400	1.0000	-.3960
5	6	.4470	-.1570	.8430	-.7990	1.0000	.6760
5	7	.7470	-.9030	.9790	-.5270	1.0000	.7070
5	8	-.9990	-2.0000	.0000	.0000	.0000	.0000
5	9	-.9990	-2.0000	.0000	.0000	.0000	.0000
5	10	-.9990	-2.0000	.0000	.0000	.0000	.0000
5	11	-.9990	-2.0000	.0000	.0000	.0000	.0000
5	12	-.9990	-2.0000	.0000	.0000	.0000	.0000
5	13	-.9990	-2.0000	.0000	.0000	.0000	.0000
5	14	-.9990	-2.0000	.0000	.0000	.0000	.0000
5	15	-.9990	-2.0000	.0000	.0000	.0000	.0000
6	6	.6570	.9130	.9450	.5140	1.0000	-.1700
6	7	.4210	-.8260	.7890	-.1470	1.0000	.7170
6	8	-.9990	-2.0000	.0000	.0000	.0000	.0000
6	9	-.9990	-2.0000	.0000	.0000	.0000	.0000
6	10	-.9990	-2.0000	.0000	.0000	.0000	.0000
6	11	-.9990	-2.0000	.0000	.0000	.0000	.0000
6	12	-.9990	-2.0000	.0000	.0000	.0000	.0000
6	13	-.9990	-2.0000	.0000	.0000	.0000	.0000
6	14	-.9990	-2.0000	.0000	.0000	.0000	.0000
6	15	-.9990	-2.0000	.0000	.0000	.0000	.0000
7	7	.6450	.8780	.9040	.2590	1.0000	-.6700
7	8	.5200	-.8500	.8540	-.2150	1.0000	.6840
7	9	.4650	-.9460	.9310	-.7430	1.0000	-.5050
7	10	.5820	-.9710	1.0000	-.8490	.0000	.0000
7	11	-1.0000	-2.0000	.0000	.0000	.0000	.0000
7	12	-1.0000	-2.0000	.0000	.0000	.0000	.0000
7	13	-1.0000	-2.0000	.0000	.0000	.0000	.0000
7	14	-1.0000	-2.0000	.0000	.0000	.0000	.0000
7	15	-1.0000	-2.0000	.0000	.0000	.0000	.0000
8	8	.5500	.8980	.9240	.4590	1.0000	-.1600
8	9	.4430	.1430	.8120	.7320	1.0000	-.5410
8	10	.4280	-.3090	.8460	-.8600	1.0000	.3310
8	11	-1.0000	-2.0000	.0000	.0000	.0000	.0000
8	12	-1.0000	-2.0000	.0000	.0000	.0000	.0000
8	13	-1.0000	-2.0000	.0000	.0000	.0000	.0000
8	14	-1.0000	-2.0000	.0000	.0000	.0000	.0000
8	15	-1.0000	-2.0000	.0000	.0000	.0000	.0000
9	9	.6310	.9510	.9990	.7880	1.0000	-.4950
9	10	.4450	.0160	.7700	.7020	1.0000	-.7290
9	11	.5710	-.9690	.9990	-.8560	1.0000	-.3790
9	12	-.9990	-2.0000	.0000	.0000	.0000	.0000
9	13	-.9990	-2.0000	.0000	.0000	.0000	.0000
9	14	-.9990	-2.0000	.0000	.0000	.0000	.0000

9	15	-.9990	-2.0000	.0000	.0000	.0000	.0000
10	10	.5030	.8630	.9120	.3090	1.0000	-.4260
10	11	.4470	-.1320	.8280	-.8170	1.0000	.6470
10	12	-.9990	-2.0000	.0000	.0000	.0000	.0000
10	13	-.9990	-2.0000	.0000	.0000	.0000	.0000
10	14	-.9990	-2.0000	.0000	.0000	.0000	.0000
10	15	-.9990	-2.0000	.0000	.0000	.0000	.0000
11	11	.4400	.8320	.8280	.1150	1.0000	-.7420
11	12	.4320	-.8290	.8270	-.1550	1.0000	.6770
11	13	-.9990	-2.0000	.0000	.0000	.0000	.0000
11	14	-.9990	-2.0000	.0000	.0000	.0000	.0000
11	15	-.9990	-2.0000	.0000	.0000	.0000	.0000
12	12	.4120	.0720	.7860	.8080	1.0000	-.7660
12	13	.4600	-.1340	.8200	-.8110	1.0000	.6150
12	14	-.9990	-2.0000	.0000	.0000	.0000	.0000
12	15	-.9990	-2.0000	.0000	.0000	.0000	.0000
13	13	.4330	.0350	.7560	.7920	1.0000	-.7660
13	14	.4640	-.1670	.8510	-.8190	1.0000	.5860
13	15	-.9990	-2.0000	.0000	.0000	.0000	.0000
14	14	.4440	.0230	.7510	.7840	1.0000	-.7690
14	15	.4680	-.1700	.8470	-.8230	1.0000	.5850
15	15	.4440	.0310	.7580	.7860	1.0000	-.7650

BANKS START AT 23836
LAST LOCATION USED 25235

P-MODE POINT SOURCE/DETECTOR TEST CASE - ANALYSIS INPUT

ND= 2, NNE= 9, NE= 9, NT= 0, NA= 6, NRESP= 1, NEX= 2, NEXND= 0

DET	X	Y	Z	RAD	TO
1	1.0000-03	1.0000-03	6.0000+04	6.0000+04	1.1764-05
2	1.0000-03	1.0000-03	6.0000+04	6.0000+04	1.1764-05

GROUP	RESP(1)
1	5.4600-09
2	5.1300-09
3	4.8400-09
4	4.6100-09
5	4.4400-09
6	4.1300-09
7	4.0100-09
8	3.3900-09
9	3.1500-09
10	3.0900-09
11	2.6400-09
12	1.9700-09
13	1.1200-09
14	2.2900-10
15	0.0000

NUMBER OF PRIMARY ENERGY BINS 9
TOTAL NUMBER OF ENERGY BINS 9

BIN NO.	LOWER LIMIT GROUP	LOWER ENERGY LIMIT	DELTA E
		1.500+07	
1	1	1.220+07	2.800+06
2	2	1.000+07	2.200+06
3	3	8.180+06	1.820+06
4	4	6.360+06	1.820+06
5	6	4.060+06	2.300+06
6	9	2.350+06	1.710+06
7	11	1.108+06	1.242+06
8	13	1.109+05	9.971+05
9	14	3.355+03	1.075+05

NUMBER OF TIME BINS 0

NUMBER OF ANGLE BINS 6
UPPER LIMITS OF COSINE BINS

-8.8889-01	-4.4444-01	0.0000	4.4444-01	8.8889-01	1.0000+00

615 CELLS USED BY ANALYSIS, 12150 CELLS REMAIN UNUSED.

```
FAI+ ARRAY REQUIRES 1970 LOCATIONS, BEGINNING (ZEROTH LOCATION) AT 25850 AND ENDING AT 37820 IN BLANK COMMON.
 180 LOCATIONS ARE UNUSED.


     ************   F-MODE FAMS STORE FOR ITERATION NO.  0   ************

                              FAM (IFAM) ARRAY
  1          1          2        100        100          0          0          0          0
  9          0          0          0          0          0          0          0          0
 17          0         10         10          0          0          0          0          0
 25          0          0          0          0          0          0          0          0
 33          0          0      25850          0      37820          0      11970         18
 41          1          2      25850      37820          1

*DD.P     DTFA.
```

ADJOINT MODE INPUT - REDUCED PT. SOURCE/DETECTOR PROBLEM 10JAN74

THIS PRINT OCCURRED ON THE 3 DAY OF THE 5 MONTH IN THE YEAR 1976
AT 0 MINUTES PAST THE HOUR OF 10 PM .

NSTRT	NMOST	NITS	NOUIT	NGPOTN	NGPOTG	NMGP	NMTG	NCOLTP	IADJM	MAXTIM	MEDIA	MEDALB
1	100	1	1	14	0	15	15	0	1	25.00	1	0

ISOUR	NGPFS	ISBIAS	WTSTRT	EBOTN	EBOTG	TCUT	VELTH
0	14	1	1.000+00	2.500-02	0.000	0.000	2.200+05

XSTRT	YSTRT	ZSTRT	AGSTRT	UINP	VINP	WINP
1.000-03	1.000-03	6.000+04	0.000	.000000	.000000	.000000

ADJOINT CASE - USER SHOULD MODIFY OUTPUT BY OFF= .48209-07

SOURCE DATA

FS(31) =	.1132569	FS(32) =	.1064117	FS(33) =	.1003962	FS(34) =	.0956253
FS(35) =	.0920990	FS(36) =	.0856687	FS(37) =	.0831795	FS(38) =	.0703188
FS(39) =	.0653405	FS(40) =	.0640959	FS(41) =	.0547616	FS(42) =	.0408637
FS(43) =	.0232322	FS(44) =	.0047502	FS(45) =	.0000000		

GROUP PARAMETERS, GROUP NUMBERS GREATER THAN 15 CORRESPOND TO SECONDARY PARTICLES

GROUP	UPPER EDGE (EV)	VELOCITY (CM/SEC)
1	1.5000+07	5.1003+09
2	1.2200+07	4.6077+09
3	1.0000+07	4.1697+09
4	8.1800+06	3.7290+09
5	6.3600+06	3.2903+09
6	4.9600+06	2.9370+09
7	4.0600+06	2.6003+09
8	3.0100+06	2.2872+09
9	2.4600+06	2.1448+09
10	2.3500+06	1.9984+09
11	1.8260+06	1.6751+09
12	1.1080+06	1.2593+09
13	5.5020+05	7.9513+08
14	1.1090+05	3.3056+08
15	3.3546+03	2.2000+05

THIS IS AN ADJOINT PROBLEM. THE ADJOINT GROUP STRUCTURE (IA) IS RELATED
TO THE FORWARD GROUP STRUCTURE (I) BY (IA=NMTG+1-I).

THE ABOVE ARRAYS ARE GIVEN IN THE FORWARD GROUP STRUCTURE.

INITIAL RANDOM NUMBER = 346122764532

NSPLT= 0 NKILL= 0 NPAST= 0 NOLEAK= 0 IEBIAS= 0 MXREG= 42 MAXGP= 0

NSOUR= 0 NFISTP= 0 NKCALC= 0 NORMF= 0

14-MEV WT XSECTIONS FOR AIR - A-MODE INPUT

```
NUMBER OF PRIMARY GROUPS (NGP)              15
NUMBER OF PRIMARY DOWNSCATTERS (NDS)        15
NUMBER OF SECONDARY GROUPS (NGG)             0
NUMBER OF SECONDARY DOWNSCATTERS (NOSG)      0
NUMBER OF PRIM+SEC GROUPS (INGP)            15
TABLE LENGTH (ITBL)                         18
LOC OF WITHIN GROUP (SIG GG) (ISGG)          4
NUMBER OF MEDIA (NMED)                       1
NUMBER OF INPUT ELEMENTS (NELEM)             1
NUMBER OF MIXING ENTRIES (NMIX)              1
NUMBER OF COEFFICIENTS (NCOEF)               6
NUMBER OF ANGLES (NSCT)                      3
RESTORE COEFF (ISTAT)                        1
ADJOINT SWITCH (FROM MORSE)                  1


INPUT/OUTPUT OPTIONS
     IRDSG (AS READ)          0
     ISTR (AS STORE)          0
     IFMU (MUS)               0
     IMOM (MOMENTS)           0
     IPRIN (ANGLES,PROB)      0
     IPUN (IMPOSSIBLE COEF)   0
     CARD FORMAT (IDTF)       0
     INPUT TAPE (IXTAPE)      0
     MORSEC TAPE (JXTAPE)     0
     06R TAPE (I06RT)         0


PACKING VARIABLES
     SCALE FACTOR       1.00+03
     SHIFT FACTOR          2000
     XSECS PER WORD           3

STORAGE ALLOCATIONS
CROSS SECTIONS START AT     22752
LAST LOCATION USED (PERM)   23835
TEMP LOCATIONS USED         37145 TO   38000
EXCESS STORAGE (TEMP)       13310
START OF LEGENDRE COEFF     23235
CARD     0 WAS READ WHEN CARD      1 WAS EXPECTED  CHECK CROSS SECTION CARD SEQUENCE IN  ELEMENT      1 COEFFICIENT      1
CARD  1028 WAS READ WHEN CARD      1 WAS EXPECTED  CHECK CROSS SECTION CARD SEQUENCE IN  ELEMENT      1 COEFFICIENT      2
CARD  2040 WAS READ WHEN CARD      1 WAS EXPECTED  CHECK CROSS SECTION CARD SEQUENCE IN  ELEMENT      1 COEFFICIENT      3
CARD  3052 WAS READ WHEN CARD      1 WAS EXPECTED  CHECK CROSS SECTION CARD SEQUENCE IN  ELEMENT      1 COEFFICIENT      4
CARD  4064 WAS READ WHEN CARD      1 WAS EXPECTED  CHECK CROSS SECTION CARD SEQUENCE IN  ELEMENT      1 COEFFICIENT      5
CARD  5076 WAS READ WHEN CARD      1 WAS EXPECTED  CHECK CROSS SECTION CARD SEQUENCE IN  ELEMENT      1 COEFFICIENT      6
```

MIXING TABLE

MEDIA 1 CONTAINS ELEMENT 1 WITH DENSITY 1.0000+00

CROSS SECTIONS FOR MEDIA 1

GROUP	SIGT	SIGST	PNUP	PNABS	GAMGEN	NU*FIS	DOWNSCATTER PROBABILITY							
1	3.585-04	3.414-04	.0000	.9523	.0000	.0000	.9691	.0309	.0000	.0000	.0000	.0000	.0000	.0000
							.0000	.0000	.0000	.0000	.0000	.0000	.0000	
2	2.745-04	2.771-04	.0000	1.0096	.0000	.0000	.9522	.0475	.0000	.0000	.0000	.0000	.0001	.0000
							.0000	.0000	.0000	.0000	.0001	.0001		
3	1.592-04	1.652-04	.0000	1.0378	.0000	.0000	.8825	.1077	.0000	.0000	.0000	.0004	.0006	.0004
							.0006	.0019	.0014	.0024	.0021			
4	1.016-04	1.108-04	.0000	1.0906	.0000	.0000	.7440	.2189	.0000	.0000	.0000	.0011	.0015	.0021
							.0078	.0063	.0097	.0085				
5	1.009-04	1.162-04	.0000	1.1520	.0000	.0000	.6358	.2888	.0119	.0000	.0003	.0022	.0033	.0095
							.0162	.0168	.0150					
6	7.415-05	1.072-04	.0000	1.4461	.0000	.0000	.3437	.3844	.2085	.0064	.0009	.0028	.0054	.0189
							.0152	.0139						
7	5.354-05	2.021-05	.0000	.3775	.0000	.0000	.3740	.4305	.1326	.0002	.0032	.0063	.0175	.0185
							.0171							
8	6.230-05	5.521-05	.0000	.8862	.0000	.0000	.4341	.4571	.0000	.0044	.0108	.0312	.0321	.0302
9	8.705-05	8.147-05	.0000	.9359	.0000	.0000	.5492	.3010	.0302	.0127	.0266	.0407	.0395	
10	6.997-05	5.824-05	.0000	.8324	.0000	.0000	.5213	.3582	.0125	.0233	.0404	.0443		
11	6.295-05	5.388-05	.0000	.8559	.0000	.0000	.5448	.3128	.0311	.0466	.0648			
12	5.851-05	4.737-05	.0000	.8096	.0000	.0000	.5646	.3038	.0606	.0710				
13	5.843-05	3.582-05	.0000	.6131	.0000	.0000	.5996	.3381	.0623					
14	6.681-05	3.439-05	.0000	.5147	.0000	.0000	.7258	.2742						
15	7.174-05	2.805-05	.0000	.3910	.0000	.0000	1.0000							

BANKS START AT 23836
LAST LOCATION USED 25235

A-MODE POINT SOURCE/DETECTOR TEST CASE - ANALYSIS INPUT

ND= 2, NNE= 9, NE= 9, NT= 0, NA= 6, NRESP= 1, NEX= 2, NEXND= 0

DET	X	Y	Z	RAD	TO
1	1.0000+00	1.0000+00	1.0000+00	5.9999+04	1.1764-05
2	1.0000+00	1.0000+00	1.0000+00	5.9999+04	1.1764-05

GROUP	RESP(1)
1	1.5680-04
2	8.9320-04
3	3.4800-03
4	1.3920-02
5	3.4570-02
6	3.5070-02
7	1.0720-01
8	8.8980-02
9	2.3230-02
10	1.2030-01
11	2.1810-01
12	1.9830-01
13	1.4030-01
14	1.5500-02
15	0.0000

THIS IS AN ADJOINT PROBLEM. THE ADJOINT GROUP STRUCTURE (IA) IS RELATED
TO THE FORWARD GROUP STRUCTURE (I) BY (IA=NMTG+1-I).

ADJOINT GROUP PARAMETERS

GROUP	RESP(1)
2	1.5500-02
3	1.4030-01
4	1.9830-01
5	2.1810-01
6	1.2030-01
7	2.3230-02
8	8.8980-02
9	1.0720-01
10	3.5070-02
11	3.4570-02
12	1.3920-02
13	3.4800-03
14	8.9320-04
15	1.5680-04

NUMBER OF SECONDARY ENERGY BINS 0
TOTAL NUMBER OF ENERGY BINS 9
LOWER UPPER

BIN NO.	LIMIT GROUP	ENERGY LIMIT	DELTA E
		3.355+03	
1	2	1.109+05	1.000+00
2	4	1.108+06	1.000+00
3	6	2.350+06	1.000+00
4	9	4.060+06	1.000+00
5	11	6.360+06	1.000+00
6	12	8.180+06	1.000+00
7	13	1.000+07	1.000+00
8	14	1.220+07	1.000+00
9	15	1.500+07	1.000+00

NUMBER OF TIME BINS 0

NUMBER OF ANGLE BINS 6

UPPER LIMITS OF COSINE BINS

-8.8889-01	-4.4444-01	0.0000	4.4444-01	8.8889-01	1.0000+00

615 CELLS USED BY ANALYSIS, 12150 CELLS REMAIN UNUSED.

```
 FAI+ ARRAY REQUIRES11970 LOCATIONS, BEGINNING (ZEROTH LOCATION) AT25850 AND ENDING AT37820 IN BLANK COMMON.
  180 LOCATIONS ARE UNUSED.


      ************   A-MODE FAMS STORE FOR ITERATION NO.  0   ************

                          FAM (IFAM) ARRAY
   1          1          2          100        100        0          0          0          0
   9          0          0          0          0          0          0          0          0
  17          0          10         10         0          0          0          0          0
  25          0          0          0          0          0          0          0          0
  33          0          0          25850      25850      37820      37820      11970      18
  41          1          2          25850      37820      2

TIME REQUIRED FOR INPUT WAS         14


      ************   A-MODE FAMS READ FOR ITERATION NO.  1   ************

                          FAM (IFAM) ARRAY
   1          1          2          100        100        0          0          0          0
   9          0          0          0          0          0          0          0          0
  17          0          10         10         0          0          0          0          0
  25          0          0          0          0          0          0          0          0
  33          1          1          25850      25850      37820      37820      11970      18
  41          1          2          25850      37820      2
 YOU ARE USING THE DEFAULT VERSION OF STRUN WHICH DOES   NOTHING.

 ***START BATCH   1                        RANDOM=        346122764532

 SOURCE DATA

 YOU ARE USING THE IFA VERSION OF SOURCE.  SOURCE/IFA PICKS THE ENERGY IG FROM BFS AND THE DIRECTION KD FROM FAI(IG,NSR,KD).
     WATE IS SET EQUAL TO DDF./
    SWATE        IAVE     UAVE     VAVE     WAVE       XAVE       YAVE       ZAVE       AGEAVE
  1.000+02      9.92     .0440    .1168    .0072     1.000-03   1.000-03   6.000+04    0.000

 NUMBER OF COLLISIONS OF TYPE NCOLL
    SOURCE SPLIT(D)    FISHN    GAMGEN REALCOLL    ALBEDO     BDRYX    ESCAPE    E-CUT TIMEKILL R R KILL R R SURV  GAMLOST
       100        0        0        0      666         0       428        56         0         0        44         4         0

 TIME REQUIRED FOR THE PRECEDING BATCH WAS     15

 ***START BATCH   2                        RANDOM=        060557257502

 SOURCE DATA
    SWATE        IAVE     UAVE     VAVE     WAVE       XAVE       YAVE       ZAVE       AGEAVE
```

```
 1.000+02    10.26    .0435  -.0914    .0940    1.000-03   1.000-03   6.000+04    0.000

NUMBER OF COLLISIONS OF TYPE NCOLL
  SOURCE SPLIT(D)    FISHN   GAMGEN REALCOLL   ALBEDO    BDRYX   ESCAPE    E-CUT TIMEKILL R R KILL R R SURV  GAMLOST
     100        0        0        0      578        0      406       61        0        0       39        4        0

TIME REQUIRED FOR THE PRECEDING BATCH WAS     10

***START BATCH   3                          RANDOM=         025222057072

SOURCE DATA
  SWATE       IAVE     UAVE     VAVE     WAVE       XAVE       YAVE       ZAVE       AGEAVE
 1.000+02    10.49    .0094  -.0165    .0455    1.000-03   1.000-03   6.000+04    0.000

NUMBER OF COLLISIONS OF TYPE NCOLL
  SOURCE SPLIT(D)    FISHN   GAMGEN REALCOLL   ALBEDO    BDRYX   ESCAPE    E-CUT TIMEKILL R R KILL R R SURV  GAMLOST
     100        0        0        0      663        0      394       50        0        0       50        8        0

TIME REQUIRED FOR THE PRECEDING BATCH WAS     12

***START BATCH   4                          RANDOM=         151756575202

SOURCE DATA
  SWATE       IAVE     UAVE     VAVE     WAVE       XAVE       YAVE       ZAVE       AGEAVE
 1.000+02    10.27    .0741  -.0106    .0210    1.000-03   1.000-03   6.000+04    0.000

NUMBER OF COLLISIONS OF TYPE NCOLL
  SOURCE SPLIT(D)    FISHN   GAMGEN REALCOLL   ALBEDO    BDRYX   ESCAPE    E-CUT TIMEKILL R R KILL R R SURV  GAMLOST
     100        0        0        0      683        0      403       56        0        0       44        5        0

TIME REQUIRED FOR THE PRECEDING BATCH WAS     11

***START BATCH   5                          RANDOM=         337100051462

SOURCE DATA
  SWATE       IAVE     UAVE     VAVE     WAVE       XAVE       YAVE       ZAVE       AGEAVE
 1.000+02    10.07    .0016  -.0328    .0868    1.000-03   1.000-03   6.000+04    0.000

NUMBER OF COLLISIONS OF TYPE NCOLL
  SOURCE SPLIT(D)    FISHN   GAMGEN REALCOLL   ALBEDO    BDRYX   ESCAPE    E-CUT TIMEKILL R R KILL R R SURV  GAMLOST
     100        0        0        0      640        0      388       66        0        0       34        6        0

TIME REQUIRED FOR THE PRECEDING BATCH WAS     11

***START BATCH   6                          RANDOM=         336362015372

SOURCE DATA
  SWATE       IAVE     UAVE     VAVE     WAVE       XAVE       YAVE       ZAVE       AGEAVE
 1.000+02    10.32    .1051    .0132  -.0324    1.000-03   1.000-03   6.000+04    0.000

NUMBER OF COLLISIONS OF TYPE NCOLL
  SOURCE SPLIT(D)    FISHN   GAMGEN REALCOLL   ALBEDO    BDRYX   ESCAPE    E-CUT TIMEKILL R R KILL R R SURV  GAMLOST
     100        0        0        0      664        0      411       61        0        0       39        2        0

TIME REQUIRED FOR THE PRECEDING BATCH WAS     11

***START BATCH   7                          RANDOM=         327351440532
```

```
SOURCE DATA
  SWATE        IAVE     UAVE     VAVE     WAVE       XAVE       YAVE       ZAVE       AGEAVE
  1.000+02     10.25     .0069    .0608    .0044    1.000-03   1.000-03   6.000+04    0.000

NUMBER OF COLLISIONS OF TYPE NCOLL
  SOURCE SPLIT(D)    FISHN    GAMGEN REALCOLL    ALBEDO     BDRYX    ESCAPE    E-CUT TIMEKILL R R KILL R R SURV  GAMLOST
     100         0        0        0      645         0       418        56        0         0       44         9         0

TIME REQUIRED FOR THE PRECEDING BATCH WAS     11

***START BATCH    8                          RANDOM=         304652172122

SOURCE DATA
  SWATE        IAVE     UAVE     VAVE     WAVE       XAVE       YAVE       ZAVE       AGEAVE
  1.000+02     10.09     .1229   -.0152   -.0195    1.000-03   1.000-03   6.000+04    0.000

NUMBER OF COLLISIONS OF TYPE NCOLL
  SOURCE SPLIT(D)    FISHN    GAMGEN REALCOLL    ALBEDO     BDRYX    ESCAPE    E-CUT TIMEKILL R R KILL R R SURV  GAMLOST
     100         0        0        0      633         0       452        61        0         0       39         6         0

TIME REQUIRED FOR THE PRECEDING BATCH WAS     11

***START BATCH    9                          RANDOM=         255147013662

SOURCE DATA
  SWATE        IAVE     UAVE     VAVE     WAVE       XAVE       YAVE       ZAVE       AGEAVE
  1.000+02     10.38    -.0475   -.0434    .0188    1.000-03   1.000-03   6.000+04    0.000

NUMBER OF COLLISIONS OF TYPE NCOLL
  SOURCE SPLIT(D)    FISHN    GAMGEN REALCOLL    ALBEDO     BDRYX    ESCAPE    E-CUT TIMEKILL R R KILL R R SURV  GAMLOST
     100         0        0        0      581         0       419        60        0         0       40         3         0

TIME REQUIRED FOR THE PRECEDING BATCH WAS     10

***START BATCH   10                          RANDOM=         372656567632

SOURCE DATA
  SWATE        IAVE     UAVE     VAVE     WAVE       XAVE       YAVE       ZAVE       AGEAVE
  1.000+02     10.44     .0566    .1079    .0865    1.000-03   1.000-03   6.000+04    0.000

NUMBER OF COLLISIONS OF TYPE NCOLL
  SOURCE SPLIT(D)    FISHN    GAMGEN REALCOLL    ALBEDO     BDRYX    ESCAPE    E-CUT TIMEKILL R R KILL R R SURV  GAMLOST
     100         0        0        0      636         0       444        57        0         0       43         4         0

TIME REQUIRED FOR THE PRECEDING BATCH WAS     11
THIS IS AN ADJOINT PROBLEM - ADJOINT ENERGY DEPENDENT FLUENCE IS NOT DIFFERENTIAL
```

THIS PRINT OCCURRED ON THE 3 DAY OF THE 5 MONTH IN THE YEAR 1976
AT 4 MINUTES PAST THE HOUR OF 10 PM .

ORNL 4464 FISSION SOURCE

RESPONSES(DETECTOR) ADJOINT RESPONSE VALUES BASED ON HENDERSON TISSUE DOSE

DETECTOR	UNCOLL RESPONSE	FSD UNCOLL	TOTAL RESPONSE	FSD TOTAL
1	5.7698-22	.03585	1.3746-20	.19440
2	0.0000	.00000	0.0000	.00000

FLUENCE(ENERGY,DETECTOR) ENERGY DEPENDENT ADJOINT FLUENCE - IMPORTANCE/CMSQ/EV/SOURCE

DETECTOR NO. ENERGIES	1	2
3.355+03		
	9.771-27	0.000
	.437	.000
1.109+05		
	6.793-21	0.000
	.554	.000
1.108+06		
	2.275-20	0.000
	.266	.000
2.350+06		
	6.966-20	0.000
	.273	.000
4.060+06		
	7.769-20	0.000
	.300	.000
6.360+06		
	9.851-20	0.000
	.630	.000
8.180+06		
	6.151-20	0.000
	.338	.000
1.000+07		
	4.398-20	0.000
	.322	.000
1.220+07		
	2.346-20	0.000
	.143	.000
1.500+07		

DETECTOR NO 1 FLUENCE(COSINE,ENERGY,DETECTOR) ENERGY AND ANGULAR DEPENDENT ADJOINT FLUENCE

ENERGIES	3.355+03	1.109+05	1.108+06	2.350+06	4.060+06	6.360+06	8.180+06	1.000+07	1.220+07
COSINES	1.109+05	1.108+06	2.350+06	4.060+06	6.360+06	8.180+06	1.000+07	1.220+07	1.500+07
-1.000000	1.319-26	5.246-21	1.402-20	4.275-20	5.185-20	2.544-20	1.961-20	1.074-20	1.804-20
	.000	.555	.201	.266	.351	.271	.130	.152	.219
-.888889	2.025-28	7.283-22	2.818-21	1.013-20	1.297-20	3.115-21	7.349-21	5.529-21	1.701-21
	.000	.423	.403	.397	.419	.392	.733	.656	.214
-.444444	0.000	3.928-22	1.655-21	3.637-21	1.227-21	6.553-22	4.084-21	1.228-21	4.847-22
	.000	.991	1.000	.534	.434	.559	.647	.695	.394
.000000	0.000	0.000	1.664-22	4.974-22	6.634-22	3.171-21	6.303-22	6.270-21	1.184-21
	.000	.000	1.000	.850	.956	.885	.582	.567	.785
.444444	0.000	0.000	0.000	0.000	0.000	0.000	5.063-21	3.825-23	4.822-22
	.000	.000	.000	.000	.000	.000	.975	1.000	.559
.888889	0.000	0.000	0.000	0.000	0.000	8.789-20	0.000	0.000	1.578-22
	.000	.000	.000	.000	.000	1.000	.000	.000	1.000
1.000000									

DETECTOR NO 2 FLUENCE(COSINE,ENERGY,DETECTOR) ENERGY AND ANGULAR DEPENDENT ADJOINT FLUENCE

ENERGIES	3.355+03	1.109+05	1.108+06	2.350+06	4.060+06	6.360+06	8.180+06	1.000+07	1.220+07
COSINES	1.109+05	1.108+06	2.350+06	4.060+06	6.360+06	8.180+06	1.000+07	1.220+07	1.500+07
-1.000000	0.000	0.000	0.000	0.000	0.000	0.000	0.000	0.000	0.000
	.000	.000	.000	.000	.000	.000	.000	.000	.000
-.888889	0.000	0.000	0.000	0.000	0.000	0.000	0.000	0.000	0.000
	.000	.000	.000	.000	.000	.000	.000	.000	.000
-.444444	0.000	0.000	0.000	0.000	0.000	0.000	0.000	0.000	0.000
	.000	.000	.000	.000	.000	.000	.000	.000	.000
.000000	0.000	0.000	0.000	0.000	0.000	0.000	0.000	0.000	0.000
	.000	.000	.000	.000	.000	.000	.000	.000	.000
.444444	0.000	0.000	0.000	0.000	0.000	0.000	0.000	0.000	0.000
	.000	.000	.000	.000	.000	.000	.000	.000	.000
.888889	0.000	0.000	0.000	0.000	0.000	0.000	0.000	0.000	0.000
	.000	.000	.000	.000	.000	.000	.000	.000	.000
1.000000									

TIME REQUIRED FOR THE PRECEDING 10 BATCHES WAS 127

PARTICLE DEATHS	NUMBER	WEIGHT
KILLED BY RUSSIAN ROULETTE	416	.53697+01
ESCAPED	584	.32113+03
REACHED ENERGY CUTOFF	0	.00000
REACHED TIME CUTOFF	0	.00000

NUMBER OF SCATTERINGS

MEDIUM	NUMBER
1	6389
TOTAL	6389

REAL SCATTERING COUNTERS

ENERGY GROUP	REGION 1		REGION 2		REGION 3		REGION 4		REGION 5		REGION 6	
	NUMBER	WEIGHT	NUMBER	WEIGHT	NUMBER	WEIGHT	NUMBER	WEIGHT	NUMBER	WEIGHT	NUMBER	WEIGHT
1	0	0.00	0	0.00	0	0.00	0	0.00	0	0.00	0	0.00
2	0	0.00	37	3.85+01	0	0.00	0	0.00	0	0.00	0	0.00
3	0	0.00	81	8.92+01	0	0.00	0	0.00	0	0.00	0	0.00
4	0	0.00	41	4.32+01	0	0.00	0	0.00	0	0.00	0	0.00
5	0	0.00	65	7.45+01	0	0.00	0	0.00	0	0.00	2	3.40+00
6	0	0.00	54	6.54+01	0	0.00	0	0.00	0	0.00	1	2.09+00
7	0	0.00	39	4.07+01	1	1.05+00	0	0.00	0	0.00	1	3.03+00
8	0	0.00	50	5.24+01	0	0.00	1	2.08+00	0	0.00	3	1.87+00
9	0	0.00	98	9.04+01	2	2.42-01	0	0.00	0	0.00	2	5.65-01
10	0	0.00	91	8.30+01	3	2.76-01	0	0.00	0	0.00	4	1.43+00
11	1	7.33-01	65	5.90+01	3	4.20-01	0	0.00	0	0.00	1	8.56-01
12	1	6.27-01	61	5.48+01	2	3.05-01	0	0.00	0	0.00	3	1.29+00
13	6	1.99+00	66	5.54+01	1	1.00+00	5	3.23-01	0	0.00	4	2.34-01
14	3	6.22-01	103	7.77+01	1	3.98-02	3	3.22-01	0	0.00	5	3.18-01
15	1	2.22-02	132	8.49+01	6	4.75-01	12	1.29+00	11	9.14-01	7	5.91-01

ENERGY GROUP	REGION 7		REGION 8		REGION 9		REGION 10		REGION 11		REGION 12	
	NUMBER	WEIGHT	NUMBER	WEIGHT	NUMBER	WEIGHT	NUMBER	WEIGHT	NUMBER	WEIGHT	NUMBER	WEIGHT
1	0	0.00	0	0.00	0	0.00	0	0.00	0	0.00	0	0.00
2	0	0.00	0	0.00	0	0.00	0	0.00	0	0.00	0	0.00
3	0	0.00	0	0.00	0	0.00	0	0.00	0	0.00	0	0.00
4	0	0.00	0	0.00	0	0.00	0	0.00	0	0.00	0	0.00
5	0	0.00	0	0.00	0	0.00	0	0.00	0	0.00	0	0.00
6	0	0.00	0	0.00	0	0.00	0	0.00	0	0.00	0	0.00
7	0	0.00	0	0.00	1	2.06-01	0	0.00	1	2.78+00	0	0.00
8	1	6.21-01	1	1.01+00	0	0.00	1	8.83-02	0	0.00	1	2.35+00
9	0	0.00	0	0.00	0	0.00	1	1.00+00	2	7.07-01	1	1.82+00
10	3	1.55+00	1	5.23-01	0	0.00	1	9.36-01	4	2.93+00	1	8.72-02
11	2	5.69-01	2	1.06+00	0	0.00	1	7.06-01	9	5.24+00	3	9.55-01
12	0	0.00	2	1.19+00	0	0.00	1	6.56-01	8	3.28+00	4	2.04+00
13	7	2.72+00	5	2.32+00	1	8.43-02	2	1.35-01	3	3.60-01	3	1.30+00
14	1	4.30-02	7	2.27+00	7	5.27-01	1	3.14-02	8	2.55+00	14	2.29+00
15	8	8.96-01	9	4.90-01	6	3.18-01	1	8.66-02	10	7.22-01	13	1.70+00

ENERGY GROUP	REGION 13		REGION 14		REGION 15		REGION 16		REGION 17		REGION 18	
	NUMBER	WEIGHT	NUMBER	WEIGHT	NUMBER	WEIGHT	NUMBER	WEIGHT	NUMBER	WEIGHT	NUMBER	WEIGHT
1	0	0.00	0	0.00	0	0.00	0	0.00	0	0.00	0	0.00
2	0	0.00	0	0.00	0	0.00	0	0.00	0	0.00	0	0.00
3	0	0.00	2	6.13+00	3	6.30+00	0	0.00	1	1.95+00	0	0.00
4	0	0.00	0	0.00	4	1.04+01	0	0.00	0	0.00	0	0.00
5	0	0.00	0	0.00	3	9.30+00	0	0.00	0	0.00	0	0.00
6	0	0.00	3	1.43+01	2	7.03+00	0	0.00	0	0.00	0	0.00
7	1	1.42-01	2	1.44+00	4	1.56+01	0	0.00	2	1.99+00	2	1.99+00
8	3	3.64-01	2	2.12-01	1	3.95-01	5	8.51+00	2	1.34+00	4	1.95+00
9	3	1.19-01	0	0.00	3	1.52+00	4	4.56+00	3	1.61+00	7	2.74+00
10	0	0.00	0	0.00	3	2.33+00	1	6.29-01	1	8.35-01	2	1.22+00

11	3	6.48-01	3	2.59-01	4	2.67+00	5	2.54+00	3	1.62+00	4	9.86-01	
12	2	8.54-01	1	1.85-01	0	0.00	6	3.38+00	4	1.82+00	4	1.90+00	
13	11	3.11+00	8	1.98+00	11	4.34+00	6	1.47+00	5	2.16+00	4	7.18-01	
14	13	2.28+00	16	4.29+00	11	1.61+00	10	8.69-01	10	1.28+00	7	1.14+00	
15	13	1.20+00	14	1.04+00	20	1.12+00	21	2.67+00	18	3.24+00	17	1.06+00	

ENERGY GROUP	REGION 19		REGION 20		REGION 21		REGION 22		REGION 23		REGION 24	
	NUMBER	WEIGHT	NUMBER	WEIGHT	NUMBER	WEIGHT	NUMBER	WEIGHT	NUMBER	WEIGHT	NUMBER	WEIGHT
1	0	0.00	0	0.00	0	0.00	0	0.00	0	0.00	0	0.00
2	0	0.00	0	0.00	0	0.00	0	0.00	0	0.00	0	0.00
3	0	0.00	0	0.00	0	0.00	7	2.57+01	10	2.08+01	0	0.00
4	0	0.00	0	0.00	0	0.00	0	0.00	3	4.92+00	6	8.51+00
5	0	0.00	1	6.80+00	0	0.00	2	6.63+00	4	1.22+01	5	1.01+01
6	1	5.17+00	0	0.00	0	0.00	0	0.00	4	9.52+00	2	4.93+00
7	4	1.04+01	1	1.18+00	0	0.00	2	2.29+00	5	7.02+00	5	1.15+01
8	4	2.45+00	1	1.42-01	0	0.00	4	2.23+00	10	1.42+01	6	2.93+00
9	7	4.61+00	2	9.57-01	1	2.33-01	2	1.78+00	4	4.10+00	18	1.88+01
10	6	1.19+01	4	6.29-01	4	1.86+00	2	2.29+00	10	6.85+00	11	9.94+00
11	4	3.01+00	11	7.02+00	2	1.07+00	9	7.96+00	18	1.09+01	15	8.43+00
12	3	2.09+00	7	2.26+00	3	1.17+00	7	3.62+00	11	4.50+00	24	1.01+01
13	7	6.37+00	4	9.76-01	11	4.47+00	7	3.28+00	21	1.25+01	15	6.09+00
14	19	4.05+00	16	2.03+00	17	1.91+00	21	3.65+00	25	5.83+00	23	4.65+00
15	14	3.37+00	25	4.07+00	29	3.76+00	15	2.11+00	34	7.99+00	29	5.54+00

ENERGY GROUP	REGION 25		REGION 26		REGION 27		REGION 28		REGION 29		REGION 30	
	NUMBER	WEIGHT	NUMBER	WEIGHT	NUMBER	WEIGHT	NUMBER	WEIGHT	NUMBER	WEIGHT	NUMBER	WEIGHT
1	0	0.00	0	0.00	0	0.00	0	0.00	0	0.00	0	0.00
2	0	0.00	0	0.00	0	0.00	1	1.40+00	0	0.00	0	0.00
3	7	1.29+01	4	1.46+01	0	0.00	5	7.97+00	1	1.68+00	10	5.31+01
4	2	2.59+00	4	1.15+01	3	4.54+00	2	3.84+00	1	1.66+00	0	0.00
5	1	1.52+00	4	1.41+01	3	7.62+00	1	3.38+00	1	1.81+00	0	0.00
6	5	8.02+00	2	1.47+01	3	8.33+00	2	6.66+00	1	2.09+00	3	7.39+00
7	0	0.00	1	1.45+00	8	1.79+01	5	2.03+01	2	2.35+00	3	1.30+01
8	5	2.17+01	9	1.35+01	7	1.30+01	1	4.29-01	0	0.00	6	2.23+01
9	4	3.26+00	8	9.90+00	10	6.91+00	3	1.83+00	7	5.74+00	6	2.59+01
10	8	4.75+00	12	1.06+01	4	2.81+00	6	2.91+00	7	6.64+00	6	7.49+00
11	12	7.33+00	15	8.48+00	6	7.07+00	3	2.73+00	6	5.22+00	11	9.22+00
12	9	5.47+00	14	8.59+00	5	3.07+00	11	6.51+00	6	4.37+00	14	9.66+00
13	16	6.65+00	10	3.01+00	14	6.33+00	13	3.55+00	12	5.91+00	15	6.27+00
14	24	6.56+00	21	6.91+00	22	8.22+00	23	3.95+00	13	2.86+00	25	6.94+00
15	57	9.64+00	18	3.24+00	49	7.02+00	37	7.58+00	35	3.54+00	32	4.25+00

ENERGY GROUP	REGION 31		REGION 32		REGION 33		REGION 34		REGION 35		REGION 36	
	NUMBER	WEIGHT	NUMBER	WEIGHT	NUMBER	WEIGHT	NUMBER	WEIGHT	NUMBER	WEIGHT	NUMBER	WEIGHT
1	0	0.00	0	0.00	0	0.00	0	0.00	0	0.00	0	0.00
2	4	4.10+00	36	4.28+01	10	1.10+01	13	1.51+01	0	0.00	0	0.00
3	22	4.08+01	32	4.65+01	43	6.57+01	26	4.45+01	0	0.00	2	2.98+00
4	15	1.99+01	9	1.19+01	14	1.88+01	10	2.42+01	2	3.52+00	0	0.00
5	19	3.28+01	23	3.69+01	15	2.24+01	22	4.86+01	2	6.09+00	6	2.10+01
6	21	3.95+01	17	2.94+01	15	2.23+01	15	3.08+01	2	6.49+00	3	1.25+01

7	10	1.05+01	8	1.40+01	8	1.05+01	16	3.14+01	2	6.37+00	7	1.14+01			
8	13	2.41+01	11	1.12+01	15	1.91+01	14	3.08+01	6	1.39+00	0	0.00			
9	32	3.95+01	29	2.60+01	36	3.38+01	34	3.12+01	9	5.42+00	3	1.36+00			
10	33	2.95+01	28	2.19+01	30	2.51+01	31	3.56+01	11	5.75+00	4	1.83+00			
11	24	1.70+01	28	2.29+01	40	2.83+01	35	2.31+01	6	1.34+00	5	3.36+00			
12	28	1.88+01	24	1.75+01	27	2.03+01	47	3.55+01	5	1.76+00	7	4.17+00			
13	29	2.37+01	38	2.75+01	39	2.44+01	46	2.65+01	7	2.14+00	4	2.03+00			
14	46	2.09+01	45	1.92+01	58	2.58+01	53	2.75+01	23	4.26+00	22	4.65+00			
15	92	2.51+01	91	3.07+01	95	3.08+01	80	2.14+01	28	3.34+00	35	4.66+00			

ENERGY GROUP	REGION 37		REGION 38		REGION 39		REGION 40		REGION 41		REGION 42	
	NUMBER	WEIGHT	NUMBER	WEIGHT	NUMBER	WEIGHT	NUMBER	WEIGHT	NUMBER	WEIGHT	NUMBER	WEIGHT
1	0	0.00	0	0.00	0	0.00	0	0.00	0	0.00	0	0.00
2	0	0.00	3	3.53+00	7	8.08+00	29	3.55+01	7	7.59+00	15	1.69+01
3	2	3.51+00	1	1.29+00	15	2.49+01	40	5.37+01	21	2.77+01	21	2.55+01
4	3	4.31+00	1	1.34+00	12	1.56+01	18	2.53+01	10	1.44+01	9	1.21+01
5	1	1.70+00	0	0.00	17	2.49+01	17	2.70+01	18	2.85+01	9	1.48+01
6	0	0.00	0	0.00	5	8.69+00	11	1.75+01	6	1.03+01	5	6.56+00
7	1	3.77-01	1	5.72-02	11	1.16+01	17	2.15+01	9	8.57+00	7	7.49+00
8	5	1.68+01	3	7.88+00	19	1.39+01	19	1.58+01	12	8.79+00	17	1.88+01
9	7	6.52+00	2	2.52+00	23	1.35+01	28	2.57+01	24	1.73+01	25	2.76+01
10	5	5.04+00	8	5.14+00	19	1.40+01	24	1.67+01	18	1.28+01	26	2.08+01
11	3	1.19+00	8	4.49+00	20	1.67+01	22	1.63+01	22	1.68+01	32	2.84+01
12	8	4.46+00	7	4.13+00	27	1.78+01	32	2.14+01	27	2.40+01	15	1.70+01
13	9	2.39+00	12	4.76+00	31	1.84+01	20	1.32+01	22	1.24+01	32	1.77+01
14	20	3.67+00	15	3.60+00	67	3.16+01	42	1.53+01	42	1.60+01	46	1.80+01
15	33	3.93+00	36	4.87+00	72	2.50+01	73	2.30+01	70	1.74+01	85	2.71+01

TRACK LENGTH COUNTERS

ENERGY GROUP	REGION 1 NUMBER	REGION 1 WEIGHT	REGION 2 NUMBER	REGION 2 WEIGHT	REGION 3 NUMBER	REGION 3 WEIGHT	REGION 4 NUMBER	REGION 4 WEIGHT	REGION 5 NUMBER	REGION 5 WEIGHT	REGION 6 NUMBER	REGION 6 WEIGHT
1	0	0.00	0	0.00	0	0.00	0	0.00	0	0.00	0	0.00
2	0	0.00	48	1.63+05	0	0.00	0	0.00	0	0.00	0	0.00
3	0	0.00	109	5.14+05	0	0.00	0	0.00	0	0.00	0	0.00
4	0	0.00	73	4.98+05	0	0.00	0	0.00	0	0.00	0	0.00
5	0	0.00	108	6.93+05	0	0.00	0	0.00	0	0.00	2	1.00+04
6	0	0.00	100	7.32+05	0	0.00	0	0.00	0	0.00	1	1.17+04
7	0	0.00	99	6.94+05	1	7.77+03	0	0.00	0	0.00	2	7.60+03
8	0	0.00	114	7.94+05	1	2.84+03	1	1.96+03	1	7.28+01	4	1.47+04
9	1	4.13+03	169	9.08+05	2	9.75+02	1	2.28+03	0	0.00	2	3.19+03
10	0	0.00	185	1.10+06	3	1.89+03	1	1.05+04	0	0.00	5	1.40+04
11	1	1.38+04	158	9.97+05	3	6.44+03	0	0.00	0	0.00	4	2.75+04
12	1	1.10+03	164	1.13+06	3	6.05+03	0	0.00	1	6.29+03	5	3.16+04
13	8	7.57+03	196	1.17+06	5	2.51+04	1	2.74+03	1	2.55+03	8	9.71+03
14	7	8.10+03	239	1.09+06	1	1.14+02	8	5.07+03	2	1.30+03	7	2.94+03
15	2	1.55+03	320	1.26+06	8	8.81+03	5	3.11+03	1	1.36+03	8	4.34+03
							15	8.21+03	16	7.55+03		

ENERGY GROUP	REGION 7 NUMBER	REGION 7 WEIGHT	REGION 8 NUMBER	REGION 8 WEIGHT	REGION 9 NUMBER	REGION 9 WEIGHT	REGION 10 NUMBER	REGION 10 WEIGHT	REGION 11 NUMBER	REGION 11 WEIGHT	REGION 12 NUMBER	REGION 12 WEIGHT
1	0	0.00	0	0.00	0	0.00	0	0.00	0	0.00	0	0.00
2	0	0.00	0	0.00	0	0.00	0	0.00	0	0.00	0	0.00
3	0	0.00	0	0.00	0	0.00	0	0.00	0	0.00	0	0.00
4	0	0.00	0	0.00	0	0.00	0	0.00	0	0.00	0	0.00
5	0	0.00	0	0.00	0	0.00	0	0.00	0	0.00	0	0.00
6	0	0.00	0	0.00	0	0.00	0	0.00	0	0.00	0	0.00
7	0	0.00	0	0.00	2	1.10+03	0	0.00	2	2.4?+04	0	0.00
8	2	1.25+04	1	5.62+03	0	0.00	1	3.02+02	1	3.6?+03	2	5.23+04
9	0	0.00	1	5.01+03	0	0.00	2	4.83+03	3	9.48+03	2	6.93+03
10	3	6.93+03	1	2.58+03	0	0.00	2	3.71+03	5	8.98+03	2	1.32+04
11	3	6.43+03	5	2.08+04	1	1.06+04	2	1.55+04	12	6.71+04	3	5.83+03
12	1	3.27+03	4	1.59+04	0	0.00	1	1.32+03	11	5.60+04	8	3.10+04
13	10	2.81+04	9	2.35+04	2	3.34+03	4	2.56+03	8	2.26+04	7	2.19+04
14	4	7.55+03	9	2.28+04	10	4.05+03	2	9.40+02	14	4.78+04	16	1.52+04
15	12	5.40+03	11	9.69+03	9	2.92+03	3	1.82+03	15	1.67+04	24	2.90+04

ENERGY GROUP	REGION 13 NUMBER	REGION 13 WEIGHT	REGION 14 NUMBER	REGION 14 WEIGHT	REGION 15 NUMBER	REGION 15 WEIGHT	REGION 16 NUMBER	REGION 16 WEIGHT	REGION 17 NUMBER	REGION 17 WEIGHT	REGION 18 NUMBER	REGION 18 WEIGHT
1	0	0.00	0	0.00	0	0.00	0	0.00	0	0.00	0	0.00
2	0	0.00	0	0.00	0	0.00	0	0.00	0	0.00	0	0.00
3	0	0.00	3	2.73+04	3	9.04+04	0	0.00	2	1.72+04	2	1.26+04
4	0	0.00	0	0.00	4	2.57+04	0	0.00	0	0.00	0	0.00
5	0	0.00	1	1.65+04	3	5.61+04	0	0.00	0	0.00	1	2.19+04
6	0	0.00	3	5.24+04	2	7.47+04	0	0.00	0	0.00	0	0.00
7	1	3.67+02	4	1.36+05	4	1.12+05	1	1.89+04	3	1.18+04	2	2.46+03
8	3	2.66+03	5	1.28+04	4	5.34+04	6	1.11+05	5	2.73+04	7	2.44+04
9	5	2.18+03	0	0.00	5	2.42+04	7	3.84+04	4	2.03+04	9	3.92+04
10	0	0.00	1	9.87+03	4	2.22+04	4	3.85+04	2	6.94+03	5	2.08+04

11	6	1.41+04	7	1.69+04	9	2.05+04	11	6.60+04	7	1.68+04	8	3.76+04			
12	3	1.26+04	3	1.41+04	2	3.02+02	10	3.76+04	7	2.54+04	8	2.98+04			
13	16	3.55+04	13	2.14+04	19	8.26+04	15	5.12+04	8	2.59+04	10	1.35+04			
14	17	1.17+04	26	4.67+04	16	3.54+04	13	3.79+04	20	2.06+04	13	1.94+04			
15	24	1.54+04	18	1.69+04	29	1.47+04	29	3.06+04	31	3.33+04	22	1.44+04			

ENERGY GROUP	REGION 19		REGION 20		REGION 21		REGION 22		REGION 23		REGION 24	
	NUMBER	WEIGHT	NUMBER	WEIGHT	NUMBER	WEIGHT	NUMBER	WEIGHT	NUMBER	WEIGHT	NUMBER	WEIGHT
1	0	0.00	0	0.00	0	0.00	0	0.00	0	0.00	0	0.00
2	0	0.00	0	0.00	0	0.00	0	0.00	0	0.00	0	0.00
3	0	0.00	0	0.00	0	0.00	10	1.66+05	10	1.07+05	0	0.00
4	0	0.00	0	0.00	0	0.00	0	0.00	5	4.33+04	7	4.82+04
5	1	1.48+04	4	8.17+04	0	0.00	3	7.96+04	6	1.44+05	8	1.88+05
6	1	1.64+04	0	0.00	0	0.00	2	1.40+05	7	2.24+05	3	2.20+04
7	5	1.93+04	2	3.51+03	1	2.50+03	5	2.44+05	6	5.98+04	8	1.93+05
8	5	2.97+04	2	5.63+04	0	0.00	5	3.11+04	17	2.38+05	13	1.11+05
9	10	3.75+04	3	2.62+03	2	9.87+02	2	3.55+03	9	5.78+04	22	1.20+05
10	11	1.43+05	7	5.31+03	5	2.14+04	4	2.08+04	18	7.51+04	17	9.44+04
11	10	7.38+04	16	1.00+05	7	6.46+04	12	3.58+04	33	2.15+05	31	1.59+05
12	7	1.88+04	13	3.89+04	7	5.04+04	9	5.42+04	18	6.97+04	35	1.49+05
13	14	1.33+05	9	2.04+04	19	7.30+04	8	3.59+04	39	2.04+05	31	1.47+05
14	32	6.38+04	24	3.98+04	28	8.38+04	38	9.13+04	48	8.60+04	41	7.42+04
15	19	7.00+04	43	5.55+04	42	5.59+04	23	2.93+04	55	9.53+04	63	9.47+04

ENERGY GROUP	REGION 25		REGION 26		REGION 27		REGION 28		REGION 29		REGION 30	
	NUMBER	WEIGHT	NUMBER	WEIGHT	NUMBER	WEIGHT	NUMBER	WEIGHT	NUMBER	WEIGHT	NUMBER	WEIGHT
1	0	0.00	0	0.00	0	0.00	0	0.00	0	0.00	0	0.00
2	0	0.00	0	0.00	0	0.00	1	3.69+03	0	0.00	0	0.00
3	9	1.61+05	7	1.44+05	0	0.00	9	3.92+04	2	1.43+04	12	3.14+05
4	4	3.09+04	5	1.02+05	3	2.73+04	3	7.72+04	1	2.61+04	0	0.00
5	2	1.79+04	7	1.48+05	5	5.18+04	4	1.80+05	1	1.53+03	2	1.74+05
6	5	4.53+04	4	1.42+05	5	6.24+04	3	1.73+05	1	1.04+04	4	1.11+05
7	3	7.08+04	2	4.19+04	9	1.86+05	8	2.26+05	2	1.27+04	6	1.90+05
8	10	2.02+05	14	2.40+05	9	1.00+05	5	1.89+05	1	5.13+04	11	5.30+05
9	7	4.03+04	15	9.84+04	16	6.84+04	4	9.91+03	8	1.90+04	9	9.40+04
10	12	4.81+04	22	9.37+04	8	9.03+04	11	4.54+04	11	6.30+04	8	1.92+05
11	21	9.18+04	30	1.74+05	10	2.32+05	7	9.24+04	13	6.77+04	20	1.43+05
12	18	1.11+05	25	1.34+05	9	3.95+04	12	9.35+04	12	1.16+05	22	9.19+04
13	26	1.22+05	21	6.99+04	27	1.39+05	17	7.79+04	24	7.35+04	23	1.11+05
14	53	1.02+05	42	1.55+05	37	1.17+05	38	9.27+04	31	4.76+04	36	8.91+04
15	94	1.02+05	39	6.98+04	69	8.82+04	60	8.99+04	54	4.68+04	52	6.15+04

ENERGY GROUP	REGION 31		REGION 32		REGION 33		REGION 34		REGION 35		REGION 36	
	NUMBER	WEIGHT	NUMBER	WEIGHT	NUMBER	WEIGHT	NUMBER	WEIGHT	NUMBER	WEIGHT	NUMBER	WEIGHT
1	0	0.00	0	0.00	0	0.00	0	0.00	0	0.00	0	0.00
2	5	1.98+04	47	1.55+05	11	1.24+04	14	5.53+04	0	0.00	0	0.00
3	27	2.72+05	42	2.70+05	57	4.92+05	35	1.89+05	0	0.00	2	3.33+04
4	21	2.17+05	12	1.00+05	22	2.58+05	19	2.24+05	2	2.11+04	3	3.00+04
5	27	3.34+05	38	3.13+05	18	1.77+05	30	4.75+05	4	8.46+04	7	1.79+05
6	29	4.04+05	25	4.32+05	26	3.66+05	22	4.40+05	4	1.27+05	4	8.30+04

7	18	2.43+05	21	3.79+05	13	9.23+04	21	2.50+05	5	1.23+05	12	3.84+05
8	28	4.73+05	29	4.25+05	28	3.01+05	34	6.56+05	8	4.86+04	3	6.56+04
9	46	3.51+05	43	2.56+05	52	3.96+05	55	3.56+05	10	3.75+04	5	1.46+04
10	46	3.34+05	41	2.73+05	46	3.05+05	53	4.07+05	17	7.65+04	7	5.49+04
11	47	3.24+05	46	2.42+05	57	2.37+05	58	4.00+05	9	6.57+04	9	6.66+04
12	46	2.88+05	48	3.59+05	51	3.47+05	83	5.14+05	12	5.42+04	11	5.65+04
13	66	5.19+05	67	3.61+05	75	3.78+05	80	4.04+05	18	5.49+04	8	3.24+04
14	92	2.61+05	80	2.65+05	106	4.25+05	102	3.84+05	37	6.96+04	34	4.99+04
15	156	3.08+05	158	4.16+05	169	3.85+05	133	2.90+05	47	5.73+04	60	9.97+04

ENERGY	REGION 37		REGION 38		REGION 39		REGION 40		REGION 41		REGION 42	
GROUP	NUMBER	WEIGHT	NUMBER	WEIGHT	NUMBER	WEIGHT	NUMBER	WEIGHT	NUMBER	WEIGHT	NUMBER	WEIGHT
1	0	0.00	0	0.00	0	0.00	0	0.00	0	0.00	0	0.00
2	0	0.00	4	5.34+03	7	9.76+03	38	1.14+05	9	4.39+04	18	7.13+04
3	4	8.34+04	1	5.32+02	19	7.80+04	48	3.34+05	34	2.46+05	24	9.91+04
4	3	6.24+04	1	7.10+03	21	1.57+05	27	3.28+05	12	1.22+05	16	1.82+05
5	1	1.08+03	2	2.23+03	27	2.71+05	26	3.79+05	26	2.83+05	19	1.98+05
6	0	0.00	0	0.00	9	1.10+05	16	1.87+05	13	1.84+05	10	1.28+05
7	1	2.53+03	1	5.64+02	16	1.49+05	27	3.46+05	21	2.61+05	14	1.20+05
8	6	9.13+04	6	3.83+05	30	2.09+05	31	2.27+05	26	1.87+05	25	3.66+05
9	11	9.25+04	4	1.39+05	40	2.23+05	45	2.99+05	36	2.15+05	41	2.42+05
10	10	1.59+05	11	5.33+04	37	2.21+05	37	2.06+05	32	2.50+05	46	3.30+05
11	6	2.12+04	15	9.61+04	48	2.65+05	44	3.59+05	37	2.49+05	54	4.65+05
12	14	8.69+04	15	8.17+04	40	2.39+05	57	3.09+05	53	4.61+05	35	3.30+05
13	14	2.50+04	20	8.60+04	65	2.84+05	54	4.13+05	44	2.15+05	63	3.74+05
14	28	3.85+04	30	7.29+04	107	3.99+05	73	2.41+05	75	2.93+05	79	2.52+05
15	51	6.15+04	52	5.09+04	124	3.02+05	132	3.58+05	120	2.61+05	149	3.94+05

***NEXT RANDOM NUMBER IS 337274612532

********** A-MODE FAMS STORE FOR ITERATION NO. 1 **********

FAM (IFAM) ARRAY

1	1	2	100	100	0	0	0	0
9	0	0	0	0	0	0	0	0
17	0	10	10	0	0	0	0	0
25	0	0	0	0	0	0	0	0
33	1	1	25850	25850	37820	37820	11970	18
41	1	2	25850	37820	2			

********** F-MODE FAMS READ FOR ITERATION NO. 1 **********

FAM (IFAM) ARRAY

1	1	2	100	100	0	0	0	0
9	0	0	0	0	0	0	0	0

```
    17              0              10              10              0              0              0              0              0
    25              0               0               0              0              0              0              0              0
    33              1               0           25850          25850          37820          37820          11970             18
    41              1               2           25850          37820              1
YOU ARE USING THE DEFAULT VERSION OF STRUN WHICH DOES   NOTHING.

***START BATCH   1                          RANDOM=        346122764532

SOURCE DATA

YOU ARE USING THE IFA VERSION OF SOURCE.  SOURCE/IFA PICKS THE ENERGY IG FROM BFS AND THE DIRECTION KD FROM FAI(IG,NSR,KD).
   WATE IS SET EQUAL TO DOF./
  SWATE       IAVE     UAVE     VAVE     WAVE       XAVE       YAVE       ZAVE       AGEAVE
 9.892+01     10.02     .0751    .1144    .0112    1.000-03   1.000-03   1.000-03    0.000

NUMBER OF COLLISIONS OF TYPE NCOLL
  SOURCE SPLIT(D)    FISHN   GAMGEN REALCOLL   ALBEDO    BDRYX   ESCAPE    E-CUT TIMEKILL R R KILL R R SURV  GAMLOST
     100        0        0        0     1433        0      516       43       24         0       33         3        0

TIME REQUIRED FOR THE PRECEDING BATCH WAS     27

***START BATCH   2                          RANDOM=        121357431522

SOURCE DATA
  SWATE       IAVE     UAVE     VAVE     WAVE       XAVE       YAVE       ZAVE       AGEAVE
 1.073+02     10.38    -.0788   -.0799    .0128    1.000-03   1.000-03   1.000-03    0.000

NUMBER OF COLLISIONS OF TYPE NCOLL
  SOURCE SPLIT(D)    FISHN   GAMGEN REALCOLL   ALBEDO    BDRYX   ESCAPE    E-CUT TIMEKILL R R KILL R R SURV  GAMLOST
     100        0        0        0     2047        0      685       38       37         0       25         2        0

TIME REQUIRED FOR THE PRECEDING BATCH WAS     28

***START BATCH   3                          RANDOM=        352056352722

SOURCE DATA
  SWATE       IAVE     UAVE     VAVE     WAVE       XAVE       YAVE       ZAVE       AGEAVE
 1.019+02     10.11     .0648   -.0125   -.0038    1.000-03   1.000-03   1.000-03    0.000

NUMBER OF COLLISIONS OF TYPE NCOLL
  SOURCE SPLIT(D)    FISHN   GAMGEN REALCOLL   ALBEDO    BDRYX   ESCAPE    E-CUT TIMEKILL R R KILL R R SURV  GAMLOST
     100        0        0        0     2099        0      666       44       34         0       22         3        0

TIME REQUIRED FOR THE PRECEDING BATCH WAS     30

***START BATCH   4                          RANDOM=        354272442002

SOURCE DATA
  SWATE       IAVE     UAVE     VAVE     WAVE       XAVE       YAVE       ZAVE       AGEAVE
 9.651+01     10.34     .0591    .0439   -.0263    1.000-03   1.000-03   1.000-03    0.000
```

```
NUMBER OF COLLISIONS OF TYPE NCOLL
  SOURCE SPLIT(D)    FISHN   GAMGEN REALCOLL   ALBEDO    BDRYX   ESCAPE    E-CUT TIMEKILL R R KILL R R SURV  GAMLOST
      100        0        0        0     1415        0      477       44       25        0       31        3        0

TIME REQUIRED FOR THE PRECEDING BATCH WAS     20

***START BATCH    5                          RANDOM=         161635566172

SOURCE DATA
  SWATE       IAVE    UAVE    VAVE    WAVE       XAVE       YAVE       ZAVE       AGEAVE
  9.766+01    10.04   -.0030   .0707  -.0300    1.000-03   1.000-03   1.000-03   0.000

NUMBER OF COLLISIONS OF TYPE NCOLL
  SOURCE SPLIT(D)    FISHN   GAMGEN REALCOLL   ALBEDO    BDRYX   ESCAPE    E-CUT TIMEKILL R R KILL R R SURV  GAMLOST
      100        0        0        0     1616        0      497       40       27        0       33        5        0

TIME REQUIRED FOR THE PRECEDING BATCH WAS     24

***START BATCH    6                          RANDOM=         247121707102

SOURCE DATA
  SWATE       IAVE    UAVE    VAVE    WAVE       XAVE       YAVE       ZAVE       AGEAVE
  9.776+01    10.19   -.1839   .0394   .0480    1.000-03   1.000-03   1.000-03   0.000

NUMBER OF COLLISIONS OF TYPE NCOLL
  SOURCE SPLIT(D)    FISHN   GAMGEN REALCOLL   ALBEDO    BDRYX   ESCAPE    E-CUT TIMEKILL R R KILL R R SURV  GAMLOST
      100        0        0        0     1750        0      543       47       26        0       27        3        0

TIME REQUIRED FOR THE PRECEDING BATCH WAS     26

***START BATCH    7                          RANDOM=         324241522022

SOURCE DATA
  SWATE       IAVE    UAVE    VAVE    WAVE       XAVE       YAVE       ZAVE       AGEAVE
  1.073+02    10.12    .0216  -.0086  -.0038    1.000-03   1.000-03   1.000-03   0.000

NUMBER OF COLLISIONS OF TYPE NCOLL
  SOURCE SPLIT(D)    FISHN   GAMGEN REALCOLL   ALBEDO    BDRYX   ESCAPE    E-CUT TIMEKILL R R KILL R R SURV  GAMLOST
      100        0        0        0     1829        0      555       41       27        0       32        1        0

TIME REQUIRED FOR THE PRECEDING BATCH WAS     25

***START BATCH    8                          RANDOM=         211251444022

SOURCE DATA
  SWATE       IAVE    UAVE    VAVE    WAVE       XAVE       YAVE       ZAVE       AGEAVE
  9.884+01     9.95    .0760  -.0072  -.1226    1.000-03   1.000-03   1.000-03   0.000

NUMBER OF COLLISIONS OF TYPE NCOLL
  SOURCE SPLIT(D)    FISHN   GAMGEN REALCOLL   ALBEDO    BDRYX   ESCAPE    E-CUT TIMEKILL R R KILL R R SURV  GAMLOST
```

```
    100        0        0        0     1922        0      610       48       22        0       30        3        0

TIME REQUIRED FOR THE PRECEDING BATCH WAS     27

***START BATCH   9                          RANDOM=         311141471302

SOURCE DATA
  SWATE        IAVE     UAVE     VAVE     WAVE       XAVE       YAVE       ZAVE       AGEAVE
 1.017+02     10.26    -.0296    .0376    -.1100     1.000-03   1.000-03   1.000-03    0.000

NUMBER OF COLLISIONS OF TYPE NCOLL
  SOURCE SPLIT(D)    FISHN    GAMGEN REALCOLL    ALBEDO     BDRYX    ESCAPE    E-CUT TIMEKILL R P KILL R R SURV  GAMLOST
     100        0        0        0     1959         0       565        39        33         0       28         1         0

TIME REQUIRED FOR THE PRECEDING BATCH WAS     28

***START BATCH  10                          RANDOM=         121405674642

SOURCE DATA
  SWATE        IAVE     UAVE     VAVE     WAVE       XAVE       YAVE       ZAVE       AGEAVE
 9.905+01      9.77    -.1070    .0286    -.0831     1.000-03   1.000-03   1.000-03    0.000

NUMBER OF COLLISIONS OF TYPE NCOLL
  SOURCE SPLIT(D)    FISHN    GAMGEN REALCOLL    ALBEDO     BDRYX    ESCAPE    E-CUT TIMEKILL R R KILL R R SURV  GAMLOST
     100        0        0        0     1736         0       601        41        29         0       30         1         0

TIME REQUIRED FOR THE PRECEDING BATCH WAS     24
```

THIS PRINT OCCURRED ON THE 3 DAY OF THE 5 MONTH IN THE YEAR 1976
AT 15 MINUTES PAST THE HOUR OF 10 PM .

HENDERSON TISSUE DOSE - RADS[T]

RESPONSES(DETECTOR) TOTAL RESPONSE - NEUTRON RESPONSE FUNCTION FROM ORNL 4464

DETECTOR	UNCOLL RESPONSE	FSD UNCOLL	TOTAL RESPONSE	FSD TOTAL
1	5.9796-22	.33333	2.4008-20	.36791
2	0.0000	.00000	3.0437-21	1.00000

FLUENCE(ENERGY,DETECTOR) ENERGY DEPENDENT FLUENCE - NEUTRONS/CMSQ/EV/SOURCE

DETECTOR NO. ENERGIES	1	2
1.500+07	0.000	0.000
	.000	.000
1.220+07	2.866-23	0.000
	.783	.000
1.000+07	1.549-21	0.000
	.446	.000
8.180+06	8.138-21	0.000
	.335	.000
6.360+06	5.336-20	0.000
	.169	.000
4.060+06	7.338-19	0.000
	.388	.000
2.350+06	1.093-18	0.000
	.372	.000
1.108+06	9.498-18	2.725-18
	.531	1.000
1.109+05	3.332-17	0.000
	.520	.000
3.355+03		

DETECTOR NO 1 FLUENCE(COSINE,ENERGY,DETECTOR) ENERGY AND ANGULAR DEPENDENT FLUENCE

ENERGIES	1.500+07	1.220+07	1.000+07	8.180+06	6.360+06	4.060+06	2.350+06	1.108+06	1.109+05
COSINES	1.220+07	1.000+07	8.180+06	6.360+06	4.060+06	2.350+06	1.108+06	1.109+05	3.355+03
-1.000000									
	0.000	0.000	0.000	0.000	0.000	0.000	0.000	0.000	1.573-18
	.000	.000	.000	.000	.000	.000	.000	.000	.675
-.888889									
	0.000	0.000	0.000	0.000	0.000	0.000	6.524-21	1.074-18	7.936-19
	.000	.000	.000	.000	.000	.000	.807	.999	.623
-.444444									
	0.000	0.000	0.000	1.036-22	2.851-22	3.325-22	8.097-20	3.296-19	1.275-18
	.000	.000	.000	1.000	1.000	.936	.997	.652	.536
.000000									
	0.000	0.000	0.000	3.107-22	6.949-22	1.604-19	1.264-19	1.019-18	6.237-18
	.000	.000	.000	1.000	.698	.541	.801	.680	.651
.444444									
	0.000	0.000	0.000	2.105-22	4.722-21	4.858-20	7.597-20	6.271-19	3.185-18
	.000	.000	.000	.878	.403	.657	.279	.497	.679
.888889									
	0.000	4.105-23	2.218-21	9.157-21	5.362-20	2.139-19	4.058-19	1.402-18	1.962-19
	.000	.783	.446	.318	.182	.123	.313	.424	.728
1.000000									

DETECTOR NO 2 FLUENCE(COSINE,ENERGY,DETECTOR) ENERGY AND ANGULAR DEPENDENT FLUENCE

ENERGIES	1.500+07	1.220+07	1.000+07	8.180+06	6.360+06	4.060+06	2.350+06	1.108+06	1.109+05
COSINES	1.220+07	1.000+07	8.180+06	6.360+06	4.060+06	2.350+06	1.108+06	1.109+05	3.355+03
-1.000000									
	0.000	0.000	0.000	0.000	0.000	0.000	0.000	0.000	0.000
	.000	.000	.000	.000	.000	.000	.000	.000	.000
-.888889									
	0.000	0.000	0.000	0.000	0.000	0.000	0.000	9.760-19	0.000
	.000	.000	.000	.000	.000	.000	.000	1.000	.000
-.444444									
	0.000	0.000	0.000	0.000	0.000	0.000	0.000	0.000	0.000
	.000	.000	.000	.000	.000	.000	.000	.000	.000
.000000									
	0.000	0.000	0.000	0.000	0.000	0.000	0.000	0.000	0.000
	.000	.000	.000	.000	.000	.000	.000	.000	.000
.444444									
	0.000	0.000	0.000	0.000	0.000	0.000	0.000	0.000	0.000
	.000	.000	.000	.000	.000	.000	.000	.000	.000
.888889									
	0.000	0.000	0.000	0.000	0.000	0.000	0.000	0.000	0.000
	.000	.000	.000	.000	.000	.000	.000	.000	.000
1.000000									

TIME REQUIRED FOR THE PRECEDING 10 BATCHES WAS 260

REAL SCATTERING COUNTERS

ENERGY GROUP	REGION 1		REGION 2		REGION 3		REGION 4		REGION 5		REGION 6	
	NUMBER	WEIGHT	NUMBER	WEIGHT	NUMBER	WEIGHT	NUMBER	WEIGHT	NUMBER	WEIGHT	NUMBER	WEIGHT
1	0	0.00	0	0.00	0	0.00	0	0.00	0	0.00	0	0.00
2	2	3.95-02	0	0.00	0	0.00	0	0.00	0	0.00	0	0.00
3	13	2.59+00	0	0.00	0	0.00	2	1.51-01	0	0.00	0	0.00
4	6	2.00+00	0	0.00	0	0.00	2	2.34+00	1	1.21+00	0	0.00
5	31	2.53+01	0	0.00	3	3.05+00	7	3.32+00	2	6.77-01	1	6.45-01
6	12	1.52+01	0	0.00	2	1.09+00	2	2.69+00	0	0.00	3	2.99+00
7	200	9.41+01	1	6.21-01	1	7.14-01	1	1.09+00	3	1.30+00	3	2.05+00
8	50	5.79+01	4	7.35-01	1	5.40-01	11	4.80+00	4	9.28-01	2	5.49-01
9	7	8.72+00	0	0.00	2	4.75-01	1	7.25-01	3	6.96-01	0	0.00
10	97	1.32+02	3	1.03-01	8	3.18+00	12	9.14+00	0	0.00	9	5.03+00
11	165	2.42+02	4	1.05-01	19	1.16+01	16	1.05+01	13	1.38+01	24	1.87+01
12	221	3.27+02	11	5.68+00	32	1.95+01	20	1.10+01	37	3.79+01	24	1.98+01
13	367	4.96+02	29	4.26+00	85	6.50+01	51	5.14+01	114	1.09+02	100	5.30+01
14	299	3.46+02	35	1.45+01	155	2.34+02	84	9.65+01	121	1.16+02	138	1.11+02
15	0	0.00	0	0.00	0	0.00	0	0.00	0	0.00	0	0.00

ENERGY GROUP	REGION 7		REGION 8		REGION 9		REGION 10		REGION 11		REGION 12	
	NUMBER	WEIGHT	NUMBER	WEIGHT	NUMBER	WEIGHT	NUMBER	WEIGHT	NUMBER	WEIGHT	NUMBER	WEIGHT
1	0	0.00	0	0.00	0	0.00	0	0.00	0	0.00	0	0.00
2	0	0.00	0	0.00	0	0.00	0	0.00	0	0.00	0	0.00
3	0	0.00	0	0.00	0	0.00	0	0.00	0	0.00	0	0.00
4	5	3.02+00	2	2.34+00	1	2.88+00	2	2.81+00	0	0.00	0	0.00
5	1	6.64-01	4	2.59+00	8	6.39+00	6	3.55+00	4	1.86+00	4	1.71+00
6	2	1.47+00	7	7.17+00	4	3.63+00	3	4.42+00	4	2.80+00	3	4.59-01
7	15	2.52+01	20	1.70+01	22	2.17+01	38	2.29+01	4	3.35+00	6	6.85+00
8	25	8.89+00	14	1.41+01	21	1.83+01	9	5.39+00	5	3.72+00	8	6.68+00
9	4	6.68+00	5	6.23+00	5	4.70+00	4	1.55+00	0	0.00	0	0.00
10	23	2.65+01	44	4.61+01	28	3.58+01	23	2.31+01	2	2.19+00	6	1.24+00
11	74	6.58+01	109	1.21+02	94	1.24+02	67	6.91+01	16	9.71+00	13	6.86+00
12	157	2.16+02	120	1.49+02	122	1.72+02	90	1.10+02	19	1.65+01	77	6.47+01
13	312	3.34+02	209	2.45+02	325	4.36+02	249	2.29+02	93	9.77+01	94	1.16+02
14	394	4.80+02	434	4.47+02	289	2.83+02	324	3.12+02	189	1.41+02	208	2.51+02
15	0	0.00	0	0.00	0	0.00	0	0.00	0	0.00	0	0.00

ENERGY GROUP	REGION 13		REGION 14		REGION 15		REGION 16		REGION 17		REGION 18	
	NUMBER	WEIGHT	NUMBER	WEIGHT	NUMBER	WEIGHT	NUMBER	WEIGHT	NUMBER	WEIGHT	NUMBER	WEIGHT
1	0	0.00	0	0.00	0	0.00	0	0.00	0	0.00	0	0.00
2	0	0.00	0	0.00	0	0.00	0	0.00	0	0.00	0	0.00
3	0	0.00	0	0.00	0	0.00	2	9.97-02	0	0.00	1	7.53-01
4	1	7.56-01	0	0.00	0	0.00	0	0.00	2	2.43+00	2	2.80+00
5	2	5.71-01	1	1.24+00	6	7.35+00	16	7.06+00	6	4.20+00	9	3.15+00
6	0	0.00	0	0.00	5	3.82+00	9	2.77+00	5	5.78+00	10	7.96+00
7	1	1.25+00	1	6.85-01	28	1.72+01	20	1.37+01	21	1.29+01	58	2.06+01
8	12	5.62+00	2	2.11+00	20	1.13+01	21	1.05+01	15	1.03+01	34	2.12+01
9	2	1.16+00	1	1.46-02	4	2.95+00	12	1.87+01	8	8.10+00	10	5.18+00
10	8	2.94+00	10	5.53+00	35	2.81+01	27	2.49+01	42	4.22+01	19	1.58+01

11	17	1.62+01	18	7.86+00	116	8.05+01	53	5.25+01	95	9.04+01	80	5.17+01			
12	27	3.68+01	19	1.92+01	107	1.22+02	127	1.69+02	80	1.07+02	76	9.92+01			
13	147	1.68+02	173	1.45+02	374	2.65+02	324	4.48+02	422	2.90+02	370	2.61+02			
14	244	4.48+02	170	2.33+02	369	3.35+02	369	4.82+02	429	5.06+02	497	3.48+02			
15	0	0.00	0	0.00	0	0.00	0	0.00	0	0.00	0	0.00			

ENERGY	REGION 19		REGION 20		REGION 21		REGION 22		REGION 23		REGION 24	
GROUP	NUMBER	WEIGHT	NUMBER	WEIGHT	NUMBER	WEIGHT	NUMBER	WEIGHT	NUMBER	WEIGHT	NUMBER	WEIGHT
1	0	0.00	0	0.00	0	0.00	0	0.00	0	0.00	0	0.00
2	0	0.00	0	0.00	0	0.00	0	0.00	0	0.00	0	0.00
3	0	0.00	0	0.00	0	0.00	0	0.00	0	0.00	0	0.00
4	0	0.00	0	0.00	0	0.00	0	0.00	0	0.00	0	0.00
5	0	0.00	0	0.00	0	0.00	0	0.00	0	0.00	1	2.37+00
6	2	6.82-02	0	0.00	0	0.00	0	0.00	4	2.00+00	1	4.22-01
7	3	1.32+00	0	0.00	0	0.00	1	5.50-01	5	5.14+00	1	3.09-01
8	3	2.20+00	1	9.46-01	3	2.73-01	1	3.13-01	9	2.16+00	14	2.42+00
9	1	4.23-01	2	1.42+00	2	1.01+00	2	1.49+00	4	6.45-01	9	4.54-01
10	4	3.49+00	3	1.13+00	4	3.14+00	1	2.72-01	0	0.00	4	3.27+00
11	3	9.03-01	5	1.98+00	15	9.98+00	5	5.20+00	5	2.97+00	14	9.82+00
12	10	3.11+01	32	2.08+01	18	1.60+01	16	1.03+01	24	2.37+01	76	2.34+01
13	47	7.82+01	106	3.80+02	68	1.13+02	16	3.21+01	28	4.86+01	68	7.13+01
14	210	2.85+02	119	1.72+02	221	2.95+02	163	7.68+01	248	1.46+02	127	2.28+02
15	0	0.00	0	0.00	0	0.00	131	1.43+02	231	2.36+02	291	3.86+02
							0	0.00	0	0.00	0	0.00

ENERGY	REGION 25		REGION 26		REGION 27		REGION 28		REGION 29		REGION 30	
GROUP	NUMBER	WEIGHT	NUMBER	WEIGHT	NUMBER	WEIGHT	NUMBER	WEIGHT	NUMBER	WEIGHT	NUMBER	WEIGHT
1	0	0.00	0	0.00	0	0.00	0	0.00	0	0.00	0	0.00
2	0	0.00	0	0.00	0	0.00	0	0.00	0	0.00	0	0.00
3	0	0.00	0	0.00	0	0.00	0	0.00	0	0.00	1	7.67-01
4	0	0.00	0	0.00	0	0.00	0	0.00	0	0.00	0	0.00
5	1	8.60-01	0	0.00	0	0.00	0	0.00	2	7.48-01	0	0.00
6	0	0.00	3	1.27+00	0	0.00	0	0.00	3	1.27-01	0	0.00
7	8	2.68+00	4	1.77-01	3	5.61-01	0	0.00	0	0.00	1	5.04-01
8	15	4.02+00	6	1.27+00	1	1.95-01	2	8.26-01	0	0.00	2	1.22+00
9	4	3.68+00	1	2.10+00	0	0.00	0	0.00	0	0.00	5	1.23+00
10	14	1.14+01	10	2.22+00	2	1.99+00	0	0.00	4	4.21+00	4	2.69+00
11	37	3.84+01	39	1.91+01	9	2.97+00	7	1.67+00	4	2.39+00	11	5.29+00
12	21	3.04+01	43	5.37+01	2	2.94-01	19	1.77+01	10	7.33+00	6	5.67+00
13	222	1.33+02	169	1.05+02	21	8.64+00	40	1.21+02	44	5.00+01	59	1.87+01
14	167	1.77+02	318	2.75+02	228	6.46+02	70	2.06+02	72	7.58+01	77	6.55+01
15	0	0.00	0	0.00	0	0.00	0	0.00	0	0.00	0	0.00

ENERGY	REGION 31		REGION 32		REGION 33		REGION 34		REGION 35		REGION 36	
GROUP	NUMBER	WEIGHT	NUMBER	WEIGHT	NUMBER	WEIGHT	NUMBER	WEIGHT	NUMBER	WEIGHT	NUMBER	WEIGHT
1	0	0.00	0	0.00	0	0.00	0	0.00	0	0.00	0	0.00
2	0	0.00	0	0.00	0	0.00	0	0.00	0	0.00	0	0.00
3	1	5.99-03	0	0.00	0	0.00	0	0.00	0	0.00	0	0.00
4	0	0.00	0	0.00	0	0.00	0	0.00	0	0.00	0	0.00
5	1	6.37-01	1	1.35-01	1	1.69-01	1	1.35-01	0	0.00	0	0.00
6	1	2.74+00	0	0.00	2	2.42-01	1	1.15-01	0	0.00	0	0.00

7	1	3.38-02	4	1.42-01	4	3.74+00	7	7.90+00	0	0.00	0	0.00
8	1	1.11-01	4	7.11-01	1	1.64-02	7	1.26+00	0	0.00	0	0.00
9	1	6.50-02	0	0.00	0	0.00	0	0.00	0	0.00	0	0.00
10	4	2.35+00	8	8.90-01	0	0.00	3	5.04-01	0	0.00	0	0.00
11	13	1.70+00	7	1.71+00	16	6.50+00	6	1.26+00	5	1.46+00	5	2.25-01
12	19	7.29+00	13	8.09+00	11	9.09+00	11	8.25+00	10	1.08+00	10	1.01+01
13	88	3.33+01	85	1.27+02	66	2.82+01	57	5.80+01	2	3.24-01	7	1.91+00
14	120	8.87+01	147	7.02+01	33	3.61+01	192	9.26+01	37	5.69+01	30	4.83+00
15	0	0.00	0	0.00	0	0.00	0	0.00	0	0.00	0	0.00

ENERGY GROUP	REGION 37		REGION 38		REGION 39		REGION 40		REGION 41		REGION 42	
	NUMBER	WEIGHT	NUMBER	WEIGHT	NUMBER	WEIGHT	NUMBER	WEIGHT	NUMBER	WEIGHT	NUMBER	WEIGHT
1	0	0.00	0	0.00	0	0.00	0	0.00	0	0.00	0	0.00
2	0	0.00	0	0.00	0	0.00	0	0.00	0	0.00	0	0.00
3	0	0.00	1	6.72-01	0	0.00	0	0.00	0	0.00	0	0.00
4	0	0.00	0	0.00	0	0.00	0	0.00	0	0.00	0	0.00
5	0	0.00	0	0.00	0	0.00	1	1.19-01	0	0.00	0	0.00
6	1	1.58-01	0	0.00	0	0.00	0	0.00	0	0.00	0	0.00
7	3	2.51+00	1	3.21-01	0	0.00	0	0.00	0	0.00	0	0.00
8	4	1.79+00	1	1.14-01	0	0.00	0	0.00	0	0.00	0	0.00
9	0	0.00	0	0.00	0	0.00	0	0.00	0	0.00	0	0.00
10	0	0.00	1	3.62-01	0	0.00	0	0.00	0	0.00	0	0.00
11	0	0.00	3	1.05+00	1	1.20-01	3	4.13-01	2	1.17-01	0	0.00
12	5	1.68+00	0	0.00	2	2.70-01	2	4.71-01	4	2.73+00	0	0.00
13	23	3.45+00	1	7.57-01	3	9.53-01	5	1.01+00	22	3.38+00	3	1.23+00
14	12	1.25+01	13	9.70+00	10	8.81+00	64	4.57+01	24	2.04+01	37	3.26+01
15	0	0.00	0	0.00	0	0.00	0	0.00	0	0.00	0	0.00

TRACK LENGTH COUNTERS

ENERGY GROUP	REGION 1		REGION 2		REGION 3		REGION 4		REGION 5		REGION 6	
	NUMBER	WEIGHT	NUMBER	WEIGHT	NUMBER	WEIGHT	NUMBER	WEIGHT	NUMBER	WEIGHT	NUMBER	WEIGHT
1	0	0.00	0	0.00	0	0.00	0	0.00	0	0.00	0	0.00
2	2	1.27+02	0	0.00	0	0.00	0	0.00	0	0.00	0	0.00
3	17	1.95+04	0	0.00	0	0.00	3	2.25+03	0	0.00	0	0.00
4	18	1.58+05	0	0.00	0	0.00	2	1.16+04	1	3.02+04	0	0.00
5	69	3.13+05	0	0.00	4	1.60+04	10	3.82+04	6	1.93+04	2	2.38+04
6	34	2.88+05	0	0.00	4	2.34+04	5	1.14+04	1	3.66+00	4	2.10+04
7	335	1.08+06	1	5.24+03	3	1.04+04	3	1.11+04	6	3.02+04	3	1.67+04
8	115	8.44+05	4	2.39+03	2	1.48+03	13	6.87+04	7	9.28+03	5	2.46+04
9	37	3.42+05	0	0.00	2	9.01+02	3	2.02+04	3	4.51+03	2	5.48+02
10	194	1.63+06	4	2.35+03	9	3.27+04	14	6.83+04	5	1.63+04	13	6.80+04
11	318	2.52+06	5	1.15+02	27	1.04+05	24	1.56+05	17	1.01+05	36	1.81+05
12	405	3.53+06	11	2.82+04	45	1.90+05	32	1.37+05	47	3.51+05	34	1.90+05
13	546	3.44+06	33	1.14+04	110	4.35+05	74	3.71+05	140	5.98+05	129	3.11+05
14	372	1.21+06	40	8.87+04	174	6.12+05	100	3.63+05	142	3.49+05	168	4.21+05
15	0	0.00	0	0.00	0	0.00	0	0.00	0	0.00	0	0.00

ENERGY GROUP	REGION 7		REGION 8		REGION 9		REGION 10		REGION 11		REGION 12	
	NUMBER	WEIGHT	NUMBER	WEIGHT	NUMBER	WEIGHT	NUMBER	WEIGHT	NUMBER	WEIGHT	NUMBER	WEIGHT
1	0	0.00	0	0.00	0	0.00	0	0.00	0	0.00	0	0.00
2	0	0.00	0	0.00	0	0.00	0	0.00	0	0.00	0	0.00
3	0	0.00	2	4.85+03	0	0.00	0	0.00	0	0.00	0	0.00
4	6	1.15+04	5	7.40+04	3	4.95+04	4	2.19+04	0	0.00	0	0.00
5	6	7.53+04	12	9.60+04	16	5.73+04	10	8.74+04	5	2.33+04	7	3.82+04
6	3	2.28+04	9	5.39+04	9	9.70+04	6	1.06+05	5	1.59+04	6	9.45+04
7	20	1.62+05	28	1.69+05	37	2.52+05	57	2.68+05	6	2.18+04	6	4.09+04
8	36	1.41+05	29	2.66+05	31	2.55+05	24	9.10+04	8	8.15+04	15	8.58+04
9	6	1.18+05	10	7.48+04	9	3.65+04	8	1.06+04	2	3.15+03	1	3.29+04
10	40	3.39+05	68	6.14+05	48	4.56+05	38	3.28+05	4	7.50+04	7	1.25+04
11	108	8.25+05	151	9.74+05	132	9.44+05	105	5.70+05	28	9.89+04	17	6.33+04
12	222	2.05+06	181	1.47+06	169	1.30+06	150	1.22+06	27	1.21+05	97	5.58+05
13	394	1.98+06	297	2.20+06	422	2.76+06	341	1.53+06	117	6.12+05	120	1.60+06
14	478	1.81+06	498	1.60+06	352	1.07+06	398	1.20+06	213	5.12+05	242	7.74+05
15	0	0.00	0	0.00	0	0.00	0	0.00	0	0.00	0	0.00

ENERGY GROUP	REGION 13		REGION 14		REGION 15		REGION 16		REGION 17		REGION 18	
	NUMBER	WEIGHT	NUMBER	WEIGHT	NUMBER	WEIGHT	NUMBER	WEIGHT	NUMBER	WEIGHT	NUMBER	WEIGHT
1	0	0.00	0	0.00	0	0.00	0	0.00	0	0.00	0	0.00
2	0	0.00	0	0.00	0	0.00	0	0.00	0	0.00	0	0.00
3	0	0.00	0	0.00	1	1.25+01	3	3.21+02	0	0.00	2	8.97+03
4	1	2.85+04	0	0.00	0	0.00	1	4.71+04	3	3.86+04	3	2.74+04
5	3	7.79+03	3	2.93+04	10	7.91+04	24	1.03+05	11	2.88+04	14	5.40+04
6	0	0.00	1	1.29+04	12	7.00+04	13	7.32+04	7	3.54+04	17	1.53+05
7	2	5.39+04	2	1.07+04	44	2.37+05	31	1.05+05	35	1.45+05	78	1.85+05
8	15	4.20+04	5	2.20+04	37	1.93+05	38	1.57+05	34	2.59+05	67	3.61+05
9	6	1.80+04	2	3.02+02	7	3.81+04	19	2.29+05	17	1.29+05	14	8.60+04
10	13	3.78+04	15	8.40+04	51	4.05+05	45	2.57+05	60	4.88+05	37	2.56+05

11	33	2.62+05	26	9.39+04	165	6.48+05	96	5.99+05	148	8.50+05	131	5.26+05
12	39	2.86+05	30	2.00+05	166	1.25+06	201	1.47+06	128	1.16+06	124	1.11+06
13	181	1.06+06	211	8.97+05	509	1.73+06	435	3.04+06	569	1.90+06	512	1.54+06
14	286	1.71+06	200	8.31+05	452	1.22+06	476	1.69+06	504	1.96+06	582	1.49+06
15	0	0.00	0	0.00	0	0.00	0	0.00	0	0.00	0	0.00

ENERGY	REGION 19		REGION 20		REGION 21		REGION 22		REGION 23		REGION 24	
GROUP	NUMBER	WEIGHT	NUMBER	WEIGHT	NUMBER	WEIGHT	NUMBER	WEIGHT	NUMBER	WEIGHT	NUMBER	WEIGHT
1	0	0.00	0	0.00	0	0.00	0	0.00	0	0.00	0	0.00
2	0	0.00	0	0.00	0	0.00	0	0.00	0	0.00	0	0.00
3	0	0.00	0	0.00	0	0.00	0	0.00	1	1.46+02	0	0.00
4	0	0.00	0	0.00	0	0.00	0	0.00	0	0.00	1	2.21+04
5	0	0.00	1	1.01+03	1	3.35+03	0	0.00	5	1.29+04	2	2.83+03
6	2	4.02+02	2	6.88+03	0	0.00	1	1.20+04	8	1.01+05	3	2.07+03
7	4	9.83+03	0	0.00	0	0.00	3	7.39+03	13	3.99+04	16	1.57+04
8	3	1.90+04	3	2.47+04	3	5.51+03	3	6.71+03	10	1.56+04	14	9.53+03
9	2	1.58+04	3	1.87+04	4	2.27+04	2	1.25+04	1	2.21+02	8	4.76+04
10	7	6.65+04	4	3.16+04	8	8.50+04	6	5.53+04	13	5.32+04	21	8.66+04
11	8	2.12+04	6	3.06+04	22	8.22+04	19	9.81+04	38	1.15+05	91	1.62+05
12	13	9.26+04	43	2.56+05	27	1.85+05	18	1.41+05	45	6.86+05	95	5.47+05
13	57	3.98+05	129	2.19+06	106	6.64+05	207	5.24+05	321	9.56+05	186	1.67+06
14	248	9.00+05	150	8.03+05	251	9.68+05	155	4.97+05	287	9.34+05	362	1.43+06
15	0	0.00	0	0.00	0	0.00	0	0.00	0	0.00	0	0.00

ENERGY	REGION 25		REGION 26		REGION 27		REGION 28		REGION 29		REGION 30	
GROUP	NUMBER	WEIGHT	NUMBER	WEIGHT	NUMBER	WEIGHT	NUMBER	WEIGHT	NUMBER	WEIGHT	NUMBER	WEIGHT
1	0	0.00	0	0.00	0	0.00	0	0.00	0	0.00	0	0.00
2	0	0.00	0	0.00	0	0.00	0	0.00	0	0.00	0	0.00
3	0	0.00	1	2.19+04	0	0.00	0	0.00	0	0.00	2	1.21+04
4	0	0.00	0	0.00	0	0.00	0	0.00	0	0.00	0	0.00
5	2	1.58+04	2	1.03+04	0	0.00	0	0.00	3	5.14+03	0	0.00
6	0	0.00	4	1.33+04	0	0.00	0	0.00	4	2.63+03	0	0.00
7	10	2.20+04	12	2.53+04	3	1.61+03	0	0.00	0	0.00	2	1.16+04
8	21	3.29+04	14	7.29+04	2	1.83+03	3	1.31+04	1	2.61+03	2	2.72+04
9	6	4.19+04	1	4.00+04	1	4.48+01	1	5.60+03	0	0.00	5	5.39+03
10	22	1.41+05	18	7.22+04	3	2.53+04	0	0.00	5	2.73+04	5	1.64+04
11	57	2.60+05	52	1.91+05	12	1.72+04	10	1.10+04	6	5.12+04	13	3.88+04
12	47	3.20+05	59	3.46+05	6	3.21+03	25	2.85+05	17	8.14+04	7	1.85+04
13	290	9.86+05	243	7.26+05	25	5.32+04	52	6.95+05	61	4.09+05	81	1.30+05
14	214	6.61+05	379	9.40+05	260	2.33+06	84	6.06+05	85	2.56+05	89	2.06+05
15	0	0.00	0	0.00	0	0.00	0	0.00	0	0.00	0	0.00

ENERGY	REGION 31		REGION 32		REGION 33		REGION 34		REGION 35		REGION 36	
GROUP	NUMBER	WEIGHT	NUMBER	WEIGHT	NUMBER	WEIGHT	NUMBER	WEIGHT	NUMBER	WEIGHT	NUMBER	WEIGHT
1	0	0.00	0	0.00	0	0.00	0	0.00	0	0.00	0	0.00
2	0	0.00	0	0.00	0	0.00	0	0.00	0	0.00	0	0.00
3	1	4.13+01	0	0.00	0	0.00	1	1.16+04	0	0.00	0	0.00
4	0	0.00	0	0.00	0	0.00	0	0.00	0	0.00	0	0.00
5	1	5.00+03	2	2.88+03	1	1.84+03	1	2.51+03	0	0.00	0	0.00
6	2	9.57+03	0	0.00	3	1.97+03	1	7.93+02	0	0.00	0	0.00

7	5	3.30+03	4	1.73+03	5	4.56+04	11	1.12+05	0	0.00	0	0.00			
8	1	6.01+01	6	8.50+03	1	3.11+01	9	1.81+04	0	0.00	1	5.09+02			
9	1	1.35+03	0	0.00	0	0.00	1	1.45+02	0	0.00	1	1.22+04			
10	6	1.41+04	9	6.39+03	0	0.00	4	2.40+03	0	0.00	0	0.00			
11	19	1.93+04	14	3.42+04	19	5.44+04	7	8.90+03	5	3.13+03	5	1.16+03			
12	26	5.71+04	19	8.15+04	18	8.49+04	19	1.13+05	13	7.45+03	13	6.22+04			
13	126	2.80+05	104	5.82+05	83	2.43+05	80	3.06+05	3	6.37+03	8	9.78+03			
14	148	3.35+05	175	2.55+05	42	1.13+05	220	3.37+05	44	2.44+05	36	2.60+04			
15	0	0.00	0	0.00	0	0.00	0	0.00	0	0.00	0	0.00			

ENERGY GROUP	REGION 37		REGION 38		REGION 39		REGION 40		REGION 41		REGION 42	
	NUMBER	WEIGHT	NUMBER	WEIGHT	NUMBER	WEIGHT	NUMBER	WEIGHT	NUMBER	WEIGHT	NUMBER	WEIGHT
1	0	0.00	0	0.00	0	0.00	0	0.00	0	0.00	0	0.00
2	0	0.00	0	0.00	0	0.00	0	0.00	0	0.00	0	0.00
3	0	0.00	2	2.15+04	0	0.00	0	0.00	0	0.00	0	0.00
4	0	0.00	0	0.00	0	0.00	0	0.00	0	0.00	0	0.00
5	0	0.00	0	0.00	0	0.00	2	2.07+03	0	0.00	0	0.00
6	1	1.36+03	0	0.00	0	0.00	0	0.00	0	0.00	0	0.00
7	3	2.72+04	1	1.72+03	0	0.00	0	0.00	1	4.63+02	0	0.00
8	6	1.13+04	1	5.27+01	0	0.00	0	0.00	0	0.00	0	0.00
9	0	0.00	0	0.00	0	0.00	0	0.00	0	0.00	0	0.00
10	0	0.00	1	1.31+02	1	2.82+02	0	0.00	0	0.00	1	5.29+02
11	0	0.00	5	1.09+04	1	1.59+03	5	6.78+03	2	1.27+03	1	1.16+02
12	6	1.44+04	0	0.00	3	3.45+03	3	4.35+02	5	7.90+03	0	0.00
13	28	2.73+04	2	9.82+03	6	4.00+03	8	3.94+03	28	2.32+04	6	3.92+03
14	16	4.51+04	16	4.44+04	14	2.94+04	73	1.76+05	25	5.47+04	47	9.54+04
15	0	0.00	0	0.00	0	0.00	0	0.00	0	0.00	0	0.00

***NEXT RANDOM NUMBER IS 334310642242

********** F-MODE FAMS STORE FOR ITERATION NO. 1 **********

FAM (IFAM) ARRAY

1	1	2	100	100	0	0	0	0
9	0	0	0	0	0	0	0	0
17	0	10	10	0	0	0	0	0
25	0	0	0	0	0	0	0	0
33	1	0	25850	25850	37820	37820	11970	10
41	1	2	25850	37820	1			

********** A-MODE FAMS READ FOR ITERATION NO. 2 **********

FAM (IFAM) ARRAY

1	1	2	100	100	0	0	0	0
9	0	0	0	0	0	0	0	0

```
   17              0              10              10              0              0              0              0              0
   25              0              0               0               0              0              0              0              0
   33              2              1           25850           25850          37820          37820          11970             18
   41              1              2           25850           37820              2
YOU ARE USING THE DEFAULT VERSION OF STRUN WHICH DOES   NOTHING.

***START BATCH   1                          RANDOM=        337274612532

SOURCE DATA

YOU ARE USING THE IFA VERSION OF SOURCE.  SOURCE/IFA PICKS THE ENERGY IG FROM BFS AND THE DIRECTION KD FROM FAI(IG,NSR,KD).
    WATE IS SET EQUAL TO DDF./
  SWATE        IAVE    UAVE    VAVE    WAVE        XAVE        YAVE        ZAVE        AGEAVE
  9.772+01     10.34   -.0462  -.1335  -.0363      1.000-03    1.000-03    6.000+04    0.000

NUMBER OF COLLISIONS OF TYPE NCOLL
  SOURCE SPLIT(D)    FISHN   GAMGEN REALCOLL   ALBEDO     BDRYX   ESCAPE    E-CUT TIMEKILL R R KILL R R SURV  GAMLOST
     100         0        0        0      689         0      400       50        0         0       50         9         0

TIME REQUIRED FOR THE PRECEDING BATCH WAS     19

***START BATCH   2                          RANDOM=        161620631352

SOURCE DATA
  SWATE        IAVE    UAVE    VAVE    WAVE        XAVE        YAVE        ZAVE        AGEAVE
  1.001+02     10.06    .0560  -.0899   .0211      1.000-03    1.000-03    6.000+04    0.000

NUMBER OF COLLISIONS OF TYPE NCOLL
  SOURCE SPLIT(D)    FISHN   GAMGEN REALCOLL   ALBEDO     BDRYX   ESCAPE    E-CUT TIMEKILL R R KILL R R SURV  GAMLOST
     100         0        0        0      702         0      398       46        0         0       54         5         0

TIME REQUIRED FOR THE PRECEDING BATCH WAS     13

***START BATCH   3                          RANDOM=        055760642172

SOURCE DATA
  SWATE        IAVE    UAVE    VAVE    WAVE        XAVE        YAVE        ZAVE        AGEAVE
  9.572+01     10.87   -.0842  -.1125   .0158      1.000-03    1.000-03    6.000+04    0.000

NUMBER OF COLLISIONS OF TYPE NCOLL
  SOURCE SPLIT(D)    FISHN   GAMGEN REALCOLL   ALBEDO     BDRYX   ESCAPE    E-CUT TIMEKILL R R KILL R R SURV  GAMLOST
     100         0        0        0      636         0      381       45        0         0       55         4         0

TIME REQUIRED FOR THE PRECEDING BATCH WAS     11

***START BATCH   4                          RANDOM=        161330657752

SOURCE DATA
  SWATE        IAVE    UAVE    VAVE    WAVE        XAVE        YAVE        ZAVE        AGEAVE
  9.392+01     10.30   -.1314   .0462   .0731      1.000-03    1.000-03    6.000+04    0.000
```

```
NUMBER OF COLLISIONS OF TYPE NCOLL
  SOURCE SPLIT(D)    FISHN    GAMGEN REALCOLL   ALBEDO    BDRYX    ESCAPE    E-CUT TIMEKILL R R KILL R R SURV  GAMLOST
     100        0        0        0      602        0      350        45        0        0       55        5        0

TIME REQUIRED FOR THE PRECEDING BATCH WAS     11

***START BATCH   5                          RANDOM=        146574510642

SOURCE DATA
  SWATE       IAVE    UAVE    VAVE    WAVE       XAVE       YAVE       ZAVE       AGEAVE
  1.050+02    10.49   -.0255  -.0375   .0726    1.000-03   1.000-03   6.000+04   0.000

NUMBER OF COLLISIONS OF TYPE NCOLL
  SOURCE SPLIT(D)    FISHN    GAMGEN REALCOLL   ALBEDO    BDRYX    ESCAPE    E-CUT TIMEKILL R R KILL R R SURV  GAMLOST
     100        0        0        0      647        0      352        53        0        0       47        9        0

TIME REQUIRED FOR THE PRECEDING BATCH WAS     11

***START BATCH   6                          RANDOM=        323602425542

SOURCE DATA
  SWATE       IAVE    UAVE    VAVE    WAVE       XAVE       YAVE       ZAVE       AGEAVE
  1.039+02    10.81   -.0172  -.0185  -.0555    1.000-03   1.000-03   6.000+04   0.000

NUMBER OF COLLISIONS OF TYPE NCOLL
  SOURCE SPLIT(D)    FISHN    GAMGEN REALCOLL   ALBEDO    BDRYX    ESCAPE    E-CUT TIMEKILL R R KILL R R SURV  GAMLOST
     100        0        0        0      707        0      445        46        0        0       54        9        0

TIME REQUIRED FOR THE PRECEDING BATCH WAS     13

***START BATCH   7                          RANDOM=        347427643052

SOURCE DATA
  SWATE       IAVE    UAVE    VAVE    WAVE       XAVE       YAVE       ZAVE       AGEAVE
  1.009+02    10.24    .0818  -.0275  -.0536    1.000-03   1.000-03   6.000+04   0.000

NUMBER OF COLLISIONS OF TYPE NCOLL
  SOURCE SPLIT(D)    FISHN    GAMGEN REALCOLL   ALBEDO    BDRYX    ESCAPE    E-CUT TIMEKILL R R KILL R R SURV  GAMLOST
     100        0        0        0      664        0      363        49        0        0       51        7        0

TIME REQUIRED FOR THE PRECEDING BATCH WAS     12

***START BATCH   8                          RANDOM=        227353673552

SOURCE DATA
  SWATE       IAVE    UAVE    VAVE    WAVE       XAVE       YAVE       ZAVE       AGEAVE
  9.606+01     9.61   -.0569  -.0054   .0248    1.000-03   1.000-03   6.000+04   0.000

NUMBER OF COLLISIONS OF TYPE NCOLL
  SOURCE SPLIT(D)    FISHN    GAMGEN REALCOLL   ALBEDO    BDRYX    ESCAPE    E-CUT TIMEKILL R R KILL R R SURV  GAMLOST
```

```
    100        0        0        0      772        0      421       51        0        0       49        4        0

TIME REQUIRED FOR THE PRECEDING BATCH WAS     13

***START BATCH   9                          RANDOM=        100027775522

SOURCE DATA
  SWATE        IAVE     UAVE     VAVE     WAVE       XAVE       YAVE       ZAVE       AGEAVE
  1.091+02     10.13     .0959   -.0001    .1065     1.000-03   1.000-03   6.000+04   0.000

NUMBER OF COLLISIONS OF TYPE NCOLL
  SOURCE SPLIT(D)    FISHN   GAMGEN REALCOLL   ALBEDO    BORYX   ESCAPE    E-CUT TIMEKILL R R KILL R R SURV  GAMLOST
     100        0        0        0      722        0      427       46        0        0       54       10        0

TIME REQUIRED FOR THE PRECEDING BATCH WAS     13

***START BATCH  10                          RANDOM=        364164710632

SOURCE DATA
  SWATE        IAVE     UAVE     VAVE     WAVE       XAVE       YAVE       ZAVE       AGEAVE
  9.794+01      9.93     .0117   -.0883   -.0189     1.000-03   1.000-03   6.000+04   0.000

NUMBER OF COLLISIONS OF TYPE NCOLL
  SOURCE SPLIT(D)    FISHN   GAMGEN REALCOLL   ALBEDO    BORYX   ESCAPE    E-CUT TIMEKILL R R KILL R R SURV  GAMLOST
     100        0        0        0      730        0      477       43        0        0       57        9        0

TIME REQUIRED FOR THE PRECEDING BATCH WAS     12
THIS IS AN ADJOINT PROBLEM - ADJOINT ENERGY DEPENDENT FLUENCE IS NOT DIFFERENTIAL
```

THIS PRINT OCCURRED ON THE 3 DAY OF THE 5 MONTH IN THE YEAR 1976
AT 18 MINUTES PAST THE HOUR OF 10 PM .

ORNL 4469 FISSION SOURCE

RESPONSES(DETECTOR) ADJOINT RESPONSE VALUES BASED ON HENDERSON TISSUE DOSE

DETECTOR	UNCOLL RESPONSE	FSD UNCOLL	TOTAL RESPONSE	FSD TOTAL
1	6.0593-22	.05351	2.2937-20	.28590
2	0.0000	.00000	1.5623-21	.98154

FLUENCE(ENERGY,DETECTOR) ENERGY DEPENDENT ADJOINT FLUENCE - IMPORTANCE/CMSQ/EV/SOURCE

DETECTOR NO. ENERGIES	1	2
3.355+03		
	4.211-25	0.000
	.871	.000
1.109+05		
	2.276-20	0.000
	.890	.000
1.108+06		
	5.014-20	0.000
	.389	.000
2.350+06		
	7.723-20	1.433-20
	.233	1.000
4.060+06		
	1.147-19	0.000
	.480	.000
6.360+06		
	3.737-20	0.000
	.478	.000
8.180+06		
	2.219-19	0.000
	.859	.000
1.000+07		
	3.898-20	6.467-21
	.273	1.000
1.220+07		
	1.480-19	1.294-19
	.827	.941
1.500+07		

DETECTOR NO 1 FLUENCE(COSINE,ENERGY,DETECTOR) ENERGY AND ANGULAR DEPENDENT ADJOINT FLUENCE

ENERGIES / COSINES	3.355+03	1.109+05	1.108+06	2.350+06	4.060+06	6.360+06	8.180+06	1.000+07	1.220+07
	1.109+05	1.108+06	2.350+06	4.060+06	6.360+06	8.180+06	1.000+07	1.220+07	1.500+07
-1.000000	1.223-25	2.590-21	1.050-20	5.896-20	2.279-20	1.705-20	1.943-20	2.246-20	1.062-20
	.609	.352	.269	.338	.274	.234	.359	.464	.132
-.888889	9.816-26	7.360-21	7.419-21	8.948-21	2.532-20	8.375-21	2.908-21	5.450-21	4.865-21
	.984	.961	.585	.320	.603	.763	.273	.460	.568
-.444444	2.206-26	4.619-23	3.490-21	2.628-21	8.005-21	3.470-22	2.809-21	2.520-21	1.082-21
	1.000	.516	.802	.566	.755	.557	.576	.862	.583
.000000	0.000	9.658-23	4.249-21	4.363-22	1.993-21	2.532-22	1.111-21	3.706-22	4.382-20
	.000	.997	.855	.392	.707	.880	.897	.786	.999
.444444	0.000	0.000	1.731-22	9.032-22	6.560-23	1.443-22	6.777-20	1.297-24	5.547-22
	.000	.000	1.000	1.000	.598	.890	.999	1.000	.655
.888889	0.000	0.000	0.000	0.000	0.000	0.000	0.000	0.000	0.000
	.000	.000	.000	.000	.000	.000	.000	.000	.000
1.000000									

DETECTOR NO 2 FLUENCE(COSINE,ENERGY,DETECTOR) ENERGY AND ANGULAR DEPENDENT ADJOINT FLUENCE

ENERGIES / COSINES	3.355+03	1.109+05	1.108+06	2.350+06	4.060+06	6.360+06	8.180+06	1.000+07	1.220+07
	1.109+05	1.108+06	2.350+06	4.060+06	6.360+06	8.180+06	1.000+07	1.220+07	1.500+07
-1.000000	0.000	0.000	0.000	2.053-20	0.000	0.000	0.000	0.000	0.000
	.000	.000	.000	1.000	.000	.000	.000	.000	.000
-.888889	0.000	0.000	0.000	0.000	0.000	0.000	0.000	2.316-21	2.534-21
	.000	.000	.000	.000	.000	.000	.000	1.000	1.000
-.444444	0.000	0.000	0.000	0.000	0.000	0.000	0.000	0.000	0.000
	.000	.000	.000	.000	.000	.000	.000	.000	.000
.000000	0.000	0.000	0.000	0.000	0.000	0.000	0.000	0.000	4.380-20
	.000	.000	.000	.000	.000	.000	.000	.000	1.000
.444444	0.000	0.000	0.000	0.000	0.000	0.000	0.000	0.000	0.000
	.000	.000	.000	.000	.000	.000	.000	.000	.000
.888889	0.000	0.000	0.000	0.000	0.000	0.000	0.000	0.000	0.000
	.000	.000	.000	.000	.000	.000	.000	.000	.000
1.000000									

TIME REQUIRED FOR THE PRECEDING 10 BATCHES WAS 129

```
          ************   A-MODE FAMS STORE FOR ITERATION NO.  2   ************

                                FAM (IFAM) ARRAY
    1              1              2            100            100              0              0              0              0
    9              0              0              0              0              0              0              0              0
   17              0             10             10              0              0              0              0              0
   25              0              0              0              0              0              0              0              0
   33              2              1          25850          25850          37820          37820          11970             18
   41              1              2          25850          37820              2

          ************   F-MODE FAMS READ FOR ITERATION NO.  2   ************

                                FAM (IFAM) ARRAY
    1              1              2            100            100              0              0              0              0
    9              0              0              0              0              0              0              0              0
   17              0             10             10              0              0              0              0              0
   25              0              0              0              0              0              0              0              0
   33              2              0          25850          25850          37820          37820          11970             18
   41              1              2          25850          37820              1
YOU ARE USING THE DEFAULT VERSION OF STRUN WHICH DOES   NOTHING.

***START BATCH    1                          RANDOM=        334310642242

SOURCE DATA

YOU ARE USING THE IFA VERSION OF SOURCE.  SOURCE/IFA PICKS THE ENERGY IG FROM BFS AND THE DIRECTION KD FROM FAI(IG,NSR,KD).
    WATE IS SET EQUAL TO DOF./
   SWATE          IAVE      UAVE      VAVE      WAVE       XAVE       YAVE       ZAVE       AGEAVE
  1.049+02         9.79     -.0062    -.0534     .0483     1.000-03   1.000-03   1.000-03    0.000

NUMBER OF COLLISIONS OF TYPE NCOLL
   SOURCE SPLIT(D)     FISHN    GAMGEN REALCOLL    ALBEDO     BORYX    ESCAPE    E-CUT TIMEKILL R R KILL R R SURV  GAMLOST
       100         0         0         0      1567         0       516        35        24         0        41         4         0

TIME REQUIRED FOR THE PRECEDING BATCH WAS      31
```

THIS PRINT OCCURRED ON THE 3 DAY OF THE 5 MONTH IN THE YEAR 1976
AT 22 MINUTES PAST THE HOUR OF 10 PM .

HENDERSON TISSUE DOSE - RADS[T]

RESPONSES(DETECTOR) TOTAL RESPONSE - NEUTRON RESPONSE FUNCTION FROM ORNL 4464

DETECTOR	UNCOLL RESPONSE	FSD UNCOLL	TOTAL RESPONSE	FSD TOTAL
1	6.0580-22	.33333	1.4740-20	.21582
2	0.0000	.00000	0.0000	.00000

FLUENCE(ENERGY,DETECTOR) ENERGY DEPENDENT FLUENCE - NEUTRONS/CMSQ/EV/SOURCE

DETECTOR NO. ENERGIES	1	2
1.500+07	0.000	0.000
	.000	.000
1.220+07	1.792-22	0.000
	.910	.000
1.000+07	3.647-21	0.000
	.484	.000
8.180+06	7.400-20	0.000
	.788	.000
6.360+06	8.745-20	0.000
	.472	.000
4.060+06	2.749-19	0.000
	.181	.000
2.350+06	1.270-18	0.000
	.351	.000
1.108+06	4.237-18	0.000
	.264	.000
1.109+05	1.563-17	0.000
	.600	.000
3.355+03		

DETECTOR NO 1 FLUENCE(COSINE,ENERGY,DETECTOR) ENERGY AND ANGULAR DEPENDENT FLUENCE

ENERGIES	1.500+07	1.220+07	1.000+07	8.180+06	6.360+06	4.060+06	2.350+06	1.108+06	1.109+05
COSINES	1.220+07	1.000+07	8.180+06	6.360+06	4.060+06	2.350+06	1.108+06	1.109+05	3.355+03
-1.000000	0.000	0.000	0.000	0.000	0.000	1.557-20	0.000	8.169-20	0.000
	.000	.000	.000	.000	.000	1.000	.000	1.000	.000
-.888889	0.000	0.000	0.000	0.000	0.000	3.897-22	3.924-22	3.083-19	2.821-20
	.000	.000	.000	.000	.000	.837	1.000	.625	.568
-.444444	0.000	0.000	3.069-22	0.000	1.410-20	1.810-21	1.029-19	1.763-19	1.532-19
	.000	.000	1.000	.000	1.000	.774	.945	.755	.971
.000000	0.000	0.000	0.000	0.000	4.563-23	7.850-21	1.594-19	2.239-19	2.037-19
	.000	.000	.000	.000	.891	.288	.510	.308	.471
.444444	0.000	0.000	2.878-22	2.173-20	2.141-21	1.538-20	9.310-20	6.496-19	5.175-18
	.000	.000	1.000	.954	.421	.296	.372	.338	.648
.888889	0.000	2.566-22	2.845-21	1.909-20	6.010-20	2.765-19	3.964-19	5.545-19	1.417-19
	.000	.910	.526	.576	.345	.152	.134	.168	.651
1.000000									

DETECTOR NO 2 FLUENCE(COSINE,ENERGY,DETECTOR) ENERGY AND ANGULAR DEPENDENT FLUENCE

ENERGIES	1.500+07	1.220+07	1.000+07	8.180+06	6.360+06	4.060+06	2.350+06	1.108+06	1.109+05
COSINES	1.220+07	1.000+07	8.180+06	6.360+06	4.060+06	2.350+06	1.108+06	1.109+05	3.355+03
-1.000000	0.000	0.000	0.000	0.000	0.000	0.000	0.000	0.000	0.000
	.000	.000	.000	.000	.000	.000	.000	.000	.000
-.888889	0.000	0.000	0.000	0.000	0.000	0.000	0.000	0.000	0.000
	.000	.000	.000	.000	.000	.000	.000	.000	.000
-.444444	0.000	0.000	0.000	0.000	0.000	0.000	0.000	0.000	0.000
	.000	.000	.000	.000	.000	.000	.000	.000	.000
.000000	0.000	0.000	0.000	0.000	0.000	0.000	0.000	0.000	0.000
	.000	.000	.000	.000	.000	.000	.000	.000	.000
.444444	0.000	0.000	0.000	0.000	0.000	0.000	0.000	0.000	0.000
	.000	.000	.000	.000	.000	.000	.000	.000	.000
.888889	0.000	0.000	0.000	0.000	0.000	0.000	0.000	0.000	0.000
	.000	.000	.000	.000	.000	.000	.000	.000	.000
1.000000									

TIME REQUIRED FOR THE PRECEDING 10 BATCHES WAS 232

APPENDIX D

DERIVATION OF THE INTEGRAL EMERGENT ADJUNCTON DENSITY EQUATION

In Section 2.4 the integral emergent adjuncton density equation (2-117) was developed by taking the adjoint of the value equation (2-112), then requiring that adjunctons travel in the direction of the velocity vector instead of opposite to it. The MORSE code document {13} also derives this equation, but the notation which uses integral operators is difficult to follow and sufficient editorial errors exist so that the validity of the results is suspect on casual inspection. This appendix contains a parallel derivation to the one in the MORSE document, but the integral notation has been dropped and a different approach taken to obtain the adjuncton density equations. The derivation begins with the definition of the two new quantities, $H_g(\bar{x},\bar{\omega})$ and $G_g(\bar{x},\bar{\omega})$, which are denoted $H_g(\bar{r},\bar{\omega},t)$ and $G_g(\bar{r},\bar{\omega},t)$, respectively, in the MORSE document. Define:

$$H_g(\bar{x},\bar{\omega}) \equiv \Sigma_t^g(\bar{x})\ \chi^*(\bar{x},\bar{\omega}) \ , \tag{D-1}$$

and

$$H_g(\bar{x},\bar{\omega}) \equiv \int_0^\infty \Sigma_t^g(\bar{x})\ \exp\left[-\int_0^R \Sigma_t^g(\bar{x}+R'\bar{\omega})dR'\right] G_g(\bar{x}+R\bar{\omega},\bar{\omega})dR \ . \tag{D-2}$$

As pointed out in Reference 13, since $\chi_g^*(\bar{x},\bar{\omega})$ is a flux-like quantity, multiplication by the cross section makes $H_g(\bar{x},\bar{\omega})$ a type of event density.

Note that Equation D-2 differs from the definition given in the MORSE document, although the exponential integral term is redefined in the MORSE derivation to be consistent with Equation D-2.

Substitution of the following two equations from Section 2 into Equation D-2 and rearranging certain terms produces Equation D-5:

$$R_g^{\chi}(\bar{x},\bar{\omega}) = \int_0^{\infty} \exp\left[- \int_0^{R} \Sigma_t^g(\bar{x}+R'\bar{\omega})dR' \right] R_g^{\Phi}(\bar{x}+R\bar{\omega},\bar{\omega})dR \ , \tag{D-3}$$

$$\chi_g^*(\bar{x},\bar{\omega}) = R_g^{\chi}(\bar{x},\bar{\omega}) + \int_0^{\infty} \Sigma_t^g(\bar{x}+R\bar{\omega}) \exp\left[- \int_0^{R} \Sigma_t^g(\bar{x}+R'\bar{\omega})dR' \right] \tag{D-4}$$

$$\times \sum_{g'} \int \frac{\Sigma_s^{g'\leftarrow g}(\bar{x}+R\bar{\omega};\bar{\omega}'|\bar{\omega})}{\Sigma_t^g(\bar{x}+R\bar{\omega},\bar{\omega})} \chi_{g'}^*(\bar{x}+R\bar{\omega},\bar{\omega}')d\bar{\omega}'dR \ ,$$

$$H_g(\bar{x},\bar{\omega}) = \int_0^{\infty} \Sigma_t^g(\bar{x}) \exp\left[- \int_0^{R} \Sigma_t^g(\bar{x}+R'\bar{\omega})dR' \right] \left[R_g^{\Phi}(\bar{x}+R\bar{\omega},\bar{\omega}') \right. \tag{D-5}$$

$$\left. + \Sigma_t^g(\bar{x}+R\bar{\omega}) \sum_{g'} \int \frac{\Sigma_s^{g'\leftarrow g}(\bar{x}+R\bar{\omega};\bar{\omega}'|\bar{\omega})}{\Sigma_t^g(\bar{x}+R\bar{\omega})} \chi_{g'}^*(\bar{x}+R\bar{\omega},\bar{\omega}')d\bar{\omega}' \right] dR \ .$$

Since the $\Sigma_t^g(\bar{x}+R\bar{\omega})$ terms cancel and the last term can be multiplied and divided by $\Sigma_t^{g'}(\bar{x}+R\bar{\omega})$, Equation D-5 can be written as:

$$H_g(\bar{x},\bar{\omega}) = \int_0^{\infty} \Sigma_t^g(\bar{x}) \exp\left[- \int_0^{R} \Sigma_t^g(\bar{x}+R'\bar{\omega})dR' \right] \left[R_g^{\Phi}(\bar{x}+R\bar{\omega},\bar{\omega}) \right. \tag{D-6}$$

$$\left. + \sum_{g'} \int \frac{\Sigma_s^{g'\leftarrow g}(\bar{x}+R\bar{\omega};\bar{\omega}'|\bar{\omega})}{\Sigma_t^g(\bar{x}+R\bar{\omega})} H_{g'}(\bar{x}+R\bar{\omega},\bar{\omega}')d\bar{\omega}' \right] d\bar{\omega}'dR \ .$$

Comparison of Equations D-2 and D-6 shows that $G_g(\bar{x},\bar{\omega})$ can be written as:

$$G_g(\bar{x},\bar{\omega}) = R_g^{\Phi}(\bar{x},\bar{\omega}) + \sum_{g'} \int \frac{\Sigma_s^{g'\leftarrow g}(\bar{x};\bar{\omega}'|\bar{\omega})}{\Sigma_t^{g'}(\bar{x})} H_{g'}(\bar{x},\bar{\omega}')d\bar{\omega}' \quad . \tag{D-7}$$

The substitution of Equation D-2 into D-7 yields the Fredholm integral equation of the second kind for $G_g(\bar{x},\bar{\omega})$:

$$G_g(\bar{x},\bar{\omega}) = R_g^{\Phi}(\bar{x},\bar{\omega}) + \sum_{g'} \int \frac{\Sigma_s^{g'\leftarrow g}(\bar{x};\bar{\omega}'|\bar{\omega})}{\Sigma_t^{g'}(\bar{x})} \int_0^{\infty} \Sigma_t^{g'}(\bar{x}) \tag{D-8}$$

$$\times \exp\left[-\int_0^R \Sigma_t^{g'}(\bar{x}+R'\bar{\omega}')dR'\right] G_g(\bar{x}+R\bar{\omega}',\bar{\omega}')dRd\bar{\omega}' \quad .$$

The above equation is identical to Equation 2-116, which was derived from the value equation. Equations D-6, D-7, and D-8 are the counterparts of Equations 88, 89, and 90 in Appendix A of Reference 13, except that the collision operator, $C_{g\rightarrow g'}(\bar{r}',\bar{\Omega}\rightarrow\bar{\Omega}')$, has been defined by placing the $\Sigma_t^{g'}(\bar{r})$ term outside of the summation over g'. Also, the transport operator, $T_{g'}(\bar{r}\rightarrow\bar{r}',\bar{\Omega}')$, must be interpreted in the sense of the definition given above Equation 88, and not in the sense implied earlier by Equations 64 and 66. With these caveats, Equation D-8 will also be called the adjoint emergent particle density. However, it should be noted that Equation D-8 is not mathematically adjoint to the emergent particle density equation, since the kernels are not adjoint.

Comparison of Equation D-8 with Equation 2-92 reveals that the adjoint emergent particle density equation is nearly identical to the emergent particle density equation, so that the logic and coding used to simulate the emergent particle density equation could be used to simulate Equation D-8 with some modification. The adjoint source, $R_g^{\Phi}(\bar{x},\bar{\omega})$ could

be input in the same manner as the forward source, $S_g(\bar{x},\bar{\omega})$. The adjoint collision kernel can be calculated from the input multigroup cross sections for forward Monte Carlo calculations. However, one troublesome aspect of Equation D-8, as well as all adjoint equations (2-110, 2-112, 2-116, and D-6) is the transport of the adjoint particles in a direction opposite to the direction vector, $\bar{\omega}'$. This is due to the fact that the transport step starts are $\bar{x}+R\bar{\omega}'$ and terminates at $\bar{x}$.

One method of overcoming this inconvenience is to define a new quantity, $\bar{G}_g(\bar{x},\bar{\omega})$, where:

$$\bar{G}_g(\bar{x},\bar{\omega}) = G_g(\bar{x},-\bar{\omega}) \quad . \tag{D-9}$$

Then the integral form of $\bar{G}_g(\bar{x},\bar{\omega})$ is just:

$$\bar{G}_g(\bar{x},\bar{\omega}) = R_g^{\Phi}(\bar{x},-\bar{\omega}) + \sum_{g'} \int \frac{\Sigma_s^{g'\leftarrow g}(\bar{x};\bar{\omega}'|-\bar{\omega})}{\Sigma_t^{g'}(\bar{x})} \int_0^{\infty} \Sigma_t^{g'}(\bar{x}) \tag{D-10}$$

$$\times \exp\left[-\int_0^R \Sigma_t^{g'}(\bar{x}+R'\bar{\omega}')dR'\right] \bar{G}_{g'}(\bar{x}+R'\bar{\omega}',-\bar{\omega}')dRd\bar{\omega}' \quad .$$

If the variable of integration, $\bar{\omega}'$, is set to $-\bar{\omega}''$, and the source term, $R_g^{\Phi}(\bar{x},-\bar{\omega})$, is defined by:

$$\bar{R}_g^{\Phi}(\bar{x},\bar{\omega}) = R_g^{\Phi}(\bar{x},-\bar{\omega}) \quad , \tag{D-11}$$

then

$$\bar{G}(\bar{x},\bar{\omega}) = \bar{R}_g^{\Phi}(\bar{x},\bar{\omega}) + \sum_{g'} \int \frac{\Sigma_s^{g'\leftarrow g}(\bar{x};-\bar{\omega}''|-\bar{\omega})}{\Sigma_t^{g'}(\bar{x})} \int_0^{\infty} \Sigma_t^{g'}(\bar{x}) \tag{D-12}$$

(continued)

$$\times \exp\left[-\int_0^R \Sigma_t^{g'}(\bar{x}-R'\bar{\omega}'')dR\right] \bar{G}_g(\bar{x}-R\bar{\omega}'',\bar{\omega}'')dRd\bar{\omega}'' \ .$$

The integral over $\bar{\omega}''$, or any other dummy variable representing the angular direction, is taken over non-negative definite increments. Since the probability of scattering from $-\bar{\omega}$ to $-\bar{\omega}''$ depends only on the angle between $-\bar{\omega}$ and $-\bar{\omega}''$ (as assumed in Section 2.1), then

$$\Sigma_s^{g'\leftarrow g}(\bar{x};-\bar{\omega}''|-\bar{\omega}) = \Sigma_s^{g'\leftarrow g}(\bar{x};\bar{\omega}''|\bar{\omega}) \ . \qquad \text{(D-13)}$$

Thus, by changing the dummy variable $\bar{\omega}''$ to $\bar{\omega}'$, Equation D-12 becomes

$$\bar{G}_g(\bar{x},\bar{\omega}) = \bar{R}_g^{\Phi}(\bar{x},\bar{\omega}) + \sum_{g'}\int \frac{\Sigma_s^{g'\leftarrow g}(\bar{x};\bar{\omega}'|\bar{\omega})}{\Sigma_t^{g'}(\bar{x})}\int_0^{\infty}\Sigma_t^{g'}(\bar{x}) \qquad \text{(D-14)}$$

$$\times \exp\left[-\int_0^R \Sigma_t^{g'}(\bar{x}-R'\bar{\omega}')dR\right] \ \bar{G}_{g'}(\bar{x}-R\bar{\omega}',\bar{\omega}')dRd\bar{\omega}' \ .$$

The above equation has the exact form as the emergent particle density equation, and hence can be simulated by the same logic and coding without any modification. Care must be taken in the application of the $\bar{G}(\bar{x},\bar{\omega})$ simulations since all directions are reversed or in the opposite sense to the normal adjoint functions. Also, the adjoint source term, $\bar{R}_g^{\Phi}(\bar{x},\bar{\omega})$, is reversed in direction to the physical response function, which must be taken into account for a non-isotropic response function. This can be done very easily in the input.

As discussed in Reference 13 for Equation 93 in Appendix A, Equation D-14, the counterpart to Equation 93, can be thought of as the

transport of psuedo-particles or adjunctons, which travel in the "proper" direction. Comparison of these two equations is restricted since the definition of the transport operator in Equation 93 is uncertain, but it is assumed to be the same as in D-14, except for obvious notation changes. In this case, the equations are the same, with Reference 13 using the somewhat confusing convention of a different symbol for the angular direction variable to represent the change of direction from the adjoint emergent particle density equation. Since Equation 93 is called the integral emergent adjuncton density, the same name will be used for D-14.

BIBLIOGRAPHY

1. A. D. Householder, G. E. Forsythe, and H. H. Germond (Editors), "Monte Carlo Methods," National Bureau of Standards Applied Mathematical Series 12, Washington, D. C. (1951).

2. H. A. Meyer (Ed), Symposium on Monte Carlo Methods, John Wiley and Sons, Inc., New York, 1956.

3. Herman Kahn, Applications of Monte Carlo, RM-1237-AEC, RAND Corporation, Santa Monica, California, revised 1956.

4. G. Goertzel and M. H. Kalos, "Monte Carlo Methods in Transport Problems," in Progress in Nuclear Energy, Series I, Vol. 2, Pergamon Press, New York, 1958.

5. J. D. Clement, "Introduction to Monte Carlo Methods and Applications," Atlanta, Georgia (unpublished).

6. M. Clark, Jr. and K. F. Hansen, Numerical Methods of Reactor Analyses, Academic Press, New York, 1964.

7. J. M. Hammersley and D. C. Handscomb, Monte Carlo Methods, John Wiley and Sons, Inc., New York, 1964.

8. J. Spanier and E. M. Gelbard, Monte Carlo Principles and Neutron Transport Problems, Addison-Wesley Publishing Company, Reading, Massachusetts, 1969.

9. B. Davidson, Nuclear Transport Theory, Oxford University Press, London, 1958.

10. M. H. Kalos, F. R. Nakache, and J. Celnik, "Monte Carlo Methods in Reactor Computations," in Computing Methods in Reactor Physics, Gordon and Breach, Science Publishers, New York, 1968.

11. G. I. Bell and S. Glasstone, Nuclear Reactor Theory, Van Nostrand Reinhold Company, New York, 1970.

12. Lord Kelvin, "Nineteenth Century Clouds over the Dynamical Theory of Heat and Light," Phil. Mag., 6, 2 (1901).

13. E. A. Straker, P. N. Stevens, D. C. Irving, and V. R. Cain, "The MORSE Code--A Multigroup Neutron and Gamma-Ray Monte Carlo Transport Code," ORNL-4585, Oak Ridge National Laboratory, Oak Ridge, Tennessee (1970).

BIBLIOGRAPHY (Continued)

14. E. A. Straker, W. H. Scott, Jr., and N. R. Byrn, "The MORSE Code with Combinatorial Geometry," SAI-72-511-LJ, Science Applications, Inc., La Jolla, California (1972).

15. V. R. Cain, "SAMBO, A Collision Analysis Package for Monte Carlo Codes," ORNL-TM-3203, Oak Ridge National Laboratory, Oak Ridge, Tennessee (1970).

16. D. C. Irving, R. M. Freestone, Jr., and F. B. K. Kam, "05R, A General-Purpose Monte Carlo Neutron Transport Code," ORNL-3622, Oak Ridge National Laboratory, Oak Ridge, Tennessee (1965).

17. D. C. Irving, "Description of the CDC-1604 Version of the 06R Neutron Monte Carlo Transport Code," ORNL-TM-3458, Oak Ridge National Laboratory, Oak Ridge, Tennessee (1971).

18. M. H. Kalos, "A Monte Carlo Calculation of the Transport of Gamma Rays," NDA 56-7, Nuclear Development Associates, White Plains, New York (1956).

19. N. R. Byrn, "CAVEAT: A Revised Version of the General Purpose Monte Carlo Program, COHORT," TN SE-290, Teledyne Brown Engineering, Huntsville, Alabama (1970).

20. B. Eisenman and F. R. Nakache, "UNC-SAM: A FORTRAN Monte Carlo System for the Evaluation of Neutron or Gamma Ray Transport in Three-Dimensional Geometry," UNC 5093, United Nuclear Corporation, Elmsford, New York (1964).

21. E. R. Friedman, M. H. Kalos, S. Preiser, G. Rabinowitz, and J. G. Beckerley, "The Numerical Solution of the Adjoint Transport Equation for Gamma Rays by the GADJET Code," NRDL-TRC-68-27, U.S. Naval Radiological Defense Laboratory, San Francisco, California (1968).

22. M. O. Cohen, W. Guber, H. Lichtenstein, H. A. Steinberg, and E. S. Troubetzkoy, "SAM-CE: A Three Dimensional Monte Carlo Code for the Solution of the Forward Neutron and Forward and Adjoint Gamma Ray Transport Equations--Revision A," MR-7021, Mathematical Applications Group, Inc., Elmsford, New York (1972).

23. M. O. Cohen, "ANTE 2--A FORTRAN Computer Code for the Solution of the Adjoint Neutron Transport Equation by the Monte Carlo Technique," DASA 2396, Mathematical Applications Group, Inc., White Plains, New York (1970).

24. G. Goertzel, "Quota Sampling and Importance Functions in Stochastic Solution of Particle Problems," ORNL-434, Oak Ridge National Laboratory, Oak Ridge, Tennessee (1949).

BIBLIOGRAPHY (Continued)

25. R. R. Coveyou, V. R. Cain, and K. J. Yost, "Adjoint and Importance in Monte Carlo Application," Nucl. Sci. Engr., 27, 219 (1967).

26. F. H. Clark, "The Exponential Transform as an Importance-Sampling Device--A Review," ORNL-RSIC-14, Oak Ridge National Laboratory, Oak Ridge, Tennessee (1966).

27. E. J. McGrath and D. C. Irving, "Techniques for Efficient Monte Carlo Simulation, Volume III, Variance Reduction," SAI-72-590-LJ, Science Applications, Inc., La Jolla, California (1972).

28. D. W. Drawbaugh, "On the Solution of Transport Problems by Conditional Monte Carlo," Nucl. Sci. Engr., 9, 185 (1961).

29. T. W. Armstrong and P. N. Stevens, "A V^{O} Importance Function for the Monte Carlo Calculation of the Deep Penetration of Gamma-Rays," J. Nucl. Energy, 23, 331 (1969).

30. L. L. Carter, "Coupled Sampling with the Monte Carlo Method in Neutron Transport Calculations," Ph.D. Dissertation, University of Washington, Seattle, Washington (1969).

31. F. A. R. Schmidt, E. A. Straker, and V. R. Cain, "Applications of Adjoint Flux Calculations to Monte Carlo Biasing," ORNL-TM-2454, Oak Ridge National Laboratory, Oak Ridge, Tennessee (1968).

32. B. Eriksson, S. Hui, M. H. Kalos, D. Spielberg, and H. Steinberg, "Automatic Computational of Importance Sampling Functions for Monte Carlo Transport Codes--Phase I," DASA 2384, Mathematical Applications Group., Inc., White Plains, New York (1970).

33. H. Steinberg, M. H. Kalos, and E. Troubetzkoy, "Automatic Computation of Importance Sampling Functions for Monte Carlo Transport Codes--Phase II," DASA 2583, Mathematical Applications Group, Inc., White Plains, New York (1970).

34. "The Huntsville Times," Huntsville, Alabama, page 2, September 6, 1971.

35. J. D. Clement and J. R. Williams, "Gas-Core Reactor Technology," Reactor Technology, 13(3), 226 (1970).

36. G. C. Pomraning, "A Method of Solution for Particle Transport Problems," GA-6497, General Atomics, San Diego, California (1965).

BIBLIOGRAPHY (Concluded)

37. D. C. Irving, "The Adjoint Equation and Its Simulations by Monte Carlo," ORNL-TM-2879, Oak Ridge National Laboratory, Oak Ridge, Tennessee (1970).

38. S. G. Mikhlin, Linear Integral Equations, Hindustan Publishing Corporation, Delhi, India, 1960.

39. Milo Solomito, Paul N. Stevens, E. A. Straker, C. A. Burgart, and S. N. Cramer, "Methods of Biasing Secondary Gamma-Ray Production in Coupled Neutron Gamma-Ray Monte Carlo Calculations," ORNL-TM-3530, Oak Ridge National Laboratory, Oak Ridge, Tennessee (1971).

40. G. A. Korn and T. M. Korn, Mathematical Handbook for Scientists and Engineers, Second Edition, McGraw-Hill Book Company, New York, 1968.

41. W. W. Engle, "A User's Manual for ANISN," K-1693, Union Carbide Corporation, Oak Ridge National Laboratory, Oak Ridge, Tennessee (1967).

42. W. A. Rhoades and F. R. Mynatt, "The DOT III Two-Dimensional Discrete Ordinates Transport Code," ORNL-TM-4280, Oak Ridge National Laboratory, Oak Ridge, Tennessee (1973).

43. C. A. Burgart, "06R-D, A Discrete Scattering Version of 06R with Importance Sampling of the Angle of Scatter," ORNL-TM-3031, Oak Ridge National Laboratory, Oak Ridge, Tennessee (1970).

44. "Measurement of Fast Neutrons and Secondary Gamma-Ray Transport through Concrete," Trans. Am. Nucl. Soc., 1971 Winter Meeting, 14(2), 916-921 (1971).

45. Jabo Sae Tang, P. N. Stevens, and T. J. Hoffman, University of Tennessee, Knoxville, Tennessee, Private Communications.

46. E. A. Straker, "Neutron Spectrum from Point Fission and 14 MeV Sources in Infinite Air," in Shielding Benchmark Problems, A. E. Profio (Ed), ORNL-RSIC-25, Radiation Shielding Information Center, Oak Ridge National Laboratory, Oak Ridge, Tennessee (1970).

47. E. A. Straker and M. L. Gritzner, "Neutron and Secondary Gamma-Ray Transport in Infinite Homogeneous Air," ORNL-4464, Oak Ridge National Laboratory, Oak Ridge, Tennessee (1969).

48. G. L. Simmons and C. M. Eisenhauer, "Neutron Dose and Fluence Distributions in an Infinite Air Medium," NBS Technical Note 745, National Bureau of Standards, Washington, D. C. (1973).

VITA

Noel Ricky Byrn was born in Nashville, Tennessee, January 26, 1939. During his early life, he and his parents, Mr. and Mrs. Grady D. Byrn, lived in various places in Middle Tennessee, moving to Jackson, Tennessee, when he was four. Mr. Byrn attended the first grade in Jackson, but moved to Dickson, Tennessee, soon after his father returned from the European Theatre of World War II. From the second grade through high school, he attended the public schools in Dickson.

In 1957, Mr. Byrn entered Tennessee Technological University at Cookeville for his freshman year. His final three years as an undergraduate were spent at the University of Tennessee, Knoxville. He received a Bachelor of Science degree in Nuclear Engineering with honors in 1961. During his undergraduate years, Mr. Byrn was honored by membership in Tau Beta Pi, Omicron Delta Kappa, Scabbard and Blade, and the ACE Board honor societies.

Soon after graduation, Mr. Byrn entered the U. S. Army Corps of Engineers as a Second Lieutenant. After completing the Engineer Officer Orientation Course, he was assigned to the Engineer School as an instructor in Atomic Demolitions Munitions. At the end of his tour of duty, he returned to the University of Tennessee at Knoxville as an Instructor in Basic Engineering and Graphics and a part-time graduate student. Mr. Byrn obtained a Master of Science degree in Nuclear Engineering in 1966. His thesis topic was "The Effects of Nitrogen, Xenon, and Temperature on the Worth of the EGCR Control Rods."

Mr. Byrn accepted a full-time position on the Technical Staff of Northrop Space Laboratory, Huntsville, Alabama, in 1965. His principal efforts were in the area of space mission analysis. In 1966, he joined Brown Engineering in Huntsville, where he directed the development of an extensive capability for performing nuclear radiation transport calculations. Mr. Byrn also began a part-time graduate program in mathematics at the University of Alabama in Huntsville. In 1969, he received the Master of Arts degree in Mathematics, and then began his Ph.D. residency program with the support of an Atomic Energy Commission Traineeship at the Georgia Institute of Technology. After completing his residency requirements, Mr. Byrn returned to Huntsville. In 1971, he joined Science Applications, Inc., where he is presently the Director of Science and Engineering Projects for the Huntsville Division of SAI and an Assistant Vice President at the Corporate level. His principal duties are managing the efforts of over twenty scientists and engineers working in the fields of nuclear weapons effects, space radiation transport, computational fluid dynamics, meteorology, energy, and environmental impacts. He is also the principal investigator for the Army's Nuclear Analysis Study.

Mr. Byrn is married to the former Judith Abigail Nicks of Dickson, Tennessee. They have three children, Judy, age 14 years, Janice, age 12 years, and Andrew, age 10 years.